

Review

Fuzzy Control Systems for Power Quality Improvement—A Systematic Review Exploring Their Efficacy and Efficiency

Anca Miron , Andrei C. Cziker * and Horia G. Beleiu 

Department Power System and Management, Technical University of Cluj-Napoca, 28th Memorandumului Street, 400114 Cluj-Napoca, Romania; anca.miron@enm.utcluj.ro (A.M.); horia.beleiu@enm.utcluj.ro (H.G.B.)

* Correspondence: andrei.cziker@enm.utcluj.ro

Abstract: Fuzzy-based control systems have demonstrated a remarkable ability to control nonlinear processes, a characteristic commonly observed in power systems, particularly in the context of power quality enhancement. Despite this, an updated and comprehensive literature review on the applications of fuzzy logic in the domain of power quality control has been lacking. To address this gap, this study critically examines published research on the effective and efficient use of fuzzy logic in resolving quality issues within power systems. Data sources included the Web of Science and academic journal databases, followed by an evaluation of target articles based on predefined criteria. The information was then classified into seven categories, including control system type, features of the fuzzy logic controller, fuzzy logic inference strategy, power quality issue, control device, implementation methodology (efficacy testing), and efficiency improvement. Our study revealed that fuzzy-based control systems have evolved from simple type-1 fuzzy controllers to advanced control systems (type-2 fuzzy and hybrid) capable of effectively addressing complex power quality issues. We believe that the insights gained from this study will be useful to both experienced and inexperienced researchers and industry engineers seeking to leverage fuzzy logic to enhance power quality control.

Keywords: fuzzy control system; fuzzy logic controller; intelligent control systems; power quality; reactive power; harmonics; voltage variations; frequency control; control device; power systems



Citation: Miron, A.; Cziker, A.C.; Beleiu, H.G. Fuzzy Control Systems for Power Quality Improvement—A Systematic Review Exploring Their Efficacy and Efficiency. *Appl. Sci.* **2024**, *14*, 4468. <https://doi.org/10.3390/app14114468>

Received: 13 April 2024

Revised: 20 May 2024

Accepted: 21 May 2024

Published: 23 May 2024



Copyright: © 2024 by the authors. Licensee MDPI, Basel, Switzerland. This article is an open access article distributed under the terms and conditions of the Creative Commons Attribution (CC BY) license (<https://creativecommons.org/licenses/by/4.0/>).

1. Introduction

More than six decades have passed since the introduction of the fuzzy sets by Lotfi A. Zadeh [1]. It has also been 50 years since M. Mamdani [2] proposed fuzzy control based on Zadeh's papers [3,4]. The first fuzzy logic controller (FLC) appeared in [5], where the authors presented a laboratory application used to control a steam engine. These articles had a significant impact on fuzzy control research, leading to thousands of control systems based on fuzzy logic being proposed in the literature since the original FLC 49 years ago [6].

In the field of power systems, and particularly power quality (PQ) [7], one of the primary fuzzy logic applications used to control reactive power was produced in 1990. Later, more researchers presented FLCs in the literature dedicated to controlling PQ using filters and specialized devices [8–10]. Table 1 shows a historical sequence of 17 FLCs proposed for PQ improvement in the literature [11–30]. A review of the works published in the 1990s reveals that FLC research was initially focused on reactive power compensation, power factor rise, and voltage and frequency regulation, i.e., power system stability [31]. Basic information on the structure of fuzzy control systems (FCSs) in power systems was also provided during this period [32]. In the later years of the decade, new prospects of fuzzy logic were considered for power quality control, such as the use of UPQCs (Unified Power Quality Conditioners). In the next decade, many researchers proposed FLCs to control other PQ issues, including harmonic distortion and voltage sags. Additionally, the effectiveness of fuzzy logic control combined with other artificial intelligence techniques

like genetic algorithms was demonstrated in several studies [33,34]. In the last 15 years, there have been many papers focused on PQ improvement considering UPQCs, distributed generation, and other AI technologies in combination with fuzzy logic control.

Table 1. History of fuzzy logic applications dedicated to power quality control.

Year	Published Works
1991	The authors of [11] introduce frequency control in power systems using an FLC with two inputs and an output.
1993	The authors of [12] propose an FLC for reactive power compensation using automatically switched capacitor banks employing TCR/TSC ¹ .
1994	Hiyama and his colleagues propose a PID ² fuzzy stabilizer for voltage control [13].
1998	The control of a UPQC with fuzzy logic control was achieved in the research presented in [14].
2004	Jurado and Valverde demonstrate that voltage sags can be effectively eliminated by using a dynamic voltage restorer controlled by an FLC [15]. Kirawanich determines that harmonic distortion and power factor issues are improved using an FLC that commands a line conditioner [16].
2006	The authors of [17] present a Takagi–Sugeno FLC dedicated to operating an active power filter to eliminate harmonics.
2008	Using simulations made in MATLAB, the authors of [18] demonstrate the efficacy of a fuzzy hysteresis controller in controlling a UPQC.
2011	The authors of [19] consider balanced and unbalanced conditions when analyzing the performance of a shunt active filter controlled by an FLC.
2014	To improve the operation of the control system, the authors of [20] employ a type-2 FLC that controls an active power filter.
2015	A hybrid FCS that combines artificial neural networks and Takagi–Sugeno–Kang probabilistic fuzzy control performs reactive power compensation with superior results compared to conventional techniques [21].
2018	Ghafouri and his colleagues propose an adaptive fuzzy controller to stabilize power system frequency in consideration of microgrids and other distributed generation units [22].
2019	The authors of [23] propose a fuel-cell-integrated UPQC controlled by a hybrid fuzzy system to compensate PQ problems. The frequency control of modern multi-area power systems is solved with fuzzy logic in [24].
2020	The authors of [25] control a 24-pulse GTO-based STATCOM ⁴ using fuzzy logic. Echalih and his colleagues describe the use of hybrid fuzzy control to command a shunt active filter [26].
2021	Vanaja and his colleagues are researching the use of an FLC-controlled STATCOM in association with an enhanced second-order generalized integrator [27]. The voltage dynamic problem is solved using fuzzy logic considering the Malaysian power system [28].
2022	The authors of [29] propose the use of fuzzy fault-tolerant control and four-switch voltage source inverters to increase the stability of power systems.
2023	The authors of [30] present the use of ANFIS ³ to improve power quality in a microgrid.

¹ TCR/TSC—thyristor-controlled reactor/thyristor-switched capacitor, ² PID—proportional–integral–derivative, ³ ANFIS—adaptive neuro-fuzzy inference system, ⁴ STATCOM—static synchronous compensator.

Fuzzy control systems are an important component of intelligent control systems. The most significant advantage of fuzzy logic that attracts power systems specialists is its ability to handle imprecise, incomplete, and vague data, as it broadens the set theory so that a set's element belongs to it based on a membership function value, as an alternative to conventional binary methods. Therefore, FCSs provide a way to deal with uncertainties through linguistic values and logical inferential rules, allowing specialists to perform dynamic modeling and controller descriptions using simple linguistic statements [35]. FLCs have been criticized due to the absence of a systematic design and a stability analysis method, plus the financial aspects regarding the replacement of traditional PID controllers [36]. Then again, in many cases, they are the first option when working with non-linear, time-delayed,

and high-order systems [37], and are overtly acknowledged as superior replacements for their PID counterparts [8].

Modern power systems are complex and often experience uncertainty due to the diverse range of electricity consumers and prosumers they serve, as well as the presence of distributed generation units and interconnected microgrids. The integration of different generation units that rely on renewable resources such as solar energy and wind can lead to PQ issues, including voltage sags, voltage swells, voltage transients, harmonics, voltage oscillations, unbalance, and low-power factors [38]. In addition, devices and equipment with nonlinear characteristics, as well as unbalanced and varying loads, can cause non-sinusoidal and unbalanced currents and voltages, voltage fluctuations, and flicker in utility electricity networks and consumer installations [39,40].

PQ disturbances in power systems can cause a range of problems, including supplementary power losses, premature aging of components, low-power factors, equipment malfunction, and even total failure [41–43]. To help prevent these issues, international standards have been developed by organizations such as the European Norms, American National Standard Institute, IEC, and IEEE. These standards provide guidelines for power-generating companies, consumers, manufacturers, and national power system organizations on the acceptable limits of PQ disturbances. Table 2 shows the limits of PQ disturbances according to IEC 61000, EN 50160, and IEEE 519-2022 [44,45]. The thresholds of the PQ indices are the reference magnitudes against which the adjustment of voltages and currents are made.

Table 2. Power quality limits.

Issue	Index	Limits		Standard/Observations
		LV	MV	
Frequency variation	$\Delta f\%$ ¹	±1%		EN 50160
Voltage sag	$\Delta u_s\%$ ²	10–95% of fundamental		IEC 61000-4-11/ 0.5 cycle—several seconds
Harmonics	THD ³	8%	5%	IEC 61000-4-7, IEEE 519 2022
Unbalance	VUF ⁴	2% (3%)	1%	IEC 61000-2-5/ IEC 61000-2-12
Voltage transients	$\Delta V\%$ ⁵	5%	3%	IEC 61000
Voltage fluctuations/Flicker	P_{st} ⁶ P_{lt} ⁷		1 0.65	IEC/EN61000-3-3
Reactive power/Power factor (PF)	PF	0.9		
Voltage interruptions	$\Delta u_i\%$ ⁸	more than 95% of fundamental		IEC 61000-4-11/ 10 ms–60 s

¹ Frequency deviation (error); ² voltage deviation; ³ total harmonic distortion factor; ⁴ voltage unbalance factor; ⁵ voltage deviation; ⁶ short-term flicker perceptibility; ⁷ long-term flicker perceptibility; ⁸ voltage deviation.

After analyzing the information provided above, it is important to understand the significance of utilizing appropriate control systems, such as FCSs, to improve power quality. To achieve an effective and efficient controller, one must have a sound knowledge of the structure and limitations of FCSs, as well as explore their possibilities. Although FCSs have been studied and analyzed in various engineering fields, such as refrigeration, and hydraulic and pneumatic systems [46–49], only a few authors have focused exclusively and intensively on PQ improvement in power systems in recent years. These studies emphasize the usefulness of fuzzy logic and explore different aspects of control systems and power systems. In the field of microgrids, a study [50] was conducted to examine the effectiveness of fuzzy control. The study concludes that a simple FLC with only one input can provide comparable results to a traditional PI (proportional–integral) controller, but it is easier to adjust. Another study [10] classified the different types of UPQCs, along with their corresponding control strategies, to eliminate or reduce PQ issues. The authors of this study mention that fuzzy logic controllers in association with other artificial intelligence

techniques have the capability to improve PQ. Similarly, in a review [51], voltage variation compensators are examined, and the authors conclude that employing fuzzy logic in the control of these compensators can improve PQ. Devices such as active power filters are also reviewed in [10,52,53], and different control methods are discussed. One significant conclusion from these studies is that a PI controller in association with fuzzy logic provides better results than a conventional PI controller in PQ improvement.

Upon reviewing the available literature, it is evident that there are still unanswered questions regarding the use of fuzzy control for improving power quality. These questions can only be addressed by systematically analyzing the literature. Thus, the main objective of this work is to provide a comprehensive review of the applications of fuzzy logic control in power quality issues, with a focus on FCSs' effectiveness and efficiency. The review covers information on fuzzy-based control systems, input and output values, fuzzy numbers, inference rules, decisions, and defuzzification methods, as well as the implementation of fuzzy logic. The work focuses on control systems that contain fuzzy logic controllers in their simple (type-1 fuzzy) and advanced (type-2 fuzzy) forms, or in association with other conventional techniques, such as PI or hysteresis control, and novel techniques like genetic algorithm optimization. In the research, ANFIS was not considered; only control strategies that maintain the classic structure and logic-based functioning of an FLC were considered.

The Section 2 of the work details the methodology employed to obtain the articles used in the review and the criteria to assess the literature. The Section 3 presents the results of the research concerning bibliometric aspects and the seven criteria (technical characteristics): control system, FLC features, FLC inference strategy, PQ issue, control device, implementation, and assessing efficiency. This section also enlists the most relevant research. The next section of the work discusses the findings and the future work that can be completed in this area. Special attention is given to different types of PQ issues and the types of control systems used to solve them. The last section concludes with the main results of the review and underlines future directions of the present work.

2. Methodology

This literature review presents an organized analysis of relevant international studies on the topics of power quality improvement, fuzzy logic control, and devices for PQ control. To initiate the study, a comprehensive search was conducted for surveys, reviews, and state-of-the-art reviews that focused on the aforementioned subjects. These works were subsequently used as the foundation for the research and selection process of the review's portfolio. Following the trends of literature reviews [10,54], a thorough examination of diverse databases was executed to obtain information on the content of the papers to make up the final set of papers. The Web of Science database was the primary source scrutinized to obtain the list of papers, considering the data found in the titles, keywords, and abstracts of papers. Only the research areas of "Engineering", "Automation Control Systems", "Mathematics", and "Computer Science" were considered. The resulting unfiltered list was then meticulously evaluated, and papers that did not conform to the research scope were eliminated. This action led to the initial set of papers. The primary search keywords for the papers were as follows:

"power quality" OR "harmonics" OR "frequency" OR "voltage sag" OR "unbalance"
OR "reactive power" OR "voltage variation" OR "power factor" OR "flicker"

AND

"fuzzy control" OR "fuzzy logic control" OR "fuzzy controller" OR "fuzzy logic controller" OR "FLC".

Secondarily, the papers' main sources were accessed, among which were IEEE Xplore, MDPI journals, Taylor & Francis journals, Elsevier journals, and Wiley journals. Further, the papers were again selected based on a more detailed content analysis. It must be emphasized that the selected papers that went in the final set and additionally were further analyzed and listed as references were the ones that respected the review's eligibility criteria, i.e., presentation of the efficacy and effectiveness of the fuzzy logic control systems

in the process of power quality improvement. Because of this, more than half of the initial list of papers were ignored in the next stage of the study.

To provide a timeframe for the study, the research focused on studies published in the last 30 years, with particular emphasis on papers from the last 15 years. However, eligible works were included in the final set regardless of publishing year. The articles were classified based on the criteria outlined in Table 3. Additionally, taking into account the methodology from reference [10], the table includes detailed information about the criteria and their characteristics.

Table 3. Assessment criteria of the article set—overview of the criteria used to classify and assess the articles in the final set.

Analysis Criteria	Details	Examples
Control system	Control systems may include not only a typical FLC, but also other elements from conventional methods or other AI techniques.	Typical FLC (Type-1 fuzzy) Fuzzy-PI Hysteresis fuzzy control Fuzzy-PID logic controller
FLC's features	The number of inputs and outputs of the controller, the number of linguistic variables, the types of fuzzy membership functions, and defuzzification methods.	Triangular, trapezoidal, and gaussian fuzzy numbers Center of gravity defuzzification method
FLC's inference strategy	The inference strategy refers to the way the output is obtained. It is implemented in the FLC to realize the aggregation of the rules and combine them.	Mamdani Takagi-Sugeno
PQ issue	The type of disturbance affecting the power quality in power systems [38].	Frequency variation Voltage variation, harmonics, unbalance
Control device	Devices used for PQ improvement depend on the type of PQ issue and its location in the power system [39].	SVC UPQC DVR STATCOM
Implementation (efficacy proof)	The control systems were implemented and tested using simulations, that is, employing appropriate environments like MATLAB and DlgSILENT, or experimental laboratory or infield tests.	Simulations Laboratory or on-site hardware implementation
Assessing efficiency and improvements	Was the control system assessed for improvement and/or was the fuzzy controller tested considering different fuzzy numbers, inferences, and/or defuzzification methods?	Yes/No Yes—testing diverse features of FLCs or enriching FLCs with additional elements

3. Results

3.1. Bibliometric Analysis

The set of papers considered in this review includes publications from journals and conference proceedings. The results of the paper selection process from the Web of Science were as follows:

- Initial unfiltered set of papers—460 papers. This set contains the raw list of papers used in the review.
- Initial set of papers—278 papers. The initial set is a list of papers that correspond to the subject of power quality improvement using fuzzy control.
- Intermediary set of papers—122 papers. These articles were the most relevant of the initial set of papers that were published in the last 15 years (2009–2023).
- Final set of papers—135 papers. The final set of papers that was considered included the previous ones plus 13 more papers available before 2009. Going forward, all recommendations and observations we make are regarding this final set of papers.

The first noticeable applications of fuzzy control in PQ were in the 1990s. An assessment of the publications from the 1990s and 2000s showed that, yearly, less than ten articles were published in the research area of interest. Later, the number of articles grew substantially, with a maximum of 43 in 2016.

When focusing on the most relevant journal, *IEEE Access* was the most prolific, with 13 publications, followed by *Electric Power Systems Research*, *IEEE Industrial Electronics Society*, and *IET Generation, Transmission & Distribution*, with more than 8 articles each. Regarding conference proceedings, relevant papers from the initial set were distributed among many of them, but the majority were found in the proceedings published before 2020.

The most cited paper found through the selection was “Load Frequency Control of a Multi-Area Power System: An Adaptive Fuzzy Logic Approach” [55], with 207 citations in the Web of Science. The paper introduces fuzzy logic for the adaptive (type-2 FLC) control of load frequency and demonstrates through simulations that the proposed control system is more efficient than a PID system and a simple type-2 fuzzy controller.

3.2. Technical Analysis

The technical analysis aimed to evaluate the articles based on the seven specific criteria. To achieve this, a separate subsection is dedicated to each criterion. These subsections provide statistical results regarding the corresponding criterion’s characteristics and list the papers significant to each criterion.

3.2.1. Control System

Control systems based on fuzzy logic have a structure that may include not only the body of a typical FLC, but also other elements borrowed from conventional control (PI, PID, and hysteresis) or other AI techniques, such as neuronal networks and evolutive algorithms. The types of control systems that have extra elements are hybrid fuzzy controllers, which in the literature we can find as fuzzy-PI, fuzzy-PID, hysteresis fuzzy, self-tuning fuzzy, adaptive fuzzy, and neuro-fuzzy controllers.

The structure of a typical FLC (type-1 fuzzy) consists of three blocks: fuzzification, inference, and defuzzification blocks, as shown in [12]. The structure of a fuzzy-based hybrid system additionally contains blocks such as P, I, and D blocks [9], hysteresis-band blocks [18], and second-order generalized integrators [27]. A type-2 fuzzy controller has the same structure as a type-1 fuzzy controller, plus a type-reduction block positioned before the defuzzification component [55]. To increase the performance of the control process, authors use evolutionary algorithms such as genetic algorithms [33,34] and machine learning algorithms like artificial neuronal networks, which lead to ANFIS [30].

In the review and research process, we considered papers that proposed typical and hybrid fuzzy-based control systems that maintained the general structure of a fuzzy logic controller. As a result, this work does not include detailed information about adaptive neuro-fuzzy inference systems or other similar control systems. Consequently, we excluded more than 18% of the total number of papers from our initial filtered set of 278 papers due to the type of control system. The number of excluded papers was 53, with 26 of them being published within the last five years, of which [56–65] are the most significant.

The complete list of types of fuzzy-based control systems and their numbers is displayed in Figure 1. We ought to mention that we added genetic algorithm fuzzy control systems to the final list because the additional components do not change the structure of the fuzzy controller, and they are used to increase the efficiency of control systems. The chart indicates that the most popular type of control system is based on a type-1 fuzzy controller, with 49 papers proposing it. The other types of control systems are fuzzy adaptive with 19 papers, and fuzzy-PI with 17 papers. A time–distribution analysis of these control systems’ appearance shows that they have been proposed mostly in the last 15 years. The types of control systems characterized by small numbers of published papers were mainly proposed in the last five years.

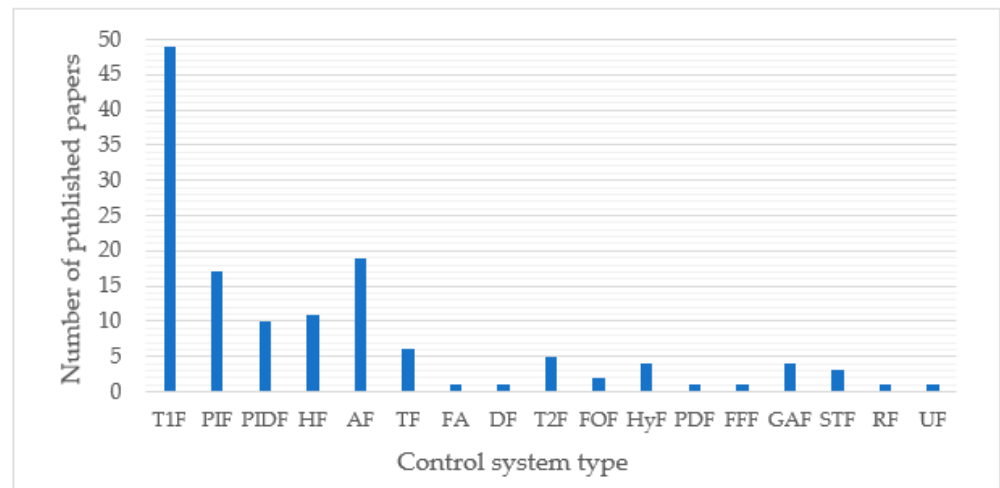


Figure 1. The numbers of published articles based on control system type. T1F—type-1 fuzzy; FPI—fuzzy-PI; FPID—fuzzy-PID; HF—hysteresis fuzzy; AF—adaptive fuzzy; TF—tuned fuzzy; FA—fuzzy-active; DF—decupled fuzzy; type-2 fuzzy; FOF—fractional-order fuzzy; HyF—hybrid fuzzy; FPD—fuzzy-PD; FFF—feed-forward fuzzy; EAF—evolutionary algorithm fuzzy; STF—self-tuned fuzzy; RF—recursive fuzzy; UF—unified fuzzy.

Table 4 enumerates 10 relevant papers which contain detailed information about the type and structure of the proposed control systems. The table presents the control systems’ type and description, plus data about the control systems’ efficacy testing and efficiency demonstrations. The articles from the table relate to the first 11 types of control system proposed in the literature: type-1 fuzzy, fuzzy-PI, fuzzy-PID, hysteresis fuzzy, adaptive fuzzy, tuned, type-2 fuzzy, evolutive algorithm fuzzy, fractional-order fuzzy, hybrid fuzzy, and self-tuned fuzzy controllers.

Table 4. Relevant papers considering the type of fuzzy-based control system.

Reference	Control System	Description	Efficacy	Efficiency
[66]	<i>Type-1 fuzzy</i>	Supercapacitors are proposed and controlled to reduce THD and regulate reactive power for wind farms	Tested through simulations	Comparison between the system with and without supercapacitors
[67]	<i>Fuzzy-PI</i>	Multi-feeder UPQC fuzzy controlled to reduce voltage and current imperfections	Software implementation for efficacy evaluation	Results compared with classical PI and type-1 fuzzy controller
[68]	<i>Fuzzy-PID</i>	Frequency and power control in insulated distribution generation units, considering also superconducting magnetic energy storage	Efficacy assessment through software implementation	Results compared with only PID and PID plus superconducting magnetic energy storage
[69]	<i>Hysteresis fuzzy</i>	Hysteresis controller bands adapted by a fuzzy controller for harmonics elimination	Demonstrated through simulations	The proposed method compared hysteresis with fixed bands with zero fixed-band controllers
[70]	<i>Adaptive fuzzy</i>	Inverters controlled for power factor tracking changes and power fluctuation decrease	Software implementation for efficacy evaluation	The proposed controller contrasted with conventional PI and Takagi–Sugeno probabilistic fuzzy controller
[71]	<i>Type-2 fuzzy</i>	Load frequency control and frequency stability considering the high penetration of distributed generation	Tested through simulations	Comparison with PI and type-1 fuzzy controller

Table 4. Cont.

Reference	Control System	Description	Efficacy	Efficiency
[72]	<i>Self-tuned fuzzy-PI</i>	Mitigation of voltage sags, voltage, and THD by using a dynamic voltage restorer and two FLCs	Efficacy assessment using simulations	Comparison between the system with and without dynamic voltage restorer
[73]	<i>Fuzzy fractional-order PI</i>	Single-phase active power filter controlled to increase power factor and limit harmonics	Simulations and experimental testing of the efficacy	Proposed methodology with the controller without fuzzy usage
[74]	<i>EV-fuzzy-PID</i>	Voltage and frequency control with automatic voltage regulator and particle swarm optimization	Software implementation for efficacy evaluation	Results show the comparison of the proposed method with another hybrid method from the literature
[75]	<i>Tuned fuzzy-PID</i>	Frequency regulation employing static synchronous series compensator (SSSC) and teaching learning optimization technique	Efficacy assessment through software implementation	The proposed method compared with the control without SSSC and with the genetic algorithm

3.2.2. Fuzzy Logic Controller Features

During the development of an FLC, researchers must consider several critical aspects: the inputs and outputs, the number of linguistic variables, the type of fuzzy numbers used in the fuzzification block, and the defuzzification method. Additionally, the FLC's rule aggregation strategy, or inference strategy, is a vital consideration. Analyzing the papers from the final set, we found the following about the features of the proposed fuzzy controllers by the researchers:

1. Number of inputs and outputs: The most used configuration is two inputs and one output, with a percentage of more than 75%, of which [76–87] are typical examples. This aspect is seen clearly in Figure 2, where other configurations that appear in more than one article are one input–one output [88], two inputs–three outputs, two inputs–two outputs, and four inputs–two outputs.
2. Number of linguistic variables: The most popular number of linguistic variables used in the fuzzification stage for the inputs and outputs was seven [78,79,82,88], followed by five and three [76,80,83]. Considering the differences between the inputs and outputs, the proposed FLCs had the same number of linguistic variables for both inputs and outputs [76], but there were also FLCs characterized by different numbers of linguistic variables [83,87]. This aspect can be seen in Table 5. Thus, we introduced both numbers of variables in the assessment. The chart from Figure 3 illustrates the number of linguistic variables.
3. Type of fuzzy numbers (membership functions): The authors extensively used a combination of trapezoidal and triangular membership functions [78,81,83,88], as shown in Figure 4. Close behind are the utilization of the triangular function, the Gauss function [79], and singletons [76]. Other functions used in the fuzzification stage, but rarely, are the bell-shaped, trapeze, and sigmoid functions. Like the number of linguistic variables, we found FLCs that use the same type of function to describe the memberships of the inputs and outputs [86], but also FLCs with different membership functions for the input and output quantities [87].
4. Defuzzification method: The center of gravity [78,81,86] is the defuzzification method normally used to obtain crisp outputs, with a percentage of 41 (55 papers). The other defuzzification methods are bisector, weighed average [76,77], and singleton, which together appear in 28 articles (20%). Unfortunately, the rest of the 51 papers did not contain clear information about the defuzzification method, even though there were data about other features of the FLC that implied the use of certain defuzzification methods. For example, when using the Mamdani style of inference from MATLAB's Fuzzy Logic Toolbox, the predefined defuzzification method is the centroid—the center of gravity—or, when using the Takagi–Sugeno style of inference, the authors can define corresponding functions to determine the crisp outputs.

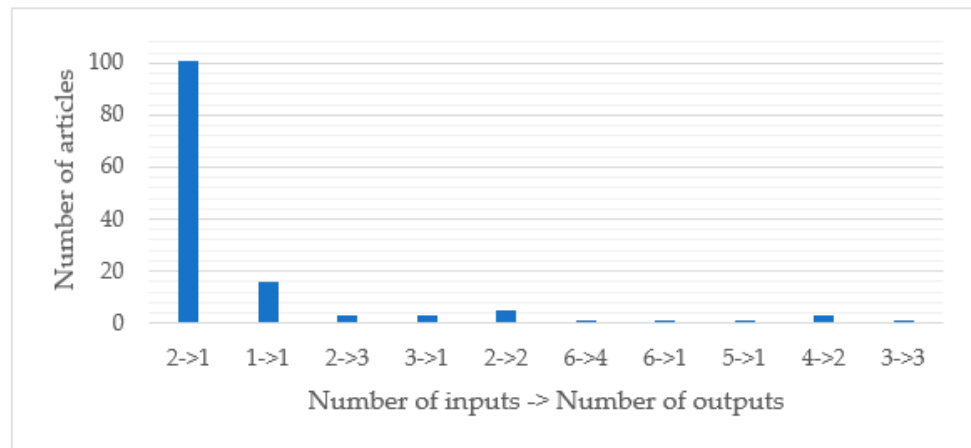


Figure 2. Article distribution regarding the number of inputs and number of outputs of the fuzzy controllers.

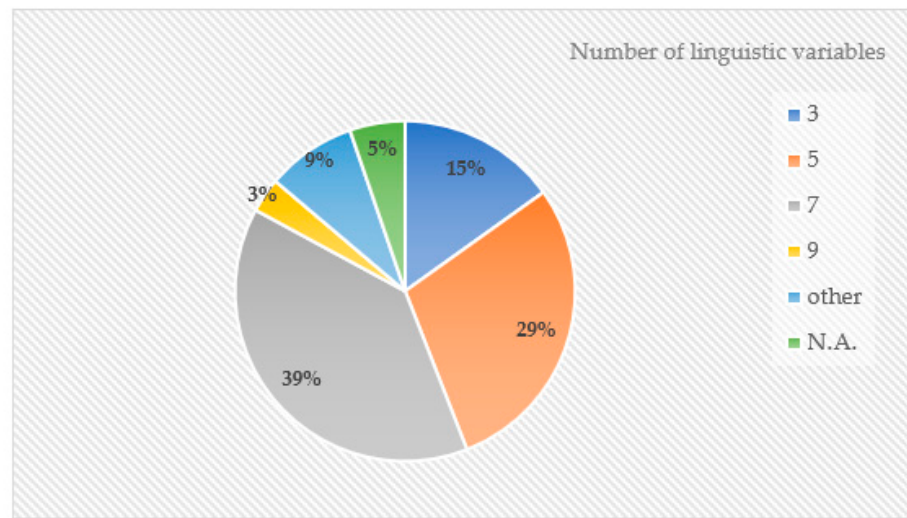


Figure 3. Article distribution regarding the number of linguistic variables of the fuzzy controllers.

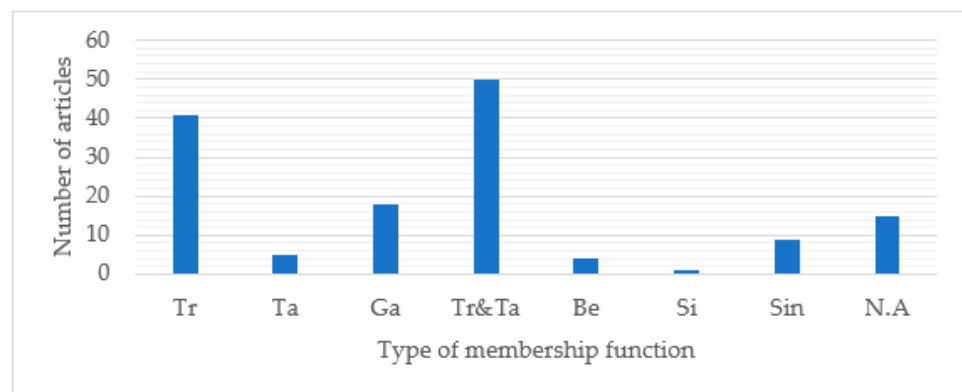


Figure 4. Article distribution regarding the type of membership function. Tr—triangle; Ta—trapeze; Ga—Gauss; Tr&Ta—triangle and trapeze; Be—bell; Si—sigmoid; Sin—singleton.

Table 5. Relevant papers considering the features of fuzzy logic controllers.

Reference	Inputs and Outputs	Number of Linguistic Variables	Fuzzy Numbers	Defuzzification Method	Efficacy	Efficiency
[76]	2->1	5	Triangle singleton	Weighted average	Processor-in-the-loop technique and simulations	Comparison with a simple repetitive controller
[77]	2->1	5 7	Triangle and trapeze triangle	Weighted average	Simulations	Demonstrated by relation with conventional droop control
[79]	2->1	7	Gaussian	Weighted average	Simulations	Comparison with PI controller
[88]	1->1	7	Triangle and trapeze	Centroid	Simulations	Comparison with a hysteresis controller with fixed bands
[80]	2->1	3 5 7	Gaussian triangle and trapeze	Centroid	Simulations	Results comparison without the control system
[74]	2->3	4 3	Triangle singleton	Weighted average	Simulations	Proposed method compared with other methods from the literature
[89]	2->2	3 5	Singleton triangle and trapeze	Weighted average	Simulations and hardware implementation	No additional methodology is tested, only the proposed method considering diverse situations
[75]	2->3	5	Triangle and trapeze	Centroid	Simulations and hardware testing	The proposed method compared with the control without SSSC and with the genetic algorithm
[85]	2->1	3 5	Triangle singleton	Weighted average	Experimental setup and simulations	Proposed adaptive fuzzy with type-1 fuzzy
[87]	2->1	3 5	Triangle gaussian	Centroid	Simulations	Results comparison without the control system

Table 5 presents 10 articles that contain whole data about all features of the proposed FLC. The table's header is divided into the four FLC features, the reference number, and the fuzzy-based control systems' efficacy testing and efficiency demonstrations.

3.2.3. Fuzzy Logic Controller's Inference Strategy

There are three main types of fuzzy control system inference strategy that are classified by the way the logical rules between the inputs and outputs are built: Mamdani, Takagi–Sugeno, and the singleton strategy [6,90].

Evaluating the final set of papers to determine the utilized inference strategy, we found that the most employed inference strategy used by the inference engine was Mamdani's. Figure 5 shows this aspect, as 41% of the authors of the analyzed articles mention the use of Mamdani's inference strategy [91]. The next most used was Takagi–Sugeno [92], followed by the Mamdani's "Min-Max" method [93] (declared by the authors, as 18 mentioned Mamdani's "Min-Max" method, or simply the "Min-Max" method). The other strategy is the singleton methodology. Unfortunately, more than 27% of the papers did not contain clear information about the inference strategy. Consequently, we did not consider these studies further when selecting the most relevant papers, which are listed in Table 6.

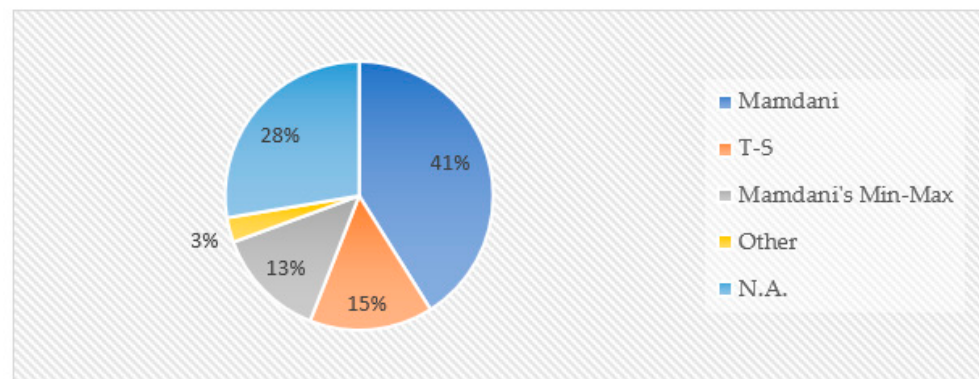


Figure 5. Article distribution regarding inference strategy. T-S—Takagi–Sugeno.

Table 6. Relevant papers considering the inference strategy of the FLCs.

Reference	Inference Strategy	Efficacy	Efficiency
[90]	<i>Takagi–Sugeno</i>	Simulations	Proposed method results are compared to results obtained with a PI controller or without a PQ improvement apparatus
[91]	<i>Mamdani</i>	Simulations and experimental tests	Comparison with a PI controller
[92]	<i>Takagi–Sugeno</i>	Simulations	Comparison with a conventional PI controller
[94]	<i>Mamdani</i>	Simulations	Comparison between different versions of the proposed fuzzy-based on-load tap changer control (OLTC) and a classic OLTC
[95]	<i>Product inference Singleton</i>	Simulations	Comparison with a PI controller
[96]	<i>Explained but not classified</i>	Simulations and experimental tests	Simulation results of the proposed method compared with results associated with a PI controller
[89]	<i>Takagi–Sugeno</i>	Simulations and experimental tests	No additional methodology is tested, only the proposed method considering diverse situations
[97]	<i>Mamdani</i>	Simulations	Comparison with a PID controller
[98]	<i>Takagi–Sugeno</i>	Simulations	Proposed adaptive fuzzy compared with conventional fuzzy controller
[99]	<i>Min inference</i>	Simulations	Results comparison without the control system

Table 6 introduces 10 significant articles that clearly describe their inference strategies; thus, it is easy for the readers to understand these aspects of fuzzy control. The table below gives data about the references, the inference style, the proposed method's efficacy, and the efficiency assessment. One can observe that five papers from the table used Takagi–Sugeno fuzzy strategies, but this aspect does not follow the data from the chart in Figure 5. We made this choice as the authors of these articles gave greater descriptions of their methodologies.

3.2.4. Power Quality Issues

The power quality issues described in the analyzed papers were very varied, from frequency variations to high-voltage THD, from voltage sags/swells to low-power factors. Considering the number of PQ issues considered, 88 studies focused on one problem,

whereas the other 46 were on multiple issues. Figure 6 illustrates these aspects, as one can see that the first seven categories describe only one disturbance, e.g., voltage sag/swell or harmonics/THD, and the last eight categories describe multiple disturbances, such as frequency variations, harmonics/THD, and reactive power (stability power systems).

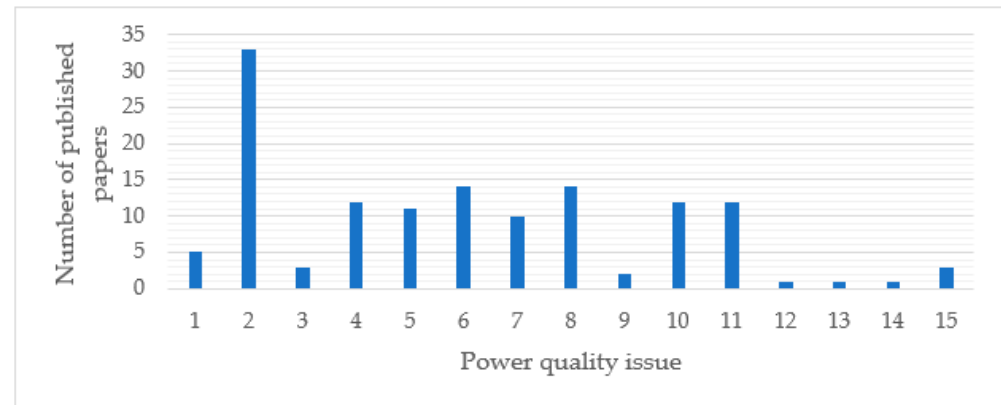


Figure 6. Article distribution considering the approached PQ issue. 1—voltage sag/swell; 2—harmonics/THD; 3—voltage unbalance; 4—frequency variations; 5—low-power factor, reactive power; 6—voltage variation; 7—load frequency control; 8—frequency, harmonics/THD, and reactive power; 9—harmonics/THD and voltage sags; 10—harmonics/THD and reactive power; 11—frequency, voltage variations, harmonics/THD and reactive power; 12—voltage sag and flicker; 13—frequency variations and flicker; 14—reactive power and flicker; 15—voltage unbalance and flicker.

Assessing the data from the chart in Figure 6, we deduced that diminishing harmonic distortions and decreasing THD was the goal of almost a quarter of the studies that used fuzzy logic control, i.e., 33 papers. Furthermore, the number of studies that focused only on one disturbance represented more than 65% of the total of 134 analyzed papers. The next most studied PQ issues were voltage variations (category 6) and the combination of frequency variations, harmonics/THD, and reactive power (category 8), which influence the stability of power systems. Closely behind, 12 studies focused on the power system's frequency control and the combinations of harmonics with reactive power, frequency variations, voltage variations, harmonics/THD, and reactive power.

Table 7 lists 10 papers that are relevant to the categories mentioned in Figure 6. The table provides information about the PQ issues addressed in each paper, a brief summary of the proposed method, and the results of the efficacy and efficiency testing of the fuzzy-based control systems.

Table 7. Relevant papers considering power quality issues.

Reference	Power Quality Issues	Description	Efficacy	Efficiency
[100]	<i>Voltage (sag/swell, imbalance), frequency, real/reactive power, and harmonics</i>	The inverter is controlled using the fuzzy space vector pulse-width modulation (FSV-PWM) technique	Simulations	The proposed method compared with the conventional ST-PWM control
[101]	<i>Harmonics reduction</i>	Seven-level modular multilevel converter (SLMMC)-based shunt active filter controlled by type-1 fuzzy	Simulations	The proposed method's results compared with PI—SLMMC control and without filter

Table 7. Cont.

Reference	Power Quality Issues	Description	Efficacy	Efficiency
[102]	<i>Load frequency control (LFC)</i>	Hybrid fuzzy control for inner loop control and genetic algorithm to optimize the control parameters	Simulations	The proposed method compared with an improved PI and adaptive fuzzy controller
[103]	<i>Voltage sag and flicker</i>	Superconducting magnetic energy storage (SMES) with hysteresis fuzzy controller	Simulations	Results comparison without the control system
[104]	<i>Voltage sag, harmonics, sudden load change</i>	Power electronic distribution transformers and adaptive PI fuzzy controller	Simulations	Comparison with a PI controller
[105]	<i>Voltage control and reactive power</i>	Capacitor banks and on-load tap changer in substations controlled by dynamic programming and type-1 fuzzy	Simulations	The proposed method's results compared with results obtained only using dynamic programming
[106]	<i>Harmonics and reactive power</i>	Three-level shunt active power filter (APF) controlled by type-1 fuzzy	Simulations	Comparison with a PI and digital RST controller
[107]	<i>Harmonics</i>	Takagi–Sugeno fuzzy controller and shunt active power filter	Simulations and laboratory testing	Results comparison without the control system
[108]	<i>LFC</i>	Indirect adaptive fuzzy control for multi-area power system	Simulations	Comparison with a PID controller
[109]	<i>Harmonics and reactive power under unbalance</i>	Type-1 fuzzy controller used to optimize the energy storage of a DC capacitor voltage of a three-phase shunt active power filter	Simulations	Results comparison without the control system and APF

3.2.5. Control Devices

Power quality control devices are introduced to eliminate and/or diminish the disturbances that negatively affect the quality of electrical energy. These devices are classified depending on their operation, physical structure, applications, and when they were first pioneered. The devices were comprehensively synthesized in the review articles [10,68,69]. In this review, we divided the control devices by their applications. Subsequently, the complete list of these devices that we found in the analyzed set of papers is summarized in Figure 7: APF (active power filter—47 papers), STATCOM, UPFC (Unified Power Flow Controller), UPQC (Unified Power Quality Conditioner), FACTS (Flexible Alternating Current Transmission System), SVC (Static Var Compensator), DVR (dynamic voltage restorer). In addition to this list, as shown in Figure 7, there is the “Controller” category, which includes the applications where the researchers combine diverse components of the power system, i.e., converters, generators, storage systems, transformers, power line conditioners, and capacitor banks, with the fuzzy-based controller to improve power quality issues. Of these devices, the most popular are the converters, with 25 appearances, followed by storage systems in 10 papers.

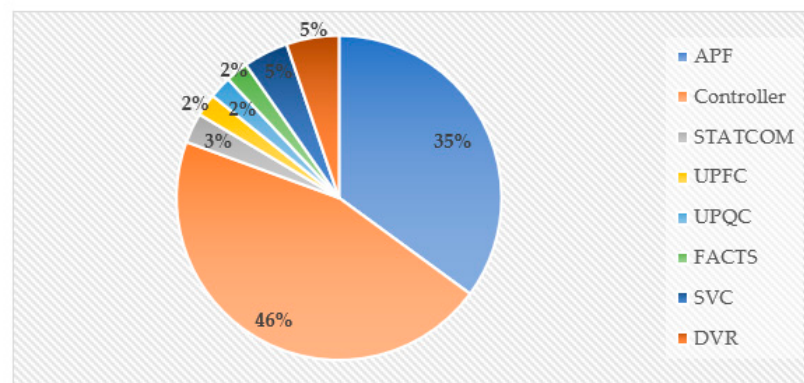


Figure 7. Article distribution considering control devices.

Table 8 is a collection of data that show information on 10 important articles. These articles used various control devices to improve the quality of power and employed FCSs. The table provides details about the characteristics of each study presented in the selected papers, which are from each category of the chart in Figure 7. Moreover, the table also gives information about the efficacy testing and efficiency demonstration of the proposed control methodology.

Table 8. Relevant papers concerning control devices.

Reference	Control Device	Description	Efficacy	Efficiency
[110]	<i>Controller (asynchronous motor)</i>	Type-1 fuzzy control asynchronous motor to increase power factor and regulate voltage	Simulations	Results comparison without the control system
[111]	<i>APF</i>	Hybrid automata–fuzzy control for THD and power factor decrease	Simulations	Comparison with a simple PI
[112]	<i>STATCOM</i>	Rise of STATCOM efficiency through sub-synchronous resonance using type-1 fuzzy	Simulations	Results comparison without the fuzzy control of STATCOM and active disturbance rejection control
[113]	<i>UPQC</i>	Mamdani and Takagi–Sugeno fuzzy controllers and phase-locked loop (PLL) control Harmonics, unbalance, and voltage variations	Laboratory experimental setup, hardware in loop real-time system	Comparison with conventional modified PLL and TS-PLL control strategy
[114]	<i>DVR</i>	Self-tuned type-2 fuzzy PI controller for voltage sag and THD alleviation	Simulations	Comparison with a type-1 fuzzy PI controller
[115]	<i>UPFC</i>	Type-1 fuzzy controls with active and reactive power variations	Simulations	Results comparison without the fuzzy control of UPFC and PID control
[116]	<i>Controller (inverter)</i>	Fuzzy supervisory with fuzzy PID control for voltage and current THD reduction	Simulations	Comparison with classic supervisory PID and classic supervisory FPID
[117]	<i>Controller (inverter)</i>	Direct power control (DPC) based on type-1 fuzzy and fuzzy PI for THD diminishing	Simulations and laboratory experiments	Results comparison with the basic DPC
[118]	<i>APF</i>	Review about the control strategies of series APF for decreasing THD, fuzzy hysteresis method	Simulations	Comparison with a simple fixed-band hysteresis, adaptive hysteresis band, and fixed hysteresis band
[16]	<i>Power line conditioner (PLC)</i>	Line current harmonic distortions and power factor Fuzzy PI controller	Software and hardware implementation	Comparison with a simple PI and a gained scheduled controller

3.2.6. Implementation (Efficacy Proof)

To verify the functionality of the control systems proposed in their papers, the researchers employed two strategies. The first strategy is based on simulations and implies the use of a dedicated simulation environment to model the controlled process together with the control system using predefined blocks or blocks and functions designed and developed by the researchers. The most popular software used to perform simulations is MATLAB, which has specialized components like Simulink and Fuzzy Logic Toolbox [118]. Other software found rarely in the papers included DIGSILENT, dSPACE, C++, and PSCAD/EMTP. The second strategy used to show the efficacy and efficiency of the proposed control methodology is physical experimental implementation. When approaching the experimental assessment, the researchers used down-scaled and equivalent power system models, signal generators, qualified measurement apparatus, dedicated sensors and transducers, and specialized microcontrollers.

In the analyzed papers, we found studies that used simulations and papers that utilized both simulations and laboratory (real-time) experiments. Figure 8 graphically shows the yearly distribution of implementation strategies employed in the surveyed articles. The chart's columns underline the preference for simulations over hardware laboratory experimentations, as software implementations represent more than 80% of the total number of 135 implementation methods used in the analyzed papers.

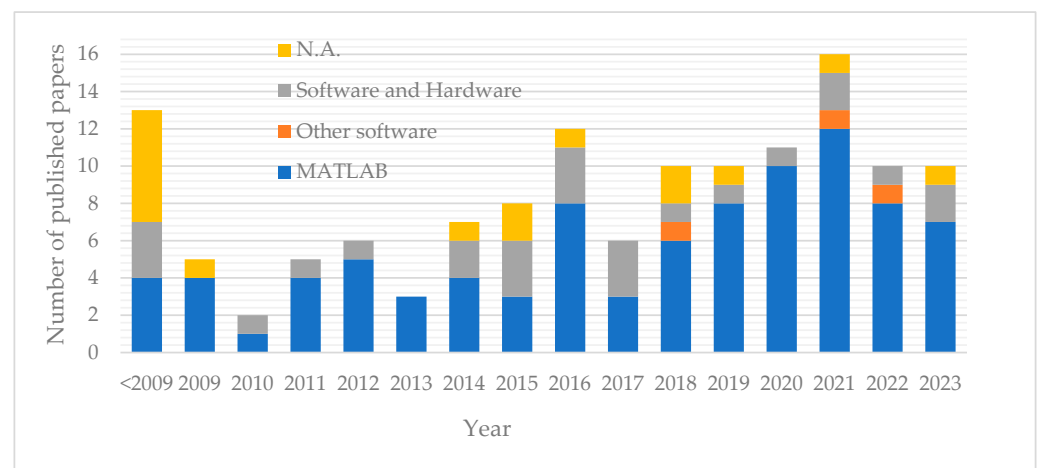


Figure 8. Yearly distribution of published papers concerning the proposed control systems' implementation and testing. Software and hardware—simulations using MATLAB and laboratory implementation; Other software—PSCAD/EMTP, dSPACE, C++, DIGSILENT; MATLAB—Simulink, SimPowerSystems, Fuzzy Logic Toolbox.

Table 9 enumerates and briefly describes the 10 chosen papers from the final set that clearly explain the implementation procedure and the obtained results. Another four papers had detailed information about the implementation process, but they are not included in the table below as they are already described in Table 8 [118], Table 7 [119], Table 6 [76], and Table 4 [120].

Table 9. Relevant papers considering the implementation of fuzzy-based systems.

Reference	Description	Implementation	Efficiency
[121]	Voltage stability, active and reactive power control in island microgrid Fuzzy adaptive impedance controller	<i>RT-LAB experiments MATLAB/Simulink</i>	Efficiency testing considering diverse operating states.
[122]	Adaptive virtual capacitor and rotational inertia control based on fuzzy logic (virtual synchronous generator VSG strategy) for frequency and voltage stability	<i>RT-LAB experiment (experimental platform hardware in loop) MATLAB/Simulink</i>	Demonstrated by comparing the proposed method with the traditional VSG control.
[123]	Modified adaptive fuzzy control with APF for power quality improvement	<i>Experimental setup—APF prototype with the proposed controller MATLAB/Simulink</i>	Simulation testing—Proposed method versus two improved sliding-mode control strategies. Hardware testing—Efficiency testing considering various conditions.
[124]	DPC is applied to parallel active filtering using type-1 fuzzy to decrease THD	<i>Laboratory experimental setup MATLAB/Simulink</i>	Simulation—Demonstrated by comparing the proposed method with the conventional DPC strategy. Hardware—Before and after filtering.
[125]	Harmonics mitigation using three-level inverter-based APF controlled by fuzzy-based dwell-time allocation algorithm (type-1 fuzzy)	<i>Laboratory implementation using digital signal processor and experimental setup MATLAB/Simulink</i>	Software—Results obtained when considering APF + fuzzy control, APF without fuzzy, and without APF. Hardware—Before and after connecting APF+ fuzzy control.
[126]	Selective harmonic compensation using microcontroller fuzzy-based control	<i>Laboratory hardware testing</i>	Proposed method vs. hysteresis, “predictive 1” and “predictive 2” control.
[127]	Harmonics current compensation using APF controlled by three type-1 fuzzy controllers	<i>MATLAB/Simulink and SimPowerSystems toolbox</i>	The proposed method’s results compared the obtained results simulating the system without the APF and fuzzy control.
[128]	Fuzzy-PI current control of DSTATCOM for power quality improvement	<i>MATLAB/Simulink</i>	Results obtained with the proposed method vs. results obtained using a simple PI controller.
[129]	Stability improvement in an island microgrid using a battery storage system controlled by a fuzzy controller	<i>DIgSILENT Power Factory software</i>	Proposed method vs. robust control.
[86]	Harmonic current compensation using hybrid power filter, P-Q theory, and fuzzy control	<i>MATLAB/Simulink Hardware implementation using FPGA</i>	Results obtained with the proposed method vs. results obtained using a simple PI controller.

3.2.7. Assessing Efficiency and Improvements

When demonstrating the efficiency of the proposed methods described in their papers, researchers chose one or more of the following four strategies enumerated below to compare the results obtained using their control methods with the results obtained when (1) no control system was employed or no PQ improvement device was utilized [87], (2) a conventional PI, PID, or control method was used as the control system [111], (3) a simple (less efficient) version of the proposed method was employed [130], or (4) other methods proposed in similar studies from the literature were used [131].

The chart in Figure 9 illustrates the yearly distribution of the efficiency demonstrations of the four strategies enumerated above. As some papers contained more than one testing strategy [131], the number of methodologies is greater than the number of papers.

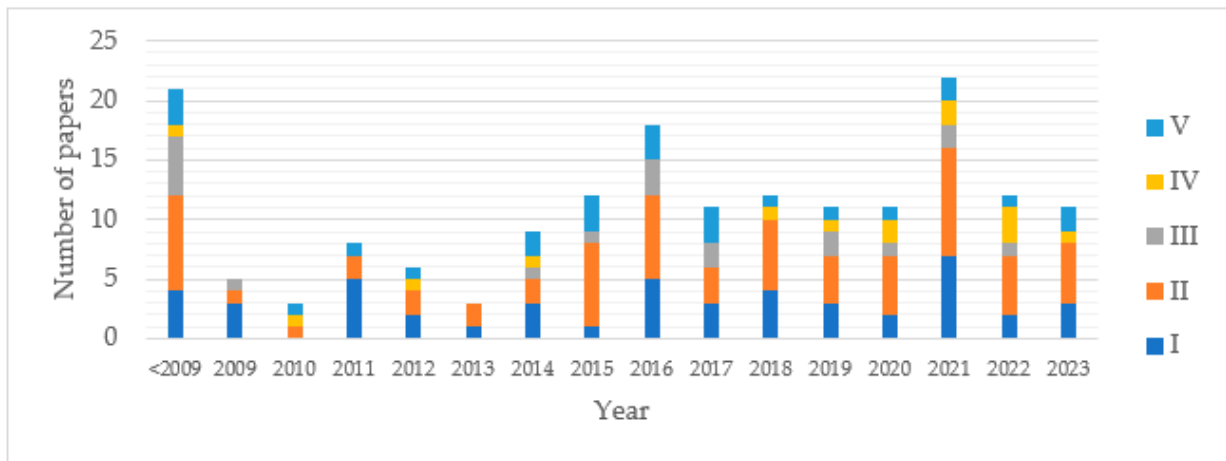


Figure 9. Yearly distribution of efficiency testing strategies in published papers. I—no control; II—PI/PID; III—other fuzzy; IV—literature methods; V—experimental.

Fuzzy logic’s strength lies in its capability to work with the nonlinearities of complex systems and the fact that no mathematical description of the control process is necessary, so only the knowledge and experience of experts are needed to provide the data to build an operative FCS [131,132]. However, a classic (type-1) FLC proved deficient when working in the presence of uncertainty factors [130]. This is the reason why many researchers studied and proposed the use of enhanced hybrid fuzzy-based controllers to obtain superior results, for example, the combination of an FLC and a PID controller, where the FLC is used to tune the three constants of the PID controller [68,75,133], or the use of evolutionary algorithms, like particle swarm optimization [74,134], to improve the parameters of the control system.

Figure 10 presents the results (number of papers per year) of the analysis of the final set in relation to the efficiency-improving methodologies used by the researchers in their studies.

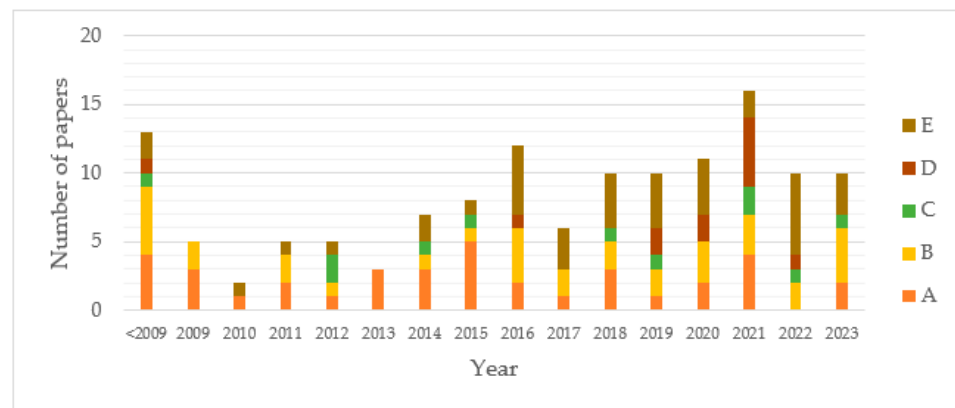


Figure 10. Yearly distribution of published papers concerning methods of efficiency improvement. A—no improvement; B—improvement using PI/PID/hysteresis; C—improvement using optimization algorithms; D—improving the features of FLC; E—improvement using other methods (adaptive, unified).

Another aspect that we considered in the analysis was the FLC’s efficiency testing and improvement concerning the fuzzy controller’s features (Sections 3.2.2 and 3.2.3), as in [132], where the authors present the difference between the Mamdani and T-S strategies when controlling an SVC for power factor reduction. From the 135 papers of the final set, as underlined in Figure 10, only 12 papers contained this type of FLC efficiency-improving methodology.

Table 10 describes 10 studies that focused on the efficiency of the fuzzy control assessment and improvement. The information in the table gives a general description of the

selected papers, information on the efficacy testing technique, and a detailed presentation of the efficiency testing and improvement method for each proposed FLC.

Table 10. Relevant papers assessing and improving the efficiency of the proposed FLCs.

Reference	Description	Efficacy	Efficiency
[63]	Frequency control using optimized type-2 fuzzy	Simulations	<i>Comparison with type-1 fuzzy and PI controller</i>
[130]	LFC in power systems with wind-generation units using robust fuzzy controller	Simulations	<i>Development and comparison of a simple type-1 fuzzy controller with the proposed hybrid fuzzy controller</i>
[64]	Online frequency regulation using fractional-order type-2 fuzzy	Simulations	<i>The proposed method vs. three methods proposed in the literature</i>
[135]	APF controlled by hybrid (inverted error deviation) fuzzy controller for decrease in harmonics	Simulations and experiments	<i>Development of both fuzzy controllers (type-1 fuzzy and hybrid) and comparison with a classic PI controller</i>
[136]	Frequency control in a microgrid with multiple types of distributed generation using hybrid type-2 fuzzy PI	Simulations	<i>The proposed method vs. conventional PI and classic type-1 fuzzy PI controller</i>
[137]	Frequency deviations and flicker issues solved using a hybrid (genetic algorithm optimizer) FLC that controls the generators	Simulations	<i>Results obtained with the proposed method compared with the results obtained without control</i>
[138]	SVC is controlled using fuzzy-PI and grey theory to improve voltage fluctuation issues	Simulations	<i>Comparison with the classic type-1 fuzzy and without the control system</i>
[139]	D-STATCOM controlled by different topologies of FLC for decrease in THD	Simulations	<i>Comparison between PI-like fuzzy controller, PI gain scheduled fuzzy controller, and hybrid fuzzy-PI controller</i>
[140]	Fuzzy load frequency control with auto-tuned membership functions and fuzzy control rules	Simulations	<i>Comparison with the classic PI controller and a hybrid fuzzy controller (FLC + particle swarm optimization)</i>
[55]	Direct adaptive fuzzy logic control for load frequency regulation in multi-area power system	Simulations	<i>The proposed method's results compared with a classic PID and a type-2 fuzzy controller</i>

4. Discussion

The analysis of the literature in the field of PQ improvement using FCSs highlights the potential of fuzzy logic in solving complex problems of modern power systems, including frequency, voltage, reactive power, harmonic distortion, and voltage unbalance control issues. Next, we focus on relevant solutions to solve these issues and future directions.

Frequency control is an essential aspect of modern power systems and is closely related to connecting distributed generation units to the grid, operating isolated microgrids, and interconnecting different areas of power systems.

Isolated microgrids that contain fluctuating generation sources (such as PV, wind, and hydro) and energy storage systems (EESs) often experience frequency fluctuations. To address this issue, researchers have used fuzzy logic to control EESs and loads, as demonstrated in [68,129,141]. Simple multiple type-1 fuzzy controllers were applied in [129,141]. Indeed, the authors of [141] use four FLCs to control the battery, dump load, load, and whole system, while [129] proposes two FLCs for active power and reactive power control, respectively. Mukherjee in [68] improved the proposed fuzzy-PID controller by tuning the PID parameters using a harmony search algorithm. These studies prove the effectiveness of FCSs through simulations by employing MATLAB [129,141] and DIGSILENT PowerFactory [129]. Efficiency is demonstrated by comparisons with other literature solutions [141], including simple PID [68] and robust control [129]. The comparison with the other methods showed that the fuzzy approach does not give frequency ripples as the robust control [129],

and the FOD performance analysis's results are superior in the case of fuzzy PID (0.21 with 1% increase in load demand), contrary to PID (0.68 in the same conditions) [68].

Frequency stability using improved FCSs when interconnecting multi-area power systems is the aim of many researchers. Thus [63,64,71,136] used simulations to demonstrate the efficacy of their hybrid type-2 fuzzy controllers and compared their proposed methods with type-1 fuzzy controllers. Aluko and his colleagues in [71] combine the UIO (Unknown Input Observer) with interval type-2 control to increase the stability and the unknown input aspect. They demonstrate in their work that the proposed type-2 FLC deals much better with undershoot frequency deviations than type-1 FLCs and PI controllers. The authors of [136] describe the combination of an interval type-2 FLC (two inputs and two outputs), a PI controller, and a dynamic selector switch to build a hybrid control system that decreases frequency ripples (maximum overshoot (MO) 0.1), contrary to type-1 fuzzy + PI (MO-0.51) and PI control (MO-0.56). The authors of [75,140] use optimization algorithms (TLBO—teaching learning-based optimization; and ABC—artificial bee colony) to adapt the parameters of the controllers. The researchers prove in [75] that their TLBO better tunes the proposed fuzzy-PID through a filter controller than a GA (ITAE = 2.74) and other methods from the literature (fuzzy PD-PI—IATE = 0.17), as the proposed method gave the lowest error (ITAE = 0.0976). The ABC algorithm tunes the two FLCs used in [140] better than PSO (particle swarm optimization), as the ISE is 3.75 for ABC-FLCs and 4.25 for PSO-FLCs, and the PI is 30.13. Smart fuzzy control that solves uncertainty factors by dealing with the FLC's outputs and values differently is proposed in [130]. Experimental validation using test setups is presented in [75,122], whereas [102] shows real-time efficacy justification. Indeed, a large-scale real-time laboratory simulation is used in [102] to compare the methods described in the paper. Thus, the BAAL (balancing authority ACE limit) for the proposed universe variable FLC was 94.84%, better than the adaptive FLC (BAAL = 92.36%) and the improved PI (BAAL = 89.06%) [102].

Maintaining voltage levels between the standard limits is a desiderate of electricity utility companies, as this aspect is required for power systems' safe operation and the normal functioning of electricity consumers' installations and apparatus. Thus, voltage control is necessary in cases of voltage sags or swells, voltage fluctuations, and variations. These scenarios appear in several situations, for example when connecting distributed generation units, as presented in [94,142,143]. A STATCOM regulated the voltage in a wind power system being controlled by a type-1 (two inputs–two outputs) fuzzy controller and gave superior results than a PI controller in a simulation study [143]. The authors of [142] demonstrated using simulations that a multi-mode fuzzy (three type-1 FLCs with three inputs and one output) controller that controlled an inverter in a power system with high-ratio PVs was better at suppressing voltage variations than a simple fuzzy controller and a simple multi-mode controller. The results showed that the multi-mode + fuzzy controller had a voltage offset equal to 12.23, and the simple fuzzy approach had a voltage offset of 34.46. Fuzzy-based reactive and active power control is proposed in [94] to regulate voltage considering an on-load tap changer and distributed generation units. Simulation and hardware in-loop tests demonstrated the superiority of the proposed method in comparison with a simple version of the control system. The authors of [119] present two FCSs (adaptive tap control and adaptive reference control) that command power transformers dedicated to voltage control, considering simulations with real data and real-time experimental tests. The adaptive reference control was the superior method. Voltage sag and flicker reduction using a hysteresis fuzzy control that drove the EES showed superior voltage stability in simulations than in a scenario without the control system [103]. The authors of [72] developed a self-tuned fuzzy-PI controller for a DVR and demonstrated through simulations that the proposed method better mitigated severe voltage sag.

Decreasing harmonic distortions of voltages and currents is solved using APFs, which in many cases are upgraded by FCSs to better serve their purpose. This situation is found in [88], where the authors designed a thyristor-controlled LC-coupling hybrid APF and used a hysteresis FLC to adjust the parameters of the filter for THD reduction in medium-

voltage-level systems. The results showed a switch loss decrease of 38% compared to using hysteresis control with a fixed band. In [84], the authors proposed an auto-tuning scheme based on an FLC to automatically calibrate the APF's control coefficient and maintain the voltage's THD within the standard limits in wind farms. Furthermore, an adaptive fuzzy method with a supervisory compensator for a three-phase APF is described in detail in [95]; more specifically, the authors use a Sugeno FLC, an adaptive law and supervisory controller, to reduce the THD from 24.71% to 1.72%. The efficacy assessment was performed using both simulations and experiments from [73,76,96,123]. The researchers in [73] used a hybrid FCS that contained a Takagi–Sugeno type-1 fuzzy controller to automatically switch between a PI and fractional-order PI controller. This approach gave greater results than employing only a PI controller, as the THD reduced from 55.8% to 2.4% and 5%. An adaptive hysteresis FLC has proven to give superior outcomes than a PI controller under various scenarios [75]. The implementation of a modified FLC on a microcontroller to control a shunt APF is described in [96]. The authors of [76] upgraded a repetitive controller with fuzzy logic, obtaining an adaptive version that showed better performance than the fixed repetitive version. This was clear, as the harmonic distortion factor decreased from 35.1% to 3.1%. The authors of [123] describe a modified adaptive FLC—more specifically, a Lyapunov-based fuzzy control. The authors compare the proposed controller with two methods from the literature through simulations. Additionally, they built a prototype that was tested in the laboratory. All tests showed that the proposed method was better, reducing the THD from 26.04% to 4.14%.

Reactive power control plays a crucial role in maintaining voltage control and power system stability. Hence, researchers often associate reactive power regulation with voltage variations and develop control systems that solve both issues simultaneously. This is the situation in [83], where the authors used a type-1 FLC to control the reactive power produced by distributed generation units. Similarly [144] describes the use of a type-1 fuzzy to adjust the SVC's capacitance for better control of reactive power and voltage control. In [145], a fuzzy self-tuning PI control together with two other regulation methods performed a three-layer coordinated reactive power compensation, and the results showed the better stability of reactive power variations than a PI-based control strategy. The reactive power control in power systems with wind generators is reflected in [93,133]. A fuzzy-PID where two FLCs give the k parameters of the PID controller plus a modulated hysteresis method is proposed in [133], and the authors show that the proposed method gave a 50.23% reduction in reactive power ripples in comparison to the conventional approach. A type -1 fuzzy with three inputs and one output is described in [93] to reduce the ripples of reactive power. All these studies used simulations to demonstrate the efficacy of the proposed methods and compared the FLCs with conventional approaches, i.e., the sensitivity method [83], no control [144], PI control [73], and conventional control [146]. Indeed, in [146], the fuzzy-based approach reduces the reactive power ripples by 40.5% in comparison with the conventional method (direct power control). For electricity consumers, reactive power control is significant as they must maintain the power factor at the connection point within a certain limit. Thus [132] presents an FLC that controls an SVC, and shows using MATLAB simulations the difference between the Mamdani and Takagi–Sugeno inferences strategies. In [147], the author describes an active power factor correction scheme that contains a boost converter controlled by an FLC with parameters optimized by a pattern search algorithm. According to simulations, the proposed method is effective and more efficient (PF = 0.99987, THD = 1.65%) than a PI controller (PF = 0.99945, THD = 2.35%).

Unbalanced three-phase voltages and currents is an issue that appears in three-phase power systems. In the literature, this problem is treated together with other PQ issues that often occur in single-phase power systems as well. For example, the authors of [99] demonstrated, through simulations, the usage of a three-phase shunt APF controlled by a self-tuning control system containing an FLC in decreasing the THD and balancing the three-phase systems of currents and voltages. The authors of [148] present an adaptive

hysteresis and FLC that controls a three-phase APF. This PQ improvement system proved to give superior results in simulations and experimental laboratory tests than a PI controller.

Considering a holistic approach to PQ improvement, that is, a reduction in all PQ disturbances, the selection of a proper control apparatus is essential. The literature demonstrates that using UPQCs controlled by hybrid FCSs is an excellent choice. The authors of [87] present the use of three type-1 fuzzy controllers to obtain switching signals for PWM logic control that command the UPQC. Simulations showed the efficacy of the proposed method in reducing THD (current from 26.58% to 5.76, and voltage from 46.93% to 3.67%), voltage sags/swells, and unbalance. A multi-feeder UPQC controlled by two FCSs is described in [67], in which a type-1 fuzzy and a fuzzy-PI controller are designed and compared through simulations. The hybrid FCS performed better in decreasing THD, unbalance, and voltage variations. The authors of [113] propose a hybrid FCS that uses two FLCs (Mamdani and Takagi–Sugeno) and the feedback integral phase-locked-loop (PLL) strategy to control a UPQC. They showed the results of the experimental assessment which proved that their method is superior to a Takagi–Sugeno-modified PLL technique in improving harmonic distortions, voltage sags, and unbalance. Indeed, with the proposed method, the THD was 2.13%, and the Takagi–Sugeno method gave a THD of 3.56%.

The tendency in recent years has been to study and propose fuzzy control inverters that connect distributed generation units but also reduce PQ issues. For example [100] describes a fuzzy space vector pulse-width modulation technique to control the inverter and improve PQ in a microgrid, without the need to depend on the utility grid. The proposed method efficacy was tested through simulations and plotting voltage, frequency, harmonics, and reactive power characteristics. The authors concluded that their method is superior to the conventional ST-PWM control, as the THD was 1.18% in comparison to 1.53%, and there were less ripples in reactive power. An FLC-based Improved Second-order Generalized Integrator (I-SOGI) scheme that controlled the assembly of a Z-source inverter that compensated a DVR solved PQ issues like balanced and unbalanced voltage sags, swells, and harmonics [131]. Additionally, the authors used the FLC (2 inputs–3 outputs) to tune the PID controller's k parameters. The simulation showed that the proposed method gave better results than other approaches from the literature. The proposed method's THD was 2%, and the results for the other methods were as follows: ANN—7.5%; RFA—5.5%; and ASO—4%.

Based on the literature review, it can be noted that type-2 and hybrid fuzzy controllers are more effective in improving PQ. Additionally, the use of membership functions that are tailored to a range of quantities, such as the type, width, and nucleus of membership functions, selected after careful examination, has also demonstrated better outcomes. Similarly, the defuzzification method and inference strategy have a significant impact on the results. For future directions in PQ improvement using FCSs, researchers should consider the use of UPQCs and other similar devices that address a large range of PQ issues.

5. Conclusions

This paper presents a comprehensive review of fuzzy-based control system applications for PQ improvement, highlighting the importance of efficacy demonstration, efficiency assessment, and improvement for FCSs. A proposed literature classification outlines seven criteria for evaluating papers that examine the characteristics of FCSs and PQ issues. The classification also presents statistics and tendencies in this area. Additionally, the most pertinent papers are selected and described in detail to provide a comprehensive overview of the subject matter.

Control systems that use hybrid fuzzy control and employ adaptive functions, optimization algorithms, and self-tuning techniques have been found to provide the best results for addressing specific issues. Such approaches have been proven to be superior to conventional and simpler fuzzy-based control methods.

To ensure the effectiveness of FCSs, it is crucial to conduct efficacy testing using a combined approach of simulations and experimental tests. This approach provides a

more comprehensive understanding of the system's performance, which is essential for ensuring the safety and reliability of FCSs. To enhance the efficiency of FLCs, it is important to explore all features and inference strategies and make sure they are the right choice for the application. To demonstrate the efficiency of the proposed methodologies, it is imperative to explore the various simulation methods mentioned in the literature and conduct experimental tests that cover a range of scenarios. By doing so, we can gain valuable insights that can help us optimize our processes and achieve better results.

This study has relevant implications not only for researchers, but also for participants. From an academic point of view, the main contributions of this paper are linked to the characteristics of fuzzy-based control systems, in particular, aspects regarding the structure, features, and inference strategies of FLCs, as well as combinations of fuzzy logic and other techniques that increase the performance of control systems. Additionally, the paper presents an analysis of the literature regarding efficiency testing, thus helping researchers in understanding new directions and tendencies. From a practitioner's viewpoint, this work presents studies from a more practical point of view, focusing on PQ issues and control devices, and including studies that describe experimental implementations and prototypes.

In conclusion, maintaining PQ within standard limits is crucial for power systems. However, due to the unpredictable and nonlinear nature of power systems, it is challenging to achieve this. Fuzzy logic, along with optimization techniques and adaptive strategies, is an appropriate approach for improving PQ. This work aims to simplify the understanding and use of fuzzy logic control in power quality issues and power quality control devices.

Regarding future directions for research, we consider further assessing published research that focused on power quality control using ANFIS and similar methodologies (data-driven fuzzy-based control) that were omitted in this research.

Author Contributions: Conceptualization, A.M. and A.C.C.; methodology, A.M.; validation, A.M., A.C.C. and H.G.B.; formal analysis, A.M. and H.G.B.; investigation, A.C.C.; resources, A.M.; data curation, H.G.B.; writing—original draft preparation, A.M. and H.G.B.; writing—review and editing, A.C.C.; visualization, H.G.B.; supervision, A.C.C.; project administration, A.M. All authors have read and agreed to the published version of the manuscript.

Funding: This research received no external funding.

Data Availability Statement: Not applicable.

Acknowledgments: This work was supported by a grant from the Ministry of Research, Innovation and Digitalization, CCCDI—UEFISCDI, project number PN-III-P2-2.1-PED-2021-4309, within PNCIDI III.

Conflicts of Interest: The authors declare no conflicts of interest.

References

1. Zadeh, L.A. Fuzzy sets. *Inf. Control* **1965**, *8*, 338–353. [[CrossRef](#)]
2. Mamdani, E.H. Application of fuzzy algorithms for control of simple dynamic plant. *Proc. IEEE* **1974**, *121*, 1585–1588. [[CrossRef](#)]
3. Zadeh, L.A. Fuzzy algorithms. *Inf. Control* **1968**, *12*, 94–102. [[CrossRef](#)]
4. Zadeh, L.A. Outline of a new approach to the analysis of complex systems and decision processes. *IEEE Trans. Syst. Man Cyber.* **1973**, *SMC-3*, 28–44. [[CrossRef](#)]
5. Mamdani, E.H.; Assilian, S. An experiment in linguistic synthesis with a fuzzy logic controller. *Int. J. Man. Mach. Stud.* **1975**, *7*, 1–13. [[CrossRef](#)]
6. Nguyen, A.-T.; Taniguchi, T.; Eciolaza, L.; Campos, V.; Palhares, R.; Sugeno, M. Fuzzy control systems: Past, present and future. *IEEE Comp. Intell. Mag.* **2019**, *14*, 56–68. [[CrossRef](#)]
7. Tomsovic, K. Fuzzy linear programming for reactive power control. In Proceedings of the 5th IEEE International Symposium on Intelligent Control, Philadelphia, PA, USA, 5–7 September 1990. [[CrossRef](#)]
8. Schwanz, D.; Bagheri, A.; Bollen, M.; Larsson, A. Active harmonic filters: Control techniques review. In Proceedings of the 17th International Conference on Harmonics and Quality of Power (ICHQP), Belo Horizonte, Brazil, 16–19 October 2016. [[CrossRef](#)]
9. Dehury, D.; Mishra, R.N.; Panda, R. Power Quality enhancement by shunt active power filter employing different control strategies: A concise review. In Proceedings of the 1st International Conference on Circuits, Power and Intelligent Systems (CCPIS), Bhubaneswar, India, 1–3 September 2023. [[CrossRef](#)]
10. Heenkenda, A.; Elsanabary, A.; Seyedmahmoudian, M.; Mekhilef, S.; Stojcevski, A.; Aziz, N.F.A. Unified Power Quality Conditioners based different structural arrangements: A comprehensive review. *IEEE Access* **2023**, *11*, 43435–43457. [[CrossRef](#)]

11. Avatchanakorn, V.; Ueda, A.; Gotoh, Y.; Mizutani, Y. Load frequency control using power demand estimation and fuzzy control. *Elect. Eng. Jpn.* **1991**, *111*, 47–57. [[CrossRef](#)]
12. So, A.T.P.; Chan, W.L.; Tse, C.T. Fuzzy logic based automatic capacitor switching for reactive power compensation. In Proceedings of the Second International Forum on Applications of Neural Networks to Power Systems, Yokohama, Japan, 19–22 April 1992. [[CrossRef](#)]
13. Hiyama, T.; Kugimiya, M.; Satoh, H. Advanced PID type fuzzy logic power system stabilizer. *IEEE Trans. Energy Conv.* **1994**, *9*, 514–520. [[CrossRef](#)]
14. Singh, B.N.; Chandra, H.; Al-Haddad, K.; Singh, B. Fuzzy control algorithm for universal active filter. In Proceedings of the Power Quality '98, Hyderabad, India, 18 June 1998. [[CrossRef](#)]
15. Jurado, F.; Valverde, M. Fuzzy logic control of a dynamic voltage restorer. In Proceedings of the 2004 IEEE International Symposium on Industrial Electronics, Ajaccio, France, 4–7 May 2004. [[CrossRef](#)]
16. Kirawanich, P.; O'Connell, R.M. Fuzzy logic control of an active power line conditioner. *IEEE Trans. Power Electr.* **2004**, *19*, 1574–1585. [[CrossRef](#)]
17. Bhende, C.N.; Mishra, S.; Jain, S.K. TS-fuzzy-controlled active power filter for load compensation. *IEEE Trans. Power Deliver.* **2006**, *21*, 1459–1465. [[CrossRef](#)]
18. Mekri, F.; Machmoum, M.; Ait Ahmed, N.; Mazari, B. A fuzzy hysteresis voltage and current control of an Unified Power Quality Conditioner. In Proceedings of the 34th Annual Conference of IEEE Industrial Electronics, Orlando, FL, USA, 10–13 November 2008. [[CrossRef](#)]
19. Mikkili, S.; Panda, A.K. Fuzzy logic controller based 3-ph 4-wire SHAF for current harmonics compensation with id-iq control strategy using simulation and RTDS hardware. In Proceedings of the IEEE Ninth International Conference on Power Electronics and Drive Systems, Singapore, 5–8 December 2011. [[CrossRef](#)]
20. Suresh, D.; Singh, S.P. Improved performance of active power filter using type-2 fuzzy logic controller. In Proceedings of the IEEE 6th India International Conference on Power Electronics, Kurukshetra, India, 8–10 December 2014. [[CrossRef](#)]
21. Lin, F.-J.; Lu, K.-C.; Ke, T.-H.; Yang, B.-H.; Chang, Y.-R. Reactive power control of three-phase grid-connected PV system during grid faults using Takagi–Sugeno–Kang probabilistic fuzzy neural network control. *IEEE Trans. Ind. Electron.* **2015**, *62*, 5516–5528. [[CrossRef](#)]
22. Ghafouri, A.; Milimonfared, J.; Gharehpetian, G.B. Fuzzy-adaptive frequency control of power system including microgrids, wind farms, and conventional power plants. *IEEE Syst. J.* **2018**, *12*, 2772–2781. [[CrossRef](#)]
23. Sundarabalan, C.K.; Puttagunta, Y.; Vignesh, V. Fuel cell integrated unified power quality conditioner for voltage and current reparation in four-wire distribution grid. *IET Smart Grid* **2019**, *2*, 60–68. [[CrossRef](#)]
24. Aluko, A.O.; Dorrell, D.G.; Pillay-Carpanen, R.; Ojo, E.E. Frequency control of modern multi-area power systems using fuzzy logic controller. In Proceedings of the IEEE PES/IAS PowerAfrica, Abuja, Nigeria, 20–23 August 2019. [[CrossRef](#)]
25. Bandopadhyay, S.; Bandyopadhyay, A. Harmonics elimination in 24 pulse GTO based STATCOM by fuzzy logic controller with switching angle optimization using grey wolf optimizer. In Proceedings of the IEEE 5th International Conference on Computing Communication and Automation (ICCCA), Greater Noida, India, 30–31 October 2020. [[CrossRef](#)]
26. Echalih, S.; Abouloifa, A.; Janik, J.M.; Lachkar, I.; Hekss, Z.; Chaoui, F.Z.; Giri, F. Hybrid controller with fuzzy logic technique for three phase half bridge interleaved buck shunt active power filter. *IFAC-PapersOnLine* **2020**, *2*, 13418–13423. [[CrossRef](#)]
27. Shunmugham Vanaja, S.D.; Albert, J.R.; Stonier, A.A. An experimental investigation on solar PV fed modular STATCOM in WECS using intelligent controller. *Int. Trans. Electr. Energ. Syst.* **2021**, *31*, e12845. [[CrossRef](#)]
28. Hoe, O.K.; Ramasamy, A.K.; Yin, L.J.; Verayah, R.; Marsadek, M.B.; Abdillah, M. Hybrid Control of Grid-Feeding and Fuzzy Logic Fault Detection in Solving Voltage Dynamic Problem within the Malaysian Distribution Network. *Energies* **2021**, *14*, 3545. [[CrossRef](#)]
29. Ayyakrishnan, M. Fuzzy Control Based Double Switching Fault Tolerant Control on Four Switch Voltage Source Inverters. *J. Electr. Eng. Technol.* **2022**, *17*, 1031–1038. [[CrossRef](#)]
30. Rupa, B.; Manohar, J.N.; Manjula, M. Power quality improvement using dual multilevel converter for micro grid-connected PV energy systems using ANFIS. *Int. J. Electr. Electron. Res.* **2023**, *11*, 550–558. [[CrossRef](#)]
31. Momoh, J.A.; Ma, X.W.; Tomsovic, K. Overview and literature survey of fuzzy set theory in power systems. *IEEE Trans. Power Syst.* **1995**, *10*, 1676–1690. [[CrossRef](#)]
32. Song, Y.-H.; Johns, A.T. Applications of fuzzy logic in power systems. I. General introduction to fuzzy logic. *Power Eng. J.* **1997**, *11*, 219–222. [[CrossRef](#)]
33. Juang, C.-F.; Lu, C.-F. Power system load frequency control by evolutionary fuzzy PI controller. In Proceedings of the IEEE International Conference on Fuzzy Systems, Budapest, Hungary, 25–29 July 2004. [[CrossRef](#)]
34. Saeidpour, E.; Parizy, V.S.; Abedi, M.; Rastegar, H. Complete, integrated and simultaneously design for STATCOM fuzzy controller with variable length genetic algorithm for voltage profile improvement. In Proceedings of the 13th International Conference on Harmonics and Quality of Power, Wollongong, NSW, Australia, 28 September–1 October 2008. [[CrossRef](#)]
35. Ibarra, L.; Webb, C. Advantages of fuzzy control while dealing with complex/ unknown model dynamics: A quadcopter example. In *New Applications of Artificial Intelligence [Internet]*; Ponce, P., Gutierrez, A.M., Rodriguez, J., Eds.; Intech Open: London, UK, 2016. [[CrossRef](#)]

36. Feng, G. A survey on analysis and design of model-based fuzzy control systems. *IEEE Trans. Fuzzy Syst.* **2006**, *14*, 676–697. [[CrossRef](#)]
37. Precup, R.-E.; David, R.-C.; Petriu, E.M.; Rădac, M.-B.; Preitl, S.; Fodor, J. Evolutionary optimization-based tuning of low-cost fuzzy controllers for servo systems. *Knowl.-Based Syst.* **2013**, *38*, 74–84. [[CrossRef](#)]
38. Jha, K.; Shaik, A.G. A comprehensive review of power quality mitigation in the scenario of solar PV integration into utility grid. *e-Prime-AEED* **2023**, *3*, 100–103. [[CrossRef](#)]
39. Hossain, E.; Tür, M.R.; Padmanaban, S.; Ay, S.; Khan, I. Analysis and mitigation of power quality issues in distributed generation systems using custom power devices. *IEEE Access* **2018**, *6*, 16816–16833. [[CrossRef](#)]
40. Remigio-Carmona, P.; González-de-la-Rosa, J.-J.; Florencias-Oliveros, O.; Sierra-Fernández, J.-M.; Fernández-Morales, J.; Espinosa-Gavira, M.-J.; Agüera-Pérez, A.; Palomares-Salas, J.-C. Current status and future trends of power quality analysis. *Energies* **2022**, *15*, 2328. [[CrossRef](#)]
41. Srivastava, M.; Goyal, S.K.; Saraswat, A.; Shekhawat, R.S.; Gangil, G. A review on power quality problems, causes and mitigation techniques. In Proceedings of the 1st International Conference on Sustainable Technology for Power and Energy Systems, Srinagar, India, 4–6 July 2022. [[CrossRef](#)]
42. Hernández-Mayoral, E.; Madrigal-Martínez, M.; Mina-Antonio, J.D.; Iracheta-Cortez, R.; Enríquez-Santiago, J.A.; Rodríguez-Rivera, O.; Martínez-Reyes, G.; Mendoza-Santos, E. A comprehensive review on power-quality issues, optimization techniques, and control strategies of microgrid based on renewable energy sources. *Sustainability* **2023**, *15*, 9847. [[CrossRef](#)]
43. Moreira, L.; Leitão, S.; Vale, Z.; Galvão, J.; Marques, P. Analysis of power quality disturbances in industry in the center region of Portugal. In *Technological Innovation for Collective Awareness Systems. DoCEIS. IFIP Advances in Information and Communication Technology*; Camarinha-Matos, L.M., Barrento, N.S., Mendonça, R., Eds.; Springer: Berlin/Heidelberg, Germany, 2014; p. 423. [[CrossRef](#)]
44. Power Quality, IEC 61000-Series Block. Available online: <https://comsys.se/our-adf-technology/power-quality-iec-61000/> (accessed on 23 March 2024).
45. *IEEE 519-2022*; Power Quality. IEEE: Piscataway, NJ, USA. Available online: <https://standards.ieee.org/ieee/519/10677/> (accessed on 23 March 2024).
46. Filo, G. A review of fuzzy logic method development in hydraulic and pneumatic systems. *Energies* **2023**, *16*, 75–84. [[CrossRef](#)]
47. Belman-Flores, J.M.; Rodríguez-Valderrama, D.A.; Ledesma, S.; García-Pabón, J.J.; Hernández, D.; Pardo-Cely, D.M. A review on applications of fuzzy logic control for refrigeration systems. *Appl. Sci.* **2022**, *12*, 1302. [[CrossRef](#)]
48. Precup, R.-E.; Nguyen, A.-T.; Blažič, S. A survey on fuzzy control for mechatronics applications. *Int. J. Syst. Sci.* **2024**, *55*, 771–813. [[CrossRef](#)]
49. Jerković Štil, V.; Varga, T.; Benšić, T.; Barukčić, M. A survey of fuzzy algorithms used in multi-motor systems control. *Electronics* **2020**, *9*, 1788. [[CrossRef](#)]
50. Castro, L.; Pérez-Londoño, S.; Mora-Flórez, J. Application of fuzzy logic based control in micro-grids. In Proceedings of the FISE-IEEE/CIGRE Conference-Living the Energy Transition, Medellín, Colombia, 4–6 December 2019. [[CrossRef](#)]
51. Sztajmec, E.; Szcześniak, P. A review on AC voltage variation compensators in low voltage distribution network. *Energies* **2023**, *16*, 6293. [[CrossRef](#)]
52. Hoon, Y.; Mohd Radzi, M.A.; Hassan, M.K.; Mailah, N.F. Control algorithms of shunt active power filter for harmonics mitigation: A review. *Energies* **2017**, *10*, 2038. [[CrossRef](#)]
53. Dash, D.K.; Sadhu, P.K. A review on the use of active power filter for grid-connected renewable energy conversion systems. *Processes* **2023**, *11*, 1467. [[CrossRef](#)]
54. Sanchez-Roger, M.; Oliver-Alfonso, M.D.; Sanchís-Pedregosa, C. Fuzzy logic and its uses in finance: A systematic review exploring its potential to deal with banking crises. *Mathematics* **2019**, *7*, 1091. [[CrossRef](#)]
55. Yousef, H.A.; AL-Kharusi, K.; Albadi, M.H.; Hosseinzadeh, N. Load frequency control of a multi-area power system: An adaptive fuzzy logic approach. *IEEE Trans. Power Syst.* **2014**, *29*, 1822–1830. [[CrossRef](#)]
56. Benhalima, S.; Chandra, A.; Rezkallah, M. Real-time experimental implementation of an LMS-adaline-based ANFIS controller to drive PV interfacing power system. *IET Renew. Power Gener.* **2019**, *13*, 1142–1152. [[CrossRef](#)]
57. Ding, X.; Yao, R.; Zhai, X.; Li, C.; Dong, H. An adaptive compensation droop control strategy for reactive power sharing in islanded microgrid. *Electr. Eng.* **2020**, *102*, 267–278. [[CrossRef](#)]
58. Irfan, M.M.; Rangarajan, S.; Collins, E.R.; Senjyu, T. Enhancing the Power Quality of the Grid Interactive Solar Photovoltaic-Electric Vehicle System. *World Electr. Veh. J.* **2021**, *12*, 98. [[CrossRef](#)]
59. Kumar, P.; Arya, S.R.; Mistry, K.D.; Babu, B.C. Performance evaluation of GRNN and ANFIS controlled DVR using machine learning in distribution network. *Optim. Control. Appl. Methods* **2023**, *44*, 987–1005. [[CrossRef](#)]
60. Fang, Y.; Li, S.; Fei, J. Adaptive Intelligent High-Order Sliding Mode Fractional Order Control for Harmonic Suppression. *Fractal Fract.* **2022**, *6*, 482. [[CrossRef](#)]
61. Fei, J.; Wang, Z.; Pan, Q. Self-Constructing Fuzzy Neural Fractional-Order Sliding Mode Control of Active Power Filter. *IEEE Trans. Neural Netw. Learn. Syst.* **2023**, *34*, 10600–10611. [[CrossRef](#)] [[PubMed](#)]
62. Lin, F.-J.; Liao, J.-C.; Chen, C.-I.; Chen, P.-R.; Zang, Y.-M. Voltage Restoration Control for Microgrid with Recurrent Wavelet Petri Fuzzy Neural Network. *IEEE Access* **2022**, *10*, 12510–12529. [[CrossRef](#)]

63. Shakibjoo, A.D.; Moradzadeh, M.; Din, S.U.; Mohammadzadeh, A.; Mosavi, A.H.; Vandeveld, L. Optimized Type-2 Fuzzy Frequency Control for Multi-Area Power Systems. *IEEE Access* **2022**, *10*, 6989–7002. [[CrossRef](#)]
64. Mohammadzadeh, A.; Kayacan, E. A novel fractional-order type-2 fuzzy control method for online frequency regulation in ac microgrid. *Eng. Appl. Artif. Intell.* **2020**, *90*, 103483. [[CrossRef](#)]
65. Liu, L.; Fei, J.; An, C. Adaptive Sliding Mode Long Short-Term Memory Fuzzy Neural Control for Harmonic Suppression. *IEEE Access* **2021**, *9*, 69724–69734. [[CrossRef](#)]
66. Hamdan, I.; Youssef, M.M.M.; Noureldeen, O. A proposed supercapacitor integrated with an active power filter for improving the performance of a wind generation system under nonlinear unbalanced loading and faults. *J. Electr. Comp. Eng.* **2023**, *2023*, 17. [[CrossRef](#)]
67. Bhavani, S.S.N.L.; Shanmukha Rao, L. Realization of novel multi-feeder UPQC for power quality enhancement using proposed hybrid fuzzy+PI controller. In Proceedings of the 2019 Innovations in Power and Advanced Computing Technologies (i-PACT), Vellore, India, 22–23 March 2019. [[CrossRef](#)]
68. Tarkeshwar, M.; Mukherjee, V. A novel quasi-oppositional harmony search algorithm and fuzzy logic controller for frequency stabilization of an isolated hybrid power system. *Int. J. Electr. Power Energy Syst.* **2015**, *66*, 247–261. [[CrossRef](#)]
69. Hien, P.T.; Huyen, D.V.; Cuong, N.D. Harmonic elimination based on fuzzy logic in combination with hysteresis control algorithm. In Proceedings of the 2017 International Conference on System Science and Engineering (ICSSE), Ho Chi Minh City, Vietnam, 21–23 July 2017. [[CrossRef](#)]
70. Shadoul, M.; Yousef, H.; Al Abri, R.; Al-Hinai, A. Adaptive fuzzy approximation control of PV grid-connected inverters. *Energies* **2021**, *14*, 942. [[CrossRef](#)]
71. Aluko, A.O.; Carpanen, R.P.; Dorrell, D.G.; Ojo, E.E. Robust state estimation method for adaptive load frequency control of interconnected power system in a restructured environment. *IEEE Syst. J.* **2021**, *15*, 5046–5056. [[CrossRef](#)]
72. Mallick, N.; Mukherjee, V. Self-tuned fuzzy-proportional-integral compensated zero/minimum active power algorithm based dynamic voltage restorer. *IET Gener. Transm. Distrib.* **2018**, *12*, 2778–2787. [[CrossRef](#)]
73. Afghoul, H.; Krim, F.; Chikouche, D.; Beddar, A. Design and real time implementation of fuzzy switched controller for single phase active power filter. *ISA Trans.* **2015**, *58*, 614–621. [[CrossRef](#)] [[PubMed](#)]
74. Al Gizi, A.J.H. A particle swarm optimization, fuzzy PID controller with generator automatic voltage regulator. *Soft Comput.* **2019**, *23*, 8839–8853. [[CrossRef](#)]
75. Pradhan, P.C.; Sahu, R.K.; Panda, S. Analysis of hybrid fuzzy logic control based PID through the filter for frequency regulation of electrical power system with real-time simulation. *J. Control Autom. Electr. Syst.* **2021**, *32*, 439–457. [[CrossRef](#)]
76. Santiprapan, P.; Booranawong, A.; Areerak, K.; Saito, H. Adaptive repetitive controller for an active power filter in three-phase four-wire systems. *IET Power Electron.* **2020**, *13*, 2756–2766. [[CrossRef](#)]
77. Fattahi, J.; Schriemer, H.; Bacque, B.; Orr, R.; Hinzer, K.; Haysom, J.E. High stability adaptive microgrid control method using fuzzy logic. *Sustain. Cities Soc.* **2016**, *25*, 57–64. [[CrossRef](#)]
78. Echalih, S.; Abouloifa, A.; Lachkar, I.; Aroudi, A.E.; Hekss, Z.; Giri, F.; Al-Numay, M.S. A Cascaded controller for a grid-tied photovoltaic system with three-phase half-bridge interleaved buck shunt active power filter: Hybrid control strategy and fuzzy logic approach. *IEEE J. Emerg. Sel. Top. Circuits Syst.* **2022**, *12*, 320–330. [[CrossRef](#)]
79. Panati, P.U.; Ramasamy, S.; Ahsan, M.; Haider, J.; Rodrigues, E.M.G. Indirect effective controlled split source inverter-based parallel active power filter for enhancing power quality. *Electronics* **2021**, *10*, 892. [[CrossRef](#)]
80. Saad, S.; Zellouma, L. Fuzzy logic controller for three-level shunt active filter compensating harmonics and reactive power. *Electr. Power Syst. Res.* **2009**, *79*, 1337–1341. [[CrossRef](#)]
81. Kocaarslan, İ.; Çam, E. Fuzzy logic controller in interconnected electrical power systems for load-frequency control. *Int. J. Electr. Power Energy Syst.* **2005**, *27*, 542–549. [[CrossRef](#)]
82. Datta, M.; Senjyu, T.; Yona, A.; Funabashi, T.; Kim, C.-H. A frequency-control approach by photovoltaic generator in a PV-diesel hybrid power system. *IEEE Trans. Energy Convers.* **2011**, *26*, 559–571. [[CrossRef](#)]
83. Calderaro, V.; Conio, G.; Galdi, V.; Piccolo, A. Reactive power control for improving voltage profiles: A comparison between two decentralized approaches. *Electr. Power Syst. Res.* **2012**, *83*, 247–254. [[CrossRef](#)]
84. Thao, N.G.M.; Uchida, K.; Kofuji, K.; Jintsugawa, T.; Nakazawa, C. An automatic-tuning scheme based on fuzzy logic for active power filter in wind farms. *IEEE Trans. Control Syst. Technol.* **2019**, *27*, 1694–1702. [[CrossRef](#)]
85. Narongrit, T.; Areerak, K.; Areerak, K. Adaptive fuzzy control for shunt active power filters. *Electr. Power Compon. Syst.* **2016**, *44*, 646–657. [[CrossRef](#)]
86. Thirumoorthi, P.; Yadaiah, N. Design of current source hybrid power filter for harmonic current compensation. *Simul. Model. Pract. Theory* **2015**, *52*, 78–91. [[CrossRef](#)]
87. Chennai, S.; Benchouia, M.T. Unified power quality conditioner based on a three-level NPC inverter using fuzzy control techniques for all voltage disturbances compensation. *Front. Energy* **2014**, *8*, 221–239. [[CrossRef](#)]
88. Sou, W.-K.; Chan, P.-I.; Gong, C.; Lam, C.-S. A fuzzy logic based adaptive source current THD controller for thyristor-controlled LC-coupling hybrid active power filter. In Proceedings of the 47th Annual Conference of the IEEE Industrial Electronics Society, Toronto, ON, Canada, 13–16 October 2021. [[CrossRef](#)]
89. Puchalapalli, S.; Singh, B. A single input variable FLC for DFIG-based WPGS in standalone mode. *IEEE Trans. Sustain. Energy* **2020**, *11*, 595–607. [[CrossRef](#)]

90. Saribulut, L.; Teke, A.; Tümay, M. Dynamic control of unified power flow controller under unbalanced network conditions. *Simul. Model. Pract. Theory* **2011**, *19*, 817–836. [[CrossRef](#)]
91. Hamzah, M.K.; Abdul Ghafar, A.F.; Mohd Hussain, M.N. Single-phase half-bridge shunt active power filter employing fuzzy logic control. In Proceedings of the 2008 IEEE Power Electronics Specialists Conference, Rhodes, Greece, 15–19 June 2008. [[CrossRef](#)]
92. Hosseinalizadeh, T.; Kebriaei, H.; Salmasi, F.R. Decentralised robust T-S fuzzy controller for a parallel islanded AC microgrid. *IET Gener. Transm. Distrib.* **2019**, *13*, 1589–1598. [[CrossRef](#)]
93. Attia, A.-F.; Sharaf, A.M. A robust FACTS based fuzzy control scheme for dynamic stabilization of generator station. *Ain Shams Eng. J.* **2020**, *11*, 629–641. [[CrossRef](#)]
94. Azzouz, M.A.; Farag, H.E.; El-Saadany, E.F. Real-time fuzzy voltage regulation for distribution networks incorporating high penetration of renewable sources. *IEEE Syst. J.* **2017**, *11*, 1702–1711. [[CrossRef](#)]
95. Fei, J.; Hou, S. Adaptive fuzzy control with supervisory compensator for three-phase active power filter. *J. Appl. Math.* **2012**, *2012*, 13. [[CrossRef](#)]
96. Anjana, P.; Gupta, V.; Tiwari, H.; Gupta, N.; Bansal, R. Hardware implementation of shunt APF using modified fuzzy control algorithm with STM32F407VGT microcontroller. *Electr. Power Compon. Syst.* **2016**, *44*, 1530–1542. [[CrossRef](#)]
97. Tur, M.R.; Wadi, M.; Shobole, A.; Ay, S. Load frequency control of two area interconnected power system using fuzzy logic control and PID controller. In Proceedings of the 7th International Conference on Renewable Energy Research and Applications (ICRERA), Paris, France, 14–17 October 2018. [[CrossRef](#)]
98. Nabipour, M.; Razaz, M.; Seifossadat, S.G.H.; Mortazavi, S.S. A novel adaptive fuzzy membership function tuning algorithm for robust control of a PV-based Dynamic Voltage Restorer (DVR). *Eng. Appl. Artif. Intell.* **2016**, *53*, 155–175. [[CrossRef](#)]
99. Benaissa, A.; Rabhi, B.; Moussi, A.; Benkhoris, M.F. Fuzzy logic controller for three-phase four-leg five-level shunt active power filter under unbalanced non-linear load and distorted voltage conditions. *Int. J. Syst. Assur. Eng. Manag.* **2014**, *5*, 361–370. [[CrossRef](#)]
100. Rao, S.N.V.B.; Kumar, Y.V.P.; Pradeep, D.J.; Reddy, C.P.; Flah, A.; Kraiem, H.; Al-Asad, J.F. Power quality improvement in renewable-energy-based microgrid clusters using fuzzy space vector PWM controlled inverter. *Sustainability* **2022**, *14*, 4663. [[CrossRef](#)]
101. Narasimhulu, V.; Ashok Kumar, D.V.; Sai Babu, C. Fuzzy logic control of SLMMC-based SAPF under nonlinear loads. *Int. J. Fuzzy Syst.* **2020**, *22*, 428–437. [[CrossRef](#)]
102. Aziz, S.; Wang, H.; Liu, Y.; Peng, J.; Jiang, H. Variable universe fuzzy logic-based hybrid LFC control with real-time implementation. *IEEE Access* **2019**, *7*, 25535–25546. [[CrossRef](#)]
103. Yunus, A.M.S.; Habriansyah, I.; Abu-Siada, A.; Masoum, M.A.S. Sag and flicker reduction using hysteresis-fuzzy control-based SMES unit. *Can. J. Elect. Comp. Eng.* **2019**, *42*, 52–57. [[CrossRef](#)]
104. Ahmed, K.Y.; Bin Yahaya, N.Z.; Asirvadam, V.S.; Saad, N.; Kannan, R.O.I. Development of power electronic distribution transformer based on adaptive PI controller. *IEEE Access* **2018**, *6*, 44970–44980. [[CrossRef](#)]
105. Liu, Y.; Zhang, P.; Qiu, X. Optimal reactive power and voltage control for radial distribution system. In Proceedings of the 2000 Power Engineering Society Summer Meeting, Seattle, WA, USA, 16–20 July 2000. [[CrossRef](#)]
106. Saidi, S.; Abbassi, R.; Chebbi, S. Fuzzy logic controller for three-level shunt active filter compensating harmonics and reactive power. *Int. J. Adapt. Control Signal Process.* **2016**, *30*, 809–823. [[CrossRef](#)]
107. Shyu, K.-K.; Yang, M.-J.; Wang, T.-W.; Wu, D.-Y. T-S fuzzy controller design based on LMI for a shunt active power filter system. In Proceedings of the 33rd Annual Conference of the IEEE Industrial Electronics Society, Taipei, Taiwan, 5–8 November 2007. [[CrossRef](#)]
108. Yousef, H. Adaptive fuzzy logic load frequency control of multi-area power system. *Int. J. Electr. Power Energy Syst.* **2015**, *68*, 384–395. [[CrossRef](#)]
109. Belaidi, R.; Haddouche, A.; Guendouz, H. Fuzzy logic controller based three-phase shunt active power filter for compensating harmonics and reactive power under unbalanced mains voltages. *Energy Procedia* **2012**, *18*, 560–570. [[CrossRef](#)]
110. Guo, C. Voltage regulation and power-saving method of asynchronous motor based on fuzzy control theory. *Open Phys.* **2022**, *20*, 334–341. [[CrossRef](#)]
111. Echalih, S.; Abouloifa, A.; Lachkar, I.; Guerrero, J.M.; Hekss, Z.; Giri, F. Hybrid automaton-fuzzy control of single phase dual buck half bridge shunt active power filter for shoot through elimination and power quality improvement. *Int. J. Electr. Power Energy Syst.* **2021**, *131*, 106986. [[CrossRef](#)]
112. Yousuf, V.; Ahmad, A. Optimal design and application of fuzzy logic equipped control in STATCOM to abate SSR oscillations. *Int. J. Circ. Theor. Appl.* **2021**, *49*, 4070–4087. [[CrossRef](#)]
113. Patjoshi, R.K.; Panigrahi, R.; Rout, S.S. A hybrid fuzzy with feedback integral phase locked loop-based control strategy for unified power quality conditioner. *Trans. Inst. Meas. Control* **2021**, *43*, 122–136. [[CrossRef](#)]
114. Mallick, N.; Mukherjee, V. Interval type 2 fuzzy logic controlled advanced dynamic voltage restorer for voltage sag alleviation. *IET Gener. Transm. Distrib.* **2019**, *13*, 3020–3028. [[CrossRef](#)]
115. Siddique, A.; Xu, Y.; Aslam, W.; Rehman, A.; Aslam, M.K. Performance of fuzzy logic-based controller for UPFC on power quality issues in transmission network. In Proceedings of the 2018 International Conference on Power System Technology (POWERCON), Guangzhou, China, 6–8 November 2018. [[CrossRef](#)]

116. Bhattacharjee, C.; Roy, B.K. Fuzzy-supervisory control of a hybrid system to improve contractual grid support with fuzzy proportional-derivative and integral control for power quality improvement. *IET Gener. Transm. Distrib.* **2018**, *12*, 1455–1465. [[CrossRef](#)]
117. Aissa, O.; Moulahoum, S.; Colak, I.; Kabache, N.; Babes, B. Improved performance and power quality of direct torque control of asynchronous motor by using intelligent controllers. *Electr. Power Compon. Syst.* **2016**, *44*, 343–358. [[CrossRef](#)]
118. Mekri, F.; Machmoum, M.; Ait-Ahmed, N.; Mazari, B. A comparative study of voltage controllers for series active power filter. *Electr. Power Syst. Res.* **2010**, *80*, 615–626. [[CrossRef](#)]
119. Spatti, D.H.; da Silva, I.N.; Usida, W.F.; Flauzino, R.A. Real-time voltage regulation in power distribution system using fuzzy control. *IEEE Trans. Power Deliv.* **2010**, *25*, 1112–1123. [[CrossRef](#)]
120. Cecati, C.; Dell'Aquila, A.; Lecci, A.; Liserre, M. Implementation issues of a fuzzy-logic-based three-phase active rectifier employing only voltage sensors. *IEEE Trans. Ind. Electron.* **2005**, *52*, 378–385. [[CrossRef](#)]
121. Jiang, E.; Zhao, J.; Shi, Z.; Mi, Y.; Lin, S.; Muyeen, S.M. Intelligent virtual impedance-based control to enhance the stability of islanded microgrid. *J. Electr. Eng. Technol.* **2023**, *18*, 3971–3984. [[CrossRef](#)]
122. Lyu, L.; Wang, X.; Zhang, L.; Zhang, Z.; Koh, L.H. Fuzzy control based virtual synchronous generator for self-adaptive control in hybrid microgrid. *Energy Rep.* **2022**, *8*, 12092–12104. [[CrossRef](#)]
123. Hou, S.; Chen, C.; Chu, Y.; Fei, J. Experimental validation of modified adaptive fuzzy control for power quality improvement. *IEEE Access* **2020**, *8*, 92162–92171. [[CrossRef](#)]
124. Ouchen, S.; Steinhart, H.; Gaubert, J.-P.; Blaabjerg, F.; Betka, A. Simulation and real time implementation of direct power control applied to parallel active filtering based on fuzzy logic controller. In Proceedings of the 7th International Conference on Systems and Control (ICSC), Valencia, Spain, 24–26 October 2018. [[CrossRef](#)]
125. Hoon, Y.; Radzi, M.A.M.; Hassan, M.K.; Mailah, N.F. Neutral-point voltage deviation control for three-level inverter-based shunt active power filter with fuzzy-based dwell time allocation. *IET Power Electron.* **2017**, *10*, 429–441. [[CrossRef](#)]
126. Dell'Aquila, A.; Lecci, A.; Liserre, M. Microcontroller-based fuzzy logic active filter for selective harmonic compensation. In Proceedings of the 38th IAS Annual Meeting on Conference Record of the Industry Applications Conference, Salt Lake City, UT, USA, 12–16 October 2003. [[CrossRef](#)]
127. Salim, C. Five-level (NPC) shunt active power filter performances evaluation using fuzzy control scheme for harmonic currents compensation. In Proceedings of the 6th International Conference on Systems and Control (ICSC), Batna, Algeria, 7–9 May 2017. [[CrossRef](#)]
128. Amoozegar, D. DSTATCOM modelling for voltage stability with fuzzy logic PI current controller. *Int. J. Electr. Power Energy Syst.* **2016**, *76*, 129–135. [[CrossRef](#)]
129. Tephiruk, N.; Kanokbannakorn, W.; Kerdphol, T.; Mitani, Y.; Hongesombut, K. Fuzzy logic control of a battery energy storage system for stability improvement in an islanded microgrid. *Sustainability* **2018**, *10*, 1645. [[CrossRef](#)]
130. Rouhanian, A.; Aliamooei-Lakeh, H.; Aliamooei-Lakeh, S.; Toulabi, M. Improved load frequency control in power systems with high penetration of wind farms using robust fuzzy controller. *Electr. Power Syst. Res.* **2023**, *224*, 109511. [[CrossRef](#)]
131. Thenmozhi, M.; Umamaheswari, S.; Stonier, A.A.; Thangavel, T. Design and implementation of photovoltaic-assisted dynamic voltage restorer using fuzzy logic controller-based improved SOGI for power quality improvement. *Electr. Eng.* **2023**. [[CrossRef](#)]
132. Khanmohammadi, S.; Hagh, M.T.; Abapour, M. Fuzzy logic based SVC for reactive power compensation and power factor correction. In Proceedings of the International Power Engineering Conference (IPEC 2007), Singapore, 3–6 December 2007.
133. Tamalouzt, S.; Belkhier, Y.; Sahri, Y.; Ullah, N.; Shaw, R.N.; Bajaj, M. New direct reactive power control based fuzzy and modulated hysteresis method for micro-grid applications under real wind speed. *Energy Sources A Recovery Util. Environ. Eff.* **2022**, *44*, 4862–4887. [[CrossRef](#)]
134. Shouran, M.; Alseid, A. Particle swarm optimization algorithm-tuned fuzzy cascade fractional Order PI-fractional order PD for frequency regulation of dual-area power system. *Processes* **2022**, *10*, 477. [[CrossRef](#)]
135. Hoon, Y.; Radzi, M.A.M.; Hassan, M.K.; Mailah, N.F. DC-link capacitor voltage regulation for three-phase three-level inverter-based shunt active power filter with inverted error deviation control. *Energies* **2016**, *9*, 533. [[CrossRef](#)]
136. Rawat, S.; Jha, B.; Panda, M.K.; Kanti, J. Interval type-2 fuzzy logic control-based frequency control of hybrid power system using DMGS of PI controller. *Appl. Sci.* **2021**, *11*, 10217. [[CrossRef](#)]
137. Lotfy, M.E.; Senjyu, T.; Farahat, M.A.-F.; Abdel-Gawad, A.F.; Lei, L.; Datta, M. Hybrid genetic algorithm fuzzy-based control schemes for small power system with high-penetration wind farms. *Appl. Sci.* **2018**, *8*, 373. [[CrossRef](#)]
138. Karami, M.M.; Itami, A. Implementation of SVC based on grey theory and fuzzy logic to improve LVRT capability of wind distributed generations. *Turk. J. Electr. Eng. Comp. Sci.* **2017**, *25*, 33. [[CrossRef](#)]
139. Varshney, A.; Garg, R. Comparison of different topologies of fuzzy logic controller to control D-STATCOM. In Proceedings of the 3rd International Conference on Computing for Sustainable Global Development (INDIACom), New Delhi, India, 16–18 March 2016.
140. Zamani, A.A.; Bijami, E.; Sheikholeslam, F.; Jafrasteh, B. Optimal fuzzy load frequency controller with simultaneous auto-tuned membership functions and fuzzy control rules. *Turk. J. Electr. Eng. Comp. Sci.* **2014**, *22*, 7. [[CrossRef](#)]
141. Das, S.; Akella, A.K. A fuzzy logic-based frequency control scheme for an isolated AC coupled PV-wind-battery hybrid system. *Int. J. Model. Simul.* **2020**, *40*, 308–320. [[CrossRef](#)]
142. Yang, X.; Qiu, Z.; Liu, F.; Jiao, K. Fuzzy logic-based multi-mode voltage control strategy for high ratio photovoltaic in a distribution network. *IET Gener. Transm. Distrib.* **2022**, *16*, 4936–4950. [[CrossRef](#)]

143. Faroug, M.A.M.; Rao, D.N.; Samikannu, R.; Venkatachary, S.K.; Senthilnathan, K. Comparative analysis of controllers for stability enhancement for wind energy system with STATCOM in the grid connected environment. *Renew. Energy* **2020**, *162*, 2408–2442. [[CrossRef](#)]
144. Naderipour, A.; Abdul-Malek, Z.; Gandoman, F.H.; Nowdeh, S.A.; Shiran, M.A.; Moghaddam, M.J.H.; Davoodkhani, I.F. Optimal designing of static var compensator to improve voltage profile of power system using fuzzy logic control. *Energy* **2020**, *192*, 116665. [[CrossRef](#)]
145. Li, M.; Li, W.; Zhao, J.; Chen, W.; Yao, W. Three-layer coordinated control of the hybrid operation of static var compensator and static synchronous compensator. *IET Gener. Transm. Distrib.* **2016**, *10*, 2185–2193. [[CrossRef](#)]
146. Sayeh, K.M.; Tamalouzt, S.; Sahri, Y. Improvement of power quality in WT-DFIG systems using novel direct power control based on fuzzy logic control under randomness conditions. *Int. J. Model. Simul.* **2023**. [[CrossRef](#)]
147. Colak, A.M. Parameters optimized with the pattern search algorithm for fuzzy control based active power factor correction. *Electr. Power Comp. Syst.* **2023**, *52*, 1115–1128. [[CrossRef](#)]
148. Panda, A.K.; Patel, R. Adaptive hysteresis and fuzzy logic controlled-based shunt active power filter resistant to shoot-through phenomenon. *IET Power Electron.* **2015**, *8*, 1963–1977. [[CrossRef](#)]

Disclaimer/Publisher’s Note: The statements, opinions and data contained in all publications are solely those of the individual author(s) and contributor(s) and not of MDPI and/or the editor(s). MDPI and/or the editor(s) disclaim responsibility for any injury to people or property resulting from any ideas, methods, instructions or products referred to in the content.

Reactive Power Compensation at Consumers Using Fuzzy Logic Control

Anca Miron

Dept. Power Systems and Management
Technical University of Cluj-Napoca
Cluj-Napoca, Romania
anca.miron@enm.utcluj.ro

Andrei C. Cziker

Dept. Power Systems and Management
Technical University of Cluj-Napoca
Cluj-Napoca, Romania
andrei.cziker@enm.utcluj.ro

Cosmin P. Dărab

Dept. Power Systems and Management
Technical University of Cluj-Napoca
Cluj-Napoca, Romania
cosmin.darab@enm.utcluj.ro

Ștefan Ungureanu

Dept. Power Systems and Management
Technical University of Cluj-Napoca
Cluj-Napoca, Romania
stefan.ungureanu@enm.utcluj.ro

Horia G. Beileu

Dept. Power Systems and Management
Technical University of Cluj-Napoca
Cluj-Napoca, Romania
horia.beileu@enm.utcluj.ro

Abstract— The research presented in this article had as objective to analyze how diverse types of fuzzy numbers, decision-making and defuzzification methods affect the efficiency of an FLC dedicated to reactive power compensation. The opening step of the research was to develop a model for the electricity consumer and determine the needs regarding the reactive power compensation. Next, the fuzzy logic controller is designed and diverse types of fuzzy numbers, decision-making and defuzzification methods are used, to decide upon the more appropriate ones. In the research MATLAB/Simulink and MATLAB/Fuzzy Logic Toolbox were employed to realize the simulations and testing of the fuzzy logic controller. The analysis uses twenty-four variants of the FLC, and the results show that the type of fuzzy sets affect the most the efficiency of the analyzed FLC.

Keywords— reactive power compensation, electricity consumer, fuzzy logic control, fuzzy sets, shunt compensation

I. INTRODUCTION

The reactive power compensation at consumers is a practice used to control the power factor and rise its value above the imposed threshold (by Romanian standards is 0.9). This is because electricity consumers (except domestic and the ones connected with them) will pay differential for their electrical energy consumption in accordance with the value of the power factor. Power factor is strictly connected to the circulation of reactive power, which on the other hand is a cause of the functioning of inductive and capacitive elements of the power systems [1].

The reactive power circulation is a characteristic of AC power systems. However, a large quantity of reactive power that moves through the power system can cause instability and diminish the quantity of active (useful) power that reaches the consumers. This is the main cause that leads the electricity consumers to use different methodologies and devices to offset the reactive power caused by their loads [2].

Power engineers and researchers study the problem of reactive power compensation and power factor correction, and it is related to power quality. Reactive power compensation, known in literature as VAR compensation is the management of reactive power [3]. The VAR compensation at consumers' side one can make using shunt compensation that provides reactive power near the resistive-inductive loads, thus the line current is minimized, so the power losses decrease, and voltage is stabilized at the load's terminals [4].

Fuzzy logic is an Artificial Intelligence Technique that copies the logic manner of humans when solving problems. It also has the capability to work with uncertainties, thus being ideal to deal with real data that one often finds in power systems [5]. The most successful and feasible applications in power systems of fuzzy logic are in control. Consequently, there are articles that propose fuzzy logic controllers (FLC) for VAR compensation [6-20]. These papers present the results of studies in which capacitor banks, SVCs, STATCOMs and / or UPFC were employed and compared in the process of VAR compensation. Additionally, the researchers compared FLCs with simple PI (proportional-integral) or PID (proportional – integral - differential) controllers [6, 8, 9, 20]. In all literature, results show that FLCs are more efficient than other controllers. In the research described in [11] two distinct types of FLC, i.e., Mamdani and Takagi-Sugeno-Kang, are used and evaluated. The authors underline the superiority of the Mamdani approach. In [15] the authors present the results of a simulation-based study, in which they assessed a FLC using triangular and trapezoidal fuzzy numbers. At the end, the conclusion was that the use of trapezoidal numbers gives better results. The above-mentioned studies do not analyze the influence of diverse types of fuzzy numbers and defuzzification methods on the FLC efficiency. Consequently, the research presented in this article had as goal to analyze how diverse types of fuzzy numbers, decision-making and defuzzification methods affect the efficiency of a FLC dedicated to VAR compensation.

The contributions of the research presented in this paper are assessment of the impact of fuzzy logic numbers, decision-making and defuzzification methods on the efficiency of a FLC dedicated to the reactive power control at consumers' side.

The rest of the paper has the following structure: second section, Background, contains aspects regarding VAR compensation and fuzzy logic controllers. The third section, Design of fuzzy logic control, describes the structure of the FLC and diverse types of fuzzy numbers, decision-making and defuzzification methods. The fourth section, Results and Discussions, presents and analyzes the obtained results and finally the fifth section, Conclusions, ends the paper with the main findings of the research.

II. BACKGROUND

A. Reactive power compensation devices

The simpler method to realize VAR compensation is by using fixed steps capacitor banks (FCBs). Other electronic based technologies for VAR compensation are the Static VAR Compensators (SVCs), and the newest ones: Static Synchronous Compensators (STATCOM), and Unified Power Flow Controllers (UPFC). These devices are connected in parallel with the loads, as Fig. 1 illustrates. One can observe in the picture that the VAR compensator is a fixed capacitor (FC) or an SVC that consists of a capacitor and reactor switched using thyristors or a STATCOM that can have diverse architectures. The role of the devices, indifferently of their construction, is to inject in the common-coupling point reactive power and balance it; thus, to have the power factor above the required threshold. The control of these devices one can does employ conventional controllers like PI / PID or FLC. An example of FCBs controlled with thyristors that get the firing angles from a FLC is proposed in [15]. The authors from [11] suggest an SVC that is a combination of a TSC and TSR for VAR compensation where the capacitor is simple-switched, and the reactor is controlled with the help of the thyristors to which the firing angles are fed by a FLC. Again, [9] suggests simple FCBs that compose the VAR compensator whose steps the authors control using a FLC.

B. Fuzzy logic controllers

Fuzzy logic controllers consist of three blocks: (1) Fuzzification block, (2) Inferences block and (3) Defuzzification block, which Fig. 2 illustrates. The fuzzification block contains the fuzzy numbers for the data that the FLC works with. The most utilized fuzzy numbers are triangular and trapezoidal, due to their simplicity. But there are other kinds of fuzzy numbers that one can use for the input and output data. The choice of the types of fuzzy numbers depends on the variations of the data that are being fuzzified. Table 1 presents five types of fuzzy numbers with their analytical and graphical representations. The Inferences block contains rules which describe the relations between the inputs and outputs. Here, during the functioning of the FLC, it is described the way the rules should be analyzed, more specifically how the key words “and,” “or” and “then” are seen, as “minimum,” “maximum,” “summation” or “product” (decision-making process).

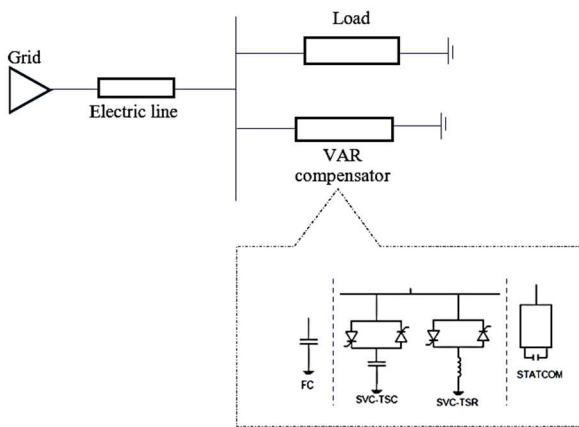
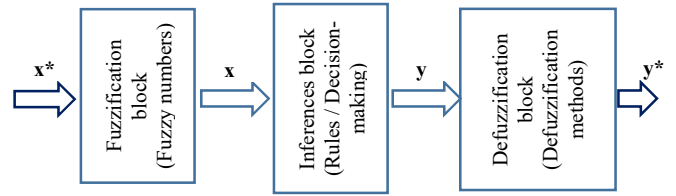


Fig. 1. Principle of shunt VAR compensation at consumers's side



x^* - input data, physical quantity.
 x - set of variables, fuzzy numbers.
 y - fuzzy surface.
 y^* - output data, physical quantity.

Fig. 2. Structure of a typical fuzzy logic controller

TABLE I. FUZZY NUMBERS [21]

No	Fuzzy number		
	Name	Mathematical representation	Graphic representation
1	Triangular	$\mu(x) = \begin{cases} 0, & x < 3 \\ \frac{x-3}{6-3}, & 3 \leq x \leq 6 \\ \frac{8-x}{8-6}, & 6 < x \leq 8 \\ 0, & x > 8 \end{cases}$	 trimf, P = [3 6 8]
2	Trapezoidal	$\mu(x) = \begin{cases} 0, & x < 1 \\ \frac{x-1}{5-1}, & 1 \leq x \leq 5 \\ 1, & 5 < x \leq 7 \\ \frac{8-x}{8-7}, & 7 < x \leq 8 \\ 0, & x > 8 \end{cases}$	 trapmf, P = [1 5 7 8]
3	Gaussian	$\mu(x) = e^{-\frac{(x-5)^2}{2 \cdot 2^2}}$	 gaussmf, P = [2 5]
4	Product of two sigmoidal	$\mu(x) = \frac{1}{1 + e^{-2(x-3)}} \cdot \frac{1}{1 + e^{5(x-8)}}$	 psigmf, P = [2 3 -5 8]
5	Pi curve	$\mu(x) = \begin{cases} 0, & x \leq 1 \\ 2 \left(\frac{x-1}{4-1} \right)^2, & 1 \leq x \leq \frac{1+4}{2} \\ 1 - 2 \left(\frac{x-4}{4-1} \right)^2, & \frac{1+4}{2} < x \leq 7 \\ 1, & 4 \leq x \leq 5 \\ 1 - 2 \left(\frac{x-5}{10-5} \right)^2, & 5 \leq x \leq \frac{5+10}{2} \\ 2 \left(\frac{x-10}{10-5} \right)^2, & \frac{5+10}{2} \leq x \leq 8 \\ 0, & x \geq 8 \end{cases}$	 pimf, P = [1 4 5 10]

a - Membership function of the fuzzy number from the fourth column

The defuzzification block is the FLC's component that has as input data the fuzzy surface obtained after the rules' execution and outputs a single data that one can use further. There are different methods to realize the defuzzification, like, center of gravity, center of surface and heights methods. Hence, when building and using a FLC, one must choose between diverse types of fuzzy numbers, defuzzification and decision-making methods; the choices differ on the application of the FLC.

In literature, the most used method to present the usefulness of FLC is by simulations. Addressing this approach, one can employ the Fuzzy Logic Toolbox (FLT) offered by MATLAB and assess it with the help of Simulink / MATLAB. This methodology one can find also in [6, 9, 11,

15, 20]. The FLT gives the possibility to use a wide variety of fuzzy numbers, decision-making and defuzzification methods. Consequently, in this research FLT is utilized, by employing four types of fuzzy sets: triangular (“trimf” in FLT), trapezoidal (“trapmf”), gaussian (“gaussmf”), and product of two sigmoidal (“psigmf”) fuzzy sets; Min-Max, Max-Prod and Sum-Prod decision-making methods and center of gravity (centroid) and center of surface (bisector) [21]. Regarding the decision-making methods that one can select with the help of the “And method,” “Or methods,” “Implication” and “Aggregation” fields (1 to 4 from Fig. 5), the FLC applies three types of decision-making methods: Max-Min, Max-Prod and Sum-Prod with the following characteristics:

- Max-Min: And methods is min, Or method – max, Implication – min, and Aggregation – max.
- Max-Prod: And methods is min, Or method – max, Implication – prod, and Aggregation – max.
- Sum-Prod: And methods is prod, Or method – sum, Implication – prod, and Aggregation – sum.

Concerning the defuzzification methods (5 from Fig. 5), the FLC utilizes two methods: centroid and bisector.

III. SIMULATION MODEL

To realize the analysis of the FLC, a Simulink model of a distribution power system that the authors from [11] propose is used. From Fig. 3 that illustrates the Simulink model, one can observe a single-phase ac power source (230 V), an electric line and three inductive-resistive loads connected to the distribution system through switches, having the loadings: Load 1 – $P=650$ W, $Q=500$ VAR; Load 2 – $P=200$ W, $Q=600$ VAR; Load 3 – $P=50$ W, $Q=200$ VAR. The two switches work as follows: the switch of load two is on at 0.4 s and off at 1.2 s and the switch of load three is on 0.8 s and off at 1.6 s. Fig. 4 pictures the variations of the active, reactive, and apparent powers respectively, and the values of the power factor at the loads side in the case that no VAR compensation is made.

The model also includes a VAR compensator, more specifically an SVC. The SVC contains two types of branches: simple switched capacitors and a thyristor-controlled reactor (TCR). The FLC, displayed in Fig. 5 controls the functioning of the TCR. The functioning of the VAR compensator is as follows: the capacitors that have the corresponding capacitance to balance the reactive power of the loads are switched on when the power factor is below the 0.9 threshold. Next, the reactor with its inductance balances the capacitor bank to maintain the power factor above 0.9. The FLC is the component that gives the thyristors the correct firing angle to obtain the matching amount of reactive power.

The fuzzy logic controller, named FLC_Q is of Mamdani type and has two inputs and one output. The inputs correspond to the reactive power and initial firing angle of the thyristors and the output is the final firing angle for the thyristors. Fig. 6 and 7 illustrate the membership functions of the inputs and output, and the fuzzy surface. The FLC is like the fuzzy logic controller presented in [11]; the difference is that it uses diverse fuzzy sets, decision-making and defuzzification methods. More specifically, it uses the four memberships functions above-mentioned, also the three decision-making and the two defuzzification methods. Accordingly, the research uses twenty-four variants of the FLC_Q, with the

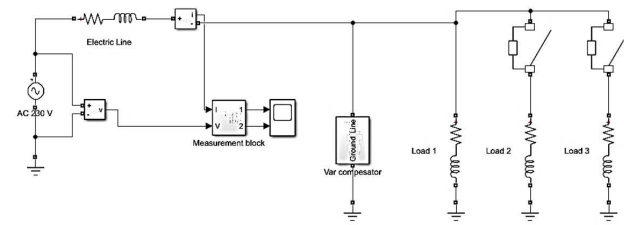


Fig. 3. Simulink model

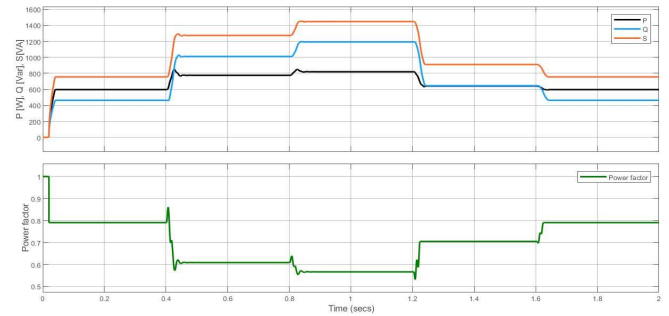


Fig. 4. The variation of the active, reactive, apparent power and power factor at loads side with no compensation

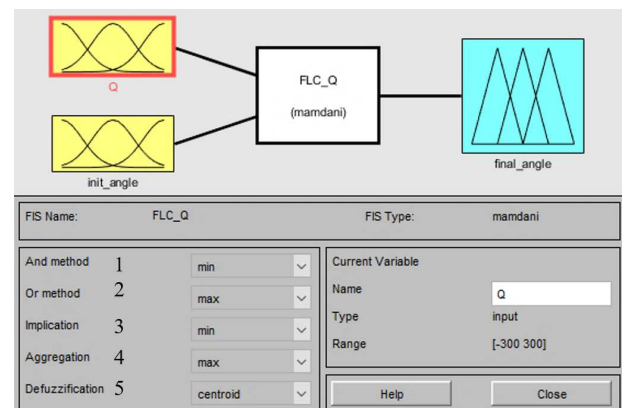


Fig. 5. The structure of the Mamdani fuzzy logic controller. 1-And methods, 2 – Or method, 3 – Implication, 4 –Aggregation, 5 – Defuzzification

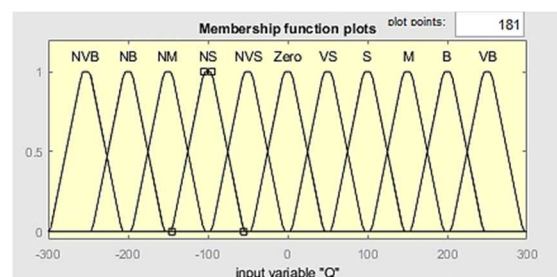


Fig. 6. Fuzzy membership functions of inputs and output for reactive power

observation that a variant contains a singular type of fuzzy sets for both the inputs and output. Table 2 enumerates the characteristics of the twenty-four FLCs.

The pictures from Fig. 6 and Fig 7 needs some explanations: Fig. 6 displays the trapezoidal fuzzy sets of the input 1 (reactive power Q) memberships functions; Fig. 7 A) shows the Gaussian fuzzy sets of the input 2 (initial angle) memberships functions; Fig. 7 B) illustrates the Product of two sigmoidal functions fuzzy sets of the output (final angle)

membership functions; and Fig. 7 C) displays the fuzzy surface obtained when the inputs and output are using triangular fuzzy sets for their memberships functions and the decision-making method is the Sum-Prod method.

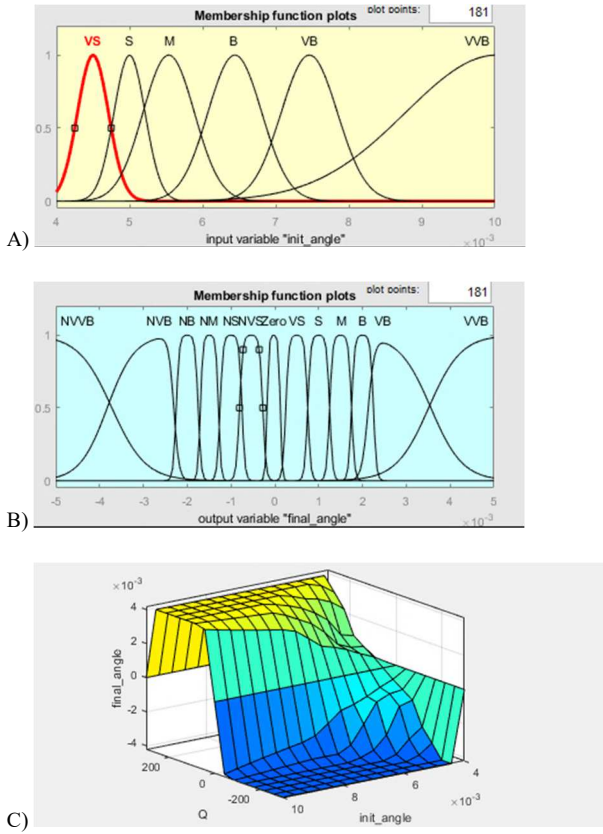


Fig. 7. Fuzzy membership functions of inputs and output for A) Initial angle, B) Final angle, and C) Fuzzy surface

TABLE II. THE 24 FUZZY LOGIC CONTROLLERS

No	Fuzzy sets ^a				Decision-making method ^b			Defuzzification method ^c	
	1	2	3	4	I	II	III	A	B
1	+				+			+	
2		+			+			+	
3			+		+			+	
4				+	+			+	
5	+				+				+
6		+			+				+
7			+		+				+
8				+	+				+
9	+					+		+	
10		+				+		+	
11			+			+		+	
12				+		+		+	
13	+					+			+
14		+				+			+
15			+			+			+
16				+		+			+
17	+						+	+	
18		+					+	+	
19			+				+	+	
20				+			+	+	
21	+						+		+
22		+					+		+
23			+				+		+
24				+			+		+

^a 1-trimf, 2-trapmf, 3-gaussmf, 4-psigmf.

^b I - Min-Max, II-Max-Prod, III-Sum-Prod.

^c A-centroid, B-bisector

IV. RESULTS AND DISCUSSIONS

The first step of the analysis is to assess the FLC_Q applying the approach used in [15] and the data from [11], named test-data. Fig. 8 illustrates the results that show the output of the FLC_Q and underline the accuracy of the designed FLC. One can see that there is no distinction between the results obtained by the authors from [11] and FLC_Q.

Next in the analysis, the FLC_Q's twenty-four variants are run on the test-data. The graphics from Fig. 9 demonstrate that there are significant differences between the results. One can detect that the type of fuzzy sets has the biggest influence upon the FLC's outputs. Between the FLC's variants with the same fuzzy sets, i.e., 1, 5, 9, 13, 17, and 21, the defuzzification method has a greater impact, in comparison with the decision-making method. Indeed, one can see minor differences between 1, 9 and 17. But, in the case of other types of fuzzy sets, i.e., 3, 7, 11, 15, 19, and 23, it is the opposite. Thus, there is a close correlation between the type of fuzzy sets and the decision-making and defuzzification methods, that they are associated with.

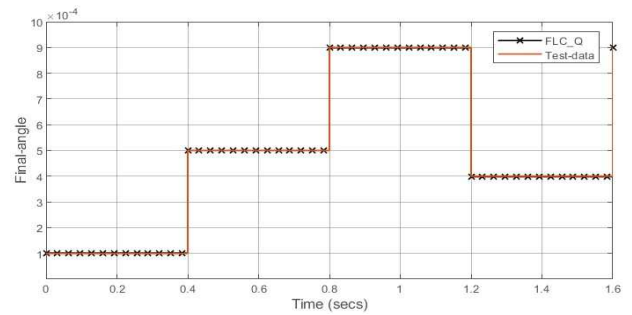


Fig. 8. Comparison of the outputs of FLC_Q and test-data

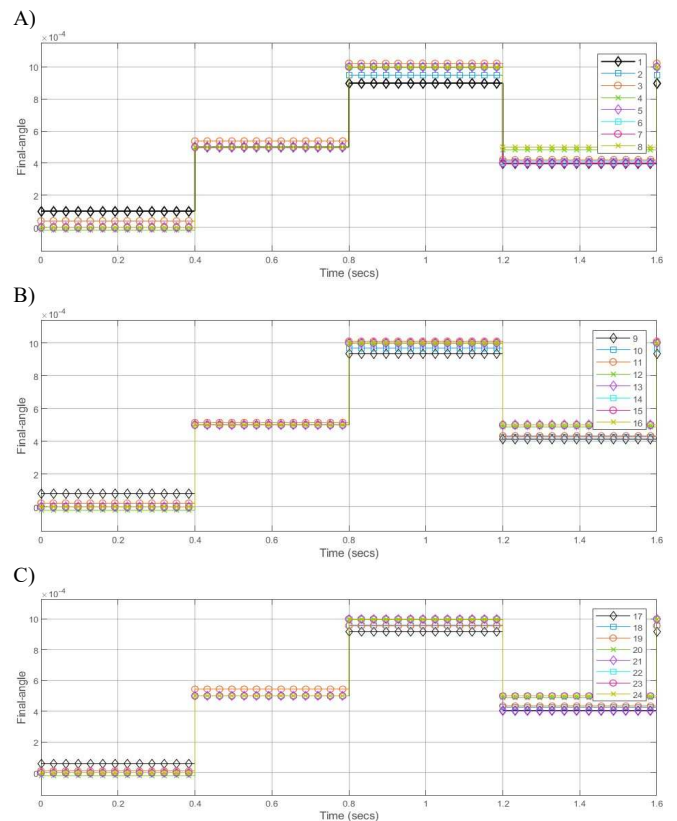


Fig. 9. Comparison between the outputs of FLC_Q's variants 24 using the test-data. A) 1-8, B) 9-16 and C) 17-24

At the end of the research, the twenty-four variants of the FLC_Q were used to control the VAR compensation in the circuit from Fig. 3 and data (simulation-data) from Fig. 4.

Fig. 10 illustrates the output values when running the FLC_Qs on the Simulink model. One can see that there are differences between the results, principally in relation to the fuzzy sets. This is evident especially during the intervals 0 – 0.4 s, 0.8 – 1.2 s, and 1.6 – 2 s in all twenty-four scenarios. Significant variations appear also because of the decision-making methods, which have a bigger influence on the outputs in contrast to the defuzzification methods. The 1.6-2 s interval shows this aspect very clearly. Thus, analyzing the decision-making methods' results, one can observe that more differentiations between the outputs appear in the case of the Sum-Prod method, i.e., cases 17-24. Regarding the defuzzification methods, the results show diverse tendencies, that are related with the type of fuzzy sets.

Fig. 11 shows the power factor values, having as main criterion the decision-making methods, then the defuzzification and finally the types of memberships fuzzy sets. The first thing that attracts the attention is that in not all cases the FLC_Q variants control properly the VAR compensation, as the reactive compensator does not maintain the power factor above the threshold of 0.9. This phenomenon appears especially in the cases when the FLCs use gaussmf and psigmf memberships functions (see cases 3, 4, 11 and 12). When comparing the defuzzification methods, the bisector method gives better results than the centroid method (see cases 4 and 8). Assessing the decision-making methods, the Sum-Prod method gives the best results, whereas the Max-Prod has the worst.

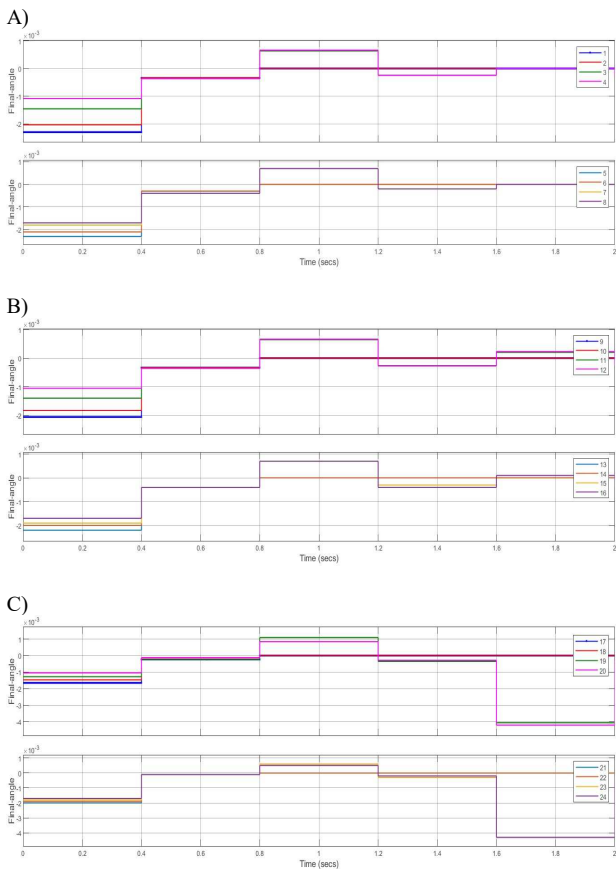


Fig. 10. Comparison between the outputs of FLC_Q's 24 variants using the simulation-data. A) 1-8, B) 9-16 and C) 17-24

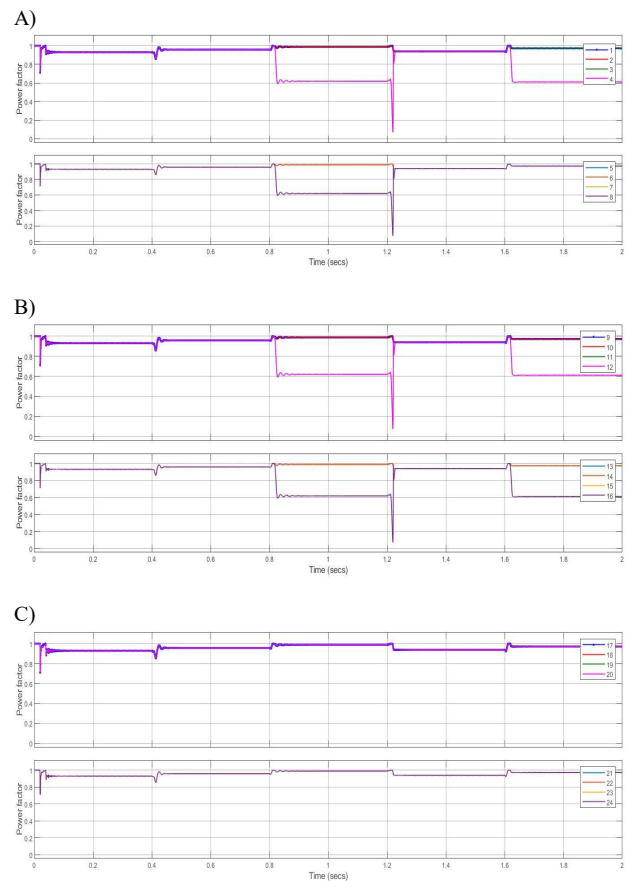


Fig. 11. Comparison between the power factor's values of FLC_Q's 24 variants using the simulation-data. A) 1-8, B) 9-16, C) 17-24

V. CONCLUSIONS

The paper presents an application of fuzzy logic control in VAR compensation at the consumer's side by employing Simulink and Fuzzy Logic Toolbox from MATLAB, and the analysis of the efficiency of the FLC. A simple single-phase model and a Mamdani fuzzy logic controller are designed for this purpose. The FLC has two inputs and one output; it commands the firing angle of an SVC used in the VAR compensation process. The FLC has twenty-four variants obtained by combining four types of fuzzy sets (triangular, trapezoidal, gaussian and product of two sigmoidal functions), three decision-making methods (Max-Min, Max-Prod and Sum-Prod) and two defuzzification methods (center of gravity and center of surfaces). The efficacy of the FLC is evaluated and demonstrated clearly. The results of the simulations demonstrate that the FLC gives a reliable performance in the power factor correction. The efficiency of the FLC's variants is evaluated and the results show that the type of fuzzy sets influence the most the FLC's efficiency. The defuzzification and decision-making methods impact the FLC's performance depending on the type of fuzzy sets they associate with.

The contributions of the research presented in the paper in comparison with the literature are the clear presentation of an FLC's features that one should consider when using fuzzy logic control and the analysis of a FLC's performance used in VAR compensation regarding the controller's characteristic components.

The main conclusion of the study is that when designing an FLC, one must study diverse types of fuzzy sets,

defuzzification and decision-making methods to determine the most appropriate for the application.

A future work that the authors consider is the analysis of the combination of diverse types of fuzzy sets in a FLC, as the proposed FLC contains in a variant only a single type of membership function.

ACKNOWLEDGMENT

This work was supported by a grant of the Ministry of Research, Innovation and Digitalization, CCCDI – UEFISCDI, project number PN-III-P2-2.1-PED-2021-4309, within PNCDI III.

REFERENCES

- [1] J. Dixon, L. Moran, J. Rodriguez and R. Domke, "Reactive Power Compensation Technologies: State-of-the-Art Review," *Proceedings of the IEEE*, vol. 93, no. 12, pp. 2144-2164, Dec. 2005, doi: 10.1109/JPROC.2005.859937.
- [2] A. N. Madhavanunni, J. Baby, S. S. Arya, J. George, J. George and D. R. Kumar, "Fuzzy logic controller for reactive power compensation," 2015 International Conference on Control Communication & Computing India (ICCC), Trivandrum, India, 2015, pp. 54-59, doi: 10.1109/ICCC.2015.7432869.
- [3] X. Zhou, K. Wei, Y. Ma and Z. Gao, "A Review of Reactive Power Compensation Devices," 2018 IEEE International Conference on Mechatronics and Automation (ICMA), Changchun, China, 2018, pp. 2020-2024, doi: 10.1109/ICMA.2018.8484519.
- [4] L. Wenxue et al., "Reactive Power Optimization in Distribution Network Considering Reactive Power Regulation Capability and Fuzzy Characteristics of Distributed Generators," 2019 4th International Conference on Power and Renewable Energy (ICPRE), Chengdu, China, 2019, pp. 387-393, doi: 10.1109/ICPRE48497.2019.9034695.
- [5] J. A. Momoh, X. W. Ma and K. Tomsovic, "Overview and literature survey of fuzzy set theory in power systems," *IEEE Transactions on Power Systems*, vol. 10, no. 3, pp. 1676-1690, Aug. 1995, doi: 10.1109/59.466473.
- [6] V. Dhyani and S. Arora, "Application of fuzzy logic control for reactive power and D.C. capacitor voltage control of Doubly Fed Induction Generator during external faults," 2013 Annual IEEE India Conference (INDICON), Mumbai, India, 2013, pp. 1-5, doi: 10.1109/INDICON.2013.6725911.
- [7] M. Golkhah and R. P. Torghabeh, "Dynamic reactive power compensating based on fuzzy logic in power transmission grids," 2008 IEEE International Conference on Industrial Technology, Chengdu, China, 2008, pp. 1-7, doi: 10.1109/ICIT.2008.4608320.
- [8] H. Zenk and A. S. Akpınar, "PI, PID and fuzzy logic controlled SSSC connected to a power transmission line, voltage control performance comparison," 4th International Conference on Power Engineering, Energy and Electrical Drives, Istanbul, Turkey, 2013, pp. 1493-1497, doi: 10.1109/PowerEng.2013.6635836.
- [9] H. B. Guliyev, "Reactive Power Adaptive Control System in Networks with Distributed Generation Based on Fuzzy Set Theory," 2019 International Artificial Intelligence and Data Processing Symposium (IDAP), Malatya, Turkey, 2019, pp. 1-5, doi: 10.1109/IDAP.2019.8875963.
- [10] Zigang Xu and Fei Wang, "Research on fuzzy logic based dynamic boundary voltage and reactive power integrated control method," 2009 Chinese Control and Decision Conference, Guilin, 2009, pp. 1645-1649, doi: 10.1109/CCDC.2009.5192237.
- [11] S. Khanmohammadi, M. T. Hagh and M. Abapour, "Fuzzy logic based SVC for reactive power compensation and power factor correction," 2007 International Power Engineering Conference (IPEC 2007), Singapore, 2007, pp. 1241-1246.
- [12] H. Mohan, M. K. Pathak and S. K. Dwivedi, "Reactive Power Based Speed Control of Induction Motor Drive using Fuzzy Logic for Industrial Applications," 2020 IEEE International Conference on Power Electronics, Smart Grid and Renewable Energy (PESGRE2020), Cochin, India, 2020, pp. 1-5, doi: 10.1109/PESGRE45664.2020.9070692.
- [13] Xu Yan, Liu Qing, Wang Fei and Zhang Kunbo, "Research on substation reactive power control with the fuzzy logic method," 2005 International Power Engineering Conference, Singapore, 2005, pp. 1-66, doi: 10.1109/IPEC.2005.206880.
- [14] P. Peng, S. -p. Su, X. Luo and L. -q. Fan, "Study on Fuzzy Dynamic Programming for Optimization of Reactive Power Compensation of Power System Including Distributed Generation," 2008 International Conference on Intelligent Computation Technology and Automation (ICICTA), Changsha, China, 2008, pp. 931-935, doi: 10.1109/ICICTA.2008.443.
- [15] Hua Li, Ruizheng Gu, Che Wen and Xuehui Zhang, "Study on control strategy of TSC reactive power compensator based on fuzzy control," 2016 International Conference on Fuzzy Theory and Its Applications (iFuzzy), Taichung, 2016, pp. 1-6, doi: 10.1109/iFUZZY.2016.8004951.
- [16] Z. Mi and F. Wang, "Substation Reactive Power and Voltage Control Using Fuzzy Control Theory," 2009 International Conference on Industrial and Information Systems, Haikou, China, 2009, pp. 417-420, doi: 10.1109/IIS.2009.85.
- [17] M. A. Djema, M. Boudour, K. Agbossou, A. Cardenas and M. L. Doumbia, "Fuzzy Logic Based Reactive Power Management for Autonomous MicroGrid," 2018 IEEE 27th International Symposium on Industrial Electronics (ISIE), Cairns, QLD, Australia, 2018, pp. 1249-1254, doi: 10.1109/ISIE.2018.8433692.
- [18] W. Zhang and Y. Liu, "Fuzzy logic controlled particle swarm for reactive power optimization considering voltage stability," 2005 International Power Engineering Conference, Singapore, 2005, pp. 1-555, doi: 10.1109/IPEC.2005.206969.
- [19] K. Arya and K. R. M. V. Chandrakala, "Fuzzy logic controller based instantaneous p-q theory for power quality improvement," 2017 International Conference on Technological Advancements in Power and Energy (TAP Energy), Kollam, India, 2017, pp. 1-4, doi: 10.1109/TAPENERGY.2017.8397354.
- [20] B. S. Rao, P. K. Gouda, S. S. Rao and K. Manohar, "Reactive Power Control in Hybrid System Using Fuzzy Logic Control," 2022 International Conference on Intelligent Controller and Computing for Smart Power (ICICCS), Hyderabad, India, 2022, pp. 1-6, doi: 10.1109/ICICCS2022.9862339.
- [21] J.-S. R. Jang, N. Gulley, MATLAB, Fuzzy Logic Toolbox, version 1, 1997, The MathWorks Inc.



Effects of voltage unbalance and harmonics on drive systems with induction motor

Horia G. Beleiu, Sorin G. Pavel, Iulian M. T. Birou, Anca Miron, Pompei C. Darab & Mohammed Sallah

To cite this article: Horia G. Beleiu, Sorin G. Pavel, Iulian M. T. Birou, Anca Miron, Pompei C. Darab & Mohammed Sallah (2022) Effects of voltage unbalance and harmonics on drive systems with induction motor, Journal of Taibah University for Science, 16:1, 381-391, DOI: [10.1080/16583655.2022.2064670](https://doi.org/10.1080/16583655.2022.2064670)

To link to this article: <https://doi.org/10.1080/16583655.2022.2064670>



© 2022 The Author(s). Published by Informa UK Limited, trading as Taylor & Francis Group.



Published online: 20 Apr 2022.



Submit your article to this journal [↗](#)



Article views: 2295



View related articles [↗](#)



View Crossmark data [↗](#)



Citing articles: 4 View citing articles [↗](#)

Effects of voltage unbalance and harmonics on drive systems with induction motor

Horia G. Beileu^a, Sorin G. Pavel^a, Iulian M. T. Birou^b, Anca Miron^a, Pompei C. Darab^a and Mohammed Sallah^{c,d}

^aDepartment of Electric Power Systems and Management, Technical University of Cluj-Napoca, Cluj-Napoca, Romania; ^bDepartment of Electric Machines and Drives, Technical University of Cluj-Napoca, Cluj-Napoca, Romania; ^cApplied Mathematical Physics Research Group, Physics Department, Faculty of Science, Mansoura University, Mansoura, Egypt; ^dHigher Institute for Engineering and Technology, New Damietta, Egypt

ABSTRACT

Due to the significant share of the induction motors (IMs) in global electricity consumption, the study of the IM in different power supply regimes is the aim of this work. In practice, these electrical receivers are not supplied from ideal voltage systems, therefore the power quality (PQ) is an important aspect in analysing the operation of this type of motors. We proposed a methodology for analysing the effects of unbalanced distorted voltages not only on the technical parameters of the IM but also on the power supply as well as on the driven mechanical system. We identified some dependencies, in analytical forms, between the sizes of interest and the considered PQ disturbances. The results showed that the supply voltage disturbances have significant effects on the induction motor, both electrically and mechanically. These effects are amplified if the IM is running at loads below 50% of the rated load.

ARTICLE HISTORY

Received 29 October 2021
Revised 31 January 2022
Accepted 6 April 2022

KEYWORDS

Induction motor; drive system; harmonics; voltage unbalance; efficiency; electromagnetic torque

1. Introduction

Power Quality (PQ) is an important aspect regarding the electromechanical receivers due to the significant share of these receivers in general electricity consumption. Electric motors and the systems they drive are the largest electrical end-use. It is estimated that the electric motor-driven systems (EMDS) account for more than half of the electricity consumed worldwide [1].

Induction motors (IMs) account for around 70% of the energy consumption of industry worldwide; thus, improving their efficiency will reduce the global consumption of electricity. There is a huge potential for energy efficiency in EMDS – around 30% of EMDS electricity use could be saved cost-effectively – which would reduce total global electricity demand by about 10% [2].

The mechanical speed of the IM is directly coupled to the frequency of the supply voltage, which limits its flexibility when supplied directly from the grid. Only about 25% of the installed IMs are supplied from power converters [3]. For IMs supplied directly from the grid, it is important to establish the tolerability limits for the different PQ disturbances, and to identify those disturbances leading to power losses, both in the machine itself and in the power grid.

The voltage unbalance represents a condition in which the three-phase voltages (or currents) differ in amplitude or displaced from their normal 120° phase

relationship or both [4]. This is a common situation in three-phase systems, and the operation of an IM is affected by the positive and negative sequence components. The negative sequence currents create a flux rotating in the direction opposite to the rotor. This flux causes increased heating, additional losses, and additional torque operating in the opposite direction to the torque produced by the positive sequence flux [4].

Harmonics is another common phenomenon in power systems. A harmonic is defined as a component with a frequency that is an integer multiple of the fundamental frequency [4]. Rotating machines are exposed to thermal effects from harmonics. Additional torque ripples are induced by the interaction between the fundamental component of the air gap flux and the harmonics currents, of the positive and negative sequences [5].

There are many studies about reducing losses and increasing the efficiency of the IM. For instance, the increasing of the IM efficiency can be achieved at every design parameter of the machine, and the PQ of the power supply should also be considered. The impact of voltage unbalance on the performance of the IMs and the systems they drive was studied [6–11].

The effect of two voltage unbalance conditions on the losses in the core of the IM was analysed [12]. The results showed that the positive sequence voltage level

has more influence on the core losses of the IM than the voltage unbalance. Whereas the effects of the positive, negative, and zero components on the torque and efficiency of the three-phase IM were evaluated [13]. Moreover, the effects on the operation performance of an IM for different unbalanced situations, considering both the negative and positive sequences are analysed [14–16].

There was a procedure presented [17] that was based on the equivalent circuits with losses segregation and using a bacterial foraging algorithm (BFA). The additional harmonic losses of the IM with the machine initial efficiency rating are evaluated in [18,19]. It was found that the increase in losses is higher in the SCIM IE3 than in the SCIM IE1. The derating factors for IM when supplied with harmonics are studied in Ref. [20]. They stated that for lower loading of the IM, the derating factors, like the NEMA MG1 or the IEC 60034-17, can underestimate the losses.

Prior research cover algorithms for efficiency estimation of IMs operating with unbalanced and distorted voltages [21,22]. In addition, the effects of harmonics and voltage unbalance on the useful life of electrical motors are presented using a simplified equivalent circuit to calculate the additional heat losses caused by power supply distortions [23]. The electromagnetic loss properties of the induction motor under unbalanced and distorted supply voltage were studied also [24].

Another study presented a comparison of the life expectancy of IE2, IE3, and IE4 Class motors under the distorted unbalanced power supply [25]. They stated that the high-efficiency motors offer an increased level of reliability and reduced maintenance requirements. The effects of voltage unbalance and harmonics on the losses of the IMs in different efficiency classes were studied [26]. It was concluded that the losses of the IM due to voltage unbalance and harmonics are greater in the higher efficiency class of IMs.

However, many of the above-mentioned studies that are based on practical experiments usually have the percent voltage unbalance or harmonic content introduced by a programmable power supply. Even if the practical setups for simulating the mentioned disturbances are chosen to reproduce common situations encountered in industry, it is not enough to achieve a systematic simulation of the PQ disturbances, considered.

In our previous work [27], we analysed the harmonic consequences on the IM. The harmonic distortion of stator current, the electromagnetic torque, the power factor (PF), and the efficiency of IM, operating in harmonics were followed.

In this work, we propose a systematic analysis of the effects of voltage unbalance and harmonics on the IM. For analysing the IM operating under unbalanced distorted voltages, we consider the following hypothesis:

Table 1. Parameters of the IM.

Symbol	Quantity	Value
P_n	nominal power	4 kW
V_n	nominal line-to-line voltage	400 V
f_n	nominal frequency	50 Hz
N_n	rated speed	1430 rpm
R_s	stator resistance	1.405 Ω
L_s	stator inductance	0.005839 H
R_r'	rotor resistance	1.395 Ω
L_r'	rotor inductance	0.005839 H
L_m	mutual inductance	0.1722
J	inertia	0.0131 kg·m ²
F	friction factor	0.002985 N·m·s
P	pole pairs	2
$\cos\varphi_n$	nominal power factor	0.82
η_n	nominal efficiency	88.5%

- The reference case, when the stator of the IM is supplied from balanced sinusoidal voltages, at grid frequency; the motor operates static at determined constant torque and speed.
- The case when the IM is supplied from unbalanced sinusoidal voltages.
- The case when the IM is supplied from balanced non-sinusoidal voltages.
- The case when the IM is supplied from unbalanced non-sinusoidal voltages, at different load percentage.

Section 2 presents the methodological aspects, and Section 3 is devoted for analysing the simulation results of the IM operating under different unbalanced conditions. Section 4 presents the consequences of the harmonics on the IM behaviour. The results obtained for the case when the IM is supplied from unbalanced distorted voltages are presented and discussed in Section 5. Finally, the conclusions and future research are presented in Section 6.

2. Methodological aspects

2.1. Modelling of the IM

We used the MATLAB/Simulink programming environment to simulate the IM under voltage unbalance and harmonics. We chose a medium-size squirrel-cage IM with a nominal power of $P_n = 4$ kW. Stator and rotor windings are star connected to an internal neutral point. The parameters of the IM are presented in Table 1.

The physical model is linear, regarding the inductivities, which are considered constant, so the phenomenon of saturation of the magnetic circuit is not considered here. The effective power factor (PF) for a three-phase non-sinusoidal and unbalanced system was calculated from the relation

$$\text{PF} = \frac{P}{S_e} = \frac{P}{3 \cdot V_e \cdot I_e} \quad (1)$$

where P is the total three-phase active power, including each frequency component, in W; S_e is the effective apparent power in the three-phase system, in VA; V_e is

the equivalent three-phase voltage, in V; I_e is the equivalent three-phase current, in A. The expressions for effective three-phase voltage and current shall be calculated from

$$V_e = \sqrt{\frac{V_a^2 + V_b^2 + V_c^2}{3}} \quad (\text{V}) \quad (2)$$

$$I_e = \sqrt{\frac{I_a^2 + I_b^2 + I_c^2}{3}} \quad (\text{A}) \quad (3)$$

where the voltages and currents represent the total rms phase values, including the fundamental and the harmonic content.

For the efficiency of the IM, we used the direct method, calculated as

$$\eta = \frac{P_{\text{out}}}{P_{\text{in}}} \cdot 100 = \frac{P_M - p_m}{P_{\text{in}}} \cdot 100 \quad (\%) \quad (4)$$

where P_{out} represents the output power, in W; P_{in} is the active input power, in W; P_M is the total power developed by the motor, in W; and p_m is the mechanical losses, in W.

We compute the output power with the equation

$$P_M = T_e \cdot \omega_m \quad (\text{W}) \quad (5)$$

where T_e is the electromagnetic torque, in N·m; and ω_m is the angular velocity of the rotor, in rad/s. The mechanical loss is determined from

$$p_m = F \cdot \omega_m^2 \quad (\text{W}) \quad (6)$$

with F represents the friction factor, in N·m·s.

2.2. Voltage unbalance

The rigorous appreciation of the unbalance regime can be made only with the symmetrical components, determined on the Stokvis-Fortescue Theorem. The voltage unbalance factor (VUF) was calculated with the following relationship [28]

$$\text{VUF} = \frac{V_{\text{neg}}}{V_{\text{pos}}} \cdot 100 \quad (\%) \quad (7)$$

where V_{neg} is the negative sequence voltage component and V_{pos} is the positive sequence voltage component.

We analysed the effects of the unbalance regime on the IM for $\text{VUF} \in 1, 2, 3, 4, 5\%$. Given that for the same value of VUF there are possible several situations, we considered three different conditions for each value of the VUF (1) different amplitudes and equal phase shifts; (2) equal amplitudes and different phase shifts; and (3) different amplitudes and different phase shifts. Because the magnitude of the positive sequence influences the IM behaviour differently for the same VUF, the above-mentioned unbalance conditions were chosen with the relation between the positive sequence

Table 2. VUF and the three-phase supply voltages for different types of voltage unbalance.

Unbalance Conditions	VUF (%)	V_a	V_b	V_c
different amplitudes, equal phase shifts, $V_{\text{pos}} < V_{\text{phn}}$	1	215∠0°	211.35∠-120°	207.7∠120°
	2	222∠0°	212.01∠-120°	207.57∠120°
	3	229∠0°	213.2∠-120°	207.25∠120°
	4	237∠0°	216.14∠-120°	207.38∠120°
	5	246∠0°	222.14∠-120°	207.38∠120°
equal amplitudes, different phase shifts, $V_{\text{pos}} = V_{\text{phn}}$	1	230∠0°	230∠-119°	230∠122°
	2	230∠0°	230∠-122°	230∠116°
	3	230∠0°	230∠-123°	230∠114°
	4	230∠0°	230∠-123.9°	230∠112.2°
	5	230∠0°	230∠-124.9°	230∠110.2°
different amplitudes, different phase shifts, $V_{\text{pos}} > V_{\text{phn}}$	1	240∠0°	235.2∠-119.7°	232.8∠120.6°
	2	240∠0°	235.2∠-118.3°	232.8∠123.4°
	3	240∠0°	235.2∠-117.3°	232.8∠125.4°
	4	240∠0°	235.2∠-116.2°	232.8∠127.6°
	5	240∠0°	235.2∠-115.1°	232.8∠129.8°

component and the nominal phase voltage V_{phn} , as follows:

- (1) different amplitudes and equal phase shifts, with $V_{\text{pos}} < V_{\text{phn}}$;
- (2) equal amplitudes and different phase shifts, with $V_{\text{pos}} = V_{\text{phn}}$;
- (3) different amplitudes and different phase shifts, with $V_{\text{pos}} > V_{\text{phn}}$.

The considered unbalanced scenarios, for simulating the IM under voltage unbalance, are presented in Table 2. In the table are shown the modules and displacement angles of the three phase-to-neutral voltages.

2.3. Harmonics

Harmonic distortion of a non-sinusoidal waveform can be determined by calculating the total harmonic distortion (THD), which represents the ration between the rms of the harmonic content and the rms value of the fundamental, expressed as a percent of fundamental, with the relation [28]

$$\text{THD} = \frac{\sqrt{\sum_{h=2}^{h_{\text{max}}} Y_h^2}}{Y_1} \cdot 100 \quad (\%) \quad (8)$$

where Y_h is the rms of the harmonic component of h order of quantity Y , which can be a voltage or current waveform. For analysing the IM behaviour under harmonics, in the supply voltages we superimposed harmonics of order $h \in 5, 7, 11, 13$, over the fundamental. The harmonics of the 5th and 11th orders are of negative sequence, and the 7th and 13th orders are of positive sequence. Firstly, we injected each considered harmonic one by one, and then combinations of them, with $\text{THD}_V \in 5, 10, 15, 20\%$, as presented in Table 3. The total rms value of voltage, including the fundamental and the harmonics, was maintained at nominal value.

Table 3. Harmonic content in the supply voltage.

Harmonic Order h	V_h (% of fund.)	V_h (V)	V_1 (V)	THD_V (%)	V_{rms} (V)
5; 7; 11; 13	5.0	11.49	229.71	5	230.0
	10.0	22.88	228.85	10	230.0
	15.0	34.11	227.40	15	229.9
	20.0	45.07	225.35	20	229.8
(5 + 7)	4.0	9.20	229.71	5	230.0
	3.0	6.90			
(5 + 7)	8.0	18.40	228.85	10	230.0
	6.0	13.80			
(5 + 7)	12.0	27.60	227.40	15	230.0
	9.0	20.70			
(5 + 7)	16.0	36.80	225.35	20	230.0
	12.0	27.60			
(5 + 7 + 11 + 13)	3.9	9.00	229.71	5	230.0
	2.6	6.00			
	1.3	3.00			
	0.9	2.00			
(5 + 7 + 11 + 13)	7.8	18.00	228.85	10	230.0
	5.2	12.00			
	2.6	6.00			
	1.7	4.00			
(5 + 7 + 11 + 13)	11.7	27.00	227.40	15	230.0
	7.8	18.00			
	3.9	9.00			
	2.6	6.00			
(5 + 7 + 11 + 13)	15.7	36.00	225.35	20	229.9
	10.4	24.00			
	5.2	12.00			
	3.5	8.00			

Table 4. VUF and THD_V of the selected scenarios.

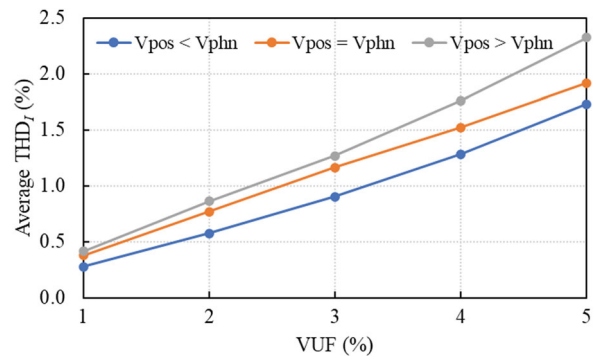
VUF (%)	THD_V (%)			
	5	10	15	20
1	S1	S2	S3	S4
3	S5	S6	S7	S8
5	S9	S10	S11	S12

2.4. Unbalanced and non-sinusoidal voltages

We chose to simulate the IM behaviour up to these limits of $VUF = 5\%$ and $THD_V = 20\%$, even if they exceed the admissible values from standards, because these limit values may occur in practice [29]. For studying the IM supplied from unbalanced distorted voltages we considered the following combinations of the VUF and THD, as presented in Table 4. For the unbalanced type, we used the case with different amplitudes and symmetrical angles with $V_{pos} < V_{phn}$. In the case of harmonic content, we considered that in the voltage waveforms are present both harmonics of orders 5 and 7, having the levels (percentage of fundamental) shown in Table 3.

3. Effects of voltage unbalance on the IM

In this section, we analyse the effects on the IM supplied from unbalanced voltages, running at 75% of rated load. The total harmonic distortion of the stator current (THD_I), the electromagnetic torque, the PF, and the efficiency of the IM are followed. For the three unbalanced situations, presented in Table 2, the results are further presented.

**Figure 1.** The average THD_I of the stator current with VUF.

3.1. Harmonic distortion of the stator current

The first analysed quantity is the harmonic distortion of the stator current. Due to voltage unbalance, the values of the stator currents of the three phases are different, so we compute the average value of the total harmonic distortion (THD_{Iav}) of the three phases. Figure 1 shows the dependency of the average value of THD_I for the three phases of the stator current with VUF, for the considered unbalanced situations. Due to the voltage system unbalance in the stator current is found in the harmonic of the third order. It can be observed from Figure 1 that the THD_{Iav} increases almost linearly with increasing VUF. Another observation is that for the same degree of unbalance, the values of THD_{Iav} differ with the magnitude of the positive sequence voltage. For example, when $VUF = 3\%$: $THD_{Iav} = 0.9\%$, for $V_{pos} < V_{phn}$; $THD_{Iav} = 1.16\%$, for $V_{pos} = V_{phn}$; and $THD_{Iav} = 1.27\%$ for $V_{pos} > V_{phn}$.

3.2. Electromagnetic torque of the IM

Voltage unbalance generates oscillations of electromagnetic torque at a frequency of two times higher than the nominal frequency. This torque component of the frequency of 100 Hz is due to currents of the negative sequence [30]. Figure 2 shows the amplitude (maximum absolute value of the difference from the dc component) of the torque oscillations, expressed as a percentage of the dc component of torque, with VUF. It can be observed that the torque oscillations increase linearly with increasing VUF. For $VUF = 5\%$, the frequency component of 100 Hz of the electromagnetic torque can reach: 54.4% of nominal torque for $V_{pos} < V_{phn}$; 57.6% for $V_{pos} = V_{phn}$; and 61.2% for $V_{pos} > V_{phn}$. To be noted that for the same value of VUF, the amplitude of the torque oscillations differs for two different unbalanced situations, $V_{pos} < V_{phn}$ and $V_{pos} > V_{phn}$, respectively, with values in the range of 11.02% to 22.75%. For example, for $VUF = 2\%$, the amplitude of torque oscillations represents 19.32% of dc component, when $V_{pos} < V_{phn}$, and 25.01%, for $V_{pos} > V_{phn}$, which means a difference of 22.75% between the two values of the amplitude of torque oscillations.

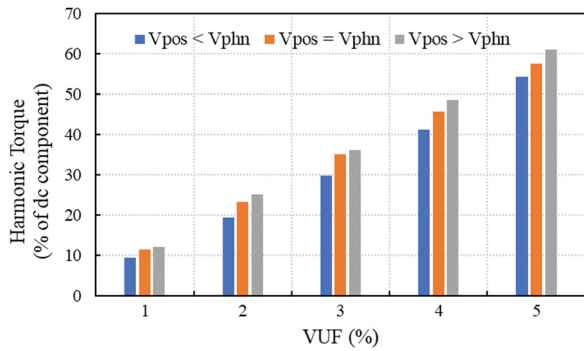


Figure 2. The amplitude of torque oscillations due to voltage unbalance.

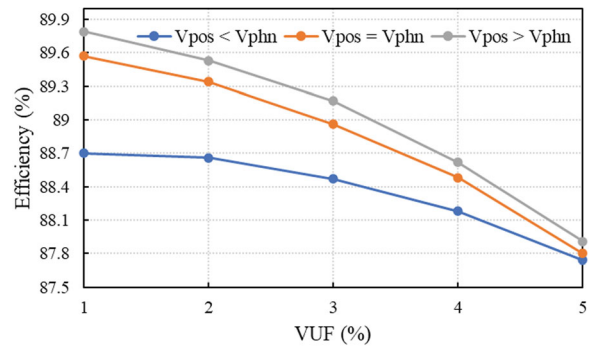


Figure 4. The efficiency of the IM due to voltage unbalance.

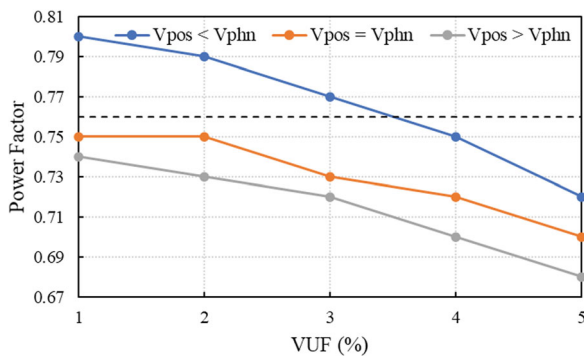


Figure 3. PF of the IM due to voltage unbalance.

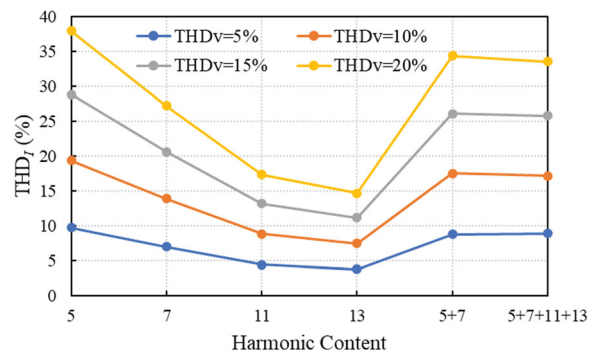


Figure 5. THD_I of the stator current with harmonic content and THD_V.

3.3. Power factor of the IM

Furthermore, we analyse the influence of the voltage unbalance on the PF of the IM. The PF variation with VUF is represented in Figure 3. In cat be observed that the PF decreases with increasing the VUF. To be noted that for the case when the $V_{pos} < V_{phn}$, the values of PF are higher than the nominal value $PF_n = 0.76$, for $VUF \in 1, 2, 3\%$; the values of PF are 0.75 and 0.72 for VUF of 4% and 5%, respectively. For the other two unbalance situations, the PF is lower than the nominal value (represented with the horizontal dashed line, in Figure 3). The differences obtained for the PF, in the considered types of unbalance, can be observed in Figure 3.

3.4. Efficiency of the IM

The efficiency of the IM running at 75% of rated load decreases with the increasing of VUF, as can be observed in Figure 4. The variation curves have a similar decreasing slope for the cases when $V_{pos} \geq V_{phn}$, but with lower values for $V_{pos} = V_{phn}$. In the case of $V_{pos} < V_{phn}$ the variation range of efficiency with VUF is narrower, but with values lower than the other two situations. The efficiency variation for the same unbalance factor, decreases with increasing of VUF and tending towards close values of efficiency for $VUF = 5\%$. The efficiency values for $VUF = 1\%$, for the cases, when $V_{pos} < V_{phn}$ and $V_{pos} > V_{phn}$, respectively, differ with 1.21%. To be noted that for $VUF = 5\%$, when

$V_{pos} < V_{phn}$, the efficiency is 87.74%, which means a decrease of $\Delta\eta\% = 2.13\%$ from the reference value $\eta_n = 89.65\%$. Another observation is that in the case of $V_{pos} > V_{phn}$ for $VUF = 1\%$, the efficiency is 89.79%, which is higher by 0.15% than the nominal value.

4. Effects of harmonics on the IM

4.1. Harmonic distortion of the stator current

The THD_I of the stator current depending on the voltage harmonic content and the THD_V is presented in Figure 5. The first remark is that in the stator current waveform are found harmonics of the same orders as those introduced in the supplying voltage. As can be observed in Figure 5, the values of THD_I depend on the order and level of the harmonics, but not on its sequence type, positive or negative.

The constant of the ratio between the level of an individual current harmonic (percentage of fundamental) $I_{h\%}$ and the level of an individual voltage harmonic $V_{h\%}$ is observed, for a given constant order h , of the harmonic present in voltage waveform. The values of this ratio are given in Table 5.

We propose a relation for permitting the calculation of the level of an individual harmonic of the stator current, of order h , when is known the level of the individual voltage harmonic, of the same order h , from the supply

Table 5. The values of the ratio $I_{h\%} / V_{h\%}$ related to the harmonic voltage order.

Harmonic Order h	$I_{h\%} / V_{h\%}$
5	1.9
7	1.4
11	0.9
13	0.7

voltage

$$I_{h\%} \approx 10 \cdot \frac{V_{h\%}}{h} (\%) \quad (9)$$

based on the graphs in Figure 5, which cross the line corresponding to the ordinates with the values $V_{h\%}$, adopted for a fictive order $h \approx 10$. Equation (9) highlights that the current harmonics with order $h < 10$ have higher levels in the current waveform than the voltage harmonic of the same order; instead for orders $h > 10$, the level of current harmonics decreases ($10/h$) times, with that of corresponding voltage harmonic.

The levels of stator current harmonics for each voltage harmonic, present in the stator voltage waveform, can be calculated with Equation (9) and the THD_I can be determined from

$$THD_I = \sqrt{\sum I_{h\%}^2} \quad (10)$$

4.2. Electromagnetic torque of the IM

The electromagnetic torque of the IM is the next analysed quantity. The torque interacts with the mechanical system of the driven machine. Figure 6 shows the amplitude (maximum absolute value of the difference from the dc component) of the electromagnetic torque oscillation $T_{eh\%}$, expressed in percentage of the nominal torque T_{en} , with the harmonic content and THD_V . As it can be observed the electromagnetic torque oscillations decrease inversely proportional to the voltage harmonic order and increase directly proportional to their level, according to the proposed relation

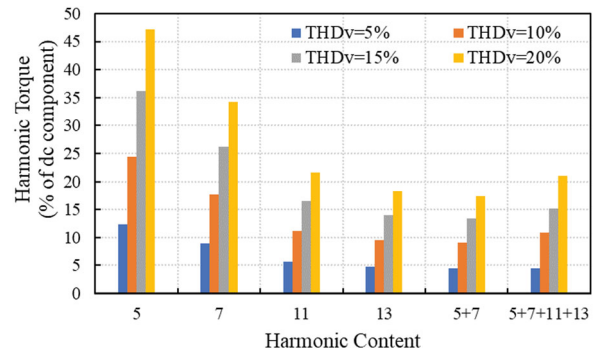
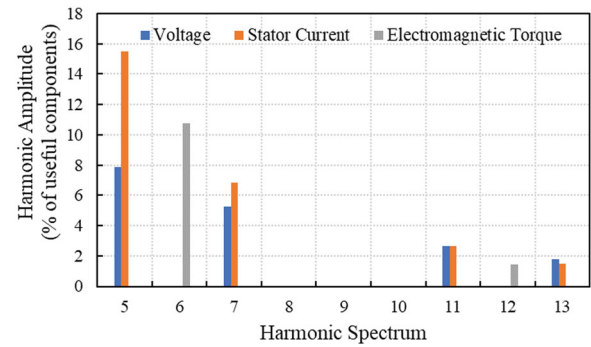
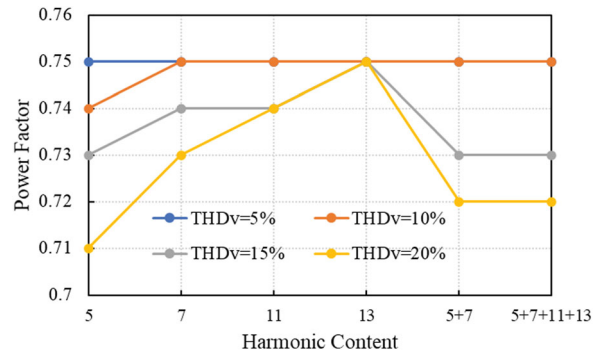
$$T_{eh\%} \approx 12 \cdot \frac{V_{h\%}}{h} (\%) \quad (11)$$

The electromagnetic torque is plotted together with the harmonic spectrum of both the stator current and the supply voltage, in Figure 7. To be noted, the occurrence of electromagnetic torques at the intermediate frequencies of harmonic pairs 5 ± 7 and 11 ± 13 .

The elevated torques at these frequencies can be regarded as mechanical resonant spectral components when coinciding with the assumed natural frequencies of the system [5]. This situation may lead to a severe increase in vibration amplitudes.

4.3. Power factor of the IM

From the electric power supply point of view, the PF of the IM represents a priority, because of the significant

**Figure 6.** The amplitude of the torque oscillations with harmonic content and THD_V .**Figure 7.** Harmonic spectrum for the amplitudes of the electromagnetic torque, voltage, and stator current.**Figure 8.** PF of the IM versus harmonic content and THD_V .

share of these electrical receivers in the global electricity consumption. Figure 8 shows the PF versus the harmonic content and the THD_V .

As a first remark, PF is maintained constant, at $PF = 0.75$, for $THD_V \in 5, 10\%$, regardless of the order or harmonic content, except the case of the fifth order harmonic, when the $PF = 0.74$; if $THD_V \geq 15\%$, there are relatively significant decreases of PF, especially when in the voltage waveform exist individual harmonics of lower orders $h \leq 7$, or when there exist combinations of harmonics with the orders and levels mentioned in Table 2. For individual harmonics of higher orders $h \geq 11, 13$, the PF is less affected.

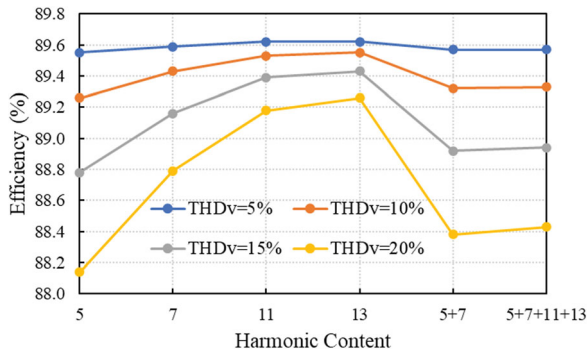


Figure 9. The efficiency of the IM versus harmonic content and THD_v.

4.4. Efficiency of the IM

In terms of energy, the efficiency is also essential along with the PF, so that its variations with harmonic content and THD_v are plotted in Figure 9. As in the case of the PF, the lower values of THD_v 15, 10% are felt to be imperceptible or to a very small extent at the efficiency level of the IM, regardless of the harmonic order or composition. Also, it can be noted that for individual harmonics of orders h=11, 13, even at THD_v = 20%, the efficiency of the IM does not decrease with more than about 0.5% of the nominal value.

More significant decreasing in the efficiency of the IM due to the harmonics are recorded in the case of fifth-order harmonic as follows: $\Delta\eta\% = 0.97\%$, when THD_v = 15%; and $\Delta\eta\% = 1.68\%$, when THD_v = 20%. In the case when in the supply voltage waveform exists harmonics of 5th and 7th orders, with the corresponding levels, mentioned in Table 2, the efficiency of the IM decreases: with $\Delta\eta\% = 0.81\%$, when THD_v = 15%; and with $\Delta\eta\% = 1.42\%$, when THD_v = 20%.

5. Effects of unbalanced distorted voltages on the IM

5.1. Harmonic distortion of the stator current

Figure 10 shows the average THD_i of the stator current, on the three phases, depending on the unbalance and the harmonics, for the considered scenarios presented in Table 3. As it can be observed in Figure 10, the more significant variations of the THD_{i,av} are due to the harmonics. For the same degree of unbalance, the values of THD_{i,av} increase with increasing of THD_v, while for the same value of THD_v on different values of VUF, the variations of THD_{i,av} are insignificant.

When the IM is supplied from unbalanced distorted voltages, in the harmonic content of the stator current are found harmonics of 3rd, 5th, and 7 orders, as presented in Figure 11, for VUF = 3% and THD_v = 10% (containing voltage harmonics of both 5th and 7th orders). The presence of the 3rd harmonic in the stator current is due to the voltage unbalance, whereas the 5th

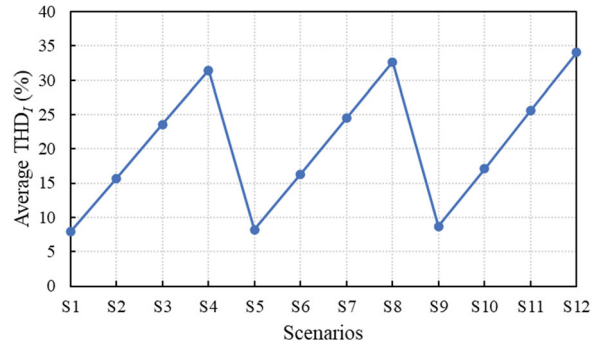


Figure 10. The Average THD_i of the stator current under voltage unbalance and harmonics scenarios.

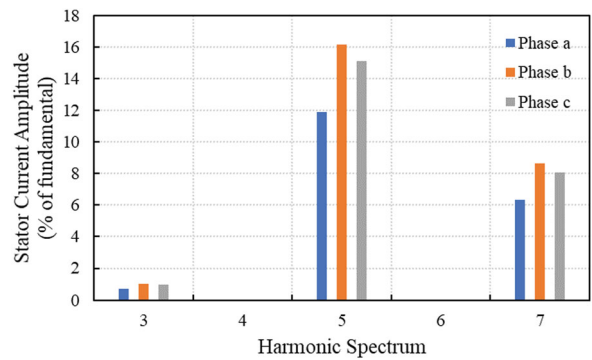


Figure 11. Harmonic spectrum of the stator current, for VUF = 3% and THD_v = 10%, when in the voltage are present harmonics of both 5th and 7th orders.

and 7th current harmonics appear due to the voltage harmonics of the same orders. In Figure 11 are presented the values of THD_i for each of the three phases of the stator current. It can be observed that the magnitudes of the 5th and 7th harmonics are greater than the 3rd harmonic, which justifies the above observation about the more significant influence of the THD_v than the VUF on the harmonic distortion of the stator current.

5.2. Electromagnetic torque of the IM

The amplitudes (maximum absolute value of the difference from the dc component) of the electromagnetic torque, expressed as a percentage of the dc component, depending on VUF and THD_v are shown in Figure 12. It can be observed that the graph could be delimited in three increasing levels, corresponding to the three degrees of unbalance of 1%, 3%, and 5%. There is a jump between each consecutive level, with a higher growth slope than the growth slopes inside each level. This highlights the fact that the unbalance regime has a greater influence on the oscillations of the electromagnetic torque than the harmonics, under the given conditions. Another observation is that the jump between S8 and S9 (degree of unbalance from 1% to 3%) is almost two times higher than the one between S4 and S5 (degree of unbalance from 3% to 5%).

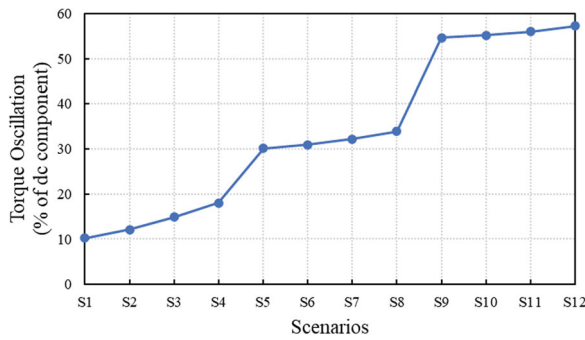


Figure 12. The amplitude of the torque oscillations under voltage unbalance and harmonics scenarios.

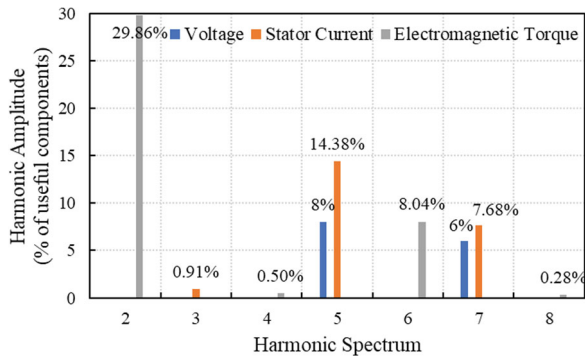


Figure 13. Harmonic spectrum of the stator current, voltage, and electromagnetic torque, for $VUF = 3\%$ and $THD_V = 10\%$, when in the voltage are present harmonics of both 5th and 7th orders.

The harmonic amplitudes, as a percentage of the useful components, of the stator current, supply voltage, and electromagnetic torque, for $VUF = 3\%$ and $THD_V = 10\%$, are presented in Figure 13. The torque oscillations of the frequency of 100 Hz, due to the voltage unbalance, represent 29.86% of nominal torque, not being influenced by the harmonics (Figures 2 and 13). The magnitude of the frequency component of 300 Hz, associated with harmonics (including harmonics of 5th and 7th orders), represents 8.04% of the nominal torque and it is not influenced by voltage unbalance (Figures 6 and 13). The torque oscillations at 4 and 8 times the fundamental frequency are generated due to the combined effect of the voltage unbalance and harmonics [30].

5.3. Power factor of the IM

Figure 14 shows the dependence of the PF on the combined effect of the voltage unbalance and harmonics. It can be observed that: for a degree of unbalance of 1% and for THD_V of 5%, 10%, and 15% (S1, S2, and S3) the values of PF are higher than the nominal value $PF_n = 0.76$ (represented with the horizontal dashed line, in Figure 14); for $VUF = 3\%$ and $THD_V = 5\%$ (S5) the $PF = 0.77$, and in S6 the $PF = PF_n = 0.76$. Another observation is that PF decreases almost linearly from

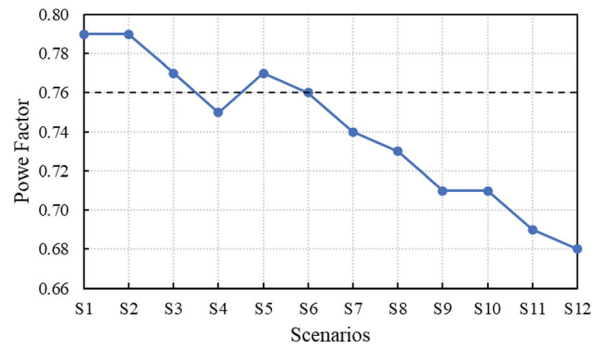


Figure 14. PF of the IM under voltage unbalance and harmonics scenarios.

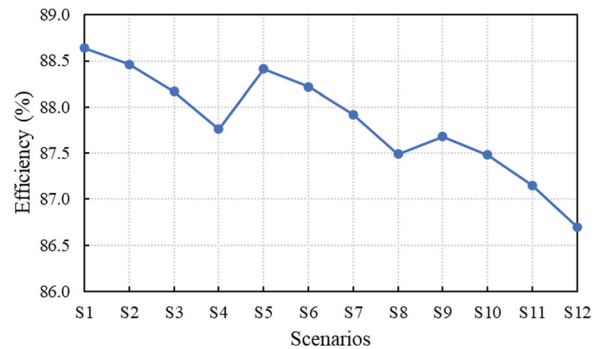


Figure 15. The efficiency of the IM under voltage unbalance and harmonics scenarios.

S5 to S12, with the minimum value of $PF = 0.68$ in S12 ($VUF = 5\%$ and $THD_V = 20\%$).

5.4. Efficiency of the IM

The efficiency of the IM, running at 75% of rated load, with the considered scenarios is plotted in Figure 15. As in the case of torque oscillations, the values of the efficiency can be spread on three levels corresponding to the three degrees of unbalance of 1%, 3%, and 5%. The efficiency of the IM decreases both with the increase of the voltage unbalance and with the increase of the harmonic distortion of the voltage waveforms. The decreasing slopes of each level, from S1–S4, S5–S8, and S9–S12, respectively, are almost of the same value; this means that the decrease associated with the harmonics (increasing THD_V from 5% to 15%) is almost the same for each considered degree of unbalance. In S8 the efficiency of the IM is 87.49%, with 0.3% lower than the efficiency value in S4, and in S12 the decrease compared to the value from S8 is 0.9%; this means that the efficiency of the IM is more affected by the increasing of VUF from 3% to 5% than the increasing of VUF from 1% to 3%. In S12 ($VUF = 5\%$ and $THD_V = 20\%$) the efficiency of the IM is $\eta = 86.7\%$ which represent: a decrease of 3.29% compared to the nominal value $\eta_n = 89.65\%$.

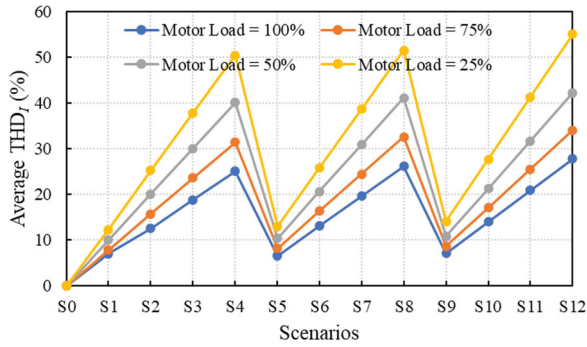


Figure 16. THD_v of the stator current under voltage unbalance and harmonics scenarios, at different load percentages.

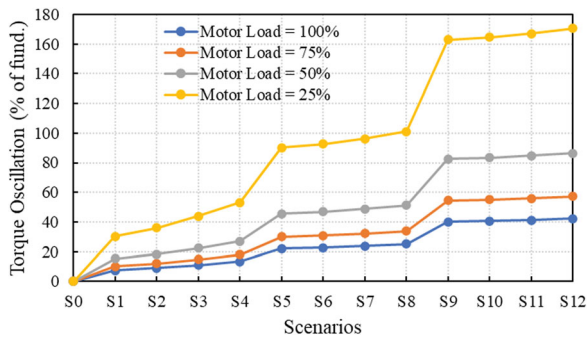


Figure 17. The amplitude of the torque oscillations under voltage unbalance and harmonics scenarios, at different load percentages.

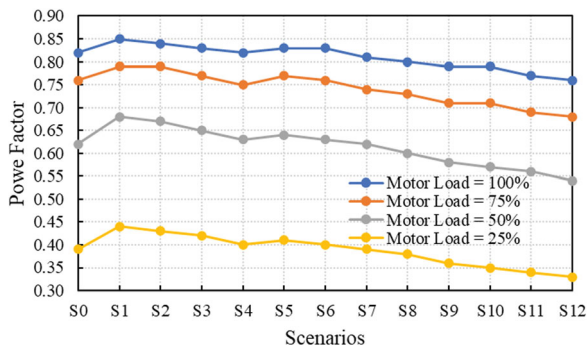


Figure 18. PF of the IM under voltage unbalance and harmonics scenarios, at different load percentages.

5.5. IM running at different motor loads

Further, we analyse the IM behaviour under non-sinusoidal and unbalanced voltages at different load percentages, of 25%, 50%, 75%, and 100%, for the considered scenarios. The scenario S0 from Figures 16–19 represents the reference case when the IM is supplied from an ideal power supply (balanced and sinusoidal voltages).

Regarding the harmonic distortion of the stator current, the THD_{av} increase with decreasing the load percentage, as can be observed in Figure 16. It can be noted that for the IM running at 25% of rated load the values of THD_{av} exceed 50%.

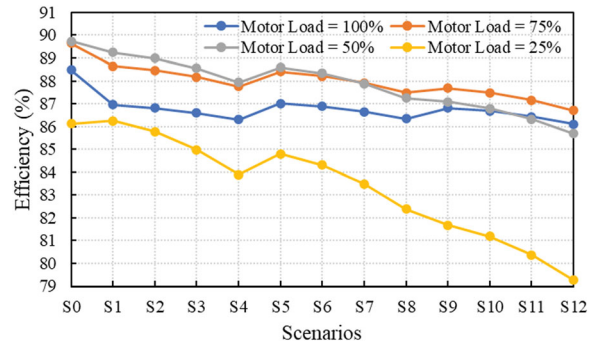


Figure 19. The efficiency of the IM under voltage unbalance and harmonics scenarios, at different load percentages.

In the case of the torque oscillations, it is observed that they are lower in amplitude the higher load percentage of the IM, as shown in Figure 17. To be noted that when the IM is loaded below 50% of rated load, the torque oscillations significantly increase, reaching amplitudes of about 170% of the nominal torque when the motor load is 25%.

Figure 18 shows the variation curves of the PF with the considered scenarios for different load percentages. It can be observed that the PF decreases with decreasing the motor loads. The PF takes values from 0.54–0.64 for the considered scenarios, while the IM load is 50%. For motor loads below 50%, the PF values decrease significantly, reaching the value of 0.33, if the IM load is 25%; this value corresponds to a decrease of 59.76% of the nominal value $PF_n = 0.82$.

The efficiency of the IM depending on the considered supplying conditions and on the percentage of motor loads is shown in Figure 19. It can be observed that IM operates at higher efficiency in case it is loaded between 50 and 75% of the rated load. For motor loads below 50%, the efficiency decreases significantly, reaching $\eta = 79.26\%$ in S12 ($VUF = 5\%$ and $THD_V = 20\%$), which represents a decrease of $\Delta\eta\% = 10.42\%$ compared to the nominal efficiency of the IM, running at nominal load, and supplied from an ideal voltage system.

6. Conclusions

For a detailed analysis of the effects of voltage unbalance on the electrical and mechanical parts of the IM, it is not enough to know only the percent voltage unbalance, but it is also important to know the magnitude of the positive sequence component. We showed that for different situations of unbalance, e.g. $V_{pos} < V_{phn}$ and $V_{pos} > V_{phn}$, for the same value of VUF, the torque oscillations can differ in amplitude by up to 22%, and the values of the efficiency differ by 1.21%. For the case of a lower value of the positive sequence component, were obtained lower values of the efficiency, but higher values of the PF.

From an electric point of view, the harmonics are felt both at the level of IM, by the variations of the PF and the efficiency, as well as at the level of the power supply system, by the current harmonics introduced in it and by the decrease of the PF. The harmonics can also cause oscillations of the electromagnetic torque. This can affect product quality where motor loads are sensitive to such variations. In cases in which substantial inertia is coupled to the rotor shaft, the electrical harmonics can excite a mechanical resonance. The resulting mechanical oscillations can cause shaft fatigue and accelerated aging of the shaft and connected mechanical parts.

Regarding the considered scenarios, when the IM is supplied from unbalanced and non-sinusoidal voltages, we showed that the voltage unbalance has a greater influence on the electromagnetic torque than the harmonics. For example, for $VUF = 3\%$ and $THD_V = 10\%$, the torque oscillations of 100 Hz frequency, due to the unbalance, is more than three times higher than the torque oscillations of 300 Hz frequency, due to the harmonics.

By simulating the considered IM under unbalanced distorted voltages at different percentage loads, it was observed that the performances of the IM are strongly affected, both electrically and mechanically, if it operates at loads below 50% of the nominal load. For $VUF = 5\%$ and $THD_V = 20\%$ in the supply of the IM, running at 25% of rated load, the amplitude of the torque oscillations reaches about 170% of the dc component, the PF decreases with almost 60% of the nominal value, and the efficiency decreases with more than 10% of the nominal efficiency.

The proposed methodology for estimating the effects of voltage unbalance and harmonics, both separately and simultaneously, on the induction motor behaviour follows the basis for a generally applicable method to assess the overall effects of the considered PQ disturbances, for any application.

As future research, we plan: (1) to adapt the current physical model of the IM to track the effects of saturation on the current unbalance and harmonics developed in the motor; and (2) to analyse the consequences of voltage unbalance and harmonics on drive systems with IMs fed by power converters.

Disclosure statement

No potential conflict of interest was reported by the author(s).

Funding

The results presented in this paper were obtained in the framework of the GNaC 2018 ARUT grant "Consequences of Power Quality Issues for Electromechanical Receivers", research Contract no. 3092/05.02.2019, with the financial support of the Technical University of Cluj-Napoca.

ORCID

Pompei C. Darab  <http://orcid.org/0000-0001-6393-233X>

Mohammed Sallah  <http://orcid.org/0000-0003-2063-8979>

References

- [1] International Energy Agency. World energy outlook 2016. Paris: IEA; 2016; [Online] Available from: <https://www.iea.org/reports/world-energy-outlook-2016>.
- [2] Waide P, Brunner CU. Energy-efficiency policy opportunities for electric motor-driven systems. Paris: International Energy Agency; 2011.
- [3] Debruyne C, Lieven V, Jan D. Harmonic effects on induction and line start permanent magnet machines. Proc. EEMODS; Rio de Janeiro, RJ, Brazil: 2013.
- [4] Baggini Angelo. Handbook of power quality, pp. 163–174. John Wiley & Sons, Ltd, The Atrium, Southern Gate, Chichester, West Sussex PO19 8SQ, England; 2008.
- [5] De La Rosa FC. Harmonics, power systems, and smart grids. 2nd ed. Boca Raton (FL): CRC Press, Taylor and Francis Group; 2015; p. 79–83.
- [6] Tabora JM, De Lima Tostes ME, De Matos EO, et al. Assessing voltage unbalance conditions in IE2, IE3 and IE4 classes induction motors. IEEE Access. 2020;8:186725–186739. DOI:10.1109/ACCESS.2020.3029794.
- [7] Agamloh EB, Peele S, Grappe J. Operation of variable-frequency drive motor systems with source voltage unbalance. IEEE Trans Ind Appl. 2017 Nov–Dec;53(6): 6038–6046. DOI:10.1109/TIA.2017.2747144.
- [8] Kini PG, Bansal RC. Effect of voltage and load variations on efficiencies of a motor-pump system. IEEE Trans Energy Convers. 2010 June;25(2):287–292. DOI:10.1109/TEC.2009.2032628.
- [9] von Jouanne A, Banerjee B. Assessment of voltage unbalance. IEEE Trans Power Delivery. 2001 Oct;16(4):782–790. DOI:10.1109/61.956770.
- [10] Siraki AG, Gajjar C, Khan MA, et al. An algorithm for nonintrusive in situ efficiency estimation of induction machines operating with unbalanced supply conditions. IEEE Trans Ind Appl. 2012 Nov–Dec;48(6):1890–1900. DOI:10.1109/TIA.2012.2225813.
- [11] Wang Y-J. Analysis of effects of three-phase voltage unbalance on induction motors with emphasis on the angle of the complex voltage unbalance factor. IEEE Trans Energy Convers. 2001 Sept;16(3):270–275. DOI:10.1109/60.937207.
- [12] Daniel Donolo P, Pezzani CM, Bossio GR, et al. Effects of negative sequence voltage on the core losses of induction motors. IEEE ANDESCON; Arequipa; 2016. p. 1–4. DOI:10.1109/ANDESCON.2016.7836232.
- [13] de Castro e Silva MD, Ferreira Filho AL, Neves ABF, et al. Effects of sequence voltage components on torque and efficiency of a three-phase induction motor. Electr Power Syst Res. 2016;140:942–949. DOI:10.1016/j.epsr.2016.03.051.
- [14] Lee C-Y. Effects of unbalanced voltage on the operation performance of a three-phase induction motor. IEEE Trans Energy Convers. 1999 Jun;14(2):202–208. DOI:10.1109/60.766984.
- [15] Guasch-Pesquer L, Youb L, González-Molina F, et al. Effects of voltage unbalance on torque and current of the induction motors. 13th International Conference on optimization of electrical and Electronic equipment (OPTIM); Brasov; 2012. pp. 647–652. DOI:10.1109/OPTIM.2012.6231766.

- [16] Neves ABF, d A, Filho LF, et al. Effects of voltage unbalance on torque and efficiency of a three-phase induction motor. 16th International Conference on harmonics and quality of power (ICHQP); Bucharest; 2014. pp. 679–683. DOI:[10.1109/ICHQP.2014.6842807](https://doi.org/10.1109/ICHQP.2014.6842807).
- [17] Santos VS, Felipe PRV, Sarduy JRG, et al. Procedure for determining induction motor efficiency working under distorted grid voltages. *IEEE Trans Energy Convers.* 2015 Mar;30(1):331–339. DOI:[10.1109/TEC.2014.2335994](https://doi.org/10.1109/TEC.2014.2335994).
- [18] Debruyne C, Corne B, Sergeant P, et al. Evaluation of the additional loss due to supply voltage distortion in relation to induction motor efficiency rating. *IEEE International Electric Machines & Drives Conference (IEMDC)*; Coeur d'Alene, ID; 2015. pp. 1881–1887. DOI:[10.1109/IEMDC.2015.7409321](https://doi.org/10.1109/IEMDC.2015.7409321).
- [19] Donolo P, Pezzani M, Bossio G, et al. Impact of voltage waveform on the losses and performance of Energy efficiency induction motors. *IEEE ANDESCON*; Santiago de Cali; 2018. p. 1–4. DOI:[10.1109/ANDESCON.2018.8564677](https://doi.org/10.1109/ANDESCON.2018.8564677).
- [20] Debruyne C, Desmet J, Derammelaere S, et al. Derating factors for direct online induction machines when supplied with voltage harmonics: A critical view. *IEEE International Electric Machines & Drives Conference (IEMDC)*; Niagara Falls, ON; 2011. pp. 1048–1052. DOI:[10.1109/IEMDC.2011.5994745](https://doi.org/10.1109/IEMDC.2011.5994745).
- [21] Al-Badri M, Pillay P, Angers P. A novel in situ efficiency estimation algorithm for three-phase induction motors operating with distorted unbalanced voltages. *IEEE Trans Ind Appl.* 2017 Nov–Dec;53(6):5338–5347. DOI:[10.1109/TIA.2017.2728786](https://doi.org/10.1109/TIA.2017.2728786).
- [22] Sousa V, Viego PR, Gómez JR, et al. Estimating induction motor efficiency under no-controlled conditions in the presences of unbalanced and harmonics voltages. *CHILEAN Conference on Electrical, Electronics Engineering, Information and Communication Technologies (CHILECON)*; Santiago; 2015. p. 567–572. DOI:[10.1109/Chilecon.2015.7400434](https://doi.org/10.1109/Chilecon.2015.7400434).
- [23] Oraee H. A quantitative approach to estimate the life expectancy of motor insulation systems. *IEEE Trans Dielectr Electr Insul.* 2000 Dec;7(6):790–796. DOI:[10.1109/94.891990](https://doi.org/10.1109/94.891990).
- [24] Zhang D, An R, Wu T. Effect of voltage unbalance and distortion on the loss characteristics of three-phase cage induction motor. *IET Electr Power Appl.* 2018;12(2):264–270. DOI:[10.1049/iet-epa.2017.0464](https://doi.org/10.1049/iet-epa.2017.0464).
- [25] Ferreira FJTE, Baoming G, de Almeida AT. Reliability and operation of high-efficiency induction motors. *IEEE Trans Ind Appl.* 2016 Nov–Dec;52(6):4628–4637. DOI:[10.1109/TIA.2016.2600677](https://doi.org/10.1109/TIA.2016.2600677).
- [26] Donolo PD, Pezzani CM, Bossio GR, et al. Derating of induction motors due to power quality issues considering the motor efficiency class. *IEEE Trans Ind Appl.* 2020 Mar–Apr;56(2):961–969. DOI:[10.1109/TIA.2020.2965859](https://doi.org/10.1109/TIA.2020.2965859).
- [27] Beleiu HG, Maier V, Pavel SG, et al. Harmonics consequences on drive systems with induction motor. *Applied Sciences.* 2020 Feb;10(4):1528. DOI:[10.3390/app10041528](https://doi.org/10.3390/app10041528).
- [28] Santoso S, McGranaghan MF, Dugan RC, et al. *Electrical power systems quality*. 3rd ed. New York (NY): McGraw Hill Companies; 2012.
- [29] IEEE Std. IEEE recommended practice for monitoring electric power quality: IEEE Standard, New York, NY 10016-5997 USA; 2019. p. 1159.
- [30] Donolo P, Bossio G, De Angelo C, et al. Voltage unbalance and harmonic distortion effects on induction motor power, torque and vibrations. *Electr Power Syst Res.* 2016;140:866–873. DOI:[10.1016/j.epsr.2016.04.018](https://doi.org/10.1016/j.epsr.2016.04.018).

Fuzzy logic controller for regulating the indoor temperature

Anca Miron
Electric Power Systems and
Management Dept.

Technical University of Cluj-Napoca
Cluj-Napoca, Romania
anca.miron@enm.utcluj.ro

Andrei C. Cziker
Electric Power Systems and
Management Dept.

Technical University of Cluj-Napoca
Cluj-Napoca, Romania
andrei.cziker@enm.utcluj.ro

Stefan Ungureanu
Electric Power Systems and
Management Dept.

Technical University of Cluj-Napoca
Cluj-Napoca, Romania
stefan.ungureanu@enm.utcluj.ro

Abstract— In recent times, globalization and energy efficiency policies have further required temperature control applications in different daily activities, especially with the greenhouse effect. In residential buildings, water and living space heating consumes most of the primary energy. The paper presents a method to keeping the comfort temperature in living space by using an approach based on an artificial intelligence technique, namely fuzzy logic. The support for the proposed method is an electrical hot-water radiator heating system with a tankless heater. The fuzzy logic controller makes a continuous regulation of the indoor temperature by adapting the temperature of the heating agent regarding the indoor and exterior temperature. To validate and test the proposed method, MATLAB-Simulink was employed. The comparison with an On/Off controller that is the most used control device due to financial benefits showed the efficiency of the fuzzy logic controller.

Keywords—fuzzy logic, indoor temperature, hot-water radiator heating, energy efficiency

I. INTRODUCTION

Households use 63% of their energy consumption in space heating [1]. In living space heating (LSH), the residential users utilize diverse types of energies: biomass, fossil fuels, electrical energy, and renewable resources. According to [2], biomass, e.g., wood, was the main primary energy source for LSH in Europe until 2015. However, in countries like Italy and Netherlands, natural gas was used to obtain thermal energy for LSH.

The global energy efficiency, ecological, and climate change policies sustain the usage of renewable and sustainable forms of energy. So, the future of LSH and water heating will imply consuming electricity from renewable resources and direct heating using renewable resources. Indeed, the results from [3] sustain that in the next 30 years, electrical energy, along with renewable resources, will be the predominant form of energies employed in LSH.

LSH with electricity (electric space heating, ELSH) can be realized through resistance, hot-water, infrared, and dry heating. Among these ELSH alternatives, hot-water heating is the most utilized because the electric heater can easily replace a natural gas heater.

Hot-water radiator heating systems (HWRHS) employ hot-water as the heating agent, radiators as the thermal energy sources, and heaters that transform the main form of energy in thermal energy. The heaters can function with natural gas, biomass, or electrical energy. HWRHS are systems for individual and central heating. In individual heating systems, two devices can produce the hot-water: tank-style heater, i.e., boiler, or a tankless heater.

Energy efficiency approaches are fundamental in all processes, as they sustain the ecological and sustainable use of resources. In LSH, through hot-water electric heating, an energy efficiency approach is to adapt the functioning of the heat source to the users' exact needs. Automatic control of the indoor temperature can complete this process. Other aspects that lead to the increase of the heating system efficiency are (i) sound isolation of the external walls of the living space, (ii) efficient electrical heaters, (iii) clean radiators, and (iv) low temperature of the heating agent.

The paper presents a method to control the temperature of the living space, i.e., indoor temperature, using fuzzy logic.

The research's suppositions are:

- A hot-water individual heating system is the support for the FLC testing,
- The hot-water source is an electric tankless heater,
- Cast iron radiators are the heat source used to increase the indoor temperature,
- The heat is transmitted through convection,
- The external walls of the living space are made of brick and are uninsulated.

The remainder of the paper is as follows: the second section describes the main theoretical parts with concern to the hot-water heating systems, the control of indoor temperature, and fuzzy logic control, respectively. The proposed method is presented in the third section, whereas the following section describes its testing. The fifth section discusses the results. The paper ends with the conclusion section, where the most critical aspects of the study's findings are enumerated.

II. BACKGROUND

A. Hot-water radiator heating system

ELSH assumes the consumption of electricity to obtain the thermal energy necessary to heat a living space, more specifically, the air, objects, persons, and all other creatures in the living space and the walls, windows, and doors. The thermal energy can be transferred through conduction, convection, and radiation. In the case of hot-water radiator heating, convection is the phenomenon that transmits thermal energy, whereas a minimal amount goes through radiation [4].

HWRHS has two variants: central (district) and individual. In district heating, a boiler-consuming natural gas typically generates the heat destined for an entire building [5]. The alternative, individual heating, is designed for a single household. The system's heater can be on natural gas or electricity. Since for the research, the support heating system is the second variant based on electricity. Further, all information presented is about this type of heating system.

An electric heater with or without a tank produces the heat. The first alternate is called a boiler, and the second is named a tankless electrical heater (TEH). Fig. 1 presents both types.

The heat is obtained using electrical energy, more precisely heating elements which temperature rises due to Joule-Lenz law. This heat is distributed by hot water (heat agent) to the radiators. The radiators heat the air in the living space; thus, the heat transfer is made using convection.

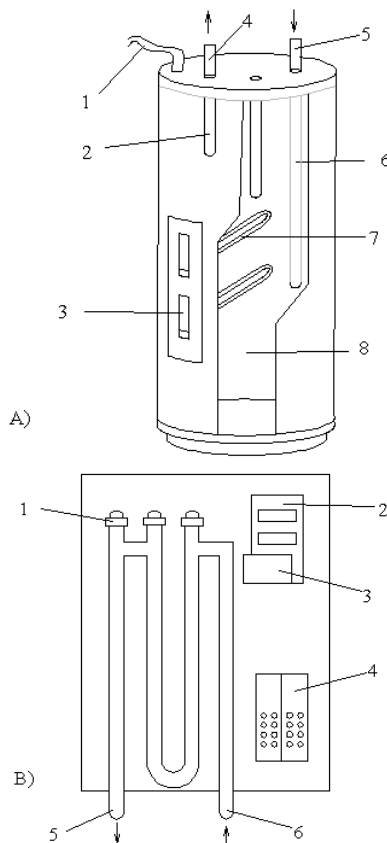


Fig. 1. Electric boiler and tankless heater
A) 1- electric supply, 2- hot water outlet, 3- thermostat, 4- hot water, 5- cold water, 6- dip tube, 7- electric heating element, 8 - water; B) 1- electric heating element, 2- electronic board, 3- display, 4- power terminal block, 5- hot water, 6- cold water

In a household with multiple rooms, each heated place has installed radiators. The hot water is circulated by a water circulation pump, which operates continuously [4]. The radiators sit next to the cold surface of the envelope; thus, they influence the thermal comfort meaningfully. Fig. 2 illustrates an HWRHS.

- The factors that influence the LSH are [4, 6]:
- The envelope of the household, i.e., the material of the exterior walls and their isolation;
- The types of windows and doors to the exterior;
- The distribution of the living space, especially in the case of big houses. Thus the use of temperature zones is recommended;
- The efficiency of the electrical heater;
- The temperature of the heating agent;
- The exterior and indoor temperature.

B. Control of indoor temperature

Control of the indoor temperature refers to the process dedicated to maintaining the temperature in the living space at a certain maximum (in the case of LSH) level or within a specific range. The automation of the process is qualified as the best approach in any application, minimizing or excluding human involvement. Consequently, the temperature is automatically controlled [7]. The results showed in numerous studies underline that the temperature is effectively and more accurately controlled compared to the manual or semiautomatic control.

In the case of LSH, the indoor temperature can be regulated with the help of On/Off, PI (proportional-integral), PID (proportional-integral-derivative), or AI (artificial intelligence) controllers. Numerous studies compare these methods in various situations [5, 7-20].

An On/Off controller is the simplest form of temperature control device [7]. The output from the controller is either on or off, with no in-between state. This device will switch the output only when the temperature goes below or above the set-point. Consequently, the output is on if the temperature's value is below the set-point and off when it is above the set-point. As the temperature crosses the set-point to modify the output state, the indoor temperature will repeatedly be cycling, going from the under to the above set-point and back. This type of regulator is utilized where accurate control is not necessary, such as when the system's mass is so great that the temperatures change very slowly. To eliminate the weak points of cycling linked with On/Off control, the researchers invented the proportional control.

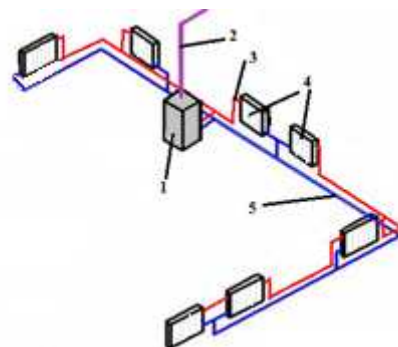


Fig. 2. Hot-water radiator heating system
1- hot-water electric heater, 2- electric supply, 3- hot water pipe, 4- radiator, 5- cold water pipe

A proportional controller reduces the average power delivered to the effector as the temperature approaches the set-point. This procedure has the effect of slackening the heater, so the control is steadier, as the temperature will not exceed the set-point but will approach it slowly. This proportionating action occurs within a proportional band. Outside of this band, which has the central set-point, the controller functions as an On/Off unit. More advanced units were built from this type of control device, from which the PID controllers are the best.

The PID unit makes two extra adjustments than the proportional controller, integral, and derivative expressed in time-based units [7]. The proportional, integral, and derivative parameters must be individually adjusted to a particular system using trial and error. The controller is suggested in systems where the load changes often, so the control unit is expected to compensate automatically due to regular changes in the set-point. The PID controllers are not appropriate for all processes, as mentioned in [8]. These control units' performance can be improved with other approaches that complement them, e.g., fuzzy controllers, as in [9], where the authors demonstrate that the hybrid is better than the conventional one. Comparing the PID and FLC devices in [10, 11], the articles conclude that the last one is faster.

C. Fuzzy logic control

Fuzzy logic control is the base of fuzzy logic controllers (FLCs). Compared with the classic controllers, which use the data with the help of precise mathematical relationships, FLCs employ inferences between several rules built with linguistic variables. The variables are fuzzy sets defined by membership functions as (1). The rules show the relations concerning the regulated quantity and the factors that influence it. Usually, these factors are the inputs to the controller. The inferences connect the quantities with which the controller works and are interpreted with the help of logic operators. Fig. 3 presents the scheme of an FLC.

The scheme describes the principle of the Mamdani configuration [21]. The FLC has three blocks: fuzzifier, inference engine, and defuzzifier. The fuzzifier realizes the preliminary transformation of the input data X and treats the quantities with the help of linguistic variables (cold, warm, and v_warm, like the ones from Fig. 4). The exit of the fuzzifier is the fuzzy sets A defined by their membership functions. These fuzzy sets relate to the raw input data and represent the inputs to the inference engine.

The inference engine selects the rules that correspond to its input data. It applies them, obtaining at the end a combination of fuzzy sets B . These sets sum up as a fuzzy surface that the defuzzifier utilizes to obtain the command output data Y of the controller.

The main advantage of FLCs is the possibility to regulate multi-parameter and non-linear processes and work with incomplete data.



Fig. 3. Scheme of an FLC
 X - Input data vector, A - input fuzzy sets vector, B - output fuzzy sets vector, Y - output data vector

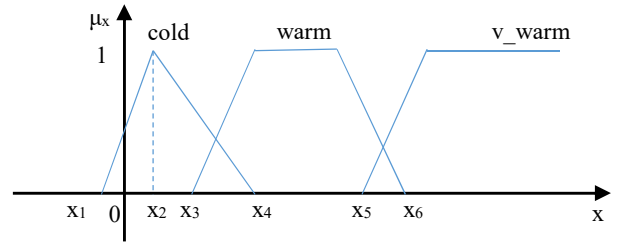


Fig. 4. Example of linguistic variables and fuzzy sets
 μ_x - membership functions, cold, warm and v_warm - linguistic variables, x - quantity

$$\mu_{cold}(x) = \begin{cases} 0 & , & x < x_1 \\ \frac{x - x_1}{x_2 - x_1} & , & x_1 \leq x \leq x_2 \\ \frac{x_4 - x}{x_4 - x_2} & , & x_2 \leq x \leq x_4 \\ 0 & , & x_4 < x \end{cases} \quad (1)$$

III. PROPOSED FUZZY LOGIC CONTROLLER

Several studies propose fuzzy logic controllers dedicated to regulating indoor temperature [15-20]. The control of indoor temperature and humidity is made with groundwater/air source reversible heat pumps and two FLCs in [15], whereas in [16] with a compressor/fan system. The system was simulated and tested with MATLAB/Simulink. Reference [15] concludes that the approach solved a complex problem without involving intricate relationships between the physical quantities. In [17] and [18], the authors compare several types of control devices, e.g., PID and PID-FLC, to determine the best solution towards obtaining the efficiency of a building by regulating the indoor temperatures. In [17], two heat sources imply the consumption of fossil fuels and renewable energy, wherein [18] a hot-water floor heating system was considered. The proposed control units were tested through simulations that showed that the combination PID-FLC is operating better than the conventional PID [17]. An attempt to develop an FLC using the MATLAB dedicated fuzzy toolbox is presented in [19]. The application has six inputs (cloud-content, outside temperature, rainfall, wind, humidity, and pressure) and an output (indoor temperature).

The proposed method has the following differences in comparison with the previous studies found in the literature:

- It considers individual hot-water radiator heating systems, with tankless electric heater;
- There are necessary two sensors for the indoor and exterior temperatures;
- The FLC continuously controls the indoor temperature by changing the temperature of the heating agent.

Further on are presented the components and the MATLAB/Fuzzy Toolbox implementation, the FIS model of the proposed FLC.

A. Fuzzifier

The FLC has the current indoor temperature and the outside temperature as inputs and the hot water temperature as output. Fig. 5 describes the linguistic variables of the controller's quantities. As the graphics show, the quantities are defined by triangular and trapezoidal fuzzy numbers

associated with the linguistic variables. Table I presents the FLC's parameters.

B. Inferences

The inferences show the relationships between the inputs and the output. They are presented in Table II and are interpreted as rules: IF T_{out} =cold and T_{in} =warm, Then $Theat$ =vwarm or IF T_{out} =cold and T_{in} =cold, Then $Theat$ =vhot. In the operational mode, the realization of the inferences is made through the Max-Min approach. This approach means that the predefined words have the following meanings: "and" as a minimum, "then" as a minimum, and "or" as a maximum. The combination of all rules determines the 3D surface from Fig. 6, which shows how the output varies concerning the two inputs. On the other hand, for a specific input data set, the inferences engine builds a specific fuzzy surface. Fig. 7 illustrates this procedure.

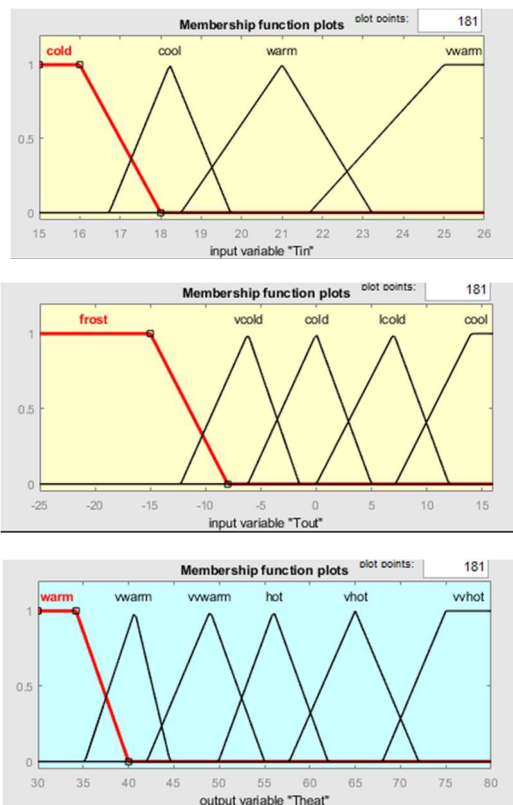


Fig. 5. Fuzzy representation of the FLC parameters
 T_{in} – indoor temperature, B) T_{out} – exterior temperature, C) $Theat$ – heating agent temperature

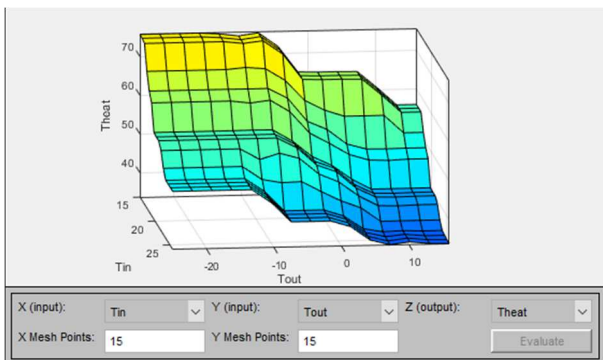


Fig. 6. Fuzzy surface of the FLC rules

C. Defuzzifier

The last block of the FLC extracts the command parameter from the final fuzzy surface obtained after the corresponding rules were applied in the previous block. The defuzzification procedure uses the Centroid method that supposes the utilization of (2).

$$Y = \frac{\int x \cdot \mu_B(x) dx}{\int \mu_B(x) dx} \quad (2)$$

In (2) the parameters have the following meaning: Y – command output found after the de-fuzzification, B – fuzzy

TABLE I. FLC PARAMETERS

Parameter	Characteristics	
	Definition / Confidence interval	Linguistic variables
T_{out}	exterior temperature [-25, 16]	frost, vcold, cold, lcold, cool
T_{in}	current indoor temperature [15, 26]	cold, cool, warm, vwarm
$Theat$	agent heat temperature [30, 80]	warm, vwarm, vvharm, hot, vhot, vvhot

TABLE II. FLC RULES

No.	Inputs		Output
	T_{in}	T_{out}	$Theat$
1	cold	frost	vvharm
2	cold	vcold	vvharm
3	cold	cold	vhot
4	cold	lcold	vhot
5	cold	cool	hot
...
16	vwarm	frost	vvharm
17	vwarm	vcold	vwarm
18	vwarm	cold	vwarm
19	vwarm	lcold	warm
20	vwarm	cool	warm

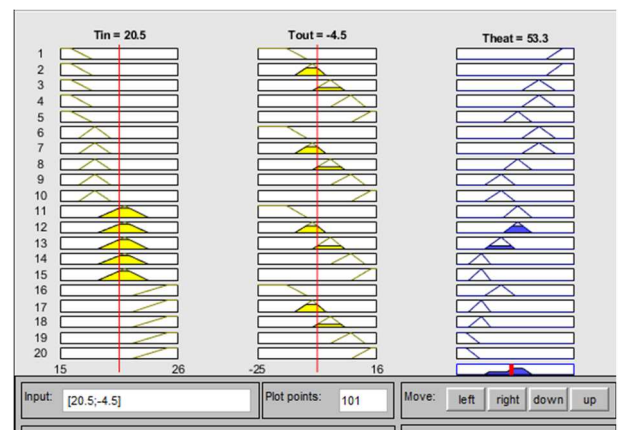


Fig. 7. FLC's inferences engine operation

output (surface) obtained after the inferences, μ_B – membership function of B .

IV. TESTING THE PROPOSED FLC

The validation of the proposed method was completed using MATLAB/Simulink. Fig. 8 illustrates the schematic implementation of the model, which contains three main blocks with the following features:

- Thermostat – has an indoor temperature sensor and commands the heating process. The set-point of the indoor temperature is 20°C. The heating begins when the temperature drops below 18°C and ends when the temperature exceeds 23°C;
- Heater – has the heat source and introduces the necessary heat to increase the temperature. The heater is a 24 kW tankless electric heater with four heating elements. The heating agent temperature, in the case of the FLC, varied between 80°C and 30°C, depending on the supply voltage and the number of operating elements;
- House – is the model of the house thermal system. The house has a 30 m x 30 m, with brick walls of 20 cm with no isolation. The windows have 1 cm, and the roof also has 20 cm.

The FLC was tested regarding a daily variation of the exterior temperature that is showed in Fig. 9, A). The performance of the FLC was tested and compared with a classic On/Off controller that was also implemented. The basic difference between the method is the temperature of the heating agent, that for the FLC is variable, whereas for the classic method is constant. Three scenarios with the constant temperature of the heating agent were considered, i.e., 40°C, 60°C, and 80°C, to have a clear picture of the process controlled by the FLC. This aspect can be seen in Fig. 9, B), which is the hot-water temperature variation. Therefore, the efficacy of the proposed FLC was successfully tested. The following section discusses the efficiency of the suggested approach.

V. DISCUSSIONS

The validation and testing of the proposed controller were positive. The results show the influence of the heating agent on the indoor temperature. Further analysis was performed on the results to have a precise picture of the impact of the proposed method in comparison with the alternative. Thus, for each controller, i.e., FLC and On/Off with three different heat agent temperatures, the heater's duration operation, electricity consumption, and daily price were calculated. Table III presents the obtained data. The results' analysis outcome shows that the heating process with an On/Off controller and low temperature for the heating agent has the longest functioning duration but the lowest energy consumption and the cheapest approach.

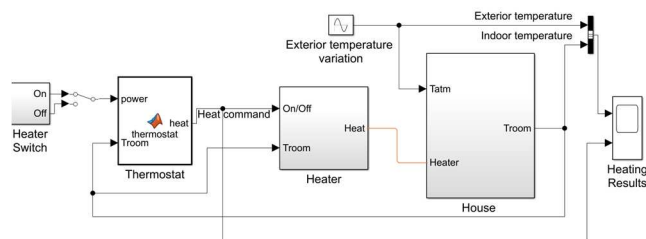


Fig. 8. MatLab/Simulink model for FLC validation

The FLC approach gets second place in energy consumption and third place for the operation duration. The other two cases have higher energy consumption, but the HLS is much quicker.

VI. CONCLUSIONS

In this paper, a fuzzy logic controller for indoor temperature regulation was proposed. The FLC has two inputs, the indoor and exterior temperatures and an output, the temperature of the heating agent.

The support heating system used is a hot-water radiator system with a tankless electric heater. The controller was developed using MATLAB/Fuzzy toolbox and tested with MATLAB/Simulink. The implemented model demonstrates the efficacy of the proposed FLC. The comparison with a classic On/Off controller that uses constant temperature for the heating agent shows that if one uses a low temperature in terms of the economy, it is the best solution. However, the comfort temperature is obtained slower in comparison with much higher temperatures. On the other hand, the FLC adapts the heating agent, offering both low consumption and quick LSH. These aspects are the strong points of the FLC.

The current model of the FLC has the disadvantage of indoor temperature cycling. A combination with a PID controller or a more complex FLC should be utilized to

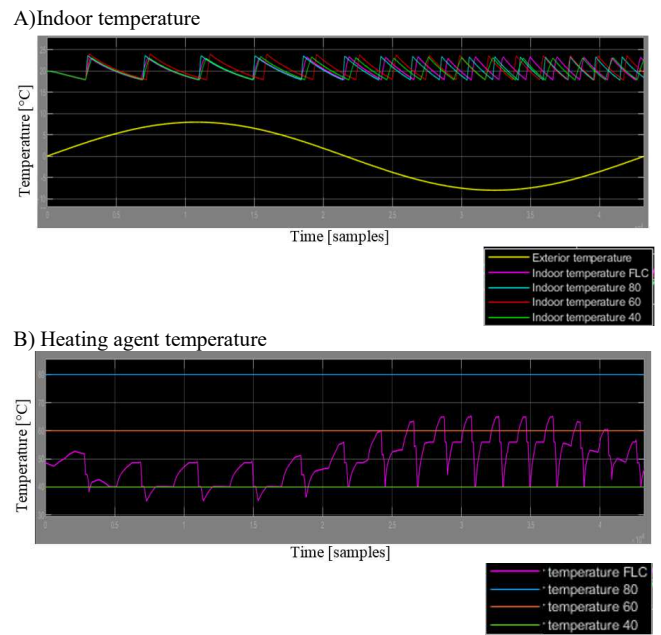


Fig. 9. Proposed method testing results

TABLE III. CONTROLLERS COMPARISON

Controller	T_{heat}^a [°C]	t_{heater}^b [hours, minutes]	E^c [kWh]	Price [Euro]
On/Off	40	3 h 45 min	37,5	4,56
On/Off	60	2 h 30 min	40	4,86
On/Off	80	1 h 45 min	42	5,11
FLC	variable	3 h	39	4,74

^a. Heat agent temperature

^b. Duration of the heater daily operation

^c. Electrical energy consumption

eliminate this weak point. Other aspects about the features of the living space could be studied, e.g., the construction materials to expand the research.

REFERENCES

- [1] ***Eurostat, "Energy consumption in households", Statistics explained, data from 2018.
- [2] N. Bertelsen and B. Vad Mathiesen, "EU-28 Residential Heat Supply and Consumption: Historical Development and Status", *Energies*, 2020, 13, 1894.
- [3] L. Kranzl et al., Heating & Cooling outlook until 2050, EU-28, HotMAPS project, 2019.
- [4] I. Sarbu, M. Mirza and E. Crasmareanu, "Heat distribution systems in buildings", The 26th Conf. on Installations for construction and ambient comfort, 6-7 th April 2017, Timisoara, Romania.
- [5] T. Benakopoulos, R. Salenbien, D. Vanhoudt and Svend Svendsen, "Improved control of radiator heating systems with thermostatic radiator valves without pre-setting function", *Energies*, 2019, 12, 3215.
- [6] M. Khan, Z. Rehman, U. Pervez, H.M I. Tariq and A. Iqbal, Central steam heating system, available online 15th of April 2021.
- [7] E.C.Ogu, Temperature control system, Thesis for B.Sc., The Department of Computer Science And Mathematics School Of Science And Technology Babcock University, Ilishan – Remo, Ogun State Nigeria, April 2011.
- [8] A.S. Sunay, O. Koçak, E. Kamberli and C. Koçum, "Design and construction of a labview based temperature controller with using fuzzy logic", available online 15th of April 2021.
- [9] A. Shome and S.D. Ashok, "Fuzzy logic approach for boiler temperature & water level control", *Inter. J of Scientific & Engin Research*, vol. 3, iss. 6, June-2012.
- [10] K.A. Kumar, P. Jyoshna and G. Seshadri, " Realization of fuzzy logic in temperature control system over PID", *Intern. J. of Engin. Research & Techn.*, vol. 3, iss. 7, pp.1506-1511.
- [11] P. Ramanathan, "Fuzzy logic controller for temperature regulation process", *Middle-East J. of Scientific Research*, vol. 20, iss. 11, pp. 1524-1528.
- [12] A.N. Isizoh, O.S. Okide, A.E. Anazia and C.D. Ogu, "Temperature control system using fuzzy logic technique", *Intern. J of Advan. Research in Artificial Intelligence*, vol. 1, no. 3, 2012, pp.27-31.
- [13] S. Afzal, M. Jamil, A. Waris, S.I. Butt and G. Mufti, "Fuzzy logic controller for boiler temperature control using labview and matlab", *Intern. J. of Control and Automation*, vol. 9, no. 9, pp.89-104.
- [14] E.S. Vincent, N. Chukwudumebi and A.T. Oluwaseun, " Application of fuzzy logic temperature controller for water bottle industry" *Comp. Engin. and Intell. Syst.*, vol.10, no.2, pp. 16-23, 2019.
- [15] T.K. Das and Y. Das, "Design of a room temperature and humidity controller using fuzzy logic", *American J of Engin. Research*, vol. 02, iss.11, pp-86-97.
- [16] J. Kumar et al, " Comparative analysis of room temperature controller using fuzzy logic & PID", *Advan. in Electr. and Electric Engin.*, vol. 3, no. 7, 2013, pp. 853-858.
- [17] B. Paris, J. Eynard, S. Grieu, T. Talbert and M. Polit, "Heating control schemes for energy management in buildings", *Energy and Buildings*, Elsevier, 2010, vol. 42, iss. 10, pp.1908- 1917.
- [18] L. Lianzhong and M. Zaheeruddin, " Hybrid fuzzy logic control strategies for hot water district heating systems", *Building Serv. Eng. Res. Technol.*, vol. 28, no.1, 2007, pp. 35-53.
- [19] P. Mondal and M. Mondal, "Temperature control inside a room using fuzzy logic method", *Intern. J. of Innovative Research in Science, Engin. and Tech.*, vol. 7, iss. 7, July 2018, pp. 7679-7685.
- [20] E. Himabindu and D. Krishna, "Design of fuzzy logic controller of residential electric water heaters", *Intern. J. of Current Engin. and Scientific Research*, vol. 5, iss. 4, 2018, pp. 207-211.
- [21] E.H. Mandami, "Applications of fuzzuy logic to approximate reasoning using linguistic synthetis", *IEEE Trans. on Syst., Man and Cybernetics*, v.c.-26, no. 12, pp. 1182-1191, 1977.

Knowledge-based system for the analysis of voltage fluctuations and flicker

Anca Miron, Andrei C. Cziker

Department of Power systems and Management
 Technical University of Cluj-Napoca
 Cluj-Napoca, Romania
 anca.miron@enm.utcluj.ro

Hadrian C. Bogariu

Department of Network's Performance Monitoring
 SDEE North Transylvania SA
 Cluj-Napoca, Romania

Abstract—Voltage fluctuations of low frequency that can cause light flicker are a power quality issue that affects several parts of the national distribution networks. In the most cases the flicker indices exceed the standards-imposed thresholds and the source of disturbance is unknown, thus becoming a troublesome situation. Considering these aspects, a knowledge-based system prototype was developed. It is dedicated to analyzing the voltage disturbances that occur in distribution networks, mainly voltage fluctuations. The paper presents the power quality issue of voltage fluctuations and flicker and the proposed artificial intelligence system.

Keywords— power quality, electric distribution networks, knowledge-based system, voltage fluctuations, light flicker

I. INTRODUCTION

Today's society is based almost entirely on electricity, since it is the most versatile form of energy. The importance of power quality has increased very much in the recent years due to several aspects: (i) the new generation of equipment are more sensitive to low power quality; (ii) the modern apparatus causes the decrease of power quality due to its components and/or functioning; (iii) the electrical energy is considered a product that must be quality assured. Accordingly, the power quality is very important for consumers and power network operators, as well.

Power quality for the networks operators is imperative for two reasons: they are compelled by standard to deliver the electrical energy with specific parameters, consequently the power quality indices must be in between imposed thresholds; and a low level of power quality negatively affects its components. Therefore, the power quality indices are permanently supervised in important nodes of the distribution and transmission networks.

The indices of the power quality are classified accordingly to their source so there are variations (power frequency, voltage magnitude, harmonics, unbalance and flicker) and events (voltage dips and swells, transients and voltage interruptions). Some of these parameters are well known by many (power frequency and voltage magnitude), but others like flicker are not.

Light flicker or simply flicker is a small repetitive change in the intensity of a light source that can be very annoying for

the human eye and to very sensible individuals can cause serious health problems. This phenomenon is determined by voltage fluctuations that vary with a specific frequency that is between 3 and 100 Hz (in standards frequency is considered under 35 Hz) [1]. Historically, only incandescent lamps were considered to suffer from voltage fluctuations. However, tests have been performed on other types of light sources like electromagnetic ballast fluorescent lamps and compact fluorescent lamps (CFL) and the results showed that those light sources can also generate flicker [1, 2, 7]. Recently, it was demonstrated that the LED lamps which are not very well designed can also suffer from flicker, because of the supply voltage fluctuations.

Voltage fluctuations may originate from the power system due to switching operations, but usually they are produced by consumers that have loads with fluctuating power. Such loads are: arc furnaces, rolling mill, motors, welders etc. The renewable generation units like wind turbines and wave power stations can also be sources for light flicker. To mitigate or eliminate this power quality disturbance, diverse methods were proposed, but there are three basic methods used in practice: (1) strengthen the network; (2) increase the short circuit power level; (3) install an active mitigation device.

In the infield power quality literature, the issue of flicker and consequently the voltage fluctuations are not very popular. The most approached aspects are the functioning of fluctuating loads [3-5], determining the source of voltage fluctuations [1], impact of voltage fluctuations on lamps [7, 9-11] and flicker measurement [1, 7, 8, 14-21].

The measurement of flicker is a complex process as it must connect the changes in the amplitude of voltage to the subjectivity of human eye and brain. Consequently, the development of flicker meter has been made in accordance with results obtained after many tests. During the experiments it was observed the impact of light flicker produced by variations of the supply voltage on human subjects. Being such a complicated measurement process, it needs expensive apparatus. A cheaper and elegant alternative to determine the existence of voltage fluctuations that are sources of flicker is the use of artificial intelligence techniques, like knowledge-based systems.

Knowledge-based systems (KBS) are computer programs that manipulate the knowledge that resides in them to solve complex problems. These systems can be successfully utilized where there is a large quantity of data about the problem that needs to be solved. The applications of these systems are very vast, and power systems is one of them.

The paper presents the results obtained after a study performed to find a simple method, which doesn't involve the use of expensive and complicated apparatus, with the main goal to identify if the flicker level is exceeding the standard limits. Thus, a prototype of a knowledge-based system dedicated to analyzing the voltage disturbances that occur in distribution systems was developed. The system has an inference engine, a knowledge base, and a graphic user interface. To be more efficient in collecting and mathematically manipulating data, the system is connected to a virtual instrument (VI) that can acquire data directly from an acquisition board or from data files.

The paper is organized as follows: the 2nd section describes the voltage fluctuations and flicker issue, as the 3rd section presents the characteristics and components of the KBS. The 4th section contains the prototype's description of the proposed KBS and VI, plus its testing. The paper's final section enumerates the conclusions of the research, about the use of artificial intelligence in power systems and power quality.

II. VOLTAGE FLUCTUATIONS AND FLICKER

Voltage fluctuations are electromagnetic disturbances characterized by small variations of the rms value, between -10 % and +10 % of the rated voltage, that can appear with a low frequency or random during a specified unit of time. This supply voltage disturbance is associated with light flicker at the end users' lamps.

The primary cause of voltage changes is at the consumers' side, when there is a time variability of the reactive power component of fluctuating loads, like arc furnaces, rolling mill drives, main winders etc. Typically, these loads' power has a high level of variation with respect to the short-circuit capacity at the point of connection to the supply. In other situations, when the light sources are close to small loads with varying power demand such as induction motors, welders, boilers, power regulators, electric saw and hammers, pumps and compressors, cranes, elevators etc., these installations became sources of flicker. Examples of the influence of such loads are presented in articles like [3-5]. In [3] a study case where the connection to the supply network of a welding machine is analyzed to find the total severity factor. There are proposed two mitigation solutions: to install a compensator device or to build a second line to strengthen the short-circuit power at the connection point.

On the side of the power system's operators, voltage fluctuation can be caused by capacitor switching and on-load transformer tap changes, which can change the inductive component of the source impedance. Variations in the generation capacity of wind turbines can also have an effect. Indeed, in [6] authors analyze the impact of wind turbines is analyzed using different techniques. In some cases, voltage

fluctuations can be caused by low frequency voltage inter-harmonics [1, 5].

Voltage fluctuation can cause many technical problems in power systems, but the physiological effect of light flicker is the most important one. This phenomenon affects directly the human beings causing fatigue, reduce of concentration levels etc. and indirectly it affects the ergonomics of the working environment.

A definition of light flicker is "impression of unsteadiness of visual sensation induced by a light stimulus whose luminance or spectral distribution fluctuates with time" [1, 7]. Over the past years numerous studies have been conducted to understand the mechanisms behind the light flicker occurrence. There are at least three different mechanisms influencing the light flicker perception by a human. These are: (i) the characteristics of the light source; (ii) the frequency response of the eye-brain of a human; (iii) the time constant of the eye-brain. In the case of lamps, the same quantity of voltage fluctuation will determine different responses. Certainly, a 60 W 230 V incandescent lamp will generate more flicker than a 60 W 120 V incandescent lamp. This is since the 60 W 120 V lamp has a thicker filament and the thermic inertia is higher. Using the results of the experimental studies the curves of irritability for incandescent lamps (Fig. 1 and 2) were established. These graphics were considered when establishing the standard flicker-meter [8, 9].

The curves from Fig. 1 indicate the dependence between the voltage fluctuation and modulation frequency of the supply voltage that causes a light flicker for an incandescent lamp of 60 W and 230 V that 50 % of people are susceptible to be negatively affected by. One can observe that the worse modulation frequency is 8.8 Hz, even for the voltage fluctuation is less than 0.5 %.

In case of random fluctuations, the worse scenario is when there are approximately 1000 changes per minute.

As new types of lamps, like CFL and LEDs, were more widely utilized, the impact of voltage fluctuation on them was analyzed. Indeed, there are described the results obtained from studying fluorescent lamps and CFL in [1, 2, 7-11] and lamps with LEDs in [12, 13].

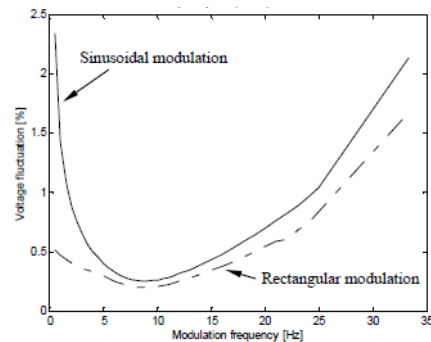


Fig. 1. Perception curves according to IEC 61000-4-15/A1 for flicker sensation sinusoidal and rectangular modulation (60W/ 230V/50Hz filament coiled lamp).

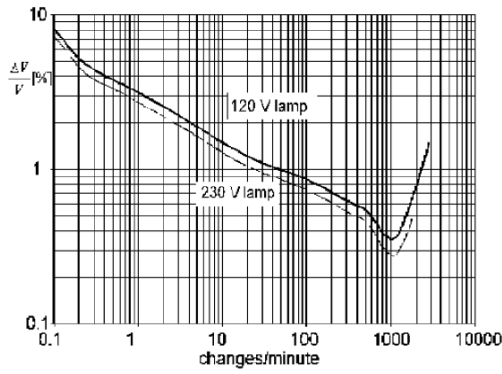


Fig. 2. Perception curves for different voltage levels

The outcomes from [9] show the average perceptibility of six human subjects for three different levels of frequency modulation of the voltage supplied to five types of light fixtures. It may be noted that with exception of a CFL with magnetic ballast, the incandescent lamp was the most sensitive to flicker. The other studies got similar results. As conclusion to these studies, in [7] it is underlined that the current standard flicker-meter is not suitable in the case of lamps different from the incandescent lamps.

The method for measuring and quantification of light flicker that is in use and widely recognized is described in [8]. The flicker-meter consists of 5 blocks, each of them having a specific role. The block diagram of the flicker-meter is described in Fig. 3.

The 1st block is a voltage adaptor that scales the input voltage with respect to its average value [7]. Thus, the flicker measurement is made based on the percentage ratio and the independence from the input voltage is guaranteed.

The 2nd, 3rd and 4th blocks represent the lamp-eye-brain chain model:

- Block 2 simulates the behavior of a 60 W 230 V incandescent lamp (standard's reference lamp) by squaring the input to separate the low frequency (0.5...30 Hz that produces the luminosity variations) voltage fluctuation from the main voltage signal.
- As the human eye has a selective, frequency – dependent behavior to the change in the light luminosity, its functioning is made through block 3. The block eliminates from the signal given by the previous block the continuous and above 100 Hz components. This block contains two in cascade filters: a first-order high-pass filter with a cutoff frequency of 0.05 Hz, and a 4th order band-pass filter that has the purpose to weighting based upon the characteristics of the lamp. This filter is based on the threshold curve of perceptibility obtained experimentally.
- Block 4 gives the instantaneous response to light flicker. It consists of a squaring multiplier and sliding mean filter. The first component simulates the nonlinear response of the eye-brain chain and the second simulates the short-term storage effect of the brain.

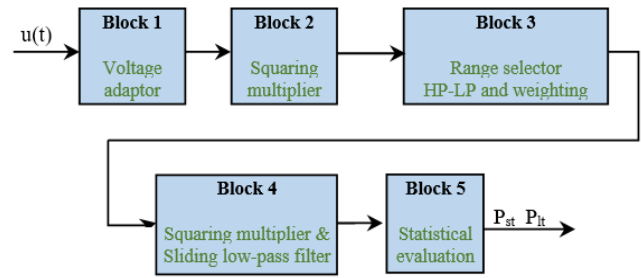


Fig. 3. Block diagram of the standard flicker meter

The 5th block statistically processes the output from the former block. The input data (instantaneous flicker levels) is divided in classes regards to the values that exceed the perceptibility value during a certain percentage of the observation time. There are two observation periods: short time – 10 minutes and longtime – 2 hours.

The indices for the flicker quantification are P_{st} and P_{lt} , that represent the flicker severity for short-term, and long-term periods. The mathematical relationships of the indices are listed below.

$$P_{st} = \sqrt{0,0314 \cdot P_{0,1} + 0,0525 \cdot P_{1s} + 0,0657 \cdot P_{3s} + 0,28 \cdot P_{10s} + 0,08 \cdot P_{50s}} \quad (1)$$

where the constants are the weighting coefficients and $P_{0,1}$ is the instantaneous sensation of flicker exceeded during 0.1% of the observation period and the index s refers to the average values: $P_{1s} = P_{0,7} + P_1 + P_{1,5}$, $P_{3s} = P_{2,2} + P_3 + P_4$, $P_{10s} = P_6 + P_8 + P_{10} + P_{13} + P_{17}$ and $P_{50s} = P_{30} + P_{50} + P_{80}$.

$$P_{LT} = \sqrt[3]{\frac{1}{N} \cdot \sum_{i=1}^N P_{STi}^3} \quad (2)$$

where N is the number of short-term severity indices over the long-term observation period that is 2 hours and P_{STi} are the values of the indices.

The standard EN 50160 specifies the index to be used for flicker is P_{LT} over a week, which is the minimum measurement period. It must be less than 1 during 95 % of the observation period.

Over the years, different methods for measurement of flicker were proposed [1, 14 - 21]. In [14] the authors suggest a graphical method; the use of LabVIEW and wavelet transform is suggested in [15] for monitoring the level of the voltage fluctuations that can cause light flicker. A method based on Kalman filters is proposed in [16, 17]. Algorithms based on Fourier transform for the calculation of light flicker are suggested in [18-21].

The conclusion of the recent papers is that in the present flicker-meter, the block that simulates the lamp behavior to voltage variations is not accurate in all cases. Hence, the standard should be reviewed and updated, and the block should be changed, according to the today's lamps.

III. KNOWLEDGE-BASED SYSTEMS

Knowledge-based systems are artificial intelligence techniques that use specialized information and logic-based reasoning to solve problems from a specific domain. The objectives of KBS are [22]: (1) provides a high intelligence level; (2) assists people in discovering and developing unknown fields; (3) offers a vast amount of knowledge in different areas; (4) aids in management of knowledge stored in the knowledge base; (5) solves social problems in a better way than traditional computer-based information systems; (6) acquires new perceptions by simulating unknown situations; (7) offers significant software productivity improvement; (8) significantly reduces cost and time to develop computerized systems. Considering these aspects, the main characteristics of a KBS are: it works for narrow domains in a reactive and proactive manner, the data manipulation is symbolic/connectionist and nonalgorithmic, it takes decisions based on knowledge and uses partial and uncertain information, data or knowledge.

The KBS consists of a Knowledge Base (KB) and a search program called Inference Engine (IE) that employs the information available in the KB. The KBS communicates with the users through a User Interface (UI). These three components represent the basic structure of a KBS. As one can see in Fig. 4 a general KBS can also contain explanation and self-learning modules. Other modules can be added to a KBS leading to form more complex architectures: data acquisition module, dynamic module, explanation base etc.

There are several types of KBS. Most applications in economy, medicine, engineering, education, military etc. are expert system, linked systems, case-based systems, database with an intelligent user interface and intelligent tutoring systems. The weak points of these software tools are the lack of imagination and ingenuity in solving problems and usage of symbolic characters that in some situations is difficult to handle.

The applications of KBS in power systems are many, some of them are presented in papers like [23-29]. The authors in [23] present an integrated expert system for analyzing and classification of all useful data regarding an electricity company's clientele. Its purpose is to determine which customer is susceptible to have caused fraud, and consequently increase the non-technical losses.

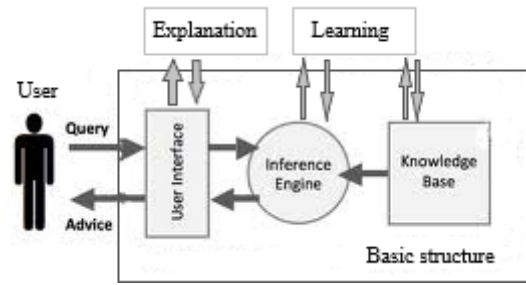


Fig. 4. General structure of a KBS

Another example is a prototype of a case-reasoning expert system which is recommended in [25].

The KB of the system was developed using info from various situations. The system was build using CLIPS as the logic programming program. In [29] a hybrid system that contains two units: an expert system and a fuzzy logic system is proposed. To determine the condition of a transformer, the input data is first analyzed and classified by the expert system which output data is fed to the fuzzy logic system that gives the state of the transformer.

Development of KBSs can be done using two approaches; the choice depends on the final product required features. The tendency is to use expert system shells when developing prototypes, like EXYS, and specific logic programming languages, like PROLOG and LISP. The main difference between the two methods is that a KBS developed using a shell has limited features regarding the UI and IE. In comparison a KBS made from the ground with a dedicated logic language is efficient by means of user interaction and reasoning strategy. The main strong point of using shells is the rapidity in obtaining KBSs.

IV. PROPOSED SYSTEM

The proposed system is a prototype that has the main purpose to determine if the flicker severity index exceeds the standard imposed thresholds that is $P_{LT} \leq 1$, for at least 95 % of the minimum observation period, a week.

The system uses a virtual instrument and a knowledge-based system. The data flow and system's algorithm are described through the diagram from Fig. 5.

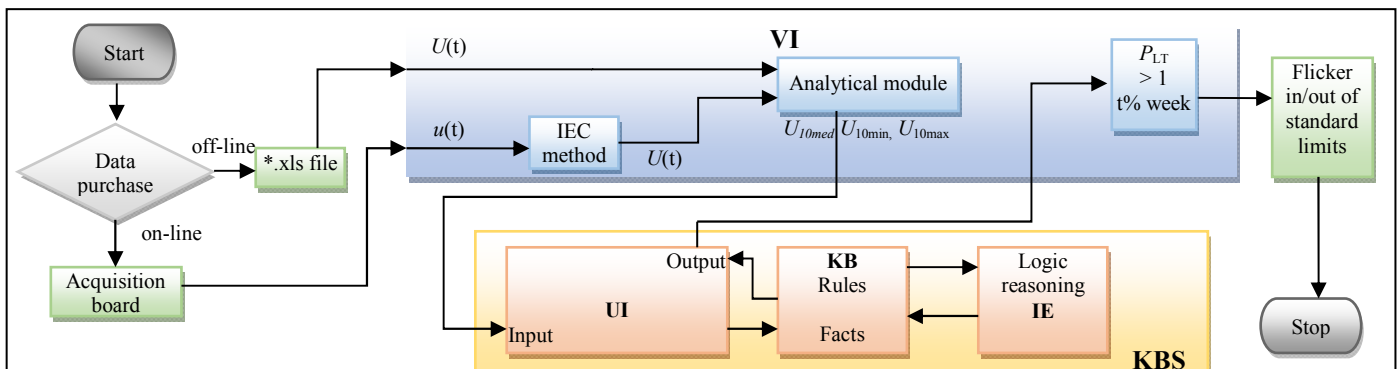


Fig. 5. Proposed system algorithm and data flow

The VI was build using LabVIEW graphical programming environment. It consists of a frontal panel and a diagram block. The frontal panel communicates with the users, being the component through which the VI acquires the input data and displays the results. Fig. 6 shows the frontal panel of the developed VI. The VI can operate on-line when in connection to a data acquisition board ($u(t)$, Fig. 5) or off-line in which situation it reads the input data from sheet-spread files ($U(t)$, Fig. 5). The VI's task is to prepare the measurement data for the KBS (U_{10med} , U_{10min} and U_{10max} , Fig. 5), as the later one can't make complicated calculus. In the on-line state the VI acquires the instantaneous voltage values and calculate according to standard the rms voltage values. Then again in the off-line case it is supposed that these values are already measured, so the VI only reads the data. In the next step the VI calculates the average, minimum and maximum rms voltage values over sample periods of 10 minutes and transfers the information for a period of a week to the KBS.

The KBS was developed with the help of CLIPS expert system shell. The KBS contains a KB, an IE and a UI. The KBS is the result of the research of data regarding the voltage fluctuations in the local distribution networks over an observation period of one year, namely 2018. This large amount of data was used to build the knowledge base of the KBS, namely the rules base.

The KB is the main part of the KBS. It contains two types of data: rules and facts. The first ones form the rules base and contain knowledge about the relationship between the voltage fluctuations and flicker's level. The rules base was build using production rules for the knowledge representation. The form of a rule is: "IF condition THEN action". In the stage of the KB development more than 100 sample periods mostly characterized by a flicker index P_{LT} between 0.8 and 3 were studied. It was observed that in most of the situations the dependence between the rms voltage and flicker level is obvious and proper rules could be implemented. However, there were found special cases, which were implemented as examples. Some of the rules used to build the KB are enumerated in Fig. 7.

The facts of the KB represent the input data that characterize the issue, so their values change according to the stage of the problem, contrary to rules.

The IE of the knowledge-based system is based on the forward chaining inference. The inference structure consists of the following actions:

- selection of the rules, which have in the "IF" section the facts acquired;
- conflicts solving that leads to one executable rule;
- execution of the action in the "THEN" section of the selected rule.

The working of the KBS is ended with the answer to the question: "During the evaluation week the flicker level is according to standard or not?" The result obtained by the KBS is transferred to the VI that displays the result.

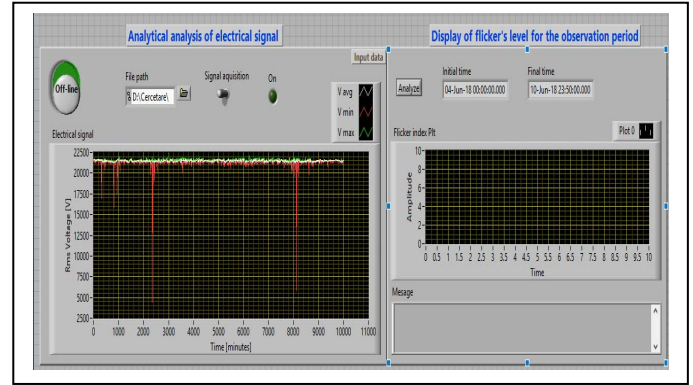


Fig. 6. Virtual instrument's frontal panel

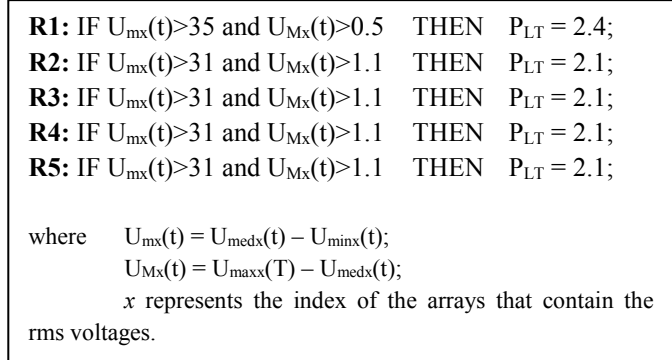


Fig. 7. Selective rules of the KBS's rules base

The UI of the KBS is predefined by the expert system shell. In the proposed system this component is not accessible to the user, but it becomes visible to the user if the KBS is operating independent from the VI. In this situation the user interacts directly to the KBS: giving the facts, asking questions etc.

The KBS receives data from the VI and transfers the results using temporarily created data files that after using are deleted from memory.

The proposed system was tested using data samples from spread-sheet files that were both like the special and general situations implemented in the KB. The results show that:

- System identified correctly in all cases if the standard limits for flicker have been exceeded;
- The P_{LT} presents an error of maximum $\pm 9\%$ for values above 1.5. This is because when building the KB, more concern was taken for the situation where P_{LT} is between 1.01 and 1.5.

V. CONCLUSIONS

The voltage fluctuations affect the fundamental quality of utility service – that is, the ability to provide lighting that is steady and consistent. Flicker is a subjective phenomenon that is caused by the amplitude variation of the supply voltage, thus its measurement is provide with the help of complex and expensive apparatus. A cheaper approach to determine the

existence of voltage fluctuations that determine light flicker is by means of artificial intelligence techniques, like KBS.

The proposed method uses a VI and a KBS. The role of the VI is to acquire and prepare input data for the KBS. The decision regarding the flicker severity is made by the later. The system's KB was build using data regarding the flicker's level over a year observation period. For representing the knowledge were used production rules, and with the help of more than 100 preparation samples were written more than 20 rules.

Validation samples were prepared from the acquired data. The system's testing showed its efficiency in the identification of the long-term flicker index.

Future research is planned for the identification of the flicker's sources and the growth of the KB to recognize more voltage disturbances.

ACKNOWLEDGMENT

Regards to the regional distribution network operators, "SDEE Transylvania Nord" for the support and help with the data used to develop the proposed knowledge-based system.

REFERENCES

- [1] P. Alexberg, "On tracing flicker sources and classification of voltage disturbances", thesis for the degree of doctor in Philosophy, Chalmers University, 2007, ISBN 978-91-7291-936-5.
- [2] R.C. Dugan, M.F. McGranaghan, S. Santoso, H.W. Beaty, "Electric power system quality", McGraw Hill, New York, 2003
- [3] A. Baggini, Handbook of Power Quality, John Wiley & Sons, Ltd, 2008, Araceli Hernández Bayo, "Voltage fluctuations and flicker – Case Study", pp. 33-42.
- [4] L. Tang, S. Kolluri, M. F. McGranaghan, "Voltage flicker prediction for two simultaneously operated ac arc furnaces", IEEE Transactions on Power Delivery, Vol. 12, No. 2, April 1997.
- [5] J.-L. Guan, M.-T. Yang, J.-C. Gu, H.-H. Chang, "Effect of harmonic power fluctuation on voltage flicker", Proceedings of the 11th WSEAS International Conference on SYSTEMS, Agios Nikolaos, Crete Island, Greece, July 23-25, 2007, pp. 230 - 236
- [6] M. K. Sharma, Advances in measurement systems, InTech, Ltd., Ch. 15, J.J. Gutierrez, J. Ruiz, A. Lazkano and L.A. Leturiondo, "Measurement of voltage flicker: application to grid-connected wind turbines", Advances in Measurement Systems, pp. 366-379, ISBN 978-953-307-061-2.
- [7] Standard IEEE std. 1159-1995. "IEEE recommended practice for monitoring electric power quality."
- [8] IEC 61000-4-15: 2003 Electromagnetic compatibility (EMC) - Part 4. Testing and measurement techniques. Section 15. Flickermeter - Functional and design specifications.
- [9] PQTN Brief No. 24, "Perception thresholds of flicker in modern lighting," published by EPRI Power Electronics Applications Center, September 1995.
- [10] PQTN Brief No. 36, "Lamp flicker predicted by gain-factor measurements," published by EPRI Power Electronics Applications Center, July 1996.
- [11] PQTN Brief No. 37, "Lamp flicker in compact fluorescent lamps and four-foot fluorescent lighting," published by EPRI Power Electronics Applications Center, August 1996.
- [12] H. Sharma, F. Sharp, "Flicker/voltage fluctuation response of modern lamps including those with dimmable capability and other low voltage sensitive equipment", 22nd International Conference on Electricity Distribution, Stockholm, 10–13 June, 2013.
- [13] A. Gil-de-Castro, S.K. Rönnerberg, M.H.J. Bollen, "Light intensity variation (flicker) and harmonic emission related to LED lamps", Electric Power Systems Research, vol. 146, 2017, pp. 107–114.
- [14] V. F. Polec, V. Maier, S. G. Pavel, H. G. Beleiu and C. Ciorca, "Graphic functions analytical identification at flicker evaluation", 2014 16th International Conference on Harmonics and Quality of Power (ICHQP), 425 - 429, ISBN: 978-1-4673-6487-4 14.
- [15] Z. Li, "Voltage fluctuation and flicker monitoring system using LabView and wavelet transform", Journal of Computers, vol. 5, no. 3, March 2010, pp. 417-424.
- [16] Z. Hanzelka, A. Bien, "Voltage Disturbances – Flicker and Flicker measurement", Power Quality Application Guide, April 2006.
- [17] A. Girgis, E. Makram, "Measurement of voltage flicker magnitude and frequency using a Kalman filtering based approach". Canadian Conf. On Computer Engineering, May 1996. Flicker measurement.
- [18] K. Srinivasan. "Digital measurement of voltage flicker". IEEE Trans. Power Del, vol. 6, pp. 1593-1598, Oct. 1991. Flicker measurement.
- [19] S. Nuccio. "A digital instrument for measurement of voltage flicker". IEEE Instrumentation and Measurement Technology Conf. Ottawa, Canada, May 1997.
- [20] M. Chen. "Digital algorithms for measurement of voltage flicker". IEE Proc.-Gener. Transmission. vol. 144, pp 175-180, Mar. 1997.
- [21] A. Hernandez, J. Mayordomo, R. Asensi and L. Beites. "A new frequency domain approach for flicker evaluation of arc furnaces". IEEE Trans. Power Del. vol. 18, pp. 631-638, Apr. 2003.
- [22] R.A. Akerkar, P.S. Sajja, "Knowledge-based systems", Jones & Bartlett Learning Publishing House, 2009, ISBN: 978-0763776473.
- [23] C. León, F. Biscarri, I. Monedero, J.I. Guerrero, J. Biscarri, R. Millán, "Integrated expert system applied to the analysis of non-technical losses in power utilities", Expert Systems with Applications, vol. 38, 2011, pp. 10274–10285.
- [24] B. Zhang, X. Li, S. Wang, "A novel case adaptation method based on an improved integrated genetic algorithm for power grid wind disaster emergencies", Expert Systems with Applications, vol. 42, 2015, pp. 7812–7824.
- [25] J.A. Matelli, E. Bazzo, J.C. da Silva, "Development of a case-based reasoning prototype for cogeneration plant design", Applied Energy, vol. 88, 2011, pp. 3030–3041.
- [26] R. K.Rayudu, "A knowledge-based architecture for distributed fault analysis in power networks", Engineering Applications of Artificial Intelligence, vol. 23, 2010, pp. 514–525.
- [27] K. Tuitemwong, S. Premrudeepreechacham, "Expert system for protection coordination of distribution system with distributed generators", Electrical Power and Energy Systems, vol. 33, 2011, pp. 466–471.
- [28] W.C. Flores, E.E. Mombello, J.A. Jardini, G. Rattá, A.M. Corvo, "Expert system for the assessment of power transformer insulation condition based on type-2 fuzzy logic systems", Expert Systems with Applications, vol. 38, 2011, pp. 8119–8127.
- [29] R.J. Sárfi, A.M.G. Solo, "Development of a hybrid knowledge-based system for multiobjective optimization of power distribution system operations", IAAI-05 /, pp. 1547-1554.

The Impact of Multiple Small PV Units on Distribution Networks. Romanian Case-study

Anca Miron, Andrei C. Cziker, Ștefan Ungureanu and Horia Gh. Beleiu

Dept. of Power Systems and Management
 Technical University of Cluj-Napoca
 Cluj-Napoca, Romania
 anca.miron@enm.utcluj.ro

Abstract— The paper presents the results obtained at the end of a study whose main goal was to answer the question: What will happen in a distribution network if there will be a large injection of power from a big number of small PV units? This situation is typical for rural distribution networks where the domestic consumers have their own PV generation units, thus becoming prosumers. The study began with the modeling of the usual domestic consumer from rural regions. After this step being finalized, the implementation of the distribution network in a simulation software followed. For this stage MatLab/Simulink was used. Thus, different situations were simulated in order to determine a full understanding of the possible problems that can appear, and consequently to be able to take the proper actions to minimize the negative impact. The results of the simulations show that in a typical summer day, when the PV units produce electricity at 100% of their capacity and the loads' consumption is the lowest, the voltage in the point of injection in distribution network can reach values that will determine the faulty operation of the consumers due to the protection apparatus' activation. Various configurations for the grid have been considered. Also, the study points out that integrating PV units by residential consumers can also help the electric grid to better maintain voltage variations in cases of larger distribution lines.

Keywords— *distribution network; PV unit; domestic consumer; power quality; computer simulation; prosumer*

I. INTRODUCTION

In the latest years, because of the environmental problems, financial advantages and technical development, the number of small generation units, that use renewable energy, has increased very much and keeps rising. In Romania, this fact is encouraged by the creation of governmental regulations supporting the use of renewable energy. In addition, it is the decreasing of the prices of these „green energy” generation units, especially PVs (photovoltaic panels). Thus, a questionnaire in a Romanian rural region performed to determine the domestic consumers' behavior showed that more than 20 % of the consumers from the sample study reflect about the installation of an on-roof PV units to decrease their electricity bill.

The paper presents the results obtained at the end of a study whose main goal was to answer the question: What will happen in a distribution network if there will be a large injection of

power from a big number of small PV units? This situation is typical for rural distribution networks where the domestic consumers have their own PV generation units (i.e. farms with rooftop installation, local agricultural businesses, and households).

The impact of PV units on distribution networks is researched worldwide [1-12]. In [1] the authors present the effects on the grid of PV-home systems in the Palestine region. The effects that were observed are: the decrease of technical losses, the increase of the voltage level near the consumers that have the PV units and the decrease of the power factor from 0.866 to 0.802 on the consumers' side of the transformer.

Using high resolution solar resource assessment with sky imager and quasi-state distribution system simulation, the authors of [2] write about the effects of high PV penetration on distribution networks and conclude that: (1) the impacts of high PV penetration depend on feeder topology and characteristics; (2) the use of a single PV generation profile overestimates the tap operation number up to 260% resulting from an overestimation of power ramp rates and magnitudes – therefore, multiple realistic profiles should be used; and (3) distributed PV resources increase the feeder hosting capacity significantly compared to a centralized setup. In comparison with this study, other one that is described in [3] whose focal target was to determine the opportunities and challenges of PVs, underline the advantages of these small generation units: benefits in voltage profile, low power losses etc.

The problem of voltage stability in distribution systems with large-scale PV generation is analyzed in [4-6]. The simulations' results from [4] show that reactive power prioritization (without any reactive current limits) is not effective for long term voltage stability, as it will lead to voltage collapse due to significant active power reduction in the power network. An application of phasor measurement units is used successfully in [6] for the analysis of the Japanese power system dynamics with high penetration of PVs.

The impact of voltage fluctuations produced by PVs because of cloud transients are studied in [7]. The results demonstrate that the phenomenon can cause light flicker, but its level won't exceed the thresholds from the imposed standard.

Other power quality problem caused by the PV inverters, namely harmonics, are discussed in [8]. At the end of the study, the authors conclude that “Despite the current THD of PV system is higher for low solar irradiance conditions, the voltage distortion for these conditions are lower than in high solar irradiance conditions. When the high solar irradiance conditions are considered, the higher harmonic voltage distortions are observed since the PV system output power increases for these conditions.”

In [9] and [10] the impact of energy storage components of PV systems is researched. Thus, the authors from [9] began their study with the question: “Are PV battery systems causing ramping problems?” At the end, they determined that the answer is “No”, the PV battery systems don’t cause ramping problems.

In [12] the authors demonstrate that an unfavorable situation happens in the winter period on cold sunny days due to low temperature and high solar radiation, the PV panels have peak yield and generate a great amount of power in the grid. Low consumption in the power line (low voltage) will require in order to evacuate the energy, a higher voltage in the PCC (point of connection) to be able to transport the energy in the nearest power station.

Considering the already made studies and their results presented in the infield literature, the research described in the paper was realized by performing three steps: (i) modelling of the usual domestic consumer from rural regions (Romanian situation); (ii) implementation of the distribution network that was used as support for the research; (iii) simulation of diverse scenarios in order to determine a full understanding of the possible problems that will appear, and subsequently to be able to take the proper actions to minimize the negative impact.

The main contributions of the study are:

- Modelling of the rural domestic consumer based on a questionnaire whose results express the behavior of Romanian rural consumers from rural regions;
- Implementation of the distribution network considering real domestic consumers and PV units, accordingly with their harmonic contents;
- Scenarios based on the situations found in an actual Romanian distribution network.

The rest of the paper is organized as follows: Section 2 describes the first step (domestic consumers modelling) of the study and its results. Section 3 presents the implemented distribution network that was used to realize the simulations and the scenarios that were considered. The simulations’ results are enumerated in the fourth section, and the conclusions of the study are underlined in the last section of the paper.

II. DOMESTIC CONSUMERS MODELLING

The modelling of the domestic consumers began with a questionnaire completed by 60 domestic consumers from a rural region. The consumers answered questions regarding their electrical apparatus characteristics, the way they use this apparatus and their intentions concerning the decrease of their electricity consumption and consequently the electricity bill. In

table 1 the most used electrical apparatus by the consumers is listed, and how often they are used during a usual week all-round year. Other apparatus that were found at 20 – 40 % of the consumers are heating devices like induction hob, hair dryer and kitchen appliances. Domestic apparatus that were used by less than 10 % of the consumers are: freezer and diverse small appliances. Regarding the electric lamps, it can be observed from the table that more than half of the consumers use light devices with LEDs and CFLs (compact fluorescent lamps), and only 25 % still use incandescent lamps.

Concerning their behavior, more than 86 % of the consumers have specified that they don’t use the apparatus if not needed, i.e. forget to shut down the lamps. So, it can be concluded that they are responsible and act efficiently regarding the electricity consumption.

To the question “What will you do to decrease the electricity consumption”, more than 20 % of the consumers answered that they consider the installation of rooftop PV generation units, about 70 % of them think to change their apparatus with new ones that have a higher class regarding the energy efficiency and the rest consider to use their devices more effective.

In conclusion to the questionnaire, it can be said that the rural domestic consumer is “energy responsible”, he/she uses modern appliances and is opened to increase energy efficiency.

The data from the questionnaire was used to obtain the rural domestic consumer universal model (RDCUM), that was used to simulate the distribution network.

TABLE I. DOMESTIC CONSUMERS’ APPARATUS

No.	Apparatus	Consumers [percentage from 60]	Frequency of utilization
1	Refrigerator	100 %	Daily
2	Battery charger	100 %	Daily
3	TV	100 %	Daily
4	Washing machine	100 %	Daily to once a week
5	Vacuum cleaner	95 %	Twice – once a week
6	Microwave oven	90 %	Daily
7	PC / Notebook	90 %	Daily
8.	Mixer	88 %	Once a week / rare
9	Hair dryer	83 %	Three times / twice a week
10	Electrical boiler	50%	Daily
11	Resistance oven	45%	Once / twice a week
12	Lamps with LEDs	56.7%	Daily
13	CFLs	55%	Daily
14	Incandescent lamps	25%	Daily
15	Fluorescent lamps	6.7%	Daily

The model contains the apparatus from table 1 and other appliances that were mentioned by the consumers and it can be adapted to the contents of the real consumers. Furthermore, RDCUM's apparatus are considered with their harmonic content that was obtained from previous studies [13-20].

The RDCUM can be seen in Fig. 1., where the apparatus is represented as loads on the fundamental frequency and current sources for the harmonics. The harmonic characteristics of four appliances are illustrated in Fig. 2.

III. DISTRIBUTION SYSTEM IMPLEMENTATION

The second stage of the research was to implement the distribution system in the simulation software. For this purpose were used:

- the model from the previous step,
- data from a real Romanian distribution network (electric lines and transformer's features),
- the model of the PV system.

The distribution network is typical for Romanian rural regions and consists of a main transformer and the corresponding electric lines that connect the consumers with the main power system. In table 2 are enumerated the distribution network elements and their features.

The distribution system implementation is illustrated in Fig. 3. It can be seen that the consumers are supplied through three feeders and they are distributed along the network accordingly with a real situation, i.e. unbalanced on the three phases of the three-phase distribution network.

All 60 domestic consumers were designed as single-phase loads of 1 kW and accordingly with their options from the questionnaire.

TABLE II. DISTRIBUTION NETWORK ELEMENTS

No.	Network's element	Element's characteristics
1	Transformer, T	DYn, 20/0.4 kV
2	Electric line, L1.1	0.037+j0.02 Ω
3	Electric line, L1.2	0.037+j0.02 Ω
4	Electric line, L1.3	0.05+j0.006 Ω
5	Electric line, L1.4	0.099+j0.04 Ω
6	Electric line, L1.5	0.091+j0.035 Ω
7	Electric line, L2.1	0.037+j0.02 Ω
8	Electric line, L2.2	0.073+j0.013 Ω
9	Electric line, L2.3	0.05+j0.006 Ω
10	Electric line, L2.4	0.08+j0.035 Ω
11	Electric line, L3.1	0.037+j0.02 Ω
12	Electric line, L3.2	0.07+j0.013 Ω
13	Electric line, L3.3	0.09+j0.04 Ω
14
15	Electric line, L3.8	0.068+j0.011 Ω

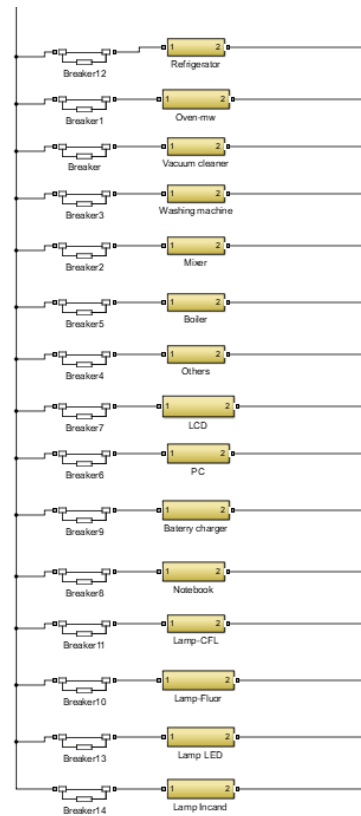


Fig. 1. MatLab/Simulink implementation of RDCUM.

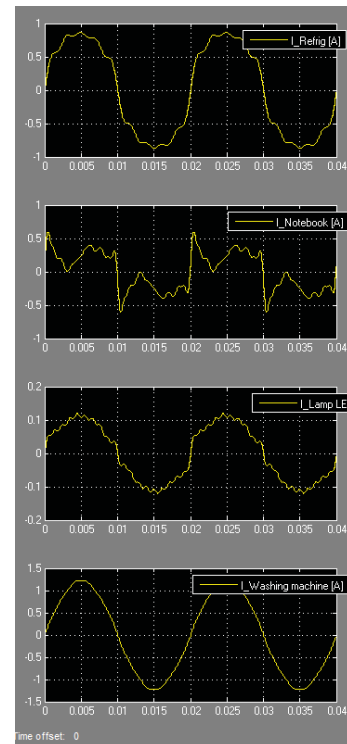


Fig. 2. Harmonic currents of RDCUM's appliances. a) Refrigerator's b) Notebook's, c) Lamp's with LEDs and d) Washing machine's current waveform.

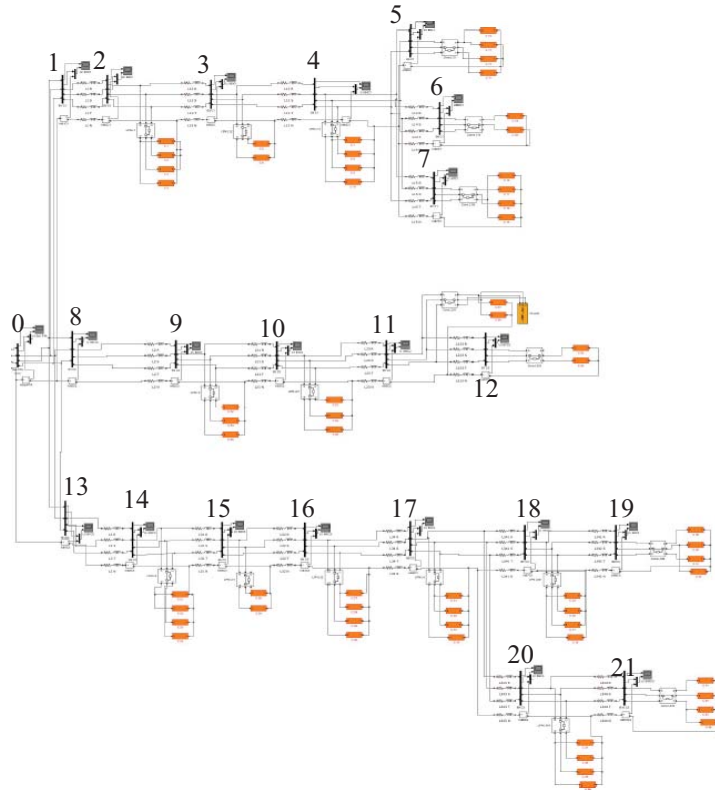


Fig. 3. MatLab/Simulink implementation of the research's support distribution network (without the PVs).

As regards the PVs and in view of the consumers preferences (the 13th consumers that considered to install PVs), two different classes of PVs were implemented: 4x240 W and 4x380 W.

The PV systems were considered as sources of harmonic currents, as their connection to the network is by an inverter that distorts the waveform of the current and consequently the voltage. For this purpose a typical single-phase inverter was used. Fig. 4 presents the current's harmonic spectrum of the inverter.

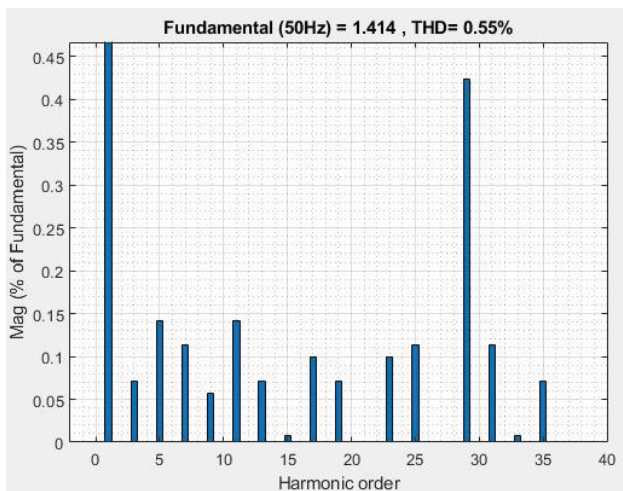


Fig. 4. Current's harmonic spectrum of the inverter.

IV. SIMULATIONS' RESULTS

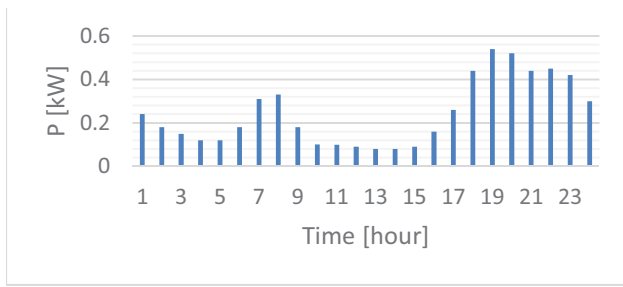
The final stage of the research was performed in concordance with the profiles of the typical consumer's average daily consumption and the peak power generated by a PV system from the considered rural region. The active power profiles for the consumption and generation are illustrated in Fig. 5. From them, one can observe that:

- (1) there are two peaks in the consumption, at 8 am and 7 pm, whereas at 1 pm is the lowest level;
- (2) the PVs generate the maximum power at around mid-day in January, in March and October between 10 and 12 am, and in July from 9 am until 2 pm.

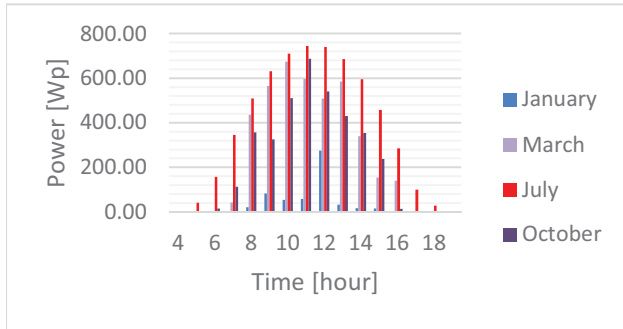
Considering the variations in consumption and generation, 12 scenarios were build: A, B, ..., M (Table III). For the simulations, the 13th PV systems were positioned at the end of the feeders, i.e. consumers connected at nodes 6, 7, 12, 19 and 21.

TABLE III. SCENARIOS

Scenario		Consumption		
		Peak 8 am	Minimum	Peak 7 pm
PV generation	January	A	B	C
	March	D	E	F
	July	G	H	I
	October	J	L	M



(a)



(b)

Fig. 5. Average profiles for (a) consumer's consumption, (b) PV generation.

Fig. 6 shows the voltage profiles obtained from the simulations.

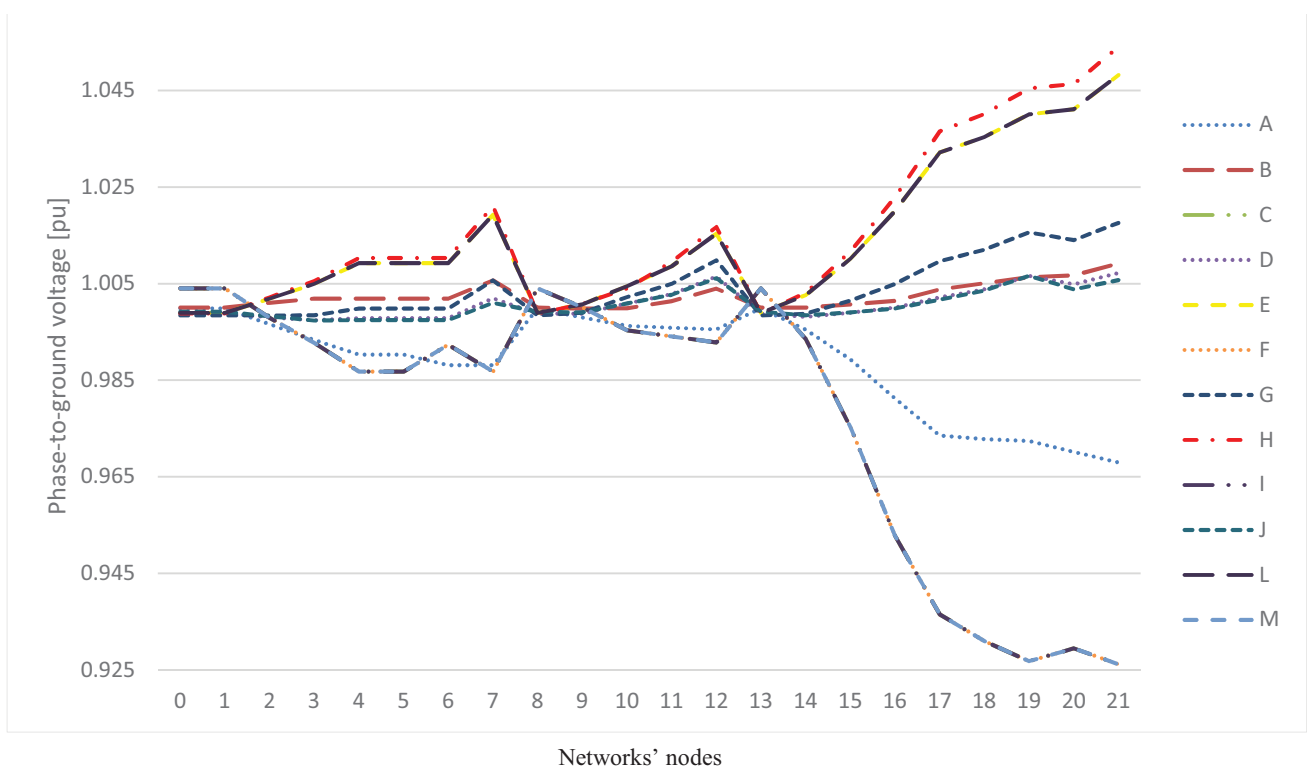


Fig. 6. Voltage profiles for scenarios A to M in nodes 0...21.

From the obtained data, the followings can be observed:

- At the consumption peak, at 7 pm there is no PV generation. Thus for scenarios C, F, I and M the rms voltage can drop below -5% of the nominal voltage (U_n), but within the $\pm 10\% U_n$ (imposed though Romanian standard). This happens at the end of feeder 3, because node 21 is the furthers from the supply node;
- At the first consumption peak, 8 am, in January (scenario A), the PV generation is very low, that it is neglected, so the voltage can drop close to -5% U_n ;
- In the other similar scenarios, D, G and J the PV generation can reach 50 % from the peak that is July mid-day, thus the voltage profile becomes smoother. Indeed, the voltage varies between +1% U_n , in all nodes of the networks;
- At the lowest consumption time, which it is the time of the highest generation level, scenarios E, H and J, from March to October the voltage level can grow dangerously close to +5% U_n (that is the limit imposed by standard for prosumers). In scenario J the level exceeds the imposed threshold, thus the protective apparatus will disconnect the corresponding prosumer.

Regarding the harmonic pollution, even though the consumers have many loads that are sources of harmonic currents, the voltage THD highest value was 2.67 %, so it didn't exceed the imposed threshold.

V. CONCLUSIONS

In the late years, the domestic consumers have the possibility to become prosumers. Thus, a questionnaire realized in a Romanian rural locality shows that 21% of the questioned consumers consider to install PV systems in order to decrease their electricity consumption from the public supply network and consequently their electricity bills.

The results of the questionnaire show that the typical rural domestic consumer has mostly modern appliances, i.e. LED lamps and microwave ovens, and has a responsible behavior (considering the use of electrical energy).

A real Romanian distribution network with the corresponding consumers and the PV systems were simulated considering the consumers' consumption profiles and PV systems generation in the studied Romanian region. The results show that the voltage level can exceed the +5% U_n and consequently activate the protective apparatus. This event happens in July at mid-day, when the consumption level is the lowest and the generation is the highest, and affects only the prosumer or the near consumers, but the rest of the feeders are not affected. The same conclusion was reached regarding the harmonic pollution: a consumer that has many harmonic pollution sources will affect its neighbors, on the same feeder, but not the entire distribution network.

At the end of the study, it can be concluded that the installation of multiple small PV systems in the rural region will increase the voltage level at the end of the feeders, but also its stability. However, if the PV system is not properly dimensioned, it can cause the prosumers to be disconnected from the grid due to the voltage rise.

ACKNOWLEDGMENT

This work was supported by a grant of the Romanian Ministry of Research and Innovation, CCCDI – UEFISCDI, project number PN-III-P1-1.2-PCCDI-2017-0404 / 31PCCDI / 2018, within PNCDDI III.

REFERENCES

[1] M.A. Omar and M.M. Mahmoud, "Grid connected PV- home systems in Palestine: A review on technical performance, effects and economic feasibility", *Ren. and Sust. Energy Reviews*, vol. 82, 2018, pp. 2490–2497.

[2] A. Nguyen, M. Velay, J. Schoene, V. Zheglov, B. Kurtz, K. Murray, B. Torre and J. Kleissl, "High PV penetration impacts on five local distribution networks using high resolution solar resource assessment with sky imager and quasi-steady state distribution system simulations", *Solar Energy*, vol. 132, 2016, pp. 221–235.

[3] S. Pujan Jaiswal, V. Shrivastava and D. K. Palwalia, "Opportunities and challenges of PV technology in power system", *Materials Today: Proceedings*, <https://doi.org/10.1016/j.matpr.2020.01.269>.

[4] E. Munkhchuluun, L. Meegahapola and A. Vahidnia, "Long-term voltage stability with large-scale solar-photovoltaic (PV) generation", *Electrical Power and Energy Systems*, vol. 117, 2020, no. 105663.

[5] J. Yaghoob, M. Islam and N. Mithulananthan, "Analytical approach to assess the loadability of unbalanced distribution grid with rooftop PV units", *Applied Energy*, vol. 211, 2018, pp. 358–367.

[6] T. Kerdphol, Y. Matsukawa, M. Watanabe and Y. Mitani, "Application of PMUs to monitor large-scale PV penetration infeed on frequency of 60 Hz Japan power system: A case study from Kyushu Island", *Electric Power Systems Research*, vol. 185, 2020, no.106393.

[7] N.B.G. Brinkel, M.K. Gerritsma, T.A. AlSkaif, I. Lampropoulos, A.M. van Voorden, H.A. Fidler and W.G.J.H.M. van Sark, "Impact of rapid PV fluctuations on power quality in the low-voltage grid and mitigation strategies using electric vehicles", *Electrical Power and Energy Systems*, vol. 118, 2020, no.105741.

[8] I.C. Barutcu, E. Karatepe and M. Boztepe, "Impact of harmonic limits on PV penetration levels in unbalanced distribution networks considering load and irradiance uncertainty", *Electrical Power and Energy Systems*, vol. 118, 2020, no.105780.

[9] D. Haberschusz, K.-P. Kairies, O. Wessels, D. Magnor and D.U. Sauer, "Are PV battery systems causing ramping problems in the German power grid?", *Energy Procedia*, vol. 135, 2017, pp. 424–433.

[10] L.H. Koh, Gao Zhi Yong, W. Peng and K.J. Tseng, "Impact of Energy Storage and Variability of PV on Power System Reliability", *Energy Procedia*, vol. 33, 2013, pp. 302 – 310.

[11] C. Mateoa, R. Cossenta, T. Gómez, G. Pretticob, P. Friasa, G. Fullib, A. Meletioub and F. Postigo, "Impact of solar PV self-consumption policies on distribution networks and regulatory implications", *Solar Energy*, vol. 176, 2018, pp. 62–72.

[12] M. Mussard, "Solar energy under cold climatic conditions: A review", *Ren. and Sust. Energy Reviews*, vol. 74, 2017, pp. 733-745.

[13] S. P. Elphick, "The modern domestic load and its impact on electricity distribution network", Master of Engineering – Research thesis, School of Electrical, Computer and Telecommunications Engineering, University of Wollongong, Australia, 2011.

[14] A. Gil-de-Castro, S. K. Rönnerberg, M. H.J. Bollen, A. Moreno-Muñoz, "Study on harmonic emission of domestic equipment combined with different types of lighting", *Int. J. of Electr. Power and Energy Syst.*, vol. 55, 2014, pp. 116–127

[15] A. Dolara, S. Leva, "Power quality and harmonic analysis of end user devices", *Energies*, vol. 5, 2012, pp. 5453-5466.

[16] P. R. Nasini, N. R. Narra, A. Santosh, "Modeling and harmonic analysis of domestic/industrial loads", *Inter. J. of Engineering Research and Applications (IJERA)*, vol. 2, issue 5, September- October 2012, pp.485-491.

[17] A. Iagar, G. N. Popa, C. M. Dinis, "The influence of home nonlinear electric equipment operating modes on power quality", *WSEAS Trans. on Syst.*, vol. 13, 2014, pp. 357-367.

[18] C. Kocatepe, R. Yumurtacı, O. Arıkan, M. Baysal, B. Kekezoğlu, A. Bozkurt, C. F. Kumru, "Harmonic Effects of Power System Loads: An Experimental Study", *Power Quality Issues*, Chapter 7, pp. 175 – 200, Intech licensee.

[19] George, A. Bagaria, P. Singh, S. R. Pampattiwar, S. Periwal, "Comparison of CFL and LED lamp – harmonic disturbances, economics (cost and power quality) and maximum possible loading in a power system", 2011, *Int. Conf. and Utility Exhibition on Power and Energy Syst. Issues & Prospects for Asia (ICUE)*, IEEE, pp. 1-5.

[20] A. Miron, A. Cziker, M. Chindriş and D. Sacerdotianu, "Impact of distributed generation on weak distribution networks. study case on a Romanian microgrid," 2016 *International Conference on Applied and Theoretical Electricity (ICATE)*, Craiova, 2016, pp. 1-6, doi: 10.1109/ICATE.2016.7754627.

Software Tool for Real-Time Power Quality Analysis

Anca MIRON, Mircea Dorin CHINDRIȘ, Andrei Cristinel CZIKER
Technical University of Cluj-Napoca, Cluj-Napoca, 400114, Romania
 anca.miron@enm.utcluj.ro

Abstract—A software tool dedicated to the analysis of power signals containing harmonic and interharmonic components, unbalance, voltage dips and voltage swells is presented. The software tool is a virtual instrument, which uses innovative algorithms based on time and frequency domains analysis to process power signals. In order to detect the temporary disturbances, edge detection is proposed, whereas for the harmonic analysis Gaussian filter banks are implemented. Considering that a signal recovery algorithm is applied, the harmonic analysis can be made even if voltage dips or swells appear. The virtual instrument input data can be recorded or online signals; the last ones being get through a data acquisition board. The virtual instrument was tested using both virtually created and real signals from measurements performed in distribution networks. The paper contains a numeric example made on a synthetic digital signal and an analysis made in real-time.

Index Terms—application software, fault detection, harmonic analysis, signal processing algorithms, time domain analysis.

I. INTRODUCTION

In the last years, as the computer science and PCs have rapidly progressed, the power engineers were encouraged to implicate them in solving diverse problems from the power systems field, e.g. modeling, simulation, measurements, process control, protections etc. Furthermore, dedicated software tools have been developed to sustain and improve the engineers work: MatLab, ETAP, PSCAD, MathCAD, LabVIEW etc. [1]

Among these software products, LabVIEW occupies a special place as it is a graphical programming environment. This particular characteristic of LabVIEW brings it near the electrical engineers that don't need specialized programming knowledge to work with it. The software products developed in LabVIEW are virtual instruments (VIs), which imitate physical instruments like: oscilloscopes, multi-meters, power quality analyzers etc. Considering that VIs work like any software, they can be used as simulation tools in a closed virtual world in which the user can observe the behavior of complex system (in this way being of great help in understanding various phenomena), but also as measurement tools [2].

Virtual instruments bring many advantages: flexibility, display facilities, data storage capability (computers have more memory than stand alone instruments) and importing

information methods; whereas the drawbacks are concerning the need of highly developed hardware.

Recently, in the field of power systems many authors propose the virtual instrumentation approach in various situations, such as simulation in [2] and [3], measurement in [4] – [8], detection in [9] and process control in [10]. Thus in [2] is showed a virtual instrument developed for the simulation of different operating states of power systems. A measurement system dedicated for the harmonics, voltage transients and flicker is proposed in [4]. The system is composed of a transducer, a computer with data acquisition board, a remote server and a virtual instrument that connects the components and makes the signal analysis. In [5] a VI build for the frequency measurement is described. The authors verified different four methods in order to obtain the best one for the fundamental frequency detection under non-stationary conditions. The virtual instrumentation is also used in [6] for the measurement of the fundamental frequency. In [7] the virtual instrumentation approach is proposed in order to determine the characteristics of the passive components under non-sinusoidal conditions. The authors model R, L and C components using the Z-domain. Finally, they obtained dynamic models of the passive components and simulate the non-sinusoidal condition with the help of a VI. The detection of loads characteristics and the simulation of power flow using the Park transform components using a virtual instrument are described in [8].

In this paper a virtual instrument dedicated for the analysis of power signals, in order to determine the existence and characteristics of harmonic distortion, unbalance, voltage dips and voltage swells is proposed. The processing algorithms are based on time and frequency domains analysis. The edge detection using Morlet function is applied to identify the temporary disturbances. A time approach is considered to extract the characteristics of the detected voltage dips and swells. As a special algorithm is used to recover the signals affected by the temporary r.m.s. (root-mean-square) voltage modification, the stationary disturbances analysis can also be performed on the entire analysis window that is of 0.2 s. The Gaussian filter banks are used to determine the quality indices of harmonic and interharmonic components. Besides the standard power quality indices, the VI also calculates new indices that can quantify in a more appropriate way the real operating state.

The paper is organized as follows: Section 2 describes the signal processing algorithm proposed for the detection and analysis of the studied disturbances. The VI components are presented in section 3, which contains information about the proposed power quality indices. Some numeric examples made with synthetic and real signals are showed in section

This paper was supported by the project “Develop and support multidisciplinary postdoctoral programs in primordial technical areas of national strategy and research – development - innovation” 4D-POSTDOC, contract nr. POSDRU/89/1.5/S/52603, project co-funded from European Social Fund through Sectorial Operational Program Human Resources 2007-2013.

4. The paper ends with a section of conclusions where are described the main aspects and advantages of the developed virtual instrument.

II. SIGNAL PROCESSING ALGORITHM

Currently, the power signals processing needed to assess the power quality indices is made by physical analyzers that have to respect several rules imposed by the in force standards (series IEC 61000 [11] – [13]). The most precise of them are instruments of Class A, implicated specially in measurements that require highly precision and legally recognition. The other two classes of precision, B and S, are not so restricted, considering that the manufacturer can use diverse methods.

Further on, the proposed methodology for the signal processing is presented in comparison with the conditions imposed for class A of performance instruments, and the drawbacks of standard methods are underlined.

The requirement in the case of harmonic pollution is to use a method (suggested the Fourier transform) that brings good results for a measurement window of 10 time cycles at 50 Hz fundamental frequency (0.2 s). As the upper order harmonics have negligible levels (comparing the lower ones), only the harmonics below the 50th order are considered of interest, and the parasite frequencies must be removed using a suitable filter. Regarding the unbalance, the symmetrical components are used and all the calculi are performed only for the fundamental component. Concerning the voltage dips and voltage swells, no method for the detection is recommended; only aspects about the disturbance characteristics and quantification are described. Accordingly, a voltage dip starts when the measured voltage as the r.m.s. on a cycle and updated every half of cycle is below the threshold (0.9 from the reference voltage) and ends when the voltage is above the threshold plus the hysteresis voltage [11]. On the other hand, in the infield literature [14]-[24] several methods based on wavelet transform, S transform and artificial intelligence are proposed for the detection and quantification of voltage dips and swells. Indeed, in [15] and [16] the authors apply the wavelet transform with the Daubechies mother wavelet to identify voltage dips, voltage swells, outages and transients. Morlet wavelet is used in [21] to perform a multi-resolution analysis for detection of transients. In [23] the S transform is the mathematical basis of the pattern recognition technique for the detection, classification and quantification of power quality disturbances waveforms. An expert system developed for the classification and analysis of power systems events is described in [24].

As presented in standards, the signal analysis for disturbances detection and quantification is recommended to be made individually for each disturbance. This is because the requested methodologies don't give accurate results if the analysis is made considering the coexistence of two or more disturbances. But using the standard methods, important information is lost, such as the harmonic distortion during temporary disturbances, and the influence of voltage dips and swells on the unbalance.

To eliminate the drawbacks of standard methodologies, the authors have developed an algorithm for the processing of power signals affected by harmonics, unbalance, voltage

dips and/or voltage swells. Regarding the width of the analysis window, as the standard recommends the algorithm uses time windows corresponding to 10 cycles at 50 Hz (Fig. 3. (A)).

The proposed algorithm works as is shown in the flow chart from Fig. 1. First the input data (the discrete three-phase signal) is read, and then it passes through an arithmetic block, that uses edge detection to identify any sudden change that appeared in the sequence of signal values. If so, a time domain analysis is performed to check the type of the disturbance: transient or temporary disturbance.

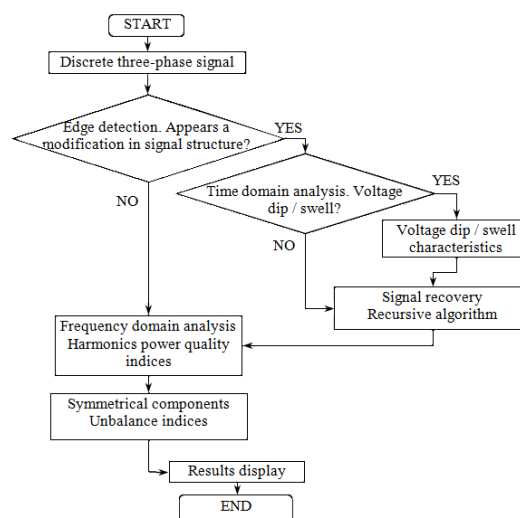


Figure 1. Logic diagram of the algorithm for the signal analysis

The existence of a temporary disturbance implies the quantification of the voltage dip or swell that was detected by determining its duration and amplitude. The next step supposes the recovery of the signal affected by the temporary disturbance, in order to be able to apply the harmonic analysis on the entire window. After the quality indices of the harmonics are calculated, the unsymmetrical components method is applied to quantify the unbalance.

The mathematical basis for the identification and analysis of temporary disturbances is described in [25]. Further on, only the mathematical relationships are presented, as they were included in the signal processing algorithm. Mathematical expressions (1) and (2) describe the edge detection method. They represent the convolution between the analyzed digital signal $u(n)$, and the Morlet function $f(n)$ [25].

$$P(k) = \left| \sum_{n=0}^{M-1} u(n) \cdot f_r(k, n) \right| \quad (1)$$

$$f_r(k, n) = f\left(\frac{n-k}{2}\right) \quad (2)$$

where $P(k)$ is the string values that contains information about the sudden changes appearance;
 $f_r(n)$ - a translation of the identification function;
 M - the number of the electric signal samples;
 $k = 0 \dots M - 1$.

The amplitude of the voltage dip or swell is calculated using the r.m.s. value updated every quarter of cycle.

The signal recovery is made using a time domain recursive algorithm. After the signal passes through this

stage, the signal has no temporary disturbance, so the harmonic analysis can be easily performed.

The standard FFT (Fast Fourier Transform) method brings errors in the case of interharmonics and fundamental frequency deviation, the use of other methods have been studied and proposed in the specialty literature [26] – [34]. Thus, DFT (Discrete Fourier Transform) with adaptive window width and wavelet transform in combination with Hartley transform are proposed in [26] and [27]. A method that offers no leakage even under frequency drift based on group-harmonic energy distribution minimizing algorithm is described in [28]. The authors from [29] and [30] use wavelet transform combined with the neuronal calculus and the support vector machine for the interharmonic estimation. Reference [31] describes a mixed approach between the recursive corrected phase wavelet transform and the frequency depending windowing for tracking harmonics. The generalized S transform and clonal selection algorithm are proposed in [32] for the (inter)harmonic estimation. Four parametric spectral estimation methods are analysed in [33]. The comparison of the methods showed that the covariance and the modified covariance methods provide relatively good performances in harmonic detection. Although the proposed methods have a high accuracy in the distortion quantification, they cannot properly identify the interharmonic components.

The method proposed for harmonic and interharmonic detection and estimation uses FFT and Gauss window. The method mathematical basis is described in [35] and [36] where it was used for the processing of speech signals. The method focuses on the properties of filter banks formed by the Fourier transform and Gauss window. The estimation precision is high, as the calculus showed that interharmonics multiple of 0.05 Hz were properly detected. The advantage of the method is that it has a computational complexity much less than the similar methods, but it offers the same precision. The block diagram of the harmonic analysis method is described in Fig. 2, and the mathematical relationships needed for the calculus of the harmonic and interharmonic orders and amplitudes are:

$$k' = k + 0.5 + \frac{\sigma}{2} \cdot [\ln(a_k) - \ln(a_{k+1})]; \quad (3)$$

and

$$U'_k = \sqrt{\sigma \cdot \pi} \cdot \exp\left(\ln[a(k)] \cdot \frac{[k' - k]^2}{\sigma}\right) \quad (4)$$

where k represents the harmonic or interharmonic order, a_k – the k^{th} order Fourier coefficient modulus of the analyzed signal, σ – constant that determines the width of the Gauss window, U'_k – k^{th} harmonic or interharmonic component amplitude

The harmonic components angles are estimated using the next mathematical relationships [37]:

$$\varphi_k = \text{sign}(\alpha_{k,c}) \cdot \arctan\left(\frac{-\alpha_{k,s}}{\alpha_{k,c}}\right); \quad (5)$$

$$\alpha_k = (H^T \cdot H)^{-1} \cdot H^T \cdot s(n); \quad (6)$$

$$\alpha_{k,s} = A_k \cdot \sin\left(\varphi_k - \frac{\pi}{2}\right); \quad (7)$$

$$\alpha_{k,c} = A_k \cdot \cos\left(\varphi_k - \frac{\pi}{2}\right);$$

$$H = \begin{bmatrix} A_1 \cdot \cos(f_1 \cdot 0) & \dots & A_k \cdot \cos(f_k \cdot 0) & \dots & A_N \cdot \cos(f_N \cdot 0) \\ \vdots & & \vdots & & \vdots \\ A_1 \cdot \cos(f_1 \cdot n) & \dots & A_k \cdot \cos(f_k \cdot n) & \dots & A_N \cdot \cos(f_N \cdot n) \\ \vdots & & \vdots & & \vdots \\ A_1 \cdot \cos(f_1 \cdot (M-1)) & \dots & A_k \cdot \cos(f_k \cdot (M-1)) & \dots & A_N \cdot \cos(f_N \cdot (M-1)) \end{bmatrix} \quad (8)$$

In the previous relationships $n = 0 \dots M-1$ represents the signal samples index, whereas $k = 1 \dots N$ is the harmonic and interharmonic components order.

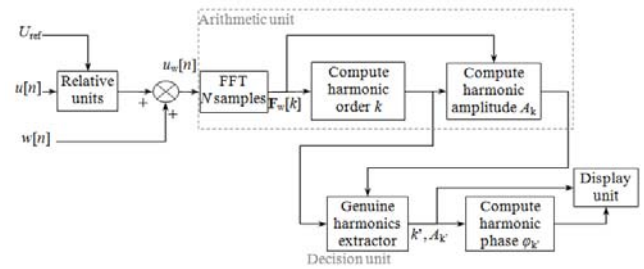


Figure 2. Block diagram of the harmonic analysis algorithm

The proposed algorithm for distorted power signals analysis was verified using the mathematical platform MathCAD, and applied on synthetic signals. The simulation data showed very good results in the detection and analysis of voltage dips/swells, harmonics (interharmonics) and unbalance. Further on, the algorithm was implemented in a virtual instrument using LabVIEW graphic programming environment.

III. PROPOSED VIRTUAL INSTRUMENT

The virtual instrument is a virtual signal analyzer that processes three-phase electric signals in order to detect and analyze harmonics/ interharmonics, unbalance, voltage dips and voltage swells. The digital signals must be sampled with a frequency of 6.4 kHz, which means 128 samples per cycle. The sampling frequency can be changed if the user requires other value, but it cannot be less than 100 samples per cycle. This is because the algorithm needs at least 5 kHz sampling frequency to properly identify interharmonics orders.

The VI is composed of the:

- frontal panel - illustrated in Fig. 3, is the graphic user interface (GUI);
- block diagram (code source) - is described in Fig. 3 (D);
- icon with connector panel - to identify the software and to be able to introduce and subordinate it in other VIs.

The code source was build in four steps corresponding to the signal reading, temporary disturbances detection and analysis, signal recovery, stationary disturbances analysis and power quality indices display. Fig. 3 (D) illustrates the block diagram in the temporary disturbances detection and analysis stage.

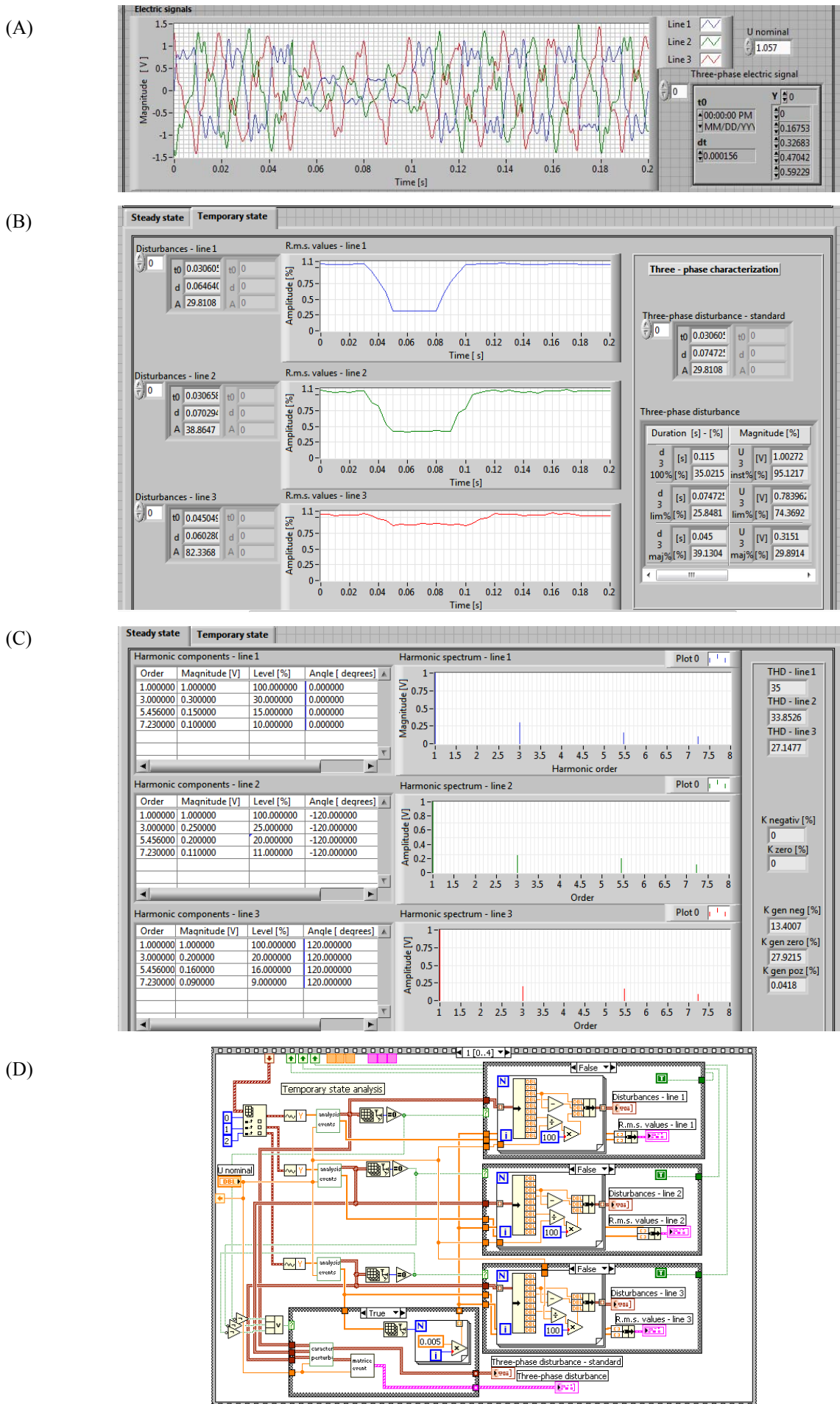


Figure 3. Graphic user interface of the virtual signal analyzer
 (A) Input signal display, (B) Temporary state quality indices, (C) Steady state quality indices

The VI input data is the digital signal sequence of values, which is obtained through a data acquisition board (the signal can be also transmitted using a data file). In Fig. 3, (A) is shown the part of the GUI that displays the digital signal, which was read and prepared to be analyzed. After processing the signal, the characteristics of the identified disturbances are displayed in two windows corresponding to the steady and temporary state, respectively.

In the case of the steady state, the power quality indices calculated are (Fig. 3, (B)) [38]:

- THD for each phase;
- Harmonic order, magnitude, level and angle for each phase. The harmonic specific features are displayed tabular and graphical;
- Unbalance factors;
- Generalized unbalance factors.

The temporary state is distinguished by the presence of voltage dips and swells, which are quantified through: start time, duration and amplitude for each phase, three-phase quantification as the standard requires, and three-phase characterization using the voltage dip/swell matrix.

The generalized unbalance factors were introduced in order to quantify properly the steady unbalance harmonic state. The quality indices take in consideration the fundamentals and the harmonic components, too. The mathematical relationships are detailed described in [38]:

- Generalized zero unbalance factor

$$k_{gU}^0 = \frac{U_g^0}{U_g^+} \cdot 100 [\%] \quad (9)$$

- Generalized negative unbalance factor

$$k_{gU}^- = \frac{U_g^-}{U_g^+} \cdot 100 [\%] \quad (10)$$

where

$$U_g^+(t) = \frac{1}{3} \cdot \sqrt{\left[\sum_k \left[\begin{array}{l} (U_k^a)^2 + (U_k^b)^2 + (U_k^c)^2 + \\ 2 \cos(\alpha_{k-ab}^+) \cdot U_1^a \cdot U_1^b + \\ 2 \cos(\alpha_{k-bc}^+) \cdot U_1^b \cdot U_1^c + \\ 2 \cos(\alpha_{k-ca}^+) \cdot U_1^c \cdot U_1^a \end{array} \right] \right]} \quad (11)$$

$$\begin{aligned} \alpha_{1-ab}^+ &= \varphi_1^a - \varphi_1^b \\ \alpha_{1-bc}^+ &= \varphi_1^b - \varphi_1^c, \\ \alpha_{1-ca}^+ &= \varphi_1^c - \varphi_1^a \end{aligned} \quad (12)$$

$$U_g^0(t) = \frac{1}{3} \cdot \sqrt{\left[\sum_k \left[\begin{array}{l} (U_k^a)^2 + (U_k^b)^2 + (U_k^c)^2 + \\ 2 \cos(\alpha_{k-ab}^0) \cdot U_k^a \cdot U_k^b + \\ 2 \cos(\alpha_{k-bc}^0) \cdot U_k^b \cdot U_k^c + \\ 2 \cos(\alpha_{k-ca}^0) \cdot U_k^c \cdot U_k^a \end{array} \right] \right]} \quad (13)$$

$$\begin{aligned} \alpha_{k-ab}^0 &= \varphi_k^a - \varphi_k^b + k \cdot \frac{2\pi}{3} \\ \alpha_{k-bc}^0 &= \varphi_k^b - \varphi_k^c + k \cdot \frac{2\pi}{3}, \\ \alpha_{k-ca}^0 &= \varphi_k^c - \varphi_k^a + k \cdot \frac{2\pi}{3} \end{aligned} \quad (14)$$

$$U_g^-(t) = \frac{1}{3} \cdot \sqrt{\left[\sum_k \left[\begin{array}{l} (U_k^a)^2 + (U_k^b)^2 + (U_k^c)^2 + \\ 2 \cos(\alpha_{k-ab}^-) \cdot U_k^a \cdot U_k^b + \\ 2 \cos(\alpha_{k-bc}^-) \cdot U_k^b \cdot U_k^c + \\ 2 \cos(\alpha_{k-ca}^-) \cdot U_k^c \cdot U_k^a \end{array} \right] \right]} \quad (15)$$

$$\begin{aligned} \alpha_{k-ab}^- &= \varphi_k^a - \varphi_k^b + (2-k) \cdot \frac{2\pi}{3} \\ \alpha_{k-bc}^- &= \varphi_k^b - \varphi_k^c + (1+k) \cdot \frac{2\pi}{3}, \\ \alpha_{k-ca}^- &= \varphi_k^c - \varphi_k^a + (1-2k) \cdot \frac{2\pi}{3} \end{aligned} \quad (16)$$

and $k=1, \dots, \infty$.

In order to underline and quantify the influence of positive sequence harmonic components, the positive unbalance factor was proposed [38]:

$$k_{gU}^+ = \frac{U_g^+ - U_1^+}{U_g^+} \cdot 100 [\%] \quad (17)$$

A three-phase quantification of the voltage dips and swells using a temporal-quantitative approach is used in order to have detailed characterization of the way the temporary event varies in time. Thus, the voltage dip/swell matrix is proposed to describe more accurately the temporary disturbances in distribution networks. It is defined as follows:

Duration	Amplitude
$d_{3\ 100\%}$	$U_{3\ inst\%}$
$d_{3\ lim\%}$	$U_{3\ lim\%}$
$d_{3\ maj\%}$	$U_{3\ maj\%}$

Figure 4. Voltage dips / swell matrix

where $d_{3\ 100\%} = 100 [\%]$,
 $d_{3\ lim\%} = (d_{lim} / d_{inst}) \cdot 100 [\%]$,
 $d_{3\ maj\%} = (d_{maj} / d_{inst}) \cdot 100 [\%]$.

The temporal quantities are defined as:

- $d_{inst} = t_{finst} - t_{iinst}$ is the duration of the event that happened between the moment that the r.m.s. voltage begins to change, leading towards the disturbance and the moment when the r.m.s. voltage is stable showing that the disturbance ended;
- $d_{lim} = t_{flim} - t_{ilim}$ - duration of the disturbance itself;
- $d_{maj} = t_{fmaj} - t_{imaj}$ - time duration when the r.m.s. voltage has its lower or higher value.

The matrix quantitative parameters have the mathematical expressions:

- Minor percentage amplitude $U_{3\ inst\%}$

$$U_{inst\%} = \frac{U_{fref} + U_{iref} - U_{maj}}{U_{ref}} \cdot 100 [\%] \quad (18)$$

- Major percentage amplitude $U_{3\ maj\%}$

$$U_{maj\%} = \frac{U_{maj}}{U_{ref}} \cdot 100 [\%] \quad (19)$$

- Standard percentage amplitude $U_{lim\%}$

$$U_{lim\%} = \frac{U_{lim} - U_{maj}}{U_{ref}} \cdot 100 [\%] \quad (20)$$

This quality index can be used to classify voltage dips and voltage swells, consequently to take the adequate measures.

IV. NUMERICAL EXAMPLES

The virtual instrument testing process was made in two stages. In the first stage several digital signals comparable with the ones found in distribution networks, and complex signals that can be hardly found in practice were virtually build. The 2nd category of signals was chosen to verify the accuracy for interharmonics and voltage dips/swells detection and quantification. On the other hand, the standard methodologies for harmonic analysis and voltage dip detection were implemented as VIs in order to make a proper comparison between the recommended methods and the proposed ones. Further on a representative numeric example performed on a synthetic digital signal is illustrated. Fig. 3, (A) illustrates the three-phase analyzed signal that is non-sinusoidal (with harmonic and interharmonic components), unbalanced and contains a voltage dip. The signal analytic expression is:

$$u_{1,2,3}(t) = \sqrt{2} \cdot \sum U^{1,2,3}_k \cdot \sin(2\pi \cdot 50 \cdot k \cdot t + \varphi^{1,2,3}_k) \quad (21)$$

where k is the harmonic or interharmonic order,

$U^{1,2,3}_k$ - harmonic or interharmonic component magnitude,

$\varphi^{1,2,3}_k$ - phase angles of the harmonic or interharmonic component for each phase.

The quantities values, voltage dip instantaneous characteristics (start time $t^{1,2,3}_0$, duration $d^{1,2,3}$ and magnitude $A^{1,2,3}$) are enumerated in Table I.

TABLE I. ELECTRIC SIGNAL CHARACTERISTICS

Harmonic components					
k	1	3,25	5,5138	7,72	11
U^1_k [V]	220	66	44	22	2
U^2_k [V]	242	77	48	19	1
U^3_k [V]	217	70	33	26	1
φ^1_k [degrees]	0	0	0	0	0
φ^2_k [degrees]	240	240	240	240	240
φ^3_k [degrees]	120	120	120	120	120
Voltage dip characteristics					
t^1_0 [s]	0.04	d^1 [s]	0.12	A^1 [%]	30
t^2_0 [s]	0.042	d^2 [s]	0.11	A^2 [%]	40
t^3_0 [s]	0.043	d^3 [s]	0.1	A^3 [%]	90

The usage of the VI, which incorporates the standard signal processing methodology brought the results from Fig. 4 and Fig. 5, where is illustrated the harmonic spectrum and the voltage r.m.s. values, respectively. Considering that the standard FFT excludes the harmonic analysis in the presence of a voltage dip, and to be able to make a proper comparison with the proposed method, the steady state analysis was made without the temporary disturbance. Table II displays, for steady and temporary states, the results in a tabular manner.

The harmonic spectrum obtained using the standard method shows the fundamental component, but the other interharmonic components result as interharmonic groups. Thus, the standard method gives incomplete information regarding the order, level and phase angles of the interharmonic components, and consequently improper

information about the real situation of the distribution networks steady state.

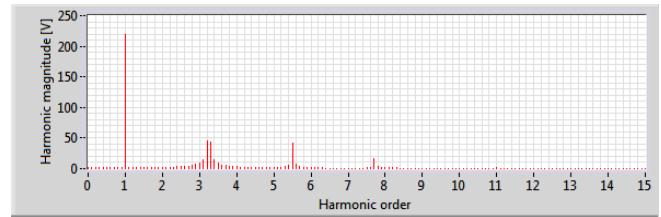


Figure 4. Harmonic spectrum on phase – line 1, using the standard FFT analysis

Analyzing the same signals by using the VI containing the proposed algorithm (where the existence of all disturbances is taken in consideration), the following results were obtained: harmonic spectrum (Fig. 6), voltage dip characteristics and allure (Fig. 7), which use graphics for presentation, whereas a more detailed display is made through Table III.

The output data that characterizes the harmonic pollution, presented in Table III, indicates a accurate estimation of the harmonic and interharmonic components, i.e. their order, magnitudes, levels and phase angles, too.

The voltage dip allure shows that both the standard and the proposed methods give precise results concerning the amplitude of the disturbance. A closest analysis highlights that the proposed method is more accurate in determining the start and end moment, that is the duration and the disturbances' shape.



Figure 5. Digital signal time variation using r.m.s. values. Standard method

TABLE II. RESULTS OBTAINED WITH THE STANDARD METHODS

Signal characteristics	Phase		
	1	2	3
k	1 – interharmonic group between 3 and 4 – interharmonic group between 5 and 6 – interharmonic group between 7 and 8		
$U^{1,2,3}_k$ [V]	220 – 65 interharmonic group magnitude – 43 interharmonic group magnitude – 20 interharmonic group		
$\varphi^{1,2,3}_k$ [degrees]	Couldn't be determined		
t_0 [s]	0.03	0.03	0
d [s]	0.13	0.13	0
A [%]	30	40	0

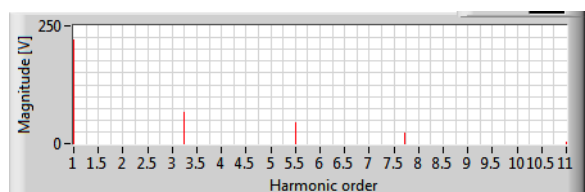


Figure 6. Harmonic spectrum on phase 1 using the proposed method

As the validation of the VI was successful for synthetic digital signals, an application was built to verify the VI using real signals. Thus a data acquisition board (DAB) was used and a special VI was developed to make the connection between the virtual signal analyzer and the DAB. The results, obtained using the VI, were compared with the ones obtained using a physical power quality analyzer.

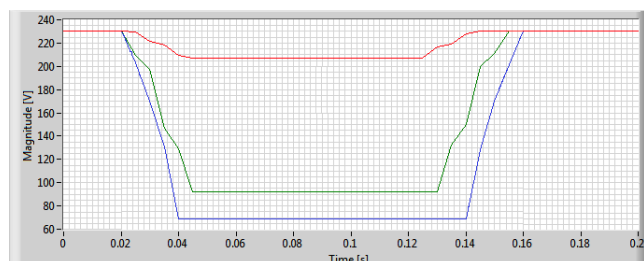


Figure 7. Electric signal time variation using rms values. Proposed method

TABLE III. RESULTS OBTAINED USING THE PROPOSED VI

Phase	1	2	3
Signal characteristics			
k	1, 3.25, 5.5138, 7.72, 11		
$U^{1,2,3}_k$ [V]	220, 66, 44, 22, 2	242, 77, 48, 19, 1	217, 70, 33, 26, 1
$\phi^{1,2,3}_k$ [degrees]	0, 0, 0, 0, 0	240, 240, 240, 240, 240	120, 120, 120, 120, 120
t_0 [s]	0.025	0.025	0
d [s]	0.12	0.109	0
A [%]	30	40	0

V. CONCLUSION

The paper describes a virtual signal analyzer dedicated for the harmonic and interharmonic components, unbalance, voltage dips and voltage swells detection and quantification. To eliminate the drawbacks of the signal processing methods that are recommended by the power quality standards and to raise the accuracy of the steady and temporary states characterization, the authors propose a new approach, which supposes the use of new signal processing methods. The proposed methodology was implemented in a virtual instrument that performs the temporary disturbance detection and analysis based on time domain analysis and harmonic and interharmonic analysis based on frequency domain analysis, plus a signal recovery action if the signals are affected by voltage dips and swells. The signal analysis is made using a 10 cycles interval (0.2 s).

The voltage dips and swells detection is made using the convolution between the analyzed signal and the Morlet function. The proposed method offers the advantages of less calculus and higher precision in disturbance duration and allure determination.

The harmonic analysis is realized by applying the Fourier transform on a signal windowed with the Gauss function. This approach brings a very high precision in interharmonic components detection, but it has disadvantage of difficulty in information extraction.

The novelty of the methodology, comparing the standard one, is the introduction of the signal recovery when the signal is affected by voltage dips and swells, thus the steady state analysis can be performed in the same 10 cycles window, along with the temporary disturbances. The signal recovery is made using a recursive algorithm that gradually

modifies the signal magnitude until it is reached the level before the temporary disturbance occurrence.

The VI besides the standard power quality indices determines also new indices that were suggested with the purpose to obtain a more accurate imagine of the real operation state of distribution networks. Consequently, the generalized unbalance factors and voltage dip/swell matrix were introduced.

As the VI was tested using virtual and real digital signals, the results showed very good detection of (inter)harmonics and a faithful allure of the voltage dips and swells.

The virtual signal analyzer has the following advantages: cheaper than physical analyzers, faster, processes both stationary and temporary disturbances in the same analysis window and easy to perform modification in its structure. Regarding the last aspect, in the future the authors intend to complete the VI in order to detect and quantify more disturbances.

REFERENCES

- [1] Anca Miron, M. Chindriș, A. Cziker, "Complex electric signals analysis using virtual instrumentation", *Int. Rev. Comp. Soft.*, September 2011, Vol.6 n. 5, pp. 667-677.
- [2] G.-R. Gillicha, D. Frunzaverdea, N. Gillicha, D. Amariei, "The use of virtual instruments in engineering education", *Procedia Social and Behavioral Sciences*, Vol. 2, Iss. 2, pp. 3806-3810, 2010. [Online]. Available: <http://dx.doi.org/10.1016/j.sbspro.2010.03.594>
- [3] W. Xinling, Z. Cheng, "Design and simulation of voltage fluctuation rate monitor system based on virtual instrument technology", *Energy Procedia*, Vol. 17, 2012, pp. 450 - 455. [Online]. Available: <http://dx.doi.org/10.1016/j.egypro.2012.02.119>.
- [4] G. Bucci, E. Fiorucci, C. Landi, "Digital measurement station for power quality analysis in distributed environments", *IEEE Trans. Instrum. Meas.*, Vol. 52, No. 1, February 2003, pp. 75 - 84. [Online]. Available: <http://dx.doi.org/10.1109/TIM.2003.809080>.
- [5] A. López, J.-C. Montañó, M. Castilla, J. Gutiérrez, M. D. Borrás, J. C. Bravo, "Power system frequency measurement under non-stationary situations", *IEEE Trans. Power Del.*, Vol. 23, No. 2, April 2008, pp. 562 - 567. [Online]. Available: <http://dx.doi.org/10.1109/TPWRD.2007.916018>
- [6] I. Orović, M. Orlandić, S. Stanković, Z. Uskoković, "A Virtual instrument for time-frequency analysis of signals with highly non-stationary instantaneous frequency", *IEEE Trans. Instrum. Meas.*, Vol. 60, No. 3, March 2011, pp. 791 - 803. [Online]. Available: <http://dx.doi.org/10.1109/TIM.2010.2060227>
- [7] L. Ferrigno, C. Liguori, A. Pietrosanto, "Measurements for the characterization of passive components in non-sinusoidal conditions", *IEEE Trans. Instrum. Meas.*, Vol. 51, No. 6, December 2002, pp. 1252 - 1258. [Online]. Available: <http://dx.doi.org/10.1109/IMTC.2001.929527>
- [8] J.-H. Teng, S.-Y. Chan, J.-C. Lee, R. Lee, "A LabVIEW based virtual instrument for power analyzers", *IEEE Proc. Int. Conf. Power Syst. Tech.*, Vol. 1, 2000, pp. 179-184. <http://dx.doi.org/10.1109/ICPST.2000.900052>
- [9] A. Monti, F. Ponci, S. Pelizzari, L. Cristaldi, "A virtual instrument for time-frequency analysis of Park power components", *Elect. Power Qual. Utilisation*, J. Vol. XIII, No. 1, (2007) 121 - 128.
- [10] F. Adamo, F. Attivissimo, G. Cavone, N. Giaquinto, "SCADA/HMI systems in advanced educational courses", *Proc. IEEE Instrum. Meas. Tech. Conf.*, Vol. 2, 2005, pp. 1097 - 1101. [Online]. Available: <http://dx.doi.org/10.1109/IMTC.2005.1604312>
- [11] IEC 61000-4-30 Testing and Measurement Techniques - Power Quality Measurement Methods.
- [12] IEC 61000-4-7: Electromagnetic compatibility (EMC) - Part 4-7: Testing and measurement techniques - General guide on harmonics and interharmonics measurements and instrumentation, for power supply systems and equipment connected thereto.
- [13] SR EN 50160:2007 - Characteristics of the voltage supplied by the distribution power networks.
- [14] S.Z. Djokic, J.V. Milanovic, S.M. Rowland, "Advanced voltage sag characterization ii: point on wave", *Gener., Transm. & Distrib.*, IET, Issue Date: January 2007, Volume: 1 Issue: 1, On page(s): 146 - 154,

- ISSN: 1751-8687. [Online]. Available: <http://dx.doi.org/10.1049/iet-gtd:20050434>
- [15] S. Nath, A. Dey, A.Y. Chakrabarti, "Detection of power quality disturbances using wavelet transform", *World Academy of Science, Engineering and Technology* 49, 2009, pp. 869 – 873.
- [16] S. Chen, H.Y. Zhu, "Wavelet transform for processing power quality disturbances", *EURASIP J. Advan. Signal Proces.*, Vol. 2007, article ID 47695.
- [17] N.C.F. Tse, "Practical application of wavelet to power quality analysis", *Power Engineering Society General Meeting*, 24-28 June 2007, ISBN: 1-4244-1298-6, pp. 1-6.
- [18] N. Ghaffarzadeh, B. Vahidi, "A New protection scheme for high impedance fault detection using wavelet packet transform", *Advances in Electrical and Computer Engineering*, Vol. 10, No. 3, 2010, pp. 17 – 20. [Online]. Available: <http://dx.doi.org/10.4316/AECE.2010.03003>
- [19] Z. Wang, Y. Zhang, J. Zhang, J. Ma, "Recent research progress in fault analysis of complex electric power systems", *Advances in Electrical and Computer Engineering* Vol. 10, No. 1, 2010, pp. 28 – 33. [Online]. Available: <http://dx.doi.org/10.4316/AECE.2010.01005>
- [20] T. Zheng, E.B. Makram, A.A. Girgis, "Power system transient and harmonic studies using wavelet transform", *IEEE Trans. Power Deliv.*, Vol.14, No.4, October 1999, pp. 1461 – 1468. [Online]. Available: <http://dx.doi.org/10.1109/61.796241>
- [21] S.-J. Huang, C.-T. Hsieh, C.L. Huang, "Application of Morlet wavelets to supervise power system disturbances", *IEEE Trans. Power Deliv.*, Vol.14, No.1, January 1999, pp. 235 – 243. [Online]. Available: <http://dx.doi.org/10.1109/61.736728>
- [22] A.M. Gaouda, M.M.A. Salama, M.R. Sultan, A.Y. Chikhani, "Power quality detection and classification using wavelet-multiresolution signal decomposition", *IEEE Trans. Power Deliv.*, Vol.14, No.4, October 1999, pp. 1469 – 1473. [Online]. Available: <http://dx.doi.org/10.1109/61.796242>
- [23] A.Y. Chilukuri, P.K. Dash, K.P. Basu, "Time-frequency based pattern recognition technique for detection and classification of power quality disturbances", *TENCON 2004, 2004 IEEE Region 10 Conference*, Vol. 3, pp. 260 – 263. [Online]. Available: <http://dx.doi.org/10.1109/TENCON.2004.1414756>
- [24] E. Styvaktakis, M.H.J. Bollen, I.Y.H. Gu, "Expert system for classification and analysis of power systems events", *IEEE Trans. Power Deliv.*, Vol. 17, No. 2, April 2002, pp. 423 – 428. [Online]. Available: <http://dx.doi.org/10.1109/61.997911>
- [25] Anca Miron, M. Chindriș, A. Cziker, "Identification of electromagnetic disturbances in modern power systems", *Journal of Sustainable Energy*, Vol. 3, No. 1, March 2012, pp. 55 - 61, ISSN: 2067-5534
- [26] M. Caciotta, S. Giarnetti, F. Leccese, Z. Leonowicz, "Comparison between DFT, Adaptive window DFT and EDFT for power quality frequency spectrum analysis", *Intern. Conf. Modern Elect. Power Syst. 2010*, Wroclaw, Poland, paper 16.1.
- [27] D.N. Gheorghe, M.D. Chindriș, et.al, "Signal Analysis in polluted power networks", *J. Sustain. Energ.*, Vol.1, No.1, March, 2010, paper 1.7.
- [28] H.C. Lin, C.H. Chen, L.Y. Liu, "Harmonics and interharmonics measurement using group-harmonic energy distribution minimizing algorithm", *Engineering Letters*, 19:3, EL_19_3_17, August 2011, pp. 1 – 6.
- [29] J.S. Huang, M. Negnevitsky, D.T. Nguyen, "Wavelet transform based harmonic analysis", *Australasian universities power engineering conference and IEAust electric energy conference*, 26-29 September 1999, Darwin, pp. 152-156.
- [30] S. Tuntisak, S. Premrudeepreechacharn, "Harmonic detection in distribution systems using wavelet transform and support vector machine", *Proc. Conf. IEEE Power Tech. Lausanne*, pp. 1540-1545, July 2007. [Online]. Available: <http://dx.doi.org/10.1109/PCT.2007.4538544>
- [31] C.D.P. Crovato, A.A. Susin, "Frequency dependent windowing for tracking harmonics and interharmonics in power systems. Survey and the recursive corrected phase wavelet transform", *Annals of the VIII Brazilian Conf. Power Qual.*, CBQEE 2009, Blumenau, Brazil, paper 82.
- [32] H. Quan, Y. Dai, "Harmonic and interharmonic signal analysis based on generalized S-transform", *Chinese J. Electron.*, Vol. 19, No. 4, Oct. 2010, pp. 656 – 660.
- [33] A.S. Yilmaz, A. Alkan, M.H. Asyali, "Applications of parametric spectral estimation methods on detection of power systems harmonics", *Electric Power Syst. Research*, No. 78(2008), pp. 683 – 693. [Online]. Available: <http://dx.doi.org/10.1016/j.epsr.2007.05.011>
- [34] J. M. Knezevic, V. A. Katic, "The hybrid method for on-line harmonic analysis", *Advances in Electrical and Computer Engineering*, Vol. 11, No. 3, 2011, pp. 29 – 34. [Online]. Available: <http://dx.doi.org/10.4316/AECE.2011.03005>
- [35] R. H. McEachern, "Speech information extractor", US Patent 5.214.708, 25 May, 1993.
- [36] F.J. Harris, "On the use of windows for harmonic analysis with the discrete Fourier transform", *Proc. IEEE*, Vol. 66, No.1, 1978, pp. 51
- [37] S. O.Hing-Cheung, "On Linear Least squares Approach for Phase Estimation of Real Sinusoidal Signals", *IEICE Trans. Fundamentals*, Vol. E88-A, No. 12, December 2005.
- [38] A. Cziker, A. Miron, M. Chindriș, "Power quality indices for unbalance characterization in non-sinusoidal condition", *14th Intern. Research/Expert Conf. „Trends in the Development of Machinery and Associated Technology” TMT 2010*, 11-18 September 2010, pp. 481-484.

Monitoring Power Quality in Microgrids Based on Disturbances Propagation Algorithms

Anca Miron^{1, a}, Mircea D. Chindriș^{1, b} and Andreas Sumper^{2, c}

¹Technical university of Cluj-Napoca, 28th Memorandumului Street, Cluj-Napoca, Romania

²Universitat Politecnica de Catalunya, 647th Av. Diagonal, 2nd Floor, Barcelona, Spain

^aanca.miron@enm.utcluj.ro, ^bmircea.chindris@enm.utcluj.ro,
^candreas.sumper@upc.edu (Anca Miron)

Keywords: power quality, microgrid, virtual instrumentation, unbalance, harmonics, voltage dips, voltage swells.

Abstract. The paper shows how the surveying of power quality in microgrids working under unbalanced harmonic distorted operating states with possible voltage dips and voltage swells existence can be accomplished implying a small amount of time and measurement activities. The surveying methodology uses the disturbances propagation phenomenon to determine the power quality indices in all of interest nodes of the microgrid utilizing the voltages and currents characteristics in one or several strategic nodes. The disturbances propagation is based on the sequence component theory applied for all detected harmonics and for the microgrids components. The proposed surveying methodology was implemented in a virtual instrument capable to acquire the voltages and currents waveforms, to analyze them in order to identify the disturbances characteristics, to calculate the disturbances propagation and display the power quality indices in all of interest nodes of the microgrid. The virtual instrument was tested using several microgrid topologies and scenarios.

Introduction

Microgrids represent the new tendencies that meet the world's new energy policy that is to protect and mitigate the impact on the environment. A microgrid is a regionally limited power system that contains small generation units, energy storage and loads. The microgrid usually operates connected to a traditional centralized power network, but it can work also in the isolated mode. The generation units and loads are interconnected at low voltage (LV) or rarely at medium voltage (MV). Microgrid generation units can include fuel cells, wind turbines, photovoltaic (solar) panels and other small power installation that use renewable energy resources.

A microgrid has three main characteristics [1 – 4]: it is seen by the main power network as a single controllable unit, enabling it to deliver the cost of large units; it has a particular topology imposed by the energy needs (in order to satisfy the power necessities); it needs a high level of power quality and a high supply safety in order to supply all consumers. This last feature imposes the knowledge of power quality (PQ) indices in all common coupling points of the microgrid. To establish accurate values of PQ indices in microgrids, a lot of complex measurements have to be performed at the same time. It is obvious that, for technological and economical reasons, it is almost impossible to accomplish this task. On the other hand, the complexity of electromagnetic phenomena imposes laborious and fineness activities for a truthful modelling of microgrids elements and of electromagnetic phenomena. An easier approach to determine the PQ indices in all of interest nodes of the microgrid is to measure the characteristics of PQ indices in the main nodes and then calculate them in the rest of the microgrid by applying a propagation algorithm. This methodology can be used because the disturbances propagate through the microgrid influenced by the microgrid components on one hand and on the other hand by the disturbances type themselves. Consequently, the PQ indices have diverse values in different points of the microgrid.

The analysis of disturbances propagation is a complex issue, involving many complicated mathematic calculus, subsequently it is very appropriate the development of software tools that contain the propagation algorithm and are dedicated for the analysis of PQ. Encouraged by the

importance of PQ in microgrids and the disturbances propagation approach, the authors have developed a virtual instrument (VI) that calculates the propagation of electromagnetic disturbances (basically harmonic distortion, unbalance, voltage dips and voltage swells) in microgrids and the PQ indices. The propagation of stationary disturbances (e.g. harmonics and unbalance) is a power flow issue during steady state, whereas the temporary disturbances (e.g. voltage dips and swells) can be also treated like usual power flow during the stationary periods (when its rms values doesn't vary) of the disturbance when the voltage amplitude is the lowest (for dips) or the highest (for swells). This approach was used because only the PQ indices are pursued, whereas for a more accurate analysis of the temporary disturbances propagation a time domain analysis is required.

The common power flow analysis methods that are based on the positive sequence representation, which are usually used for large power distribution systems, are not appropriate for microgrids and modern LV distribution power networks, because they have an unbalanced and harmonic polluted working state. Furthermore, the today's power flow software tools are not adapted for the microgrids analysis, because they initially have been developed for large systems. A drawback in the existing technical literature regarding the steady state modelling of microgrids is that it assumes only positive sequence representation for power flow analysis [5, 6]. Then again, the concept of three phase power flow analysis has been widely presented in literature [7 - 14], and the proposed methods were chosen in accordance with the network topology and the applied methodologies. The compensation methods have been proposed for power flow analysis of radial networks and weakly meshed grids in [7] and [8], respectively. The power flow analysis of looped (ring) or general network structures are conducted based on Gauss and/or Gauss-Seidel methods in [9, 10] and Newton – Raphson method in [11 – 13]. The sequence components theory has been used in [12 – 15] to develop a three phase power flow solver for general network topologies with synchronous generating units. Using the sequence components frame in the power flow analysis effectively reduces the problem size and the computational burden as compared to the phase frame approach. Moreover, due to the weak coupling between the three sequence networks, the system equations can be solved using parallel programming [13]. Considering the unbalance and harmonics, the propagation implemented in the proposed survey methodology is based on the sequence components theory. Comparing the approaches presented in the literature [13 – 15], the proposed method adapts the sequence components theory for all harmonics. Thus the microgrid is decomposed in three independent sequence components, and the power flow is determined for each sequence harmonic component. In accordance with the proposed approach, all the microgrid elements are modelled with their sequence components: electric lines, power transformers, linear balanced consumers (constant power) and distributed generation units (constant power). The temporary disturbances propagation is made considering the technical literature [16, 17].

In the last years, the computer science development has encouraged the involvement of PCs in resolving various issues related to power systems, such as protections, control, measurements, processes control, modelling etc. Thus, specialized dedicated software tools were created in order to support and improve the engineers work: LabVIEW, DIgSILENT, EDSA, MatLab etc.

The software products developed using LabVIEW graphical programming environment are virtual instruments (VIs). These software tools emulate physical instruments, but they operate like usual software and consequently they can be used so. Thus on one side, VIs are utilized to design the measurement system, but on the other side, they are used as simulation tools in a closed virtual world in which the user can observe the behaviour of complex systems in different contexts, being of great help in understanding various phenomena [18]. Recently, in the field of power systems, many authors have used the virtual instrumentation approach to simulate different operating states of power systems [19], solve issues related to measurements [20 – 24], to detect the loads characteristics [25], to design and simulate the voltage fluctuation rate monitor [26], to control different processes [27]. Analyzing the technical literature, the developed software tool is among the few VIs dedicated for simulation of power systems processes.

The rest of the paper is organized as follows: the next section describes the proposed survey methodology, then the developed VI is presented, its usage and a study case that validates the algorithm and the VI are presented. The paper ends with a section of conclusions where the importance of developed VI is underlined.

Proposed power quality monitoring method using disturbances propagation algorithm

The proposed methodology was build on the supposition that the start point of the disturbances propagation is the injection point of the disturbances, where the measurement have been made, or the distributed generation units whose characteristics are known are connected. Besides, the complexity of the propagation phenomenon imposes: (i) the analysis of power signals in order to determine and quantify the PQ indices, which were performed using novel algorithms [28, 29] and new indices [30, 31]; (ii) the microgrid to be modelled in accordance with the non-sinusoidal unbalanced operating state, thus the electric lines and transformers parameters were calculated considering the skin effect; (iii) the electric quantities and microgrids parameters were used in per unit and with sequence components. It must be added that the proposed method can be applied for both radial and looped microgrid, and typical power networks topologies.

The remainder of the section describes the propagation algorithm, microgrid modelling and the mathematical basis of the disturbances propagation through the grids components.

Disturbances propagation algorithm. The algorithm for the disturbances propagation is described in Fig. 1 and supposes the following stages:

- analysis of acquired signals, in order to determine the existence of electromagnetic disturbances, their types and PQ indices in the measurement points;
- transformation of the electric quantities in per unit and sequence components quantities;
- calculus of microgrids parameters, considering the real operating state (skin effect);
- microgrids topology (radial and looped) identification in order to track the effects on the disturbances propagation;
- sequence components (positive, negative and zero) of the analyzed microgrid, in per unit calculus;
- analysis of disturbances propagation using the corresponding mathematical block (Fig. 5). Calculus block stopping condition is met when all electric quantities (currents and voltages) in all of interest microgrid nodes are determined;
- computation of power signals characteristics, i.e. the PQ level in all of interest microgrid nodes.

In Fig. 1 $u(t)$ and $i(t)$ represent the acquired sampled power signals; $U^{A,B,C}_k$ and $I^{A,B,C}_k$ the voltages and currents harmonic components on the three phases; $U^{+, -, 0}_k$ and $I^{+, -, 0}_k$ the sequence components for each k^{th} order harmonic; k_U^- , k_U^0 and THD_U symbolize the PQ indices corresponding the analyzed disturbances; Z_T , Z_L microgrid electric parameters, whereas $Z^{+, -, 0}_T$ and $Z^{+, -, 0}_L$ sequence components of the microgrid electric parameters.

Microgrid modelling. The electric lines (overhead lines and cables) are modelled using only the series parameters: resistance (R_l) and reactance (X_l), thus the characteristic impedance, Z_l .

$$\underline{Z}_l = R_l + j\omega L_l = R_l + jX_l \text{ } [\Omega/\text{m}]. \quad (1)$$

The electric line model is illustrated in Fig. 2. The resistance was determined considering the d.c. component, and the a.c. gain parameter, k_{ca} – relationship (2).

The a.c. gain parameter depends on the frequency, conductor's type, resistivity and permeability as mathematical relationships (2) and (3) show [32].

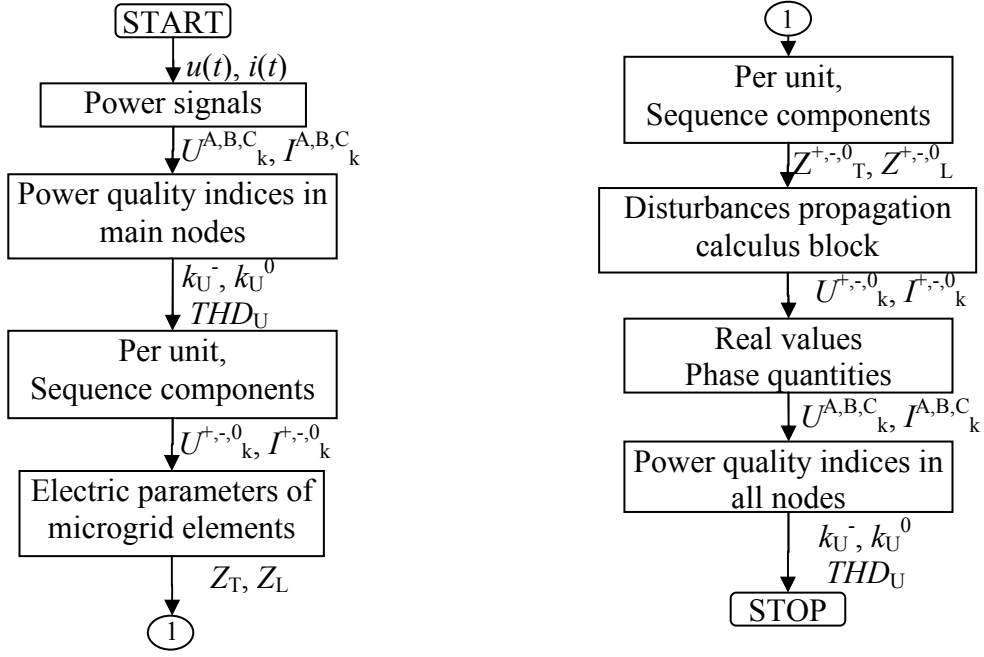


Fig. 1. Logic diagram of propagation algorithm

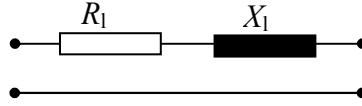


Fig. 2. The equivalent electric scheme of an electric line

$$k_{ca} = \frac{m \cdot r}{2} \cdot \frac{ber(m \cdot r) \cdot bei'(m \cdot r) - bei(m \cdot r) \cdot ber'(m \cdot r)}{(ber'(m \cdot r))^2 + (bei'(m \cdot r))^2} \quad (2)$$

$$m = \sqrt{\frac{\omega \cdot \mu}{\rho}} \quad (3)$$

where r is the conductor's radius, [m]; μ – material permeability, [H/m]; R_{cc} – d.c. resistance, [Ω /m]; R_l – a.c. resistance, [Ω /m]; μ_r – relative permeability; ρ – conductor's resistivity, [$\Omega \cdot \text{mm}^2$ /m]; ber și bei – real and imaginary parts of the Bessel functions, which are described below.

The transformers are modelled considering the electric scheme from Fig. 3. Thus the electric parameters are determined using the characteristic features of the transformer [33].

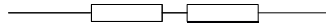


Fig. 3. Single-phase scheme of the three-phase power transformer

The consumers, which are considered linear loads, are modelled using a static model characterized by series parameters – resistance and reactance (impedance), Fig. 4. The electric parameters are calculated using the consumer nominal power and voltage.

$$\underline{Z}_c = R_c + j\omega L_c = R_c + jX_c, [\Omega] \tag{4}$$

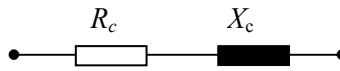


Fig. 4. Equivalent single-phase electric scheme of the linear consumer

Propagation calculus block. In the propagation analysis the following assumptions have been accepted: (i) the electric lines and power transformers are linear elements, thus they do not cause harmonic currents or voltages; (ii) the non-linear consumers are considered invariant harmonic current sources (this means that the harmonic order, amplitude and initial phase don't vary in time); (iii) the microgrid is supplied with a symmetric system of sinusoidal voltages from the power system (in the connected mode); (iv) the distributed generation units are considered invariant.

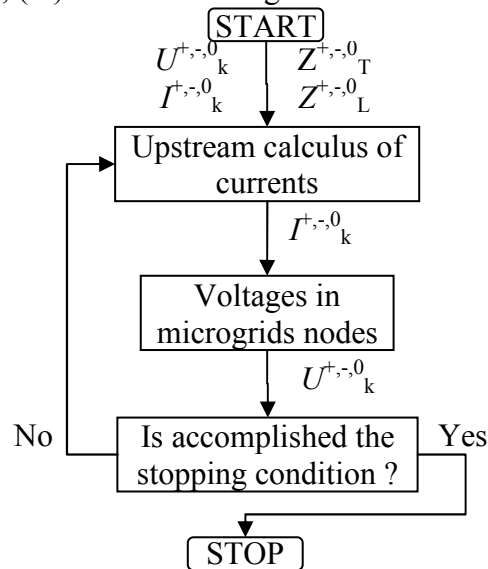


Fig. 5. Logic diagram of the disturbances propagation calculus block

The propagation phenomenon study was made using an iterative method (the backward/forward sweep), which was modified for the non-sinusoidal unbalanced operating state. This kind of approach supposes a three-phase modelling of the grid elements, in view of the fact that the electric quantities can be different for the three phases. Consequently the superposition method and the sequence components theory were implied. Thus each three-phase harmonic current/voltage system was analyzed as an unbalanced system. Moreover, utilizing this approach and taking into account the characteristics of sequence components belonging to the microgrid elements, the microgrid is seen as three sequence independent microgrids: positive, negative and zero sequence. Fig. 6 illustrates a power network along with its three sequence components [35, 36].

The positive and negative sequence components of power transformers behave in the same way, irrespective of magnetic core type and the connection scheme. The mathematical formula showing the relationship between the sequence harmonic voltages and currents are:

$$\begin{aligned} \underline{U}_{A,h}^{+/-} &= \underline{I}_{A,h}^{+/-} \cdot \underline{Z}^{+/-} + k \cdot \underline{U}_{a,h}^{+/-} \\ \underline{U}_{B,h}^{+/-} &= \underline{U}_{A,h}^{+/-} \cdot a^2 \\ \underline{U}_{C,h}^{+/-} &= \underline{U}_{A,h}^{+/-} \cdot a \end{aligned} \tag{5}$$

where k is a parameter depending on the transformer connection, h is the harmonic's order, $\underline{U}_{A/B/C,h}^{+/-}$ - positive/negative primary harmonic phase-to-earth voltages, $\underline{U}_{a/b/c,h}^{+/-}$ - positive/negative secondary harmonic phase-to-earth voltages, $\underline{Z}^{+/-}$ - positive/negative transformer impedance, $\underline{I}_{A,h}^{+/-}$ - positive/negative sequence harmonic currents that flow through the primary windings and are characterized by the following mathematical relationships:

$$\underline{I}_{A,h}^+ = \frac{1}{n_T} \cdot \underline{I}_{a,h}^+, \quad \underline{I}_{A,h}^- = \frac{1}{n_T} \cdot \underline{I}_{a,h}^- \quad (6)$$

In (6), $\underline{I}_{a,h}^+$ and $\underline{I}_{a,h}^-$ are the positive and negative sequence harmonic currents from the secondary winding, and n_T is the transformer ratio.

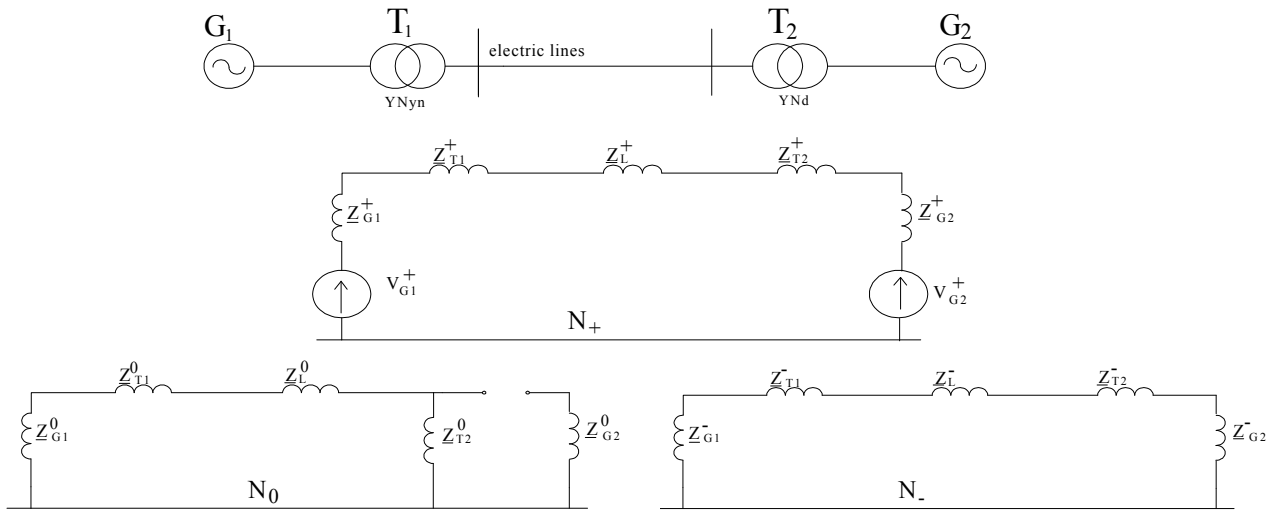


Fig. 6. Decomposition of a power grid in its sequence components (grid's parameters are in per unit)

The zero sequence components of secondary currents produce important magnetic fluxes only if they can not appear on the primary side, too.

$$\begin{aligned} \underline{U}_{A,h}^0 &= \underline{I}_{A,h}^0 \cdot \underline{Z}^0 + k \cdot \underline{U}_{a,h}^0 \\ \underline{U}_{B,h}^0 &= \underline{U}_{A,h}^0 \\ \underline{U}_{C,h}^0 &= \underline{U}_{A,h}^0 \end{aligned} \quad (7)$$

where $\underline{U}_{A/B/C,h}^0$ and $\underline{U}_{a/b/c,h}^0$ are the zero sequence primary and secondary voltages, \underline{Z}^0 - the zero sequence transformer impedance; $\underline{I}_{A,h}^0$ - the primary zero sequence current.

A voltage dip or swell that appears at a voltage level propagates at the same voltage level, at higher voltage levels and/or lower voltage levels, too. The propagation at lower voltage levels takes place without a considerable change in amplitude; in contrast, when it propagates upstream the source point suffer a amplitude decrease. The first step in the propagation analysis of voltage dips/swells imposes the knowledge of dips/swells characteristics; then it follows the study of the grid elements influence on voltage dip/swell characteristics and vice-versa. Considering only the electric lines and transformers, the last ones have the biggest influence on the voltage dips propagation.

The power transformers working in the power networks have different connections that influence the voltage dips/swells; as a result, a voltage dip/swell that propagate downstream, from the high voltage to the low voltage side of a transformer, has different characteristics in the primary if

compares with the secondary. An accurate analysis of transformers influence upon the voltage dips propagation is made in [16]. In accordance with this study, transformers can be divided in three categories: (i) transformers for which every secondary voltages are the difference between two primary voltages. This category includes transformers with connections Dy, Yd and Yz; (ii) transformers that eliminates only the zero sequence components; this model applies for transformers with group connections Y_{NY} and Y_{Yn} , and Dd, Dz_n , respectively; (iii) transformers that do not modify the voltage. For this kind of transformers, the secondary voltage (p.u.) is equal with the primary voltage (p.u.). This category encompasses transformers with Y_{NYn} connection.

Virtual instrument

The proposed methodology was implemented in a VI, named PowerDiNet_PQMo, capable to determine the PQ indices in a microgrid functioning under non-sinusoidal unbalanced operating state, with possible voltage dips or swells appearance. The VI can work off-line (taking the data from a file that contains the measurements) or on-line (with the help of an data acquisition board the input power signals are acquired). The graphic user interface is illustrated in Fig. 7, whereas the source code is presented in Fig. 8.

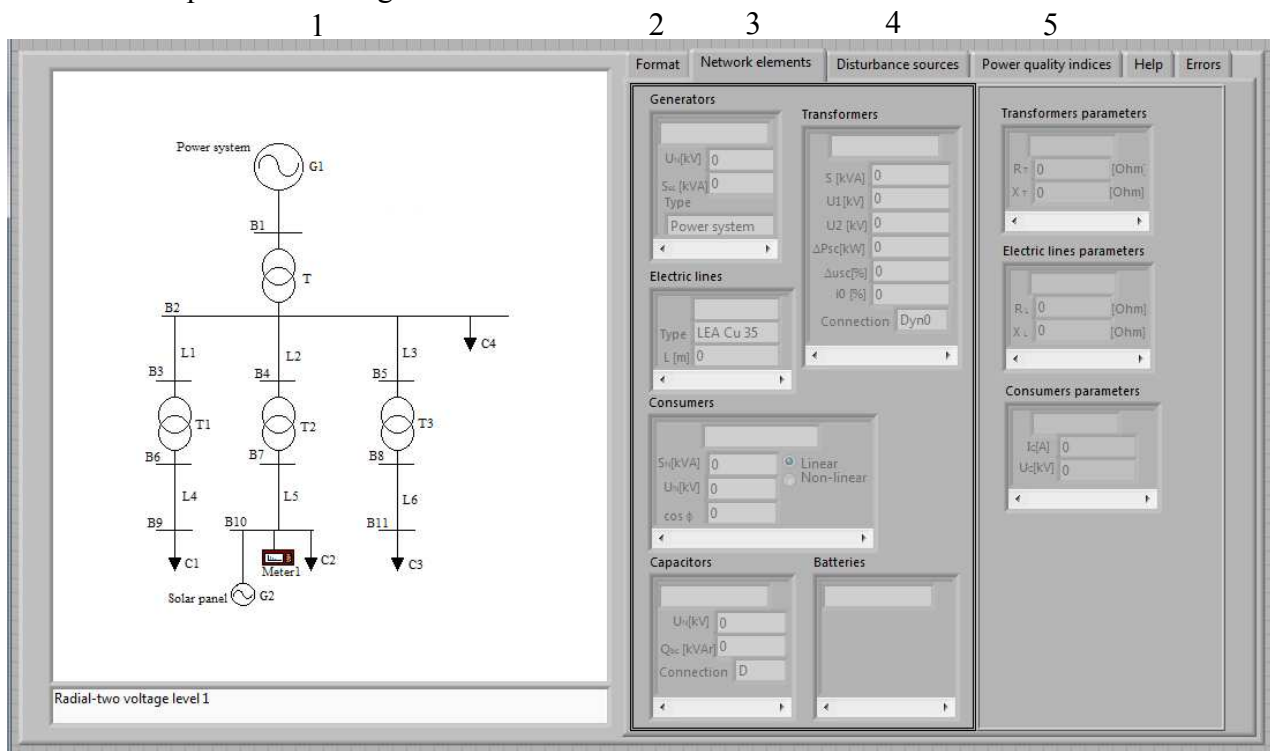


Fig. 7. PowerDiNet_PQMo graphic user interface

PowerDiNet_PQMo usage is easy and sequential: first the user has to choose the microgrid topology (predefined or custom), the electric parameters calculus (typical or complex), the power quality analysis (standard and/or custom) and the way the data should be displayed (standard and/or report) by accessing submenu “Format” (Fig. 7 – 2). In Fig. 7 – 1, is illustrated a predefined microgrid topology, whereas the custom topology supposes the user builds its microgrid using a special support grid and power system elements. The typical electric parameters means the calculus of microgrid parameters is performed without the skin effect, contrary the complex option implies the calculus of the electric parameters considering the skin effect. Standard power quality analysis is as [37] recommends, and the custom analysis is using the methods described in [28, 29] able to identify interharmonics and three-phase voltage dips and swells. On the next step, the microgrid components (generation units, transformers, electric lines, consumers, capacitors and batteries) characteristics have to be introduced (Fig. 7 – 3), whereas the input power signals, $u(t)$ and $i(t)$ are introduced in the 3rd step (Fig. 7 – 4). After these 3 stages, the VI processes the input data and

Table 1. Microgrid elements characteristics

Microgrid element	Characteristics
G1	$P_{sc} = 20 \text{ MVA}$, $U_N = 110 \text{ kV}$
T	$S_N = 1.6 \text{ MVA}$, $U_1/U_2 = 110/20 \text{ kV}$, $u_{sc} = 6\%$, $\Delta P_{sc} = 21.05 \text{ kW}$, $\Delta P_\theta = 2.1 \text{ kW}$, Y_{Nd-11}
T1	$S_N = 0.4 \text{ MVA}$, $U_1/U_2 = 20/0.4 \text{ kV}$, $u_{sc} = 4\%$, $\Delta P_{sc} = 4.3 \text{ kW}$, $\Delta P_\theta = 0.8 \text{ kW}$, Dy_n-11
L1	Over-head line, $l = 20 \text{ km}$, $s = 70 \text{ mm}^2$, Steel - Aluminum
L4	Cable, $l = 0.1 \text{ km}$, $s = 150 \text{ mm}^2$, Copper
C1	$P_N = 300 \text{ kW}$, $PF = 0.8$, $U_N = 0.4 \text{ kV}$
T2	$S_N = 0.1 \text{ MVA}$, $U_1/U_2 = 20/0.4 \text{ kV}$, $u_{sc} = 2\%$, $\Delta P_{sc} = 1.5 \text{ kW}$, $\Delta P_\theta = 0.29 \text{ kW}$, Y_{Yn-0}
L2	Over-head line, $l = 2 \text{ km}$, $s = 70 \text{ mm}^2$, Steel - Aluminum
L5	Cable, $l = 0.1 \text{ km}$, $s = 50 \text{ mm}^2$, Copper
C2	$P_N = 80 \text{ kW}$, $PF = 0.8$, $U_N = 0.4 \text{ kV}$
T3	$S_N = 0.63 \text{ MVA}$, $U_1/U_2 = 20/0.4 \text{ kV}$, $u_{sc} = 5\%$, $\Delta P_{sc} = 6.2 \text{ kW}$, $\Delta P_\theta = 1.2 \text{ kW}$, Dy_n-0
L3	Over-head line, $l = 10 \text{ km}$, $s = 70 \text{ mm}^2$, Steel - Aluminum
L6	Cable, $l = 0.1 \text{ km}$, $s = 240 \text{ mm}^2$, Copper
C3	$P_N = 500 \text{ kW}$, $PF = 0.8$, $U_N = 0.4 \text{ kV}$
G2	$P_{sp} = 100 \text{ kW}$, $U_N = 0.4 \text{ kV}$
C4	$P_N = 500 \text{ kW}$, $PF = 0.9$, $U_N = 20 \text{ kV}$

The scenario settings are: predefined microgrid, typical calculus of the microgrid parameters, standard PQ analysis and indices, and standard-window display of results. Processing the input data, the VI identified harmonics and unbalance, thus the PQ indices and their propagation through the microgrid are illustrated in Table 2; Fig. 9 presents the load flow. As the calculus was made for each phase, in the scheme are illustrate only the maximum values that indicate the worse situation. It can be seen that the voltage unbalance is very low, and the other consumers are not influenced by the non-linearity or unbalance of the solar panels.

Table 2. Power quality indices

Busbar	THD_U [%]	k_U^- [%]	k_U^0 [%]
B1	0	0	0
B2	2.7	0	0
B3	0	0	0
B4	11	0.1	0
B5	0	0	0
B6	0	0	0
B7	12	0	0.1
B8	0	0	0
B9	0	0	0
B10	12.1	0	0.1
B11	0	0	0

THD_U [%] – voltage's total harmonic distortion factor,

k_U^- – voltage's negative unbalance factor,

k_U^0 – voltage's zero unbalance factor.

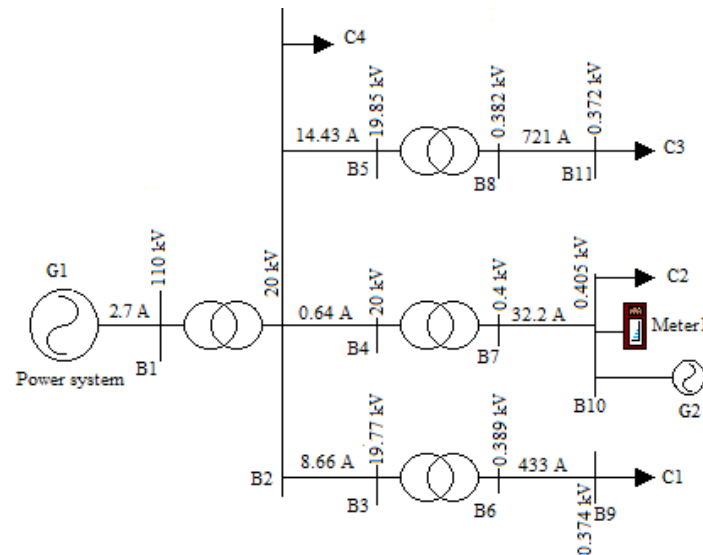


Fig. 9. Load flow through the microgrid

Summary

The authors proposed a low-cost and time saver methodology for power quality monitoring in microgrids working under non-sinusoidal unbalanced conditions, with possible voltage dips and swells existence. The method is based on the disturbances propagation phenomenon, which was analyzed with the help of sequence components applied for all detected harmonic components. The propagation algorithm was implemented in a virtual instrument that offers the possibility of analyzing the PQ in microgrids, but also to simulate their functioning. The VI was tested using diverse microgrids topologies with different scenarios (regarding consumers, distributed generation units and disturbances levels). The paper describes a functioning scenario of a microgrid that supplies four types of consumers from the main power network and solar panels. As a result of the performed analysis on the showed example and on other microgrids, the followings have been observed:

- The disturbances propagate entirely along the electric lines, but their characteristics change when they pass through the grid's transformers, depending on the transformer connection;
- The zero sequence components of harmonics from the secondary side of transformers that have the Dy_n connection, cannot be found on the primary side;
- The disturbances source doesn't influence the other consumers because the power system is strong enough to reduce its effects. In the situation the microgrid is working in isolated mode and the generation unit is of big power comparing the consumer near it, its influence can be sensed.

The usage of the presented software tool offers the following advantages:

- 1). Low-cost and time saver comparing the classical measurement apparatus and survey methodologies;
- 2). Analysis of microgrids power quality indices using both the standard methodology but also an advanced analysis for interharmonics identification that uses novel algorithms. It can be observed that the VI can easily be used for arbitrary distribution power networks;
- 3). Friendly graphic interface;
- 4). Workable results in a short time.

Acknowledgements

This paper was supported by the project "Development and support of multidisciplinary postdoctoral programmes in major technical areas of national strategy of Research - Development - Innovation" 4D-POSTDOC, contract no. POSDRU/89/1.5/S/52603, project co-funded by the European Social Fund through Sectoral Operational Programme Human Resources Development 2007-2013.

References

- [1] N. Hatziargyriou, H. Asano, Microgrids: An Overview of Ongoing Research, Development, and Demonstration Projects, <http://eetd.lbl.gov/EA/EMP/emp-pubs.html>, Last Accessed: June 2012
- [2] B. Lasseter, Microgrids and distributed energy resources, Sustainability Innovation Workshop, HP Laboratories, Wuhan, October 2008
- [3] Advanced architectures and control concepts for more microgrids, European project, coord. Nikos Hatziargyriou, ICCS Company, Finished in December 2009, www.microgrids.eu, Last Accessed: June 2012
- [4] T.L. Vandoorn, B. Renders, L. Degroote, B. Meersman and L. Vandeveldel, Active load control in islanded microgrids based on the grid voltage, *IEEE Trans. Smart Grid*, 2(1) (2011) 139 – 151.
- [5] H. Chen, J. Chen, D. Shi and X. Duan, Power flow study and voltage stability analysis for distribution systems with distributed generation, *IEEE Power Eng. Soc. General Meeting*, Montreal, QC, Canada, 2006.
- [6] W. Bo, W. Sheng, L. Hua and X. Hua, Steady-state model and power flow analysis of grid connected photovoltaic power system, *Proc. IEEE Intern. Conf. Ind. Tech.*, (2008) 1–6.
- [7] D. Shirmohammadi, H. Hong, A. Semlyen and G. Luo, A compensation-based power flow method for weakly meshed distribution and transmission networks, *IEEE Trans. Power Syst.*, 3 (2), (1988) 753–762.
- [8] C. Cheng and D. Shirmohammadi, A three-phase power flow method for real-time distribution system analysis, *IEEE Trans. Power Syst.*, 10 (2) (1995) 671–679.
- [9] J. Teng, A modified Gauss-Seidel algorithm of three-phase power flow analysis in distribution networks, *Intern. J. Elect. Power Energy Syst.*, 24 (2) (2001) 97–102.
- [10] J. Vieira, W. Freitas and A. Morelato, Phase-decoupled method for three-phase power-flow analysis of unbalanced distribution systems, *Proceedings Inst. Elect. Eng. Generation, Transmission Distribution*, 151 (5) (2004) 568–574.
- [11] V. Costa, M. Oliveira and M. Guedes, Developments in the analysis of unbalanced three-phase power flow solutions, *Intern. J. Elect. Power Energy Syst.*, 29 (2) (2007) 175–182.
- [12] K. Lo and C. Zhang, Decomposed three-phase power flow solution using the sequence component frame, *Proc. Inst. Elect. Eng., Gen., Transm. Distrib.*, 140 (3) (1993) 181–188.
- [13] M. Abdel-Akher, K. Nor and A. Rashid, Improved three-phase power-flow methods using sequence components, *IEEE Trans. Power Syst.*, 20 (3) (2005) 1389–1397.
- [14] M. Abdel-Akher, K. Nor and A. Abdul-Rashid, Development of unbalanced three-phase distribution power flow analysis using sequence and phase components, in *Proc. 12th Int. Middle-East Power System Conf.*, (2008) 406–411.
- [15] M. Z. Kamh, R. Iravani, Unbalanced model and power flow analysis of microgrids and active distribution systems, *IEEE Tran. Power Deliv.*, 25 (4) (2010) 2851 – 2858.
- [16] L.D. Zhang, M.H.J. Bollen, A method for characterizing unbalanced voltage dips (sags) with symmetrical components, *IEEE Power Engineering Letters*, (1998) 50-52.
- [17] L.D. Zhang, Propagation of voltage sags in power systems, PhD. thesis, Department of Electric Power Engineering and Department of Signals and Systems, Chalmers University of Technology, Goteborg, Sweden, 2000.
- [18] G.-R. Gillicha, D. Frunzaverdea, N. Gillicha and D. Amariei, The use of virtual instruments in engineering education, *Procedia Social and Behavioral Sciences*, 2 (2010) 3806–3810.
- [19] G. Bucci, E. Fiorucci and C. Landi, Digital measurement station for power quality analysis in distributed environments, *IEEE Transactions on Instrumentation and Measurement*, 52 (1) (February 2003) 75 – 84.

-
- [20] A. López, J.-C. Montaño, M. Castilla, J. Gutiérrez, M. Dolores Borrás and J. C. Bravo, Power system frequency measurement under non-stationary situations, *IEEE Trans. Power Deliv.*, 23 (2) (2008) 562 – 567.
- [21] I. Orović, M. Orlandić, S. Stanković and Z. Uskoković, A Virtual instrument for time-frequency analysis of signals with highly non-stationary instantaneous frequency, *IEEE Trans. Instr. Measurement.*, 60 (3) (2011) 791 – 803.
- [22] L. Ferrigno, C. Liguori and A. Pietrosanto, Measurements for the characterization of passive components in non-sinusoidal conditions, *IEEE Trans. Instr. Measurement*, 51 (6) (2002) 1252 – 1258.
- [23] J.-H. Teng, S.-Y. Chan, J.-C. Lee and R. Lee, A LabVIEW based virtual instrument for power analyzers, *IEEE Proc. Intern. Conf. Power Syst. Tech.*, 1 (2000) 179-184.
- [24] A. Monti, F. Ponci, S. Pelizzari and L. Cristaldi, A virtual instrument for time-frequency analysis of Park power components, *J. Electr. Power Qual. Utilis.*, XIII (1) (2007) 121 – 128.
- [25] W. Xinling and Z. Cheng, Design and simulation of voltage fluctuation rate monitor system based on virtual instrument technology, *Energy Procedia*, 17 (2012) 450 – 455.
- [26] F. Adamo, F. Attivissimo, G. Cavone and N. Giaquinto, SCADA/HMI systems in advanced educational courses, *Proc. IEEE Instrum. Measur. Tech. Conf., IMTC 2005*, 2 (2005) 1097 – 1101.
- [27] Clarke Edith, *Analysis of power systems circuits*, Technical Publishing House, 1973.
- [28] A. Miron, M.D. Chindriş and A.C. Cziker, Harmonics and interharmonics analysis of power signals using Gaussian filter banks, *Elect. Power Syst. Res.*, unpublished (submitted for publication).
- [29] A. Miron, M.D. Chindriş and A.C. Cziker, Time domain analysis of voltage dips/swells in modern power networks, *IET Gen., Transm. & Distr.*, unpublished (submitted for publication).
- [30] A. Cziker, A. Miron and M. Chindris, Power quality indices for unbalance characterization in non-sinusoidal condition, 14th Intern. Research/Expert Conf. „Trends in the Development of Machinery and Associated Technology” TMT 2010, 11-18 September 2010, pp. 481-484. [Online]. Available: <http://www.tmt.unze.ba/proceedings 2010.php>
- [31] A. Miron, M.D. Chindriş and A. Cziker, Voltage dips and swells quantification in harmonic unbalanced polluted power systems, unpublished
- [32] A. Cziker and A.C. Cziker, *Exploitation of power station and substations*, Science Book Publishing House, Cluj – Napoca, Romania, 2006.
- [33] M.J. Heathcote, *The J&P Transformer book*, Twelfth edition, A practical technology of the power transformer, Leed Educational and Professional Publishing Ltd. 1998, Woburn, Great Britain
- [34] A.J. Pansini, *Electrical distribution engineering*, The Fairmont Press Inc., Great Britain, 2007
- [35] M. Chindriş, A. Sudria, A. Cziker and Anca Miron, Propagation of unbalance in electric power systems, 9th Intern. Conf. Electr. Power Qual. Utilis., EPQU’07, Barcelona, Spain, 9 – 11 October 2007, Session 4D – Improvement and distribution loads
- [36] A. Miron, M. Chindriş and A. Cziker, Efficiency increase of power quality analysis using virtual instrumentation, *WEC REGIONAL ENERGY FORUM – FOREN 2010*, Neptun, 2010, paper s3-13-en
- [37] IEC 61000-4-30 Testing and Measurement Techniques – Power Quality Measurement Methods;



Interharmonics Analysis using Fourier Transform and Virtual Instrumentation

Anca MIRON, M. CHINDRIS and A. CZIKER

Department of Power Systems
Technical University of Cluj-Napoca
Cluj – Napoca, Romania

Anca.Miron@eps.utcluj.ro, Mircea.Chindris@eps.utcluj.ro, Andrei.Cziker@eps.utcluj.ro

Abstract—Interharmonics represent those electrical signals whose frequencies are not integer multiples of the supply fundamental frequency. They correspond to electrical components that are not synchronized with the systems fundamental frequency; due to this fact, they have a more destructive impact than harmonics on the elements of the power system. International organizations like IEC and IEEE International Force Task Committee have defined the terminology, limits and measurement guidelines for interharmonics; even though, there still are difficulties in their detection and measurement with an acceptable accuracy. The paper presents the mathematical basis of Fourier transformation and some general aspects regarding a new algorithm that authors propose for interharmonics analysis. The classic Discrete Fourier Transform is adjusted using windows with different widths accordingly to the interharmonics spectrum. The paper also contains a numerical example and the description of the virtual instrument developed specifically for interharmonics detection and evaluation.

Keywords - *interharmonics, Discrete Fourier Transform, detection and evaluation, virtual instrumentation*

I. INTRODUCTION

Due to the increasing use of electronic and switching devices, power quality is deteriorating in the electric distribution grids. A major aspect of power quality is the harmonic pollution, whose effects negatively influence all grids elements.

Harmonics represent spectral components of frequencies that are integer multiple of the fundamental frequency. Interharmonics are defined by the IEC Interharmonic Task Force as “Any frequency which is not an integer multiple of the fundamental frequency”.

By now, many standards and procedures were developed to identify and limit the unnecessary harmonics, but mostly of them for the integer multiple harmonics.

In the scientific literature there are a lot of studies regarding interharmonics sources, modeling, simulation, limits and measurement [1-6]. However the most problematic issue is the accurate determination of interharmonic frequency and amplitude, which still raises many questions.

The interharmonics emerge in all power switching converters and inverter drives. The characteristic of the switching converters (for instance, ac/dc supplies and power factor correctors) is that they are not synchronized to the power supply frequency. On the other hand, the inverter drives cause variations of the amplitude and/or phase angle of the fundamental component and/or of the harmonic components.

Today, recognized interharmonic sources are:

- Static converters, in particular direct and indirect frequency converters;
- Variable-load electric drivers;
- Arcing loads;
- Ripple controls;
- Control and protection signalling in electric lines.

Interharmonics introduced by these sources have the following possible effects:

- Noise in the audio amplifiers;
- Additional torques on motors and generators;
- Disturb zero crossing detectors (dimmers);
- Additional noise in inductive coils (magnetostriction);
- Blocking or unintended operation of ripple control receivers.

The main difficulty in the interharmonics analysis is that they are not synchronized with the fundamental frequency.

The paper firstly reviews the mathematical basis of interharmonics analysis. A new adapted algorithm based on the Fourier Transform is proposed. The paper also presents a virtual instrument (VI) for interharmonic detection and evaluation whose working principle is based on the proposed algorithm. The last part of the paper presents some numerical examples.

II. INTERHARMONICS ANALYSIS

The mathematical basis of the harmonic and interharmonic analysis is based on the Discrete Fourier Transform (DFT).

The Fourier analysis can be used on non-sinusoidal periodical signals and decomposes them into a series of sinusoidal components. The classic Fourier transform can be applied with properly results only on a periodical signal $f(t)$ with period of T , where T is the period of the fundamental frequency:

$$f(t) = c_0 + \sum_{n=1}^{\infty} [a_n \cdot \cos(n \cdot \omega \cdot t) + b_n \cdot \sin(n \cdot \omega \cdot t)]; \quad (1)$$

here, c_0 is the continuous component of the periodical signal, while $c_n = \sqrt{a_n^2 + b_n^2}$ is the amplitude of the n^{th} order harmonic. The harmonic angle in its working space $n \cdot \omega \cdot t$, with an initial origin arbitrary chosen, is $\alpha_n = \arctg \frac{a_n}{b_n}$; this value, reported to the fundamental space ($\omega \cdot t$) is $\alpha'_n = \frac{\alpha_n}{n}$.

If $f(n)$ is a sampled signal with a rate of N points per cycle, and the period T is sampled in $2p$ intervals of $\Delta t = T/(2p)$, the Fourier coefficients can be obtained using the Discrete Fourier Transform (DFT), by the following mathematical relationships:

$$A_0 = \frac{1}{T} \int_0^T f(t) dt \approx \frac{1}{2p} \sum_{i=1}^{2p} f(t_i); \quad (2)$$

$$A_n = \frac{2}{T} \int_0^T f(t) \cdot \cos(n \cdot \omega \cdot t) dt \approx \frac{1}{p} \sum_{i=1}^{2p} f(i) \cdot \cos \frac{n \cdot \pi \cdot i}{p}; \quad (3)$$

$$B_n = \frac{2}{T} \int_0^T f(t) \cdot \sin(n \cdot \omega \cdot t) dt \approx \frac{1}{p} \sum_{i=1}^{2p} f(i) \cdot \sin \frac{n \cdot \pi \cdot i}{p}; \quad (4)$$

where ω is the fundamental angular frequency. As the signal $f(n)$ is assumed to be on one fundamental period cycle, every sampled value will theoretical repeating itself every N points. In practice, the sampled non-sinusoidal signal is frequently written as:

$$y = Y_0 + \sum_{n=1}^{\infty} \sqrt{2} \cdot Y_n \cdot \sin(n \cdot \omega_1 \cdot t + \gamma_n), \quad (5)$$

where Y_n is the r.m.s. value of the n^{th} order harmonic, and γ_n is its initial angle.

The above presented relationships are used to found harmonics. The IEC Interharmonics Task Force was the first international team that tried to standardize the evaluation of interharmonics [1].

The proposed method utilize a Discrete Fourier Transform performed over a time window of exactly 10 cycles for 50 Hz systems, corresponding approximately to 200 ms. This new approach fixes the frequency resolution at 5 Hz. Using this procedure, interharmonics with frequency integer multiple of 5 Hz can be obtained. Thus, interharmonics components that are in between the integer multiple of 5 Hz would split primarily into adjacent interharmonic bins with a minimum of leak into harmonic bins. In summary, a necessary condition in interharmonic detection is that the sampled data for DFT operation must cover multiple fundamental cycles.

Two major problems appear in the interharmonic analysis:

- The non-integer multiple components calculated from DFT do exist?
- The magnitudes and frequencies of the interharmonics are correctly evaluated?

A solution for these problems is to select a time window large enough to include the periods of all signal components. This synchronization to the interharmonics is very difficult because it means to choose a window width too large. Thus the interharmonics analysis encounters many difficulties.

The authors propose a new method for interharmonic detection and analysis. It is based on the DFT with a variable time window depending on the interharmonic spectrum firstly detected. The algorithm assumes the realization of several steps:

1. Analysis is made with a window of 10 fundamental cycles;
2. Spectrum is analysed and spectral leakages are looked for. Regarding the interharmonics, there can be found three possible cases:
 - a. multiple integers of 5 Hz interharmonics (genuine interharmonics);
 - b. multiple integers of 5 Hz interharmonics (genuine interharmonics) and spectral interharmonics groups surrounding specific frequencies;
 - c. spectral interharmonics groups surrounding specific frequencies.
3. After the previous stage, depending on the results, this 3rd step may perform the following:
 - a. Interharmonics order, amplitude and angle are presented and displayed. The signal analysis ends;
 - b. The genuine interharmonics are memorized and the spectral groups are taken in consideration for another analysis;
 - c. Spectral groups are taken in consideration for another analysis.

4. This step is necessary only in the cases 3.b. and 3.c. The window width is enlarged, and a more detailed analysis is performed. To reduce the number of Fourier coefficients that have to be calculated, only the frequencies that form the spectral groups are considered.
5. Algorithm continues until there are only genuine interharmonics.

This method diminishes the huge amount of calculus that must be made if the window width is constant and raises the accuracy of amplitude and phase determination.

The above presented algorithm was implemented to create a virtual instrument in the graphic programming environment LabVIEW. Further on, the virtual instrument (VI) and its working principles are presented.

III. VIRTUAL INSTRUMENT FOR INTERHARMONICS ANALYSIS

The virtual instrument reads the electrical signals through an acquisition data board, analyzes them using DFT and evaluates the harmonic and interharmonics components.

The LabVIEW graphic programming environment was used to create this VI. LabVIEW environment helps to build applications as testing and measurement, data acquisition, instrument control, data logging, measurement analysis and report.

Forward, the two main components of the VI are presented, namely the passive (graphic user interface) and the active (operating modules) one.

A. Graphic user interface

As the graphic user interface (GUI) represents the part of the VI with which the users come in contact, a simple and easy to understand GUI was built up. Through it, users can introduce the input data and visualize the obtained results.

Frontal panel is composed of graphic objects used for making choices, introducing input data (controls) and presenting results (indicators). First of all, user must choose the way of reading signals – from a file or directly from the network through a data acquisition board, by using button 1. The figure 1 presents the off-line variant, when user has to introduce source file path. Once he made this choice, the virtual instrument reads data and illustrates the signals through window 4.

Button 3 is the control with which user can start the signals analysis. The results of this analysis are presented in a graphic (indicator 4) and tabular (indicator 5) form. For instance, Table 5 contains the characteristics of signal components: order, r.m.s., angle and level in percentage. The total harmonic distortion is presented through the indicator 6.

B. Block diagram

The bloc diagram is the active part (engine) of the VI, i.e. the VI's component that is not seen by the users. The hierarchy tree of the VI is illustrated in figure 2; it can be seen

that for each module a suggestive icon was build up (except for the ones already created and assumed); the connections between the operating modules are also illustrated.

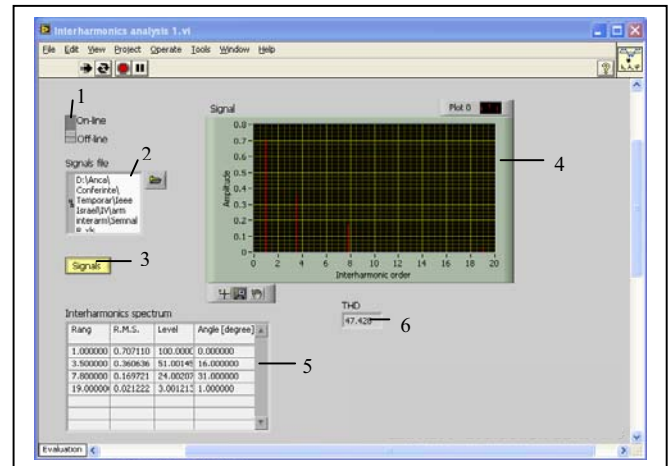


Figure 1. Frontal panel of the VI for interharmonics detection and analysis

The main program (underlined in red) has diverse sub-VIs with different roles:

- Identification of signal period;
- Determination of harmonic spectrum;
- Detection of genuine interharmonics;
- Calculus of Fourier coefficients;
- Determination of harmonics and interharmonics r.m.s., angles and levels;
- Conversion of angle units from radians to degrees;
- Calculus of the THD (Total Harmonic Distortion).

The working algorithm of the virtual instrument is as follows:

- The user selects the source of signals – file (Off-line) or data acquisition board (On-line);
- For the first variant, user must introduce the data file path for the file in which the measured data was saved;
- Read data are shown in the illustration window;
- User can start the analysis by pushing button “Analyze”;
- The read signals are processed and the results are sent to the adequate frontal panel components;
- The harmonics and interharmonics components are graphically illustrated in the window 4 and numerically in the table 5;
- Total harmonic distortion is calculated and sent to the proper indicator.

In figure 3 a capture of the block diagram is presented. The most important aspect of this virtual instrument is the detection of interharmonics and the evaluation of their main parameters: order, amplitude and angle.

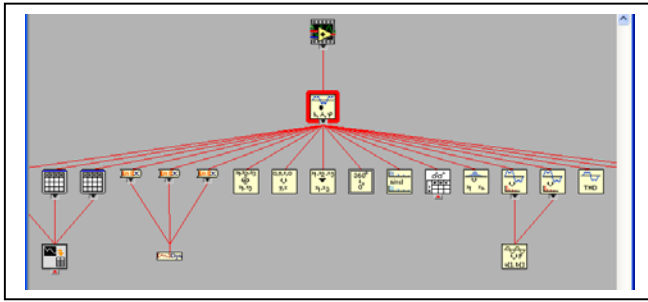


Figure 2. Virtual instrument hierarchy tree

The procedure steps are further presented:

- A period (cycle) corresponding to the fundamental frequency is taken, and the signal is analyzed;
- The obtained spectrum is verified: if there are spectral leakages, the window width is raised to 10 cycles;
- The spectrum is analyzed again and if there are genuine harmonics and interharmonics, they are memorized;
- The existence of spectral leakages imply another analysis, this time for a 100 cycles window, but only for the frequencies where these leakages were identified, and so on, until there are only genuine interharmonics of significant r.m.s. (> 0.001 units).

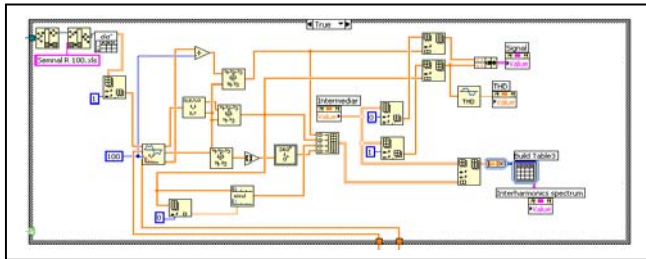


Figure 3. The block diagram of the virtual instrument

The last step is essential, because it shortens the time calculus even if the window width is very large.

A numerical example shows the working principle. A non-sinusoidal waveform sampled was analyzed; the results of first step are presented in figure 4, highlighting an important spectrum leakage. The final analyze, put in evidence some interharmonics, as shown in figure 1.

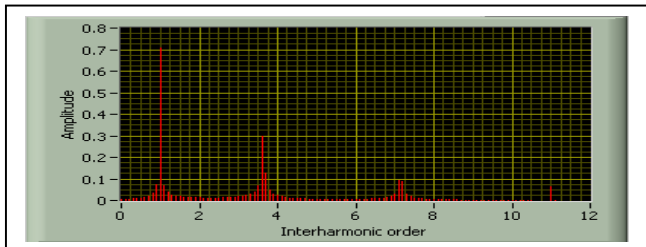


Figure 4. Interharmonics spectrum leakage after the first step analysis

IV. CONCLUSIONS

Interharmonics have become an important aspect of power quality. They are defined as “Any frequency which is not an integer multiple of the fundamental frequency”. Because of the fact that they are not synchronized with the systems fundamental frequency, they have a more destructive impact than harmonics on the elements of the power system.

The international power quality committees have defined the terminology, limits and measurement guidelines for interharmonics; even though, there still are difficulties in their detection and measurement with an acceptable accuracy.

The paper presents general aspects about interharmonics analysis using the Discrete Fourier Transform and the standardized method of interharmonics measurement. A virtual instrument developed for interharmonics detection and analysis is also described.

The working principle of the virtual instrument is based on an adapted Fourier transform, its use bringing many advantages:

- “accurate” detection and analysis of interharmonics;
- short time analysis even for large window width;
- friendly graphic interface, easy to use even by the non-specialized engineer.

REFERENCES

- [1] ***CEI/IEC 1000 – 2 – 1, “Electromagnetic Compatibility, Part 2: Environment, Section1: Description of the environment – Electromagnetic environment for low – frequency conducted disturbances and signaling in public supply systems”, 1st edition 1990.
- [2] ***IEC – 61000 – 2 – 2, “Compatibility levels for low-frequency conducted disturbances and signaling in public low-voltage power supply systems”, 2nd edition, 2000.
- [3] Gallo D., Langella R., Testa A., “Interharmonics Part 1: Aspects related to modeling and simulation”, L’Energia Elettrica – Volume 81 (2004) – „Ricerche”, pp. 168 – 173.
- [4] Gallo D., Langella R., Testa A., “Interharmonics Part 2: Aspects related to measurement and limits”, L’Energia Elettrica – Volume 81 (2004) – „Ricerche”, pp. 174 – 181.
- [5] ***Interharmonics in power systems, IEEE Interharmonic Task Force, Cigre 36.05/Cired 2 CC02 Voltage Quality Working Group, 199.
- [6] Gunther E., s.a., “Interharmonics in Power Systems”, Cigre 2000.
- [7] Zhang D., Xu W., Liu Y., “The phase sequence characteristics of interharmonics”, IEEE Transactions on Power Delivery, Vol.20, No.4, October 2005, pp. 2563 – 2569.
- [8] Li C., Xu W., Tayjasant T., “Interharmonics: basic concepts and techniques for their detection and measurement”, Electric Power System Research 00(2003) 1 – 10, www.elsevier.com/locate/epsr.
- [9] Rusek J., “Interharmonics generated by induction machines”, Electrical Power Quality and Utilization, Magazine Vol. II, No.2, 2006, pp. 49 – 52.
- [10] Hanzelka Z., Bien A., “Power Quality Application Guide. Interharmonics 3.1.1”, Leonardo Power Quality Initiative, July 2004.
- [11] Lobos T., Leonowicz Z., Rezmer J., Koglin H. – J., “Advanced signal processing methods of harmonics and interharmonics”, <http://zleonowicz.republika.pl/art/amsterdam.pdf>.
- [13] Miron Anca, Chindris M., Cziker A., “Interharmonic Issue in the Electric Power Systems”, PSC 2007, 21-23 November 2007, Timisoara, Romania.



Propagation of Unbalance in Electric Power Systems

M. Chindriș, A. Cziker, Anca Miron, H.Bălan

Dept. of Electric Power Engineering
Technical University of Cluj – Napoca
Cluj – Napoca, Romania
Mircea.Chindris@eps.utcluj.ro

Ana Iacob

ICMET Craiova, Research, Development and Testing
National Institute of Electrical Engineering, Romania

A. Sudria

Dept. Ingeniería Eléctrica – CITCEA
Universidad Politécnica de Catalunya
Barcelona, Spain
sudria@citcea.upc.edu

Abstract—Power quality has become an important issue for electric power engineering. Nowadays, the distribution electric networks have unbalanced operating regimes, mainly produced by the great number of single-phase loads. Unbalanced line currents produce unbalanced voltage drops on the three phases of the supply system. Consequently, the voltage system within the supply network will become unbalanced. Voltage unbalance influences different components of the electric networks: the effects on the motors are the growths of losses, supplementary heating, and finally, the motors life is shortened. In the distribution and transmission electric networks the main effect of the unbalanced currents is the existence of additional power losses. Taking into account the above mentioned aspects, it is necessary to study the propagation of unbalance through the electric power system, upstream from the LV distribution level. By using the symmetrical components theory, transformers with different types of connections were studied, and their influence on the unbalance propagation was analyzed. A numerical example is presented for the propagation of unbalance from the secondary side of a transformer with Yz_n connection to its primary side.

Keywords – power quality, unbalanced regime, unbalance propagation, power transformers

I. INTRODUCTION

The modern three-phase distribution systems supply a great diversity of customers; among them, those having single-phase, two-phase and unbalanced three-phase loads have become preponderant. The operation of these consumers imposes to the distribution network a permanent unbalanced running state, characterized by different parameters of the three phases.

The unequal distribution of loads between the three phases of the supply system determines the flow of unbalanced

currents that produce unbalanced voltage drops on the electric lines; as a result, the voltage system within the supply network becomes also unbalanced.

In power systems supplying asymmetrical (unbalanced) loads, appear supplementary negative and/or zero sequence currents that cause additional power losses and faults in the electric power system and the unacceptable overheating of three-phase asynchronous machines belonging to different customers [1].

The paper presents a study regarding the propagation of unbalance distortion through electric networks, upstream from the LV to higher voltage levels.

The paper (I) summarizes some theoretical aspects regarding unbalance distortion in three-phase distribution networks; (II) describes the methodology of the investigation and (III) analyzes the influence of types of connections and magnetic cores on the voltage unbalance propagation through transformers, with a numerical example for a Yz_n case. In the end, conclusions about the studied phenomenon are derived.

II. UNBALANCE IN THREE-PHASE DISTRIBUTION NETWORKS

To study the unbalanced operation of a power system, the symmetrical components theory is used. According to Stokvis-Fortescue theorem, every three-phase asymmetrical system of phasors can be decomposed into three symmetrical systems of positive, negative and zero sequence respectively. This aspect can be seen in figure 1 where every sequence system contains three phasors characterized by equal magnitudes; in the case of positive and negative sequences, components are rotated between them with 120 electrical degrees in counter-clockwise

direction and negative clockwise direction, respectively. In the case of zero sequence components, there is no rotation between phasors. If an asymmetrical system of line currents is taken into consideration, the relationship between the initial system and the symmetrical sequence systems can be written as follows:

$$\begin{pmatrix} \underline{I}_A \\ \underline{I}_B \\ \underline{I}_C \end{pmatrix} = \begin{pmatrix} 1 & 1 & 1 \\ 1 & a^2 & a \\ 1 & a & a^2 \end{pmatrix} \cdot \begin{pmatrix} \underline{I}^+ \\ \underline{I}^- \\ \underline{I}^0 \end{pmatrix}, \quad (1)$$

where $\underline{I}_A, \underline{I}_B$ and \underline{I}_C are the line current phasors; $\underline{I}^+, \underline{I}^-$ and \underline{I}^0 are the positive, negative and zero symmetrical systems, respectively; $a = e^{j120^\circ}$ is the rotation operator. The reverse relationship is:

$$\begin{pmatrix} \underline{I}^+ \\ \underline{I}^- \\ \underline{I}^0 \end{pmatrix} = \frac{1}{3} \begin{pmatrix} 1 & a & a^2 \\ 1 & a^2 & a \\ 1 & 1 & 1 \end{pmatrix} \cdot \begin{pmatrix} \underline{I}_A \\ \underline{I}_B \\ \underline{I}_C \end{pmatrix}. \quad (2)$$

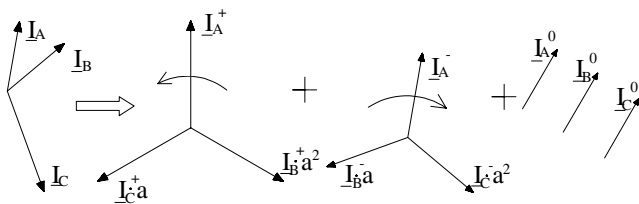


Figure 1. Decomposition of a unsymmetrical phasors system in three symmetrical phasors systems

These sequence systems are not only theoretical, they correspond to the reality: the positive sequence components are created by the synchronous or asynchronous generators while the negative and zero sequence components appear at the place of unbalance. Each of them can be separately measured and influences in a different way the power system. For example, in the case of motors, the positive sequence components produce the useful torque while the negative sequence components produce fields that create braking torques. On other hand, the zero sequence components is the one that get involved in the cases of interferences between the electric and the telecommunication transmission lines [1].

Other influences on balanced elements (generators and loads) connected to the power system are as follows:

- Negative sequence currents can produce the overheating of synchronous generator rotors, the transformers saturation and ripples in rectifiers;
- Zero sequence currents cause excessive power losses in neutral conductors and interferences with protection systems;

- In unbalanced electric systems, power losses grow and the loading capacity of the transmission networks diminishes.

To quantify the amount of imbalance, a set of different parameters is implemented. For illustration, the current unbalance can be quantified using the following definitions:

- Unbalance factor: $k_I^- = \frac{I^-}{I^+}$; (3)

- Asymmetry factor: $k_I^0 = \frac{I^0}{I^+}$; (4)

- Total unbalance factor: $k_I = k_I^0 + k_I^-$; (5)

- Complex unbalance factor: $\underline{k}_I^- = \frac{\underline{I}^-}{\underline{I}^+}$; (6)

- Complex asymmetry factor: $\underline{k}_I^0 = \frac{\underline{I}^0}{\underline{I}^+}$; (7)

where I^+, I^- and I^0 are the magnitudes of the positive, negative and zero-sequence current, respectively.

The values of these parameters must not exceed the planning given limits; e.g. according to [2], the maximum value of voltage unbalance factor must be 2% during 95% of the observation period (1 week by default).

III. ANALYSIS METHOD

To analyze the propagation phenomenon of voltage/current unbalance from the LV consumers' level to the next upper voltage level of the distribution electric system, network elements must be modeled. Transformers and electric lines models were determined considering the sequence components theory. The positive and negative sequence impedances are equal in the case of the electric lines and transformers and are represented by the electric line impedances and the transformers normal leakage impedances. Zero sequence impedances of electric lines depend on their type (cable or overhead lines) and on the type of the return circuit of the current. Transformer zero sequence impedances depend on its rating, constructive and connection type. An electric power system decomposed in sequence equivalent systems is presented in figures 2, where the magnitudes are presented in p.u. [5].

From the propagation phenomenon point of view, unbalance currents and voltages entirely propagate through the electric lines; consequently, only transformers will be further on analyzed.

For both positive and negative sequence components, transformers react in the same way regardless of the magnetic core and connections type [6].

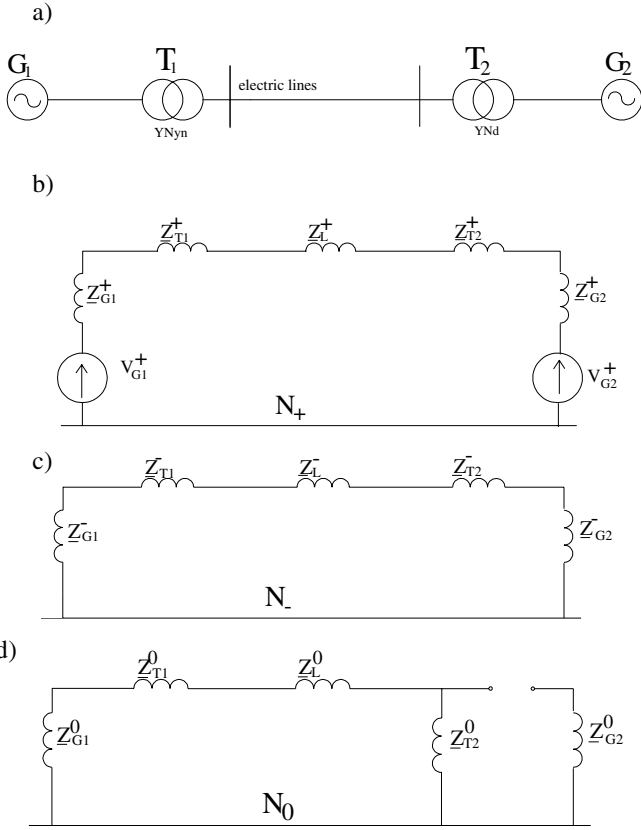


Figure 2. Electric power networks: a) Single-phase diagram; b) Positive sequence equivalent diagram ; c) Negative sequence equivalent diagram, d) Zero sequence equivalent diagram.

The relationships between voltages and currents in case of these two sequence components are:

$$\begin{cases} \underline{U}_A^+ = \underline{I}_A^+ \cdot \underline{Z}^+ - K \cdot \underline{U}_a^+ \\ \underline{U}_B^+ = \underline{U}_A^+ \cdot a^2 \\ \underline{U}_C^+ = \underline{U}_A^+ \cdot a \end{cases} \quad (8)$$

$$\begin{cases} \underline{U}_A^- = \underline{I}_A^- \cdot \underline{Z}^- - K \cdot \underline{U}_a^- \\ \underline{U}_B^- = \underline{U}_A^- \cdot a \\ \underline{U}_C^- = \underline{U}_A^- \cdot a^2 \end{cases} \quad (9)$$

where K is a generalized coefficient calculated considering transformer connections, $\underline{U}_{A,B,C}^{+/-}$, $\underline{U}_{a,b,c}^{+/-}$ are the primary and secondary positive/negative sequence voltages respectively; $\underline{Z}^{+/-}$ - the positive/negative sequence transformers impedance, $\underline{I}_A^{+/-}$ - the positive/negative sequence primary current and

$$\underline{I}_A^{+/-} = -\frac{1}{n_T} \cdot \underline{I}_a^{+/-} \quad (10)$$

In the relationship (10) $\underline{I}_a^{+/-}$ is the secondary positive/negative current and n_T is the transformer voltage ratio. The values of generalized coefficient K are presented in table 1 where N_p represents the primary turn number while N_s has the same meaning for the secondary windings.

TABLE 1. Transformers ratio depending on its connections

Connection	K	Connection	K
Yy	$\frac{N_p}{N_s}$	Dy	$\frac{N_p}{\sqrt{3} \cdot N_s}$
Yd	$\frac{\sqrt{3} \cdot N_p}{N_s}$	Dd	$\frac{N_p}{N_s}$
Yz	$\frac{2 \cdot N_p}{\sqrt{3} \cdot N_s}$	Dz	$\frac{2 \cdot N_p}{3 \cdot N_s}$

The zero sequence secondary currents produce important magnetic fluxes only if they can not appear in the primary side.

If the zero sequence secondary currents appear in the primary side, the total magnetic flux produced by the secondary and primary components may be neglected [6]. The zero sequence transformer impedance, $\underline{Z}^0 = R^0 + j \cdot X^0$, has big values for groups of three single-phase transformers or shell-type transformers. In those cases where zero sequence currents can flow in both primary and secondary lines, the zero sequence impedance is the normal leakage transformer impedance. Where zero sequence currents can not flow in both sides of the transformer, the zero sequence impedance is equivalent to infinity comparatively to other sequence impedances [7]. The relationships between the zero sequence voltages and currents are:

$$\begin{cases} \underline{U}_A^0 = \underline{I}_A^0 \cdot \underline{Z}^0 - K \cdot \underline{U}_a^0 \\ \underline{U}_B^0 = \underline{U}_A^0 \\ \underline{U}_C^0 = \underline{U}_A^0 \end{cases} \quad (11)$$

where $\underline{U}_{A,B,C}^0, \underline{U}_{a,b,c}^0$ are the primary and secondary zero sequence voltages, \underline{Z}^0 is the zero sequence transformer impedance and \underline{I}_A^0 is the zero sequence primary current.

In relationships (8), (9) and (11) the secondary sequence voltages were calculated using the following formula [5]:

$$[\underline{U}]_s = [\underline{Z}]_s \cdot [\underline{I}]_s \quad (12)$$

where $[\underline{U}]_s$, $[\underline{Z}]_s$, $[\underline{I}]_s$ are the secondary voltage, network impedance and current sequence components matrix respectively.

IV. UNBALANCE PROPAGATION

A. General aspects

In the issue of unbalanced voltage and currents propagation through the distribution system, the main element is the transformer. Transformer connection influences in different ways this phenomenon: there are transformers through which unbalance propagate unchanged and contrary, transformers that reduce the unbalance factors.

The solving of the unbalanced operating state of a three-phase transformer means the finding of the following quantities:

- primary and secondary phase-to-phase voltages;
- primary and secondary line currents;
- current through the neutral conductor (if it is any).

To establish the solution of this problem, the following data are required:

- transformers rated parameters;
- primary phase-to-phase voltages (considered symmetric);
- consumers parameters that produce the unbalanced loading.

Because finding the solution of this issue in the general case is complicated, the analysis will be made considering that the supply voltage system is perfectly symmetric; the transformer's magnetization current is neglected and the transformer is a linear load, in consequence the superposition of effects is admitted.

B. Numerical example

In this chapter, the propagation phenomenon of voltages and currents unbalance through the distribution systems containing a Yz_n transformer is analyzed. This transformer was chosen because of its special behavior when supplying unbalanced loads; it has the following features: star connection on HV side, interconnected star connection with neutral grounding on LV side, and three limb core-types. Figure 3 presents the transformer voltage phasors diagram.

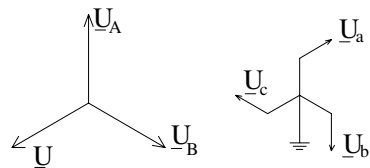


Figure 3. Transformers voltage phasors diagram

For the secondary interconnected star winding, each phase voltage is composed of voltages of two limbs crossed by currents that flow in opposite senses; due to this fact, the zero sequence current produces zero sequence fluxes that mutually cancel each other, and consequently the global zero sequence flux for each limb is null. The currents path through the windings is showed in figure 4 where N_p , N_s are the primary

and secondary number of turns; I_1 , I_2 , and I_3 are the secondary unbalanced currents.

To investigate how unbalance propagates through the transformer, mathematical modeling was used. For this purpose, the electric network presented in Figure 5 was considered; in this diagram, \underline{Z}_p and \underline{Z}_s are transformers primary and secondary impedances; \underline{Z}_L and \underline{Z}_N are the line and neutral conductor impedances, respectively; \underline{Z}_1 , \underline{Z}_2 and \underline{Z}_3 are the unbalanced consumer impedances.

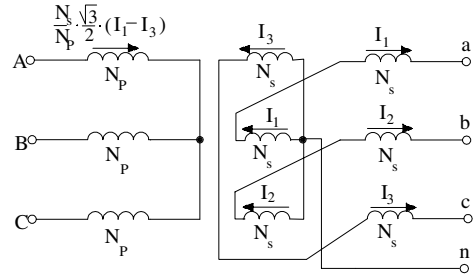


Figure 4. Line currents flow through the transformers windings

The transformer and electric line have the following parameters [9]:

- rated power $S_T = 160$ [kVA];
- rated primary voltage $U_p = 6$ [kV], rated secondary voltage $U_s = 0.4$ [kV] ;
- normal transformer load leakage impedance $\underline{Z}_T = 5.49 + i \cdot 8.06$ [Ω];
- transformer zero sequence impedance $\underline{Z}^0 = 14.77 + i \cdot 134.19$ [Ω];
- line and neutral conductor impedances $\underline{Z}_L = \underline{Z}_N = 0.143 + i \cdot 0.017$ [Ω].

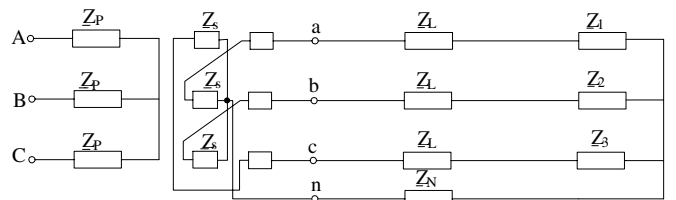


Figure 5. Electric distribution network diagram

The distribution network supplies three single-phase consumers of $S_1 = 17$ [kVA], $S_2 = 40$ [kVA] and $S_3 = 30$ [kVA] with power factor $\lambda = 0.8$. The complex forms of LV line currents are: $I_1 = 28.18 - i \cdot 29.30$,

$I_2 = -86.33 - i \cdot 25.74$ and $I_3 = 19.19 + i \cdot 65.15$, while the neutral current is $I_N = -38.95 + i \cdot 10.10$. Accordingly to the relationship (2), the following expressions of symmetrical components on the LV side of the network can be obtained:

- line currents:

$$\underline{I}_a^+ = 46.82 - i \cdot 46.8; \underline{I}_a^- = -5.65 + i \cdot 14.12;$$

$$\underline{I}_a^0 = -12.98 + i \cdot 3.36; k_I^- = 22.98[\%];$$

- load voltages

$$\underline{U}_a^+ = 222.49 + i \cdot 5.89; \underline{U}_a^- = -1.05 - i \cdot 1.92;$$

$$\underline{U}_a^0 = 7.67 - i \cdot 1.03.$$

Based on transformer behavior, relationships (8 – 11) allow calculating the voltage symmetrical components on the HV side of the transformer as follows:

$$\underline{U}_{AB}^+ = -5.23 - i \cdot 3.03 [kV]; \quad \underline{U}_{AB}^- = 0.012 - i \cdot 0.011 [kV];$$

$$\underline{U}_{AB}^0 = 0 [V].$$

These values let us to quantify the amount of voltage unbalance on the two sides of the transformer. Relationships (3) to (5) give the value of the total voltage unbalance factors at the LV and HV level of the studied electric network: $k_{s-U}^- = 0.98 [\%]$ for the secondary and $k_{p-U} = 0.28 [\%]$ for the primary. The comparative analysis of the obtained results shows a decrease of voltage unbalance from the secondary to primary of the studied transformer. Consequently, it can conclude that this type of transformer reduces the voltage unbalance if this type of perturbation propagates from the LV level to MV one.

In the same way, other types of transformers used to supply four wires LV networks were studied in order to evaluate their behavior from the point of view of unbalance propagation from the secondary side to the primary side. As a result of this research, the transformers were classified in three categories as presented below:

- transformers that do not change the unbalance from one level of voltage to another one: $Y_N Y_n$ (in this case, the neutral conductors can be loaded 100%);
- transformers that reduce the unbalance level, but neutral conductor can be loaded only at 10% of the rated current: $Y y_n$;
- transformers that reduce the unbalance level and the neutral conductor can be 100% loaded: $D y_n, Y z_n$.

V. CONCLUSIONS

The main conclusions of this paper relate to the transformers influence on the unbalance propagation. To analyze the transformer behavior from this point of view the symmetrical components theory was implemented. This theory

allows decomposing an unbalanced system of phasors into three symmetrical systems of positive, negative and zero sequence respectively. As a result any unbalanced power system may be studied as the superposition of three linear balanced systems.

This method was used in modeling the components of the power systems, namely electrical lines and transformers. Due to the fact that electric lines do not influence the unbalance propagation, transformers having different connections and magnetic core structure were analyzed via appropriate mathematical modeling.

The paper presents the detailed numerical study in the case of transformers with primary star connection and secondary interconnected star with neutral grounding connection. It is proved that this type of transformer mitigate the voltage unbalance in the primary side due to its special behavior regarding the zero-sequence components of the secondary line currents.

General comments are also presented regarding the behavior of other types of transformers.

ACKNOWLEDGMENT

The authors acknowledge the financial support given by the National Council for Scientific Research of Romania under grant CEEEX 153/2006.

REFERENCES

- [1] A. Cziker, M. Chindris, "Mitigation of the unbalanced steady state to industrial consumers. Theory and Applications", (in Romanian), MEDIAMIRA Publishing House, Cluj-Napoca 2003, Romania.
- [2] *** "Power Quality in European Electricity Supply Networks", Union of the Electricity Industry – EURELECTRIC, 2002.
- [3] C. Lazaroiu, N. Golovanov, "Propagation of voltage unbalance in power systems supplying AC traction loads", The 6th International Power Systems Conference, 03-04.11.2005, Timisoara, Romania, pp. 317 - 322.
- [4] N. Nimpitiwan et al. ., "The propagation of disturbances in power distribution systems", Transmission and Distribution Conference and Exposition, 2003 IEEE PES Volume 1, Issue , 7-12 Sept. 2003, pp. 6 - 12 Vol.1.
- [5] R. Tirnovan, S. Darie, "Faults and abnormal functioning regimes in electric networks", (in Romanian), MEDIAMIRA Publishing House, Cluj-Napoca 2004, Romania, p.33.
- [6] I. Boldea, "Transformers and electrical machines" (in Romanian), Didactic and Pedagogic Publishing House, Bucharest 1994, Romania, pp. 60 – 61.
- [7] M. J. Heathcote, "The J & P Transformer Book, Twelfth edition, A Practical Technology of The Power Transformer", Reed Educational and Professional Publishing Ltd 1998, p. 844.
- [8] A. Simion, "Electric machines. Volume 1 Transformers", (in Romanian), "Gheorghe Asachi" Publishing House, Iasi, 2000, Romania.
- [9] I. Voncila et al., "Calculation of MV transformers parameters for energy consumption optimization ", (in Romanian), SNET'04, 22-24 October 2004, Bucharest, Romania.